Mechanisms of cardiac endothelial damage by ionising radiation

Zahra Gharaei

This thesis is submitted for the degree of Doctor of Philosophy

Department of Oncology

University of Sheffield

November 2015

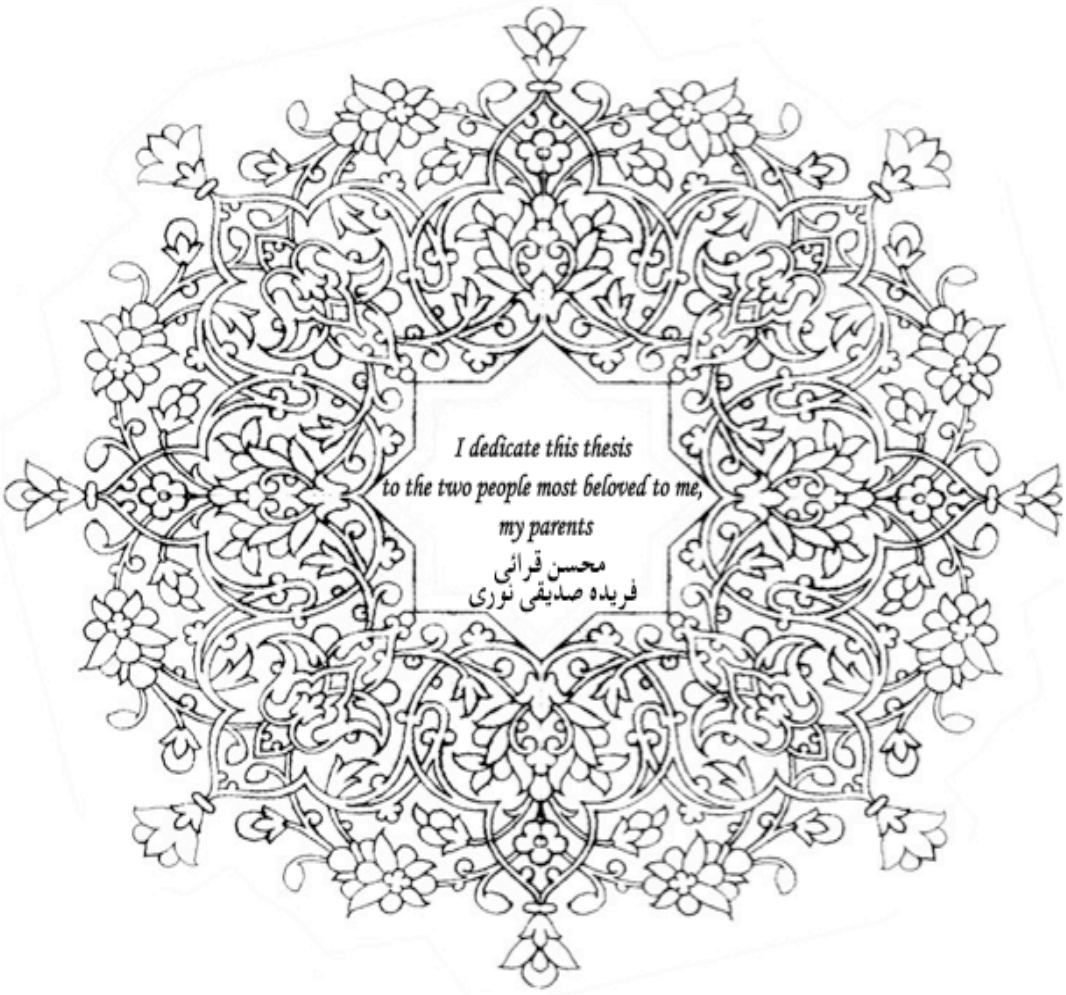
I dedicate this thesis
to the two people most beloved to me,
my parents
محسن قرائی
فریده صدیقی نوری

Acknowledgements

First of all, I am indebted to my supervisor Dr Chryso Kanthou for teaching me all the basic techniques and for her continued guidance and support, which have been invaluable in the accomplishment of this work. In particular, I would like to especially thank her for her patience and help with feedback, as well as corrections during the writing of this thesis. It was very much appreciated. I would like to extend my sincerest gratitude to my second supervisor Professor Gillian Tozer for her kind guidance and support and providing me with sound advice and helpful feedback throughout the course of this study. I would also like to say a special thank you to Professor Angie Cox for her mentoring role and in particular her kind advice, encouragement and support throughout my PhD. I appreciate exceptional support from Professor Nicola Brown and her guidance in completing my thesis.

A huge thank you to all the members of the Tumour Microcirculation Group, especially Matt Fisher, Dr Sarah Jane Lunt, Dr Debayan Mukherjee, Dr Toby Holmes and Dr Rachel Daniel and also other members of the Oncology Department, especially Jenny Globe, Sue Higham and Carmel Nichols for helping me to go through this project and made it more enjoyable, which would have not been possible without their kindness and support. Writing a thesis is difficult; however, writing in a foreign language makes it even harder. Therefore, I am eternally grateful to Dr Farzana Angum, Uzma Reem and Dr Sheila Harris for their continual help with English. This is particularly true in chapters 3 and 5 where their correction of my English and writing style and help in re-organising the structure of these chapters significantly improved the way it read. They have helped me to appreciate how the use of the English language can influence the scientific meaning of what is written. I would like to offer my thanks to the European Atomic Energy Community's Seventh Framework Program CARDIORISK grant for funding my studentship and our collaborators, Professor Wolfgang Dörr and Dr Julia Haagen for performing the localised mouse heart irradiations.

A special thanks to Reem for her friendship and encouragement over the years, especially for always being there for me when I needed her. I am really grateful for having her in my life. I would like to extend a huge thanks to my brothers Ebi and Mo, my sister Mania and best friends Mehraveh, Sara Fatemeh and Elham for their love and emotional support. I would not have been able to complete this thesis without you. I love you guys and I wish you all the best in your lives.

Finally, I am indebted to my parents for their unconditional love and being a continuous source of emotional and moral support. They have taught me to be a better person and their belief in me has made me stronger. I owe all I have accomplished to the most precious people in my life, my mom and dad.

Most importantly, thank you God for your abundant blessings in my life.

Abstract

Exposure of the heart to ionising radiation even at low to moderate doses can increase the risk of developing cardiovascular disease (CVD) many years later. This is of significance to cancer survivors who were treated with radiotherapy in the thorax. Damage to the heart microvasculature is thought to play a key role in development of radiation-induced CVD. The aim of this project was to investigate the effects of radiation on heart microvascular endothelial function using *in vitro* and *in vivo* approaches. In particular effects of radiation on angiogenesis were investigated since angiogenesis is important for heart repair after myocardial injury.

The hearts of C57BL/6 and APOE$^{-/-}$ mice were X-ray irradiated with doses of 0.2 to 16 Gray by the group's collaborators and animals were sacrificed at 20-60 weeks post-irradiation. Angiogenic sprouting was assessed in heart explants embedded in fibrin. A dose dependent reduction in angiogenic sprouting was observed, which was significant after ≥8 Gy at 20 weeks and ≥2 Gy at 60 weeks post-irradiation demonstrating that vascular damage was progressive. Radiation inhibited *in vitro* endothelial migration at doses of ≥0.2 Gy. Radiation also inhibited endothelial tubule formation in matrigel and in organotypic assays in which endothelial cells were co-cultured with fibroblasts. In addition to damaging cells directly, radiation also induces indirect effects through bystander interactions. Results showed that irradiated fibroblasts inhibited angiogenesis through soluble factors they secreted into their conditioned media. Signaling mechanisms through which radiation alters angiogenic function were studied. Results showed that transforming growth factor beta and Rho-GTPase signaling are involved in the anti-angiogenic activity of radiation.

In summary, this study established that low to moderate doses of radiation inhibit endothelial function which could contribute to the development of CVD. The study also identified signaling pathways that may be targeted to protect against radiation-induced heart microvascular damage.

Publications arising from this work

Z. Gharaei, J. Haagen, C. C. Reyes-Aldasoro, W. Dörr, G. M. Tozer and C. Kanthou (2010). Cardiac endothelial damage by ionizing radiation. *Microcirculation* (*Abstract of 60th meeting of British and Microcirculation Societies*) **17**(6): 458-493. (Oral presentation)

Z. Gharaei, C. Kanthou, G. M. Tozer, C. C. Reyes-Aldasoro, J. Haagen and W. Dörr (2010). Inhibition of cardiac endothelial cell angiogenic responses after radiation exposure, *The Medical School 6th Annual Research Meeting*. (Poster presentation)

Z. Gharaei, C. C. Reyes-Aldasoro, J. Haagen, W. Dörr, G. M. Tozer and C. Kanthou (2011). Inhibition of angiogenic capacity in the mouse heart after radiation exposure, *The Medical School 7th Annual Research Meeting*. (Poster presentation)

Z. Gharaei, J. Haagen, W. Dörr, G. M. Tozer and C. Kanthou (2012). Effect of radiation on cardiac endothelial angiogenic function. *Microcirculation* (*Abstracts of the 2nd Joint Meeting of the British and American Microcirculation Societies, 62nd Meeting of the British Microcirculation Society*) **20**(1): 77-78. (Poster presentation)

C. Kanthou, Z. Gharaei, J. Haagen, S. J. Lunt, C. C. Reyes-Aldasoro, W. Dörr, and G. M. Tozer (2012). Inhibition of angiogenesis in the mouse heart by ionizing radiation. *Cancer Research* (*American Association for Cancer Research 103rd Annual Meeting 2012*) **72**(8): 5723

Z. Gharaei, J. Haagen, W. Dörr, G. M. Tozer and C. Kanthou (2012). Inhibition of angiogenesis in the mouse heart and endothelial cells after radiation exposure, *The Medical School 8th Annual Research Meeting*. (Poster presentation)

Abbreviations

3D	three Dimensional
3D-CRT	3-Dimensional Conformal Radiation Therapy
AA	Aortic Arch
aFGF	acidic Fibroblast Growth Factor
AGIR	Advisory Group on Ionising Radiation
AHS	Adult Health Study
ALK	Activin Receptor-Like Kinase
Ang-II	Angiotensin II
ANOVA	Analysis of Variance
ALP	Alkaline Phosphatase
AP-1	Activator Protein-1
ATCC	American Type Culture Collection
ATM	Ataxia Telangiectasia- Mutated
BEIR	Biological Effects of Ionizing Radiation BEIR (A US National Academy of Science expert panel)
BER	Base Excision Repair
bFGF	basic Fibroblast Growth Factor
BMPs	Bone Morphogenic Proteins
BrDU	Bromodeoxyuridine
BSA	Bovine Serum Albumin
CA4P	Combretastatin A4 Phosphate
CEC	Cardiac Endothelial Cell
CF	Cardiac Fibroblast
CM	Conditioned Media
CNS	CNS Central Nervous System

CTGF	Connective Tissue Growth Factor
CVD	Cardiovascular Disease
DAB	Diaminobenzidine
DAPI	4',6-diamidino-2-phenylindole
DDR	DNA Damage Responses
DMEM	Dulbecco's Modified Eagle Medium
DMSO	Dimethyl Sulfoxide
DNA	Deoxyribonucleic acid
DSB	Double Strand Break
EC	Endothelial Cell
ECGS	Endothelial Growth Supplement
ECL	Chemiluminescence
EDTA	Ethylenediamine - N, N, N`, N`- tetraacetic acid
EGF	Epidermal Growth Factor
EHS	Engelbreth-Holm-Swarm
ELISA	Enzyme Linked Immunosorbent Assay
ERK	Extracellular signal Regulated Kinase
FBS	Foetal Bovine Serum
FDA	Federal Drug Administration
Gills HTX	Gill's Haematoxylin
GJICs	Gap-Junction Intracellular Communications
Gy	Gray
H&E	Haematoxylin And Eosin
HA	Heart Atrial
HBSS	Hank's Balanced Salt Solution
HD	Hodgkin's Disease
HDF	Human Dermal Fibroblast

HDL	High-Density Lipoprotein
HDMECs	Human Dermal Microvascular Endothelial Cells
HIF-1α	Hypoxia-Inducible Factor-1 alpha
HR	Homologous Recombination
HRR	Homologous Recombination Repair
HUVEC	Human Umbilical Vein Endothelial Cell
HV	Heart Ventricular Myocardium
ICAM-1	Intercellular Adhesion Molecule-1
ICRP	International Commission on Radiological Protection
IgA	Immunoglobulin A
IGF	Insulin Growth Factor
IGRT	Image-Guided Radiation Therapy
IHC	Immunohistochemistry
IL	Interleukin (IL-1; IL-1β, IL-6; IL-10; IL-12)
IMRT	Intensity-Modulated Radiation Therapy
IR	Ionizing Radiation
IRIF	Ionizing Radiation Induced Foci
JNK	c-Jun-N-terminal Kinase
LAP	Latent Associated Protein
LAPs	Latency-Associated Peptides
LDL	Low-Density Lipoprotein
LDLr	low-density lipoprotein receptor
LDS	Lithium Dodecyl Sulfate
LET	Linear Energy Transfer
LSS	Life Span Study
LTBP	Latent-TGF-β Binding Protein
MAPK	Mitogen Activated Protein Kinase

MCP-1	Monocyte Chemotactic protein - 1
MEK	Mitogen-activated protein kinase
MES	2-(*N*-morpholino)ethanesulfonic acid
MI	Myocardial Infarction
Mit C	Mitomycin C
MMP	Matrix Metalloproteinases
MMR	Mismatch Repair
MOPS	3-(*N*-morpholino)propanesulfonic acid
mRNA	messenger Ribonucleic acid
NCRP	National Council on Radiation Protection and Measurements
NCI	National Cancer institute
NER	Nucleotide Excision Repair
NF- κB	Nuclear Factor κB
NHEJ	Non-Homologous End-Joining
NO	Nitric Oxide
PAI-1	Plasminogen Activator Inhibitor-1
PBS	Phosphate Buffered Saline
PDGF	Platelet-Derived Growth Factor
PECAM-1	Platelet-Endothelial Cell Adhesion Molecule-1
PIGF	Placenta Growth Factor
ROCK	Rho-associated Protein Kinase
ROS	Reactive Oxygen Species
RSN	Reactive Nitrogen Species
RT	Room temperature
rTGFbp	Recombinant TGF-β protein
SCEs	Sister Chromatid exchanges
SCID	Severe Combined Immuno-Deficient

SEER	Surveillance, Epidemiology and End Results cancer registry
SR-A	Scavenger Receptor Class A
SSB	Single Strand Break
Sv	Sievert
t-PA	tissue-type Plasminogen Activator
TF	Tissue Factor
TFPI	Tissue Factor Pathway Inhibitor
TGF-β	Transforming Growth Factor-beta1
TM	Thrombomodulin
TMG	Tumour Microcirculation Group
TNF-α	Tumour Necrosis Factor- alpha
TβRII	TGF-β Type II receptor
u-PA	urokinase type Plasminogen Activator
UNSCEAR	United Nations Scientific Committee on the Effects of Atomic Radiation
USNRC	United State Nuclear Regulatory Commission
UV	Ultraviolet
VCAM-1	Vascular Cell Adhesion Molecule-1
VEGF	Vascular Endothelial Growth Factor
vWF	von Willebrand Factor
WPB	Wiebel-Palade Bodies
WR	Radiation-Weighting factor
α-SMA	Alpha- Smooth Muscle Actin

Table of Contents

List of Tables

List of Figures

Chapter One

Introduction

1.1 Ionizing radiation and sources

There are two types of radiation sources; natural and man-made radiation sources and people are exposed to radiation from both natural and man-made sources. Cosmic radiation (beta and gamma coming from space), terrestrial radiation (soil, water, vegetation) and internal radiation (potassium-40, carbon-14 and lead-210) are three sources of natural background radiation. Man-made radiation is used in diagnosis, screening and treatment of some diseases such as cancer. Two distinct groups of people are exposed to man-made radiation sources, those who are receiving radiation for treatment as well as occupationally exposed individuals (USNRC, 2011).

Gray (Gy) or Sievert (Sv) are two units of radioactive dose. Radiation doses are usually measured in an international unit called Gray (Gy). 1 Gray is the amount of energy (1 Joule) (e.g. Gamma-ray or X-ray) absorbed by1 kilogram of tissue/material (absorbed doses). The energy absorbed by tissue, no-matter from the type of radiation, is expressed in unit of Gy. However the biological effects of various type of radiation (e.g. X-ray or alpha particle) are different (for the same given absorbed dose, e.g. 1 Gy) and the Gy unit does not take into account these differences. Biological effects vary because different types of radiation have different energies and so different path lengths through different types of tissues. The radiation equivalent doses takes into account the different biological effectiveness of different types of radiation and the Sievert (Sv) unit, also measured in joules per kilogram, is defined as the dose in Gy multiplied by a radiation-weighting factor (WR), which depends on the type of radiation, taking into account their different linear energy transfer (LET). The Sv is particularly important in radiation protection, as it is the most relevant unit for estimating the risk from radiation exposure of developing cancer later in life (AGIR, 2010; ICRP, 2007a).

People are exposed to radiation from natural, medical and man-made sources. A world-wide average annual radiation dose (from all backgrounds) to an individual member of the general population is about 3.5 mSv. The legal limit for the occupationally exposed workers has been

set at 50 mSv. It has been reported that the exposure to dose above 100 mSV constitutes a risk of developing cancer (Masse, 2000). In Switzerland the annual exposure to radiation from natural and man-made sources has been estimated to be about 4 mSv. The exposure to man-made and natural radiation contributes 30 and 70 % respectively to the annual radiation dose (4 mSV) (Roth *et al.,* 1996).

1.2 Discovery of X-rays and radiation therapy

A new kind of ray (X-ray), was discovered by Wilhem Cornard Rontgen in 1895. This could be absorbed by a variety of materials, and produce fluorescence (reviewed by Rontgen, 1896; Rockwell, 1998). After discovery of the X- ray, the naturally radioactive materials, polonium and radium were discovered by Marie Curie in 1898. These discoveries revolutionised some fields of physics, chemistry and medicine. Techniques for delivering the radiation, treatment planning and precise dosimetric measurement were subsequently developed for radiation therapy (reviwed by Tubiana *et al.*, 1996).

In 1896, X-ray radiation was introduced in the treatment of cancer, and its positive effects on tumour cells were observed with some occasional cures (Ewing, 1934). Radiotherapy is one of the most effective ways of treatment of cancer, which can be used with curative or palliative intents to eliminate cancers or relieve their symptoms via killing cancer cells. It has been estimated that about 50 % of different cancer cases will receive radiotherapy during their treatment (Delaney *et al.*, 2005). Following transfer of energy by radiation to living cells, atoms and molecules inside become ionised and excited, which results in damage to tissues and cells. Moreover it might be used alone or in combination with chemotherapy, surgery or both (ICRP, 2007a).

These ionisation and excitation events can damage normal and cancer cells through the molecules that regulate vital cell processes (especially DNA and RNA) or via indirect damage to these molecules via creation of free radicals from interaction with tissue water (Lawrence, 2008). Howard and Plec in 1952 provided fundamental insights into cell division and showed

that radiation causes cell cycle arrest in the G2 phase (Howard and Plec, 1952). The Little et al study showed that the quiescent cells were more resistant to radiation and could repair the damage after exposure while radiation was toxic for proliferating cancer cells (Little *et al.*, 1973). Cell proliferation is not uniform. In some tissues like skin, cells proliferate rapidly, while in other tissues, such as brain, they are less or non-proliferative. The proliferative pattern of a tissue could determine the radiation toxicity. When quiescent cells are exposed to radiation, the radiation damage is not observed until they start dividing. In contrast, radiation is most effective at killing those cells that are actively dividing, as they could express the lethal damage (especially to DNA) rapidly and pass it on to the next generation. Moreover, radiation injury to cells during S phase is more fatal as cells have shorter time to repair. Cancer cells are relatively radiosensitive because they are rapidly proliferating. Moreover, cancer cells can have deficient repair mechanisms. If their DNA is damaged beyond repair they die or stop dividing (reviwed by Rockwell, 1998).

1.3 Radiation regime for radiotherapy

The radiation dose that could kill every clonogenic cell in the tumour would be the ideal dose leading to cure. However, radiation damage to surrounding normal tissue needs to be taken into account. Different normal cells show different sensitivities to radiation based on their age, proliferating nature and ability to repair. There are different choices for radiotherapy which are determined according to the tumour type, size, location, depth in body, proximity to the normal tissue as well as patient's general health, age and other medical conditions. There are three types of radiotherapy: external-beam radiation, internal and systemic radiation therapy (Lawrence, 2008; NCI, 2010). In external-beam therapy, photon beams such as X-rays or gamma rays are generated and delivered to the tumours by a linear accelerator. 3-dimensional conformal radiation therapy (3D-CRT), intensity-modulated radiation therapy (IMRT), image-guided radiation therapy (IGRT), tomotherapy, and proton therapy are types of external radiation therapy which differ in imaging techniques and the type of beams used (NCI, 2010). If a radioactive material is used and placed in the body near the tumour cells, it is called

internal radiation therapy or brachytherapy. The radioactive isotopes are sealed in tiny seeds, needles, wires or catheters and placed within the body near the tumour on a temporary or permanent basis. During brachytherapy the patients are radioactive and need to stay in special care until the radioactive source is removed or decayed adequately (Connell and Hellman, 2009; Lawrence *et al.*, 2008; NCI, 2010; Patel and Arthur, 2006).

In systemic radiation therapy, the radioactive substances (e.g. iodine), or radioactive substance, which is bound to a monoclonal antibody are injected intravenously, and are subsequently taken up by target cancer cells (e.g. radioactive iodine is used in Thyroid cancer). Patients are advised to have limited contact with other people as they might emit a very low dose of radiation. Nowadays, the radiation from external beam therapy is mostly delivered to patients in low doses fractions (Connell and Hellman, 2009; NCI, 2010; Rockwell, 1998). A single high dose of radiation can cause severe normal tissue damage. Using fractionated doses increase protection of normal tissue against radiation by having time in between to restore and repair the damage from the previous dose they received. Fractionated radiation exposure to tumour cells also increases the probability of DNA damage at their most vulnerable cell cycle point (Rockwell, 1998; Connell and Hellman, 2009).

The combination of radiotherapy and chemotherapy is called radiochemotherapy. Dose and timing of radiation therapy are dependent on tumour type and the goal of treatment. Radiotherapy might be applied along with surgery or chemotherapy. If radiation treatment is planned before surgery it is called neoadjuvant or pre-operative in order to shrink the size of tumour before surgery. The addition of radiation during surgery is called intraoperative radiation therapy, which can help shielding of normal tissues, which are too close to tumours for external therapy. Radiotherapy after surgery is called adjuvant or post-operative therapy (Calvo *et al.*, 2006; Connell and Hellman, 2009; NCI. 2010).

1.4 Mechanisms of radiation effects on tissue/cells

1.4.1 DNA damage

Radiation damage to tissues can be induced by electrons, protons, neutrons, photons (e.g. γ-rays and X-rays), α- particles and heavier particles such as carbon nuclei (Rastogi *et al.*, 2010; Sachs *et al.*, 1992;). All the molecules inside cells are in danger of being ionised as the radiation energy is deposited randomly. However, except for DNA (with only two copies), radiation has fewer effects on other molecules such as RNA and proteins, as they have several copies, which undergo a rapid turnover following exposure. Therefore, DNA is the main target of ionizing radiation. If the damage to DNA by radiation is not repaired properly, it can cause lethal consequences (Nikjoo and Khvostunov, 2003). It was observed that when radiation was delivered to the nucleus it led to a higher rate of cell death compared to when radiation was delivered to the plasma membrane or cytoplasm (Warters and Hofer, 1977). DNA consists of two strands, each strand containing four bases (adenine, cytosine, guanine and thymine), which are connected by a sugar-phosphate backbone. The two strands form a double helical structure connected by hydrogen bonds. At regular intervals, this double helix is wound around histones forming a nucleosome. The chromosome structure is made up finally by further DNA folding and looping (Wouters and Begg, 2009).

Radiation-induced damage compromises several stages, including initiation, promotion and the final stage of progression. In the initiation stage, radiation causes excitation, which means ionisation or ejection of electrons from molecules within cells. These are often termed the principal biological effects. Molecular damage occurs as a result of deposition of radiation energy inside the cells and excitation state of molecules inside such as DNA, RNA, proteins and water. Energy is transferred to molecules within 10^{-15} seconds (reviewed by Nikjoo and Khvostunov, 2003). In the promotion stage, the ejected electron caused by radiation has the ability to collide with other molecules inside the cells and result in further ionisations (Goodhead, 2006; Wouters and Begg, 2009). Transfer of energy from excited molecules to other surrounding molecules depends on the magnitude of transferred energy and initiates a

chain of events, forming clusters of ionisations and excitations. The transfer of energy to the neighbouring molecules and the ejection of secondary electrons continue until the excess energy is lost completely and the electron is trapped by electrostatic charges (reviewed by Goodhead, 1994; Nikjoo and Khvostunov, 2003).

The end products of irradiation are ionised molecules and free radicals, which could potentially result in degeneration of the biomolecules, breaking of chemical bonds in different molecule's structure and consequently cause molecular damage to DNA and other molecules. It takes approximately less than a 10^{-13} second for a primary particle to cross a cell's nucleus (Sachs *et al.*, 1992). The H and OH ions are types of hydrated electrons, which are produced by water molecules associated with DNA. Hydroxyl radicals are one of the most damaging agents. The free radical causes DNA single and double strand breaks (Nikjoo *et al.*, 2001; Nikjoo and Khvostunov, 2003).

The severity of damage depends on the magnitude of energy and number of the ionisation clusters. High-linear energy transfer (LET) radiation produces a larger cluster inside the nucleus and complex types of strand break damage. Lower energy deposition tends to create smaller clusters, with more likelihood of single strand breaks (SSBs) or double strand breaks (DSBs) of a type that are more repairable compared to the complex type of double strand DNA breaks by high-LET (Nikjoo and Khvostunov, 2003).

In has been reported that, exposure to 1 Gy irradiation (using both high and low LET radiation) in a mammalian cell will produce a large number of events including; about 10^5 ionizations with more than 1000 DNA bases damage (O'Driscoll and Jeggo, 2006; Wouters and Begg, 2009). The evaluation of clustered-damage revealed that a high-LET radiation induces a more complex damage compared to the low-LET radiation while the total yield of strands breaks was similar in both radiation types. The low-LET induced approximately 20-40 DSBs, compared to 70 DSBs in high-LET group. Within seconds or minutes of DNA damage,

the repair mechanism is triggered and activated; (Nikjoo *et al.*, 1998; Wouters and Begg, 2009).

1.4.2 Mechanisms of DNA Damage Response

Cells have specialised repair mechanisms to eliminate or minimize DNA damage. There are different DNA damage responses (DDR) to effectively reduce the cytotoxicity of radiation despite the large number of lesions produced per cell. The damage is first detected by sensor proteins, which signal to effector pathways. The three main effector pathways, as shown in Figure **1.1,** are the DNA repair pathway, programmed cell death and the damage checkpoint pathway (O'Driscoll and Jeggo, 2006; Wouters and Begg, 2009).

Different proteins in the response to DNA damage, including the sensor proteins, are recruited to the site of injury. The damaged regions are called ionising radiation induced foci (IRIF). Phosphorylation of H2AX histone protein is one of the early DDR events, which starts within 5-30 min after induction of the damage. Histone H2A is a component of the nucleosome in which DNA is packaged and H2AX is a variant of histone H2A, which is distributed throughout the nucleus. The phosphorylated H2AX, known as γH2AX, initiates the recruitment of other essential proteins to the site of damage and results in formation of IRIF (Bartek *et al.*, 2004; Kastan and Bartek, 2004; Stucki and Jackson, 2006; Wouters and Begg, 2009). The DNA repair pathways include: base excision repair (BER), mismatch repair (MMR), nucleotide excision repair (NER), SOS response and double-strand break repair (by homologous recombination and non-homologous end joining). Different cells show a wide variation in tolerance to radiation. Since DSBs affect both DNA strands and cause the loss of genetic material, it is the most harmful of radiation-induced damages (Rastogi *et al.*, 2010). Depending on the type of damage and cell conditions, damage to DNA injury in the majority of cases is repairable. However if damages caused by radiation are not repaired completely or efficiently, they could lead to biological effects such as mutation, chromosomal aberration and genetic instability (Cox, 1994).

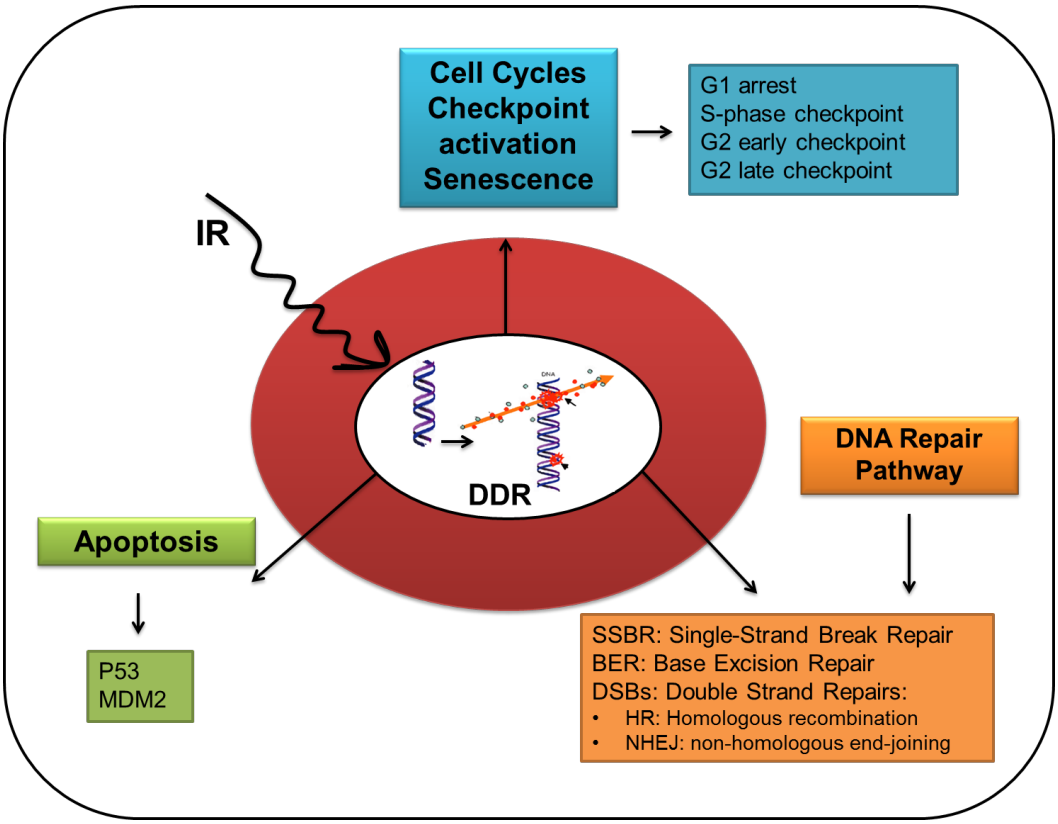

Figure 1.1 DNA damage responses. Apoptosis, DNA repair pathways and Senescence are three effector pathways that are activated following radiation exposure and DNA damage.

1.4.3 Other mechanisms of radiation effect on cells

Radiation damage to DNA, either directly or indirectly (via free radical production from irradiated water), is the classic mechanism for radiation injury. However, it has been observed that cells respond differently to low dose radiation below 1 Gy compared to responses at higher doses. For instance, high doses inevitably produce cell death, it is just the amount that varies with dose (deterministic effect), whereas there is only a probability of mutation at low doses (stochastic effect) because of the random nature of energy deposition. A linear-quadratic dose response relationship, which applies for doses above 1 Gy, is not valid for the range of very low-dose radiation (Osterreicher *et al.*, 2003). In recent years, radiation-induced responses such as adaptive responses, genomic instability, low-dose hypersensitivity and bystander effects (non-targeted responses), have been identified and observed in living organisms to account for biological effects at low radiation doses (Brooks, 2005; Matsumoto *et al.*, 2007).

1.4.4 Radiation induces Adaptive responses

The adaptive response is when a very small radiation dose (ranging between 0.01-0.2 Gy), referred to as the priming dose, induces an effective protective signaling mechanism in cell/tissues, which leads to lower than normal radiation-induced damage (make it less susceptible to radiation-induced damage), when exposed to a second higher radiation dose several hours later (Matsumoto *et al.*, 2007; reviewed by Olivieri *et al.*, 1984). When the priming dose is above 0.2 Gy, adaptive responses are not detected (Feinendegen, 1999). Some studies showed that factors involved in DNA repair (e.g. poly (ADP-ribose) poly7merase (PARP)), factors involved in cell cycle regulation (e.g. p125), as well as signal transduction pathways, are the most important mediators of adaptive responses (Matsumoto *et al.*, 2007; Wang and Ohnishi, 1997; Wiencke *et al.*, 1986). Changes in gene-expression might also be involved (Brooks, 2005). The p38 mitogen-activated protein kinase (p38MAPK) and nuclear factor κB (NF- κB)-related signaling pathways have been implicated in radioadaptive responses (Joiner *et al.*, 1996; Shimizu *et al.*, 1999). Additionally, the reactive oxygen species

and nitrogen species (ROS/RSN) have been found to have contributory roles in adaptive responses following exposure to low doses of radiation. The production of ROS/RNS could cause DNA damage that initiates further radioadaptive responses. The DNA damage by ROS/RNS results in induction of some transcription factors as well as cellular events that in turn induce radio-protective responses in cells (Matsumoto *et al.*, 2007). The adaptive response has not been observed in all cells/tissues exposed to radiation, and is dependent upon the interval between exposures, as well as radiation dose (UNSCEAR, 2006; NCRP, 2010). Underlying mechanisms are still poorly understood and require further studies.

1.4.5 Radiation induces genetic instability

DNA damage, gene mutation and chromosome aberration are some of the important early radiation-induced damages that occur in cells. These genetic instabilities in the cell genome can be passed on to the cells' progeny (Brooks, 2005; Morgan, 2011). The genetic instability has been demonstrated in irradiated cells after multiple divisions, when initially exposed to both low and high radiation doses. This phenomenon could explain some of the late effects of low-dose radiation (Morgan and Sowa, 2009; Morgan, 2011; NCRP, 2010).

1.4.6 Radiation induces low-dose hypersensitivity

It has been reported that, at doses smaller than 0.5 Gy, cell survival rate is lower than expected from the linear quadratic doses responses model that applies at higher doses. The mechanism of this effect is not fully understood yet (Joiner *et al.*, 2001; Prise *et al.*, 2005). Cells could exhibit low-dose hypersensitivity due to their cell cycle state when exposed to radiation as well as changes in DNA damage signaling and apoptosis responses. It has been observed that radiation-induced changes in DNA repair, gene expression and apoptosis differ at high and low doses. The repair mechanism pathways in the DDR may be sub-optimal at these low doses (Averbeck, 2009; NCRP, 2010).

1.4.7 Radiation induces bystander responses

There are always some cells that are not traversed by radiation but still exhibit signs of radiation damage. This could be explained as a result of signaling or communication between the irradiated cells (targeted cells) and non-irradiated cells (non-targeted cells), which is called the bystander effect (Matsumoto *et al.*, 2007). This mechanism is relatively slow due to the need to activate signaling pathway(s) in neighbouring cells but can result in chromosomal instability, mutation, cell killing and apoptosis as well as increased ROS in non-irradiated cells (Matsumoto *et al.*, 2007; NCRP, 2010; Osterreicher *et al.*, 2003; Prise and O'Sullivan, 2009).

The bystander effect, was initially described in 1992 by Nagasawa and Little. They observed that when Chinese hamster ovary cells were irradiated with 0.31 mGy of α-particles, an enhanced frequency of sister chromatid exchanges (SCEs) were observed in about 30% of the cells while only 0.1-1% of the cells were traversed by an α- particle track (Nagasawa and Little, 1992). This non-targeted bystander effect was also confirmed by other studies (Deshpande *et al.*, 1996; Huo *et al.*, 2001). Moreover, when non-irradiated cells were co-cultured with cells that had been irradiated with low radiation doses, such as X-rays, a similar bystander effect was observed (Mothersill and Seymour, 1998). In addition, a bystander effect was observed when non-irradiated cells were exposed to the culture medium from the irradiated cells (Iyer and Lehnert, 2002; Mothersill and Seymour, 1998). Radiation-induced bystander effects have been studied both *in vitro* (Prise and O'Sullivan, 2009) and under *in vivo* conditions (Kassis, 2004) and so are likely to be of relevance in humans. Additionally, bystander responses have been observed after exposure to both low and high radiation doses. The bystander effect observed at low doses increased dramatically (Osterreicher *et al.*, 2003).

The mechanism of radiation-induced bystander responses is still not fully known. Cells can communicate through direct connections between cells or through soluble factors (e.g. signaling molecules, cytokines) in the culture medium (Hamada *et al.*, 2007; Osterreicher *et al.*, 2003). A direct connection occurs through interaction between cell ligands and their receptors or through gap-junction intracellular communications (GJICs). The bystander effect

has been shown in many cells types including, fibroblasts, epithelial cells, and endothelial cells (Osterreicher *et al.*, 2003; reviewed by Matsumoto *et al.*, 2007).

Tumour necrosis factor-α (TNF-α) and transforming growth factor-β1 (TGF-β) are possible mediators of this bystander response (Barcellos-Hoff and Brooks, 2001; Ewan *et al.*, 2002; Martin *et al.*, 1997). TGF-β-related signaling can cause ROS induction (Iyer and Lehnert, 2002). Additionally, nitric oxide (NO) has been found to play an important part in radiation-induced bystander effects. It has been observed that NO excreted from irradiated cells caused a radioresistance phenotype in adjacent non-irradiated cells (reviewed by Matsumoto *et al.*, 2007). Moreover initiation of the bystander effect and increased cell proliferation in bystander cells was found to result from NO-mediated events (Han *et al.*, 2007; Shao *et al.*, 2002).

1.5 Epidemiology of radiation induced-diseases

Epidemiology is important in order to identify risk factors for exposure to different radiation doses. In radiation-associated cardiovascular disease, epidemiological evidence can be used to identify the appropriate radiation doses to use for mechanistic studies (Darby *et al.*, 2010; Little *et al.*, 2008).

1.5.1 Radiation damage on normal tissue

A few months after Rontgen's discovery, several acute biological effects such as skin burn, baldness and dermatitis, were reported. By 1959, about 360 cases of death from those exposed to radiation (X-ray and radium) were reported and the cause was mostly because of cancer (reviewed by Doll, 1995). Many studies have reported that exposure to radiation can lead to cancer and non-cancer diseases such as cardiovascular diseases (CVD) in later life (Kamiya and Sasatani, 2012; Lawrence, 2008). Such studies have led to strict regulations on the use of radiation for protection of both the general public and radiation workers. The United Nations Scientific Committee (UNSCEAR), International Commission on Radiological Protection (ICRP) and US national research council have reviewed the effects of therapeutic and atomic radiation (ICRP, 2007; reviewed by Doll, 1995; UNSCEAR, 2006; UNSCEAR, 1993).

Following the atomic bomb in Hiroshima and Nagasaki, 180,000 people were killed directly and thousands of people died shortly after exposure as a result of acute radiation. Furthermore, thousands of individuals exposed to the radiation, developed different symptoms later. An atomic bomb Casualty Commission was conducted in conjunction with the Japanese National Institute of Health to study the long-term genetic and somatic effects on radiation survivors (Cannan, 1962; reviwed by Doll, 1995). Our current knowledge of long-term radiation effects is based on principal evidences from atomic bomb survivors. Some data show that doses between 0.2-0.5 Gy could increase the risk of abortion, abnormality and development of cancer later in the unborn child, which could be 6% per Gy (reviewed by Doll, 1995; UNSCEAR, 1993). According to some evidence, there was a reduction in life expectancy following radiation exposure in the occupational exposure group (Smith and Doll, 1981; Warren, 1956). However, in other studies such as the Life Span Study, no life-shortening effect of radiation was observed (Cardis *et al.*, 1995; Shimizu *et al.*, 1991). In addition to atomic bomb survivors, radium, uranium and radon are sources of ionizing radiation in nature, which have been found to be harmful to exposed populations such as mine-workers. According to some epidemiological observations, the risk of lung cancer increased following radon exposure, which in turn depends on the proportion and intake of radon (Lubin *et al.*, 1995; Darby *et al.*, 2005).

1.5.2 Radiation induces circulatory disease

Circulatory diseases including pericardial disease, congestive heart disease, coronary heart disease and stroke are some of the leading causes of death in the world. Moreover coronary heart disease is the UK's most common cause of death, cancer being the second. Atherosclerosis is the underlying reason for stroke and coronary heart disease (Adams *et al.*, 2003; AGIR, 2010).

Non-modifiable risk factors for heart disease are sex, age and genetic predisposition and well-established modifiable factors include smoking, diabetes, low HDL and high LDL blood cholesterol. Some additional lifestyle risk factors include physical inactivity, obesity, an

atherogenic diet (high caloric density, fat, cholesterol) (Tzoulaki *et al.*, 2009). In addition to different CVD risk factors, radiation has been identified as another independent risk factor in human heart disease. CVD is one of the important determinants of late radiation morbidity and mortality (AGIR, 2010; Hoving *et al.*, 2008; Stewart *et al.*, 2006;).

Radiation coming from environmental agents or occupational or medical exposure is one of the potential risk factors associated with heart disease. During radiation treatment for cancer, normal tissue surrounding the tumour is exposed to radiation. The heart or a part of the heart is irradiated during the course of radiotherapy in the thoracic area for many cancer types such as lung and lymphoma, some head and neck cancers, spinal and mostly breast cancers. For treatment of breast cancer, patients receive radiation doses of 40-50 Gy in small fractions of about 2 Gy (Andratschke *et al.*, 2011; Hendry *et al.*, 2008; Schultz-Hector and Trott, 2007). Many epidemiological and experimental animal studies have confirmed the increased risk of CVD after radiation exposure (Adams *et al.*, 2003; Fajardo and Stewart, 1972; Stewart *et al.*, 2006). According to recent epidemiological studies, there is evidence of elevated circulatory disease at much lower radiation doses. The data from atomic-bomb survivors of Japan are the main evidence of increased risk of coronary heart disease, myocardial infarction and stroke at lower radiation doses with a linear radiation dose-response (AGIR, 2010; Shimizu *et al.*, 2010; Yamada *et al.*, 2004). Generally low dose radiation is defined as < 0.5 Gy, moderate doses as 0.5 to 5 Gy and doses higher than 5 Gy are considered as high radiation doses. For radiologists doses lesser than 5 Gy are considered as low dose (Andratschke *et al.,* 2011; Hidebrandt, 2010).

1.5.3 Radiation-induced heart disease

Many cancer survivors receive radiotherapy during their treatment and some receive doses of at least 10 Gy to their heart or the carotid arteries. It has been proven that radiation of the heart, at high doses, causes heart disease, which may manifest years later as a result of deterministic tissue damage (McGale and Darby, 2008). According to Fajardo and Stewart's experimental studies (1970), heart is one of the most radiosensitive and dose-limiting organs in

radiotherapy (Fajardo and Stewart, 1970). Some epidemiological studies published on radiation damage at high doses are discussed below.

In a study by Hancock *et al*, the risk of mortality from heart disease was assessed in patients who were given mediastinal irradiation of approximately 40 Gy. The results showed an increased death from ischemic heart disease and myocardial infarction following radiation (Hancock *et al.*, 1993). Patients who received radiotherapy for head and neck cancer showed an increase in the relative risk of stroke when compared to those who did not receive radiotherapy (Dorresteijn *et al.*, 2002).

A critical review of nearly 100 clinical reports, which were mostly concerned with higher doses (between 45 and 70 Gy to the heart and coronary arteries) for common cancer patients (e.g. breast cancer, head and neck cancer etc), showed development of atherosclerosis and stenosis in the heart arteries (reviewed by Schultz-Hector *et al.*, 1995).

The long-term (10-23 years follow up) cohort study by Aleman *et al* (2003) on 1,261 Hodgkin's disease (HD) patients, who received high doses of radiation to their heart, showed that there was increased relative risk of CVD after 10 years, especially in patients treated before the age of 21. Clinical manifestation of ischaemic heart disease, myocardial insufficiency and microvascular perfusion changes were found in heart disease patients many years after radiotherapy treatment (Adams *et al.*, 2003; Aleman *et al.*, 2003). Rutqvist *et al* showed that breast cancer patients who received radiotherapy during their treatment compared to the patients treated with surgery alone had a significant increase in mortality from heart disease (Rutqvist *et al.*, 1992). Between 1950 and 1990, the cardiac doses received by breast cancer patients during radiation treatment, were quantified by Taylor and colleagues (Taylor *et al.*, 2007). Radiation treatment of breast and chest resulted in the heart receiving doses of 0.9-14 Gy and 0.4-6 Gy for left-side and right side irradiations respectively. The risk of mortality from CVD was significant in the long-term follow up of breast cancer patients after receiving high doses (Radiation protection No 158, 2008; Taylor *et al.*, 2007). However other risk

factors for CVD such as smoking, hypertension, diabetes, age and sex are confounding factors, when trying to estimate the risk from radiotherapy of breast cancer (Chargari *et al.*, 2011; Clarke *et al.*, 2005;). Nowadays there is more emphasis on delivering lower doses of radiation in these patients.

1.5.4 Radiation-induced heart disease at low and moderate radiation doses (0.2-5 Gy)

According to epidemiological and clinical studies there is no doubt of increased risk of CVD and heart disease mortality following high doses of radiation exposure to heart and vasculature (Schultz-Hector and Trott, 2007; Stewart *et al.*, 2006;). However the association of radiation at lower doses with late occurring heart diseases has recently begun to emerge. The studies of atomic bomb survivors were the first to suggest the linear dose-response relationship between heart disease and low dose radiation with no threshold, which clearly implicate the raised risk of circulatory disease at lower and moderate doses (reviewed by McGale and Darby, 2008; Little *et al.*, 2010). The studies of the atomic bomb survivors and other exposed groups together give a better understanding of the biological mechanism of radiation-induced damage at lower doses. This is urgently needed for radiation protection purposes and to confidently select a dose-response model that can help predict the risk of heart disease from low dose radiation exposure.

1.5.5 Low and moderate doses of radiation induce heart diseases in therapeutically exposed groups

The Surveillance, Epidemiology and End Results cancer registry data (SEER) has provided a major report on study of radiation-induced heart disease in breast cancer patients who received radiotherapy as a part of primary treatment or post-operative treatment. The 308,861 women included in this cohort were treated between 1973-2001. The results showed the 22% death was from heart disease (ischaemic heart disease and myocardial infarction), with 44% higher mortality risk of left-sided breast cancer patients compared to that in right sided. The mean doses given to breast cancer patients hearts was estimated to be about 5Gy in the treatment of right-sided breast cancer and 10 Gy in the left-sided breast cancer patients (Paszat *et al.*, 1998;

Radiation protection No 158, 2008; Schultz-Hector, 1993; Schultz-Hector and Trott, 2007). The Darby *et al* study using the SEER data demonstrated that the risk of CVD continuously increased with increasing time (Darby *et al.*, 2005). The Paszat *et al* (1998) study on women registered with SEER showed that the death rate from myocardial infarction (MI) was 17% higher in women with regional stage left-sided tumours than right-sided in women who were less than 60 years of age. However, increased risk appeared only after more than 10 years of follow up (Paszat *et al.*, 1998). In breast cancer patients, who received the target doses of 40-50 Gy, it has been estimated that the heart received mean doses of about 1-2 Gy which itself can induce CVD (using the linear quadric model after correction for fractionation doses) (Schultz-Hector and Trott, 2007). The early breast cancer trialists collaborative group found that death rate from heart disease in women with early breast cancer who received radiotherapy was 27% higher than women who did not receive it. The average dose that the heart received was about 1-2 Gy (Clarke *et al.*, 2005).

There is also evidence for low-dose irradiation of the heart leading to heart disease from studies of treatment of benign disease. Carr *et al* studied 3,719 patients suffering from peptic ulcer, who were treated with fractionated radiotherapy (about 9-18 Gy) between 1936 and 1965 to the stomach in order to reduce gastric secretion of hydrochloric acid. They were compared to patients who did not receive radiotherapy (Carr *et al.*, 2005). Heart doses ranging from 1.6 to 3.9 Gy were estimated and a 24% increased risk of coronary heart disease (manifested 10 years after exposure), after adjustment for smoking and other risk factors, was observed (Carr *et al.*, 2005). In the US, among peptic ulcer patients, those who received radiotherapy up to a mean cardiac dose of about 2 Gy, had a relative risk of 1.20 compared with non-irradiated patients after adjusting for sex, age, smoking and time after treatment (McGale and Darby, 2008).

1.5.6 Low and moderate doses of radiation induce heart diseases in atomic-bomb survivors

The evidence from epidemiological studies of the Japanese atomic bomb survivors of Hiroshima and Nagasaki are the best for quantification of low doses radiation-related effects on heart diseases. The only result with estimated risk of heart disease at lower radiation dose came from this study (Hauptmann *et al.*, 2003).

The Life Span Study (LSS) includes about 86,572 people who were within 2.5-3 km of hypocentres at the time of the bombing. The doses that individuals received were estimated to be between 0 to 4 Gy (86% received <0.2 Gy) during the 47 years of follow up (1950-1997). Of the 44,771 deaths reported in the LSS cohort there were 31,881 deaths from non-cancer diseases. Furthermore, 15% of the non-cancer deaths occurred during the last seven years of the study and 250 (0.8%) of the non-cancer deaths were estimated to be associated with the radiation exposure (Preston *et al.*, 2003; Shimizu *et al.,* 2010). The LSS cohort has provided strong evidence of non-cancer diseases such as stroke, respiratory disease and especially heart diseases in atomic bomb survivors, which increases with increasing doses. There are compelling indications that the radiation-related risk is still elevated even at doses of below 1 Sv while below 0.5 Sv there is still a dose response, but it is not consistently linear as that at > 1 Sv. The subjects mostly received penetrating γ-rays (Preston *et al.*, 2003; Yamada *et al.*, 2004).

The Adult Health Study (AHS) also studied 20,000 survivors in addition to LSS in 1958. The results showed an increased risk of about 14% per Sv during the follow-up. This cohort study showed a relation between CVD and atomic bomb survivors (Kodama *et al.*, 1996). From this information, Wong *et al*, carried out a study to investigate the late effects of exposure to atomic bomb radiation on the development of 19 different non-cancer diseases (Wong *et al.*, 1993). They studied those features over a period of time, which provided information on late effects of ionising radiation on non-cancer diseases. They found that the younger subjects who were heavily exposed showed increased incidence of MI in the later years. They also updated

this study in 2004 and found a significant dose-response relationship for hypertension and MI in survivors exposed at less than 40 years of age (Yamada *et al.*, 2004).

Excess radiation-related CVD mortality and morbidity has been observed in both the LSS cohort and AHS. The estimated excess relative risk according to Shimizu *et al* (2010) was 14% (6% to 23%, P<0.001) per Gy with linear dose response even at lower doses (ERR/Gy= 0.14). However the degree of risk at doses between 0 to 0.5 Gy is unclear. In these data from risk factors such as smoking, diabetes obesity, and alcohol intake were collected and accounted in the study and according to the result none of the potential biases or confounders had significant impact on elevated radiation risk for CVD (Ozasa *et al.*, 2012; Shimizu *et al.*, 1990; Shimizu *et al.*, 2010).

1.5.7 Low and moderate doses of radiation induce heart diseases in occupational exposure

The risk of cardiovascular disease following radiation exposure has been considered among several types of radiobiologists and nuclear workers and other occupationally exposed groups, which mostly received lower radiation doses than therapeutic purposes. Long-term mortality from CVD has been investigated among many workers who were exposed; however information of individual doses was not available. The radiation doses to radiobiologists were about 1 Gy per year in early 1900 but after radiological protection guidelines were published it declined to 0.05Gy and 0.005Gy in 1950 and 1990 respectively (McGale and Darby, 2008). The mortality from cancer and heart diseases for early radiobiologists was found to be higher than in the general population (reviwed by McGale and Darby, 2008; Smith and Doll, 1981). However, the number of epidemiological studies performed on low dose radiation exposure is limited and data are conflicting.

The US radiology technologists' study has evaluated mortality from heart disease in relation to low dose radiation exposure in 90,284 individuals (received mean cardiac doses of 0-0.5 Gy). They found that the risk of circulatory system diseases increased significantly among those

who worked before 1950 compared with those after 1960 (Hauptmann *et al.*, 2003). The data from the early radiologists in the United States showed that there was an increased risk of CVD, which was contradictory with results from radiologists' cohort in the United Kingdom. This could be due to the fact that potentially confounding factors such as smoking have not been included in most of these studies (Berrington *et al.*, 2001; Hauptmann *et al.*, 2003).

The Canadian national Dose registry of radiation workers cohort (long-term follow up to 45 years of 397 individuals) study has demonstrated a strong positive association between low doses of radiation and increased risk of CVD mortality. The mean radiation dose to whole body was 8.6 mSv for men and 1.2 mSv for women from sources of exposures to X-rays, γ rays, β particles, and neutrons. However due to the potential bias (lack of adjustment for non-radiation risk factors and dosimetry uncertainties), the results should be interpreted with caution (Zielinski *et al.*, 2009).

The Three countries Study is one of the largest cohorts with follow up of about 22 years which shows an increasing trend (0.26 relative risk (RR) per Sievert) in CVD mortality following low dose radiation exposure after stratification for age, sex, socio-economic status which has reduced the potential confounding bias (Cardis *et al.*, 1995; McGale and Darby, 2008).

The Nuclear worker population can also be used to assess radiation effects at low doses. The mortality of nuclear industry workers was studied from an international (15-country) nuclear workers cohort (275,312 workers with information on socio-economic status with average radiation doses of 20.7 mSv). Data were pooled internationally together which resulted in the strength of the statistical power. The excess relative radiation doses per Sv after adjustment for socioeconomic status was estimated about 0.09 (95% CI -0.43 to 0.70). This study shows little association between excess risk of CVD and low dose radiation. However it also has limitations like many other studies and does not provide the same order of magnitude (radiation risk) as the atomic-bomb survivors' study does (ICRP , 2007; Vrijheid *et al.*, 2007). The elevated risk of CVD was also studies in the nuclear plants of Mayak Production

Association in the Urals region of Russia (data collected from 12,000 workers). These workers received a prolonged exposure from gamma radiation. After adjustment for non-radiation factors such as smoking, alcohol consumption and socioeconomic status (these information were available at the time), a significant increasing trend in the incidence of heart disease was observed (at above 1 Gy) (Azizova *et al*., 2010a; Azizova *et al*., 2010b; Bolotnikova *et al.*, 1994; ICRP, 2007). The excess relative risk (ERR) of CVD disease from some of the epidemiological studies are reviewed in the table **1.1,** in which heart received low and moderate doses of between 0-5 Gy (ICRP, 2007a; Little *et al*., 2010).

However, the positive risk of CVD in the above studies is not supported by other studies such as radiologists (Matanoski *et al.*, 1975) and radiobiologists in the UK (Berrington *et al.*, 2001). The results from these studies showed no evidence of excess CVD mortality induced by low dose radiation, in contrast with other studies that showed radiation elevated risk of heart disease as a result of exposure to low and moderate radiation doses (Hauptmann *et al.*, 2003; Hendry *et al.*, 2008; Ivanov *et al.*, 2006). Therefore the data from different studies for very low doses are inconclusive.

1.5.8 Limitation of the epidemiological studies

Non-cancer late effects of radiation on heart have been documented at doses below 5 Gy or 5 Sv among the atomic bomb survivors and in other studies as mentioned above. The analysis of Mayak and Japanese atomic-bomb survivor studies showed a linear dose-response curve for heart diseases which support the assumption of the increased risk of CVD following radiation exposure at low doses of < 0.5 Gy (Azizova *et al*., 2010a; Azizova *et al*., 2010b; Shimizu *et al*., 2010). These two studies were the only ones adjusted with the life style (smoking and drinking) and other risk factors associated with heart diseases.

Data	References	Average heart dose (range)	Number in cohorts (person, years, follow up	Excess relative risk (ERR/sv or Gy^{-1} (and 95% CI)
Japanese atomic bomb survivors	(Preston *et al*., 2003; Shimizu *et al*., 2010; Yamada *et al*., 2004)	0.15 Gy (0- 4 Gy)	86,572	ERR/Gy = 0.14 (0.06, 0.23)
USA radiology technologist	Hauptmann *et al*., 2003)	0.01 Gy (0-0.5 Gy)	90,284	RR= 1.00 (1950-1960+)
15-country nuclear workers (IARC)	Vrijheid *et al*., 2007	0.0207 (0- >0.5 Sv)	275,312	ERR/Sv = 0.09 (-0.42, 0.91)
Mayak Workers	(Bolotnikova *et al*., 1994; Azizova *et al*., 2010a, 2010b)	0.91 Gy male 0.65 Gy Females (0-5.92 Sv) External γ dose	12,000	ERR/Gy= 0.11 IHD, incidence ERR/Gy =0.07 mortality
Peptic Ulcer study	Carr *et al*., 2005	(1.6-3.9 Gy)	3,719	ERR/Gy= 0.10 (-.0.12, 0.33)

Table 1.1 Estimated positive ERRs of CVD after exposure to low/moderate radiation doses (below 5 Gy) from some of published epidemiological studies (based on Little *et al* (2010, 2012) and ICRP (2007a) publications).

However, other studies with showed no positive trend at doses below 5 Sv (McGale and Darby, 2008). There is a significant heterogeneity in other studies at low doses, which suggests that the assumption would be speculative, as they only provide no or partial adjustment/control for confounding risk factors. Therefor the existence of these potentially confounding factors could bias the results (Hauptmann *et al.*, 2003; Little *et al.*, 2008; Little *et al*., 2012). The radiation doses have been estimated in both Gy and Sv, although this makes little difference when radiation exposure was at low LET, as in most of the studies (Little *et al.*, 2009).

1.6 Effect of radiotherapy in early and late damage on normal tissue

Radiation damage to normal tissue can be classified as: i) acute effects, which are observed during radiotherapy or several weeks after the treatment and ii) late effects, which happen months or years after exposure to radiation (Stone *et al.*, 2003). The mechanism of late radiation damage is still not clear. Furthermore, decreasing the radiation dose increases latency of radiation-induced damage (Brush *et al.*, 2007). Apoptosis, activation of pro-inflammatory and prothrombic responses and lymphocyte infiltration are some of the early radiation effects on normal tissue after exposure. Acute damages are deterministic effects that happen as a result of injury to the proliferating cells that received radiation. This also includes radiation burn, skin irritation, erythema, fatigue, nausea, diarrhoea, hair loss, hematopoietic damage and so on. These effects are developed above a certain threshold (of radiation) and within hours, days and weeks. The effects are dose dependent, with larger doses producing earlier and more damage (Brush *et al.*, 2007; Stone *et al.*, 2003).

Radiation-induced damage may take months to years to develop. Late effects of radiation are fibrosis, memory loss, damage to the vasculature, bowel, infertility, cardiovascular diseases and secondary cancer (Stone *et al.*, 2003). The sustained production of pro-inflammatory and profibrotic cytokines by radiation may contribute to development of radiation-induced fibrosis and massive fibrosis results in remodelling and failing of the tissue. Radiation-induced fibrosis can also damage microvessels and causes cardiac fibrosis in the long term (Dean *et al.*, 2005; Haydont *et al.*, 2005; Pohlers *et al.*, 2009; Vozenin-Brotons *et al.*, 2003). Patients who

received radiotherapy during their treatment may develop secondary cancer years later, depending on the area of body exposed. Cancer and genetic effects are stochastic health effects of late radiation injury without a dose threshold, the probability increases linearly with increasing radiation doses but the severity of the effects is not dose-dependent (Kamiya and Sasatani, 2012; Masse, 2000; Roth *et al.*, 1996).

1.6.1 Effects of radiation on vasculature of normal tissue

Multiple studies have reported that damage to blood vessels has an important role in both early and late pathogenesis of radiation-induced normal tissue damage (Fajardo and Stewart, 1970; Fajardo and Berthrong, 1988; Hoving *et al*., 2012; Seemann *et a*l., 2012; Stewart *et al*., 2013). Some of these studies are summarized here.

A study on mouse duodenal villi damage following radiation exposure of the abdomen at 10 Gy revealed that damage and alteration of their blood vessels resulted in injury to gastrointestinal tissue. They showed that there were early changes in capillaries of mouse duodenal villi such as vasodilatation (Abbas *et al.*, 1990). A study of radiation effects on vasculature of the rat spinal cord showed that the necrosis in the central nervous system (CNS) could be related to microvascular damage (Coderre *et al.*, 2006). Pulmonary injury, which manifests as pneumonitis and fibrosis, occurs following radiation exposure of the thorax (Gross, 1977). Functional damage to pulmonary microvasculature in rabbits, at a single dose of 30 Gy, was observed and found to play a key role in radiation-induced pulmonary injury (Orfanos *et al.*, 1994). Raicu *et al* (1993) studied direct effects of irradiation on endothelial cells using a micronucleus assay. Their study identified endothelial cell damage at the genetic level, following radiation exposure (Raicu *et al.*, 1993).

In summary, vascular damage is one of the most prominent effects of early and late radiation injury in normal tissues. Furthermore, endothelial cells, which form the inner luminal lining of blood vessels, are considered to be one of the most sensitive targets for radiation damage (Fajardo and Berthrong, 1988; Raicu *et al.*, 1993).

1.6.2 Radiation damage to the heart

Heart is one of the most radiosensitive organs, and radiation-induced CVD has been found to be the most common cause of death among those who received radiotherapy, especially for thoracic tumours. Different studies on pathogenesis of radiation-induced CVD revealed that damage to both large and small vessels are the most important events in radiation-induced damage to the heart. Moreover, this is mostly due to the radiosensitivity of endothelial cells (Fajardo and Berthrong, 1988; Stewart *et al*, 2013; Stewart *et al.*, 1995). Therefore, an understanding of the mechanism of vascular damage in the delayed pathogenesis of radiation-induced CVD is required in order to modify radiation treatment, thereby reducing the side effects of radiation especially on the heart and associated vessels. The mechanism of radiation injury to the heart is due to both microvascular and macrovascular damage.

1.7 Endothelial cells

The endothelium is the thin, flattened monolayer of endothelial cells (EC) that lines the entire vascular system (lymph vessels and blood vessels). Large blood vessels (veins and arteries) are composed of three distinct layers. The intima consists of a single layer of endothelial cells on a basement membrane that line the vessel lumen. The second layer is called the media, which mostly contains multiple plates of smooth muscle cells, and the outer layer is the adventitia that contains nerves, smaller nutrient blood vessels and loose connective tissue (Karamysheva, 2008; Levick, 2003). These three layers have been shown in Figure **1.2**. Smaller vessels such as capillaries only consist of an endothelial monolayer and basement membrane without any underlying smooth muscle cells (Karamysheva, 2008; Levick, 2003; Stewart *et al*., 2010).

The endothelium controls the passage of metabolites (eg. serotonin), proteins (eg. growth factors, coagulant and anti-coagulant proteins), lipid transporting particles (low density lioprotein (LDL)) and hormones between the lumen of the vessel and the surrounding tissue. Morover, ECs have the capacity to transport white blood cells in and out of the blood flow (Cines *et al.*, 1998; Gerhardt and Betsholtz, 2003).

The endothelium has both anti-coagulant and procoagulant properties. During an unperturbed state, ECs prevent platelet adhesion and clotting by facilitating anti-thrombotic functions. Thrombin is an important enzyme involved in coagulation and it activates several coagulation enzymes as well as platelets. ECs control the activity of thrombin via the expression of tissue factor pathway inhibitor (TFPI) and thrombomodulin which prevents the formation of thrombin. When the endothelium is perturbed by chemical factors or physical forces, it transforms into a procoagulant surface. Tissue factor (TF) is exposed on the cell surface. The von Willebrand factor (vWF) is then secreted, which is a povital procoagulant factor. Once TF is exposed to the plasma membrane, it binds to factor VII and initiates the coagulation cascade leading to prothrombin activation to thrombin and formation of fibrin (Cines *et al.*, 1998; Zhang *et al.*, 2010). ECs also take part in fibrinolysis (degradation of fibrin clot) by secreting plasminogen activators such as tissue-type plasminogen (t-PA) and urokinase-type plasminogen (u-PA) activators. Both t-PA and u-PA play roles in the conversion of plasminogen to active plasmin which leads to fibrin degradation (Wojta *et al.*, 1989a; Wojta *et al.*, 1989b).

Endothelial cells make numerous dynamic contributions to cardiovascular functions such as permeability, the control of vasomotor tone, blood cell trafficking and haemostatic balance. Endothelial cells also play a role in angiogenesis and inflammatory responses (Figure **1.3**). EC deregulation plays an important part in the development of vascular disorders such as thrombotic diseases, impaired wound healing and atherosclerosis (Karamysheva, 2008; Levick, 2003). Here the inflammatory and angiogenic activities of ECs as potential inducers of CVD by radiation are discussed in more depth.

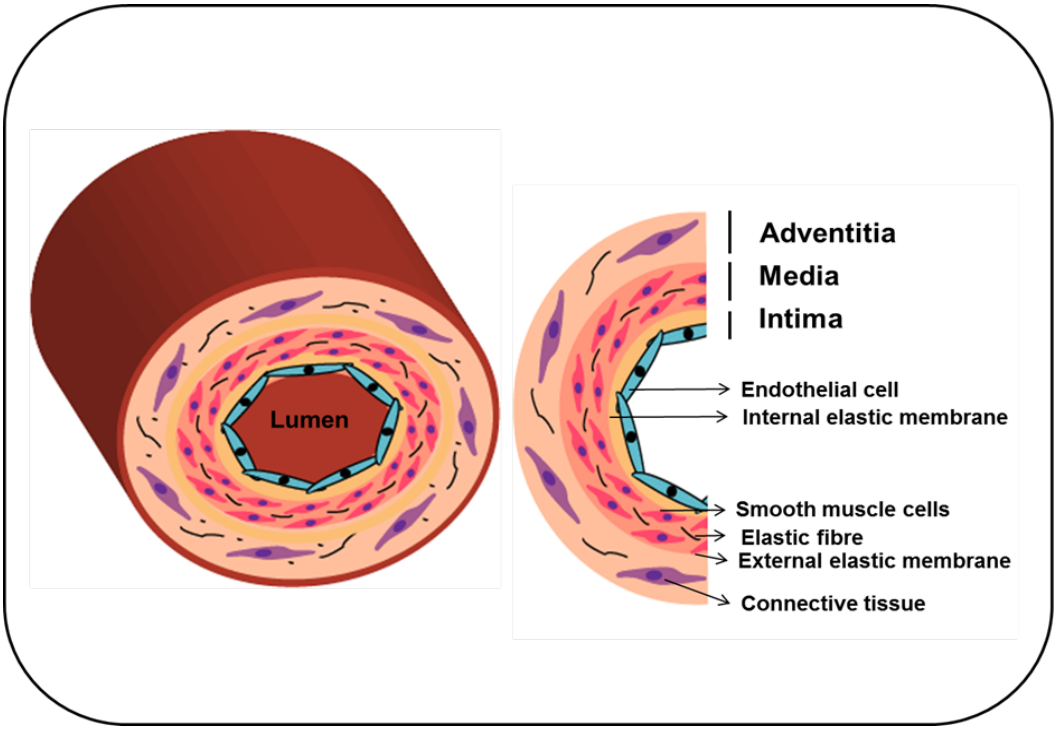

Figure 1.2 Image representing the structure of artery. The normal artery contains three layers. The first (inner) layer is intima, which comprises of endothelium that is in contact with blood. The middle layer is media, which is consisted of smooth muscle cells. Adventitia is the last (outer) layer, which contains nerves and microvessels.

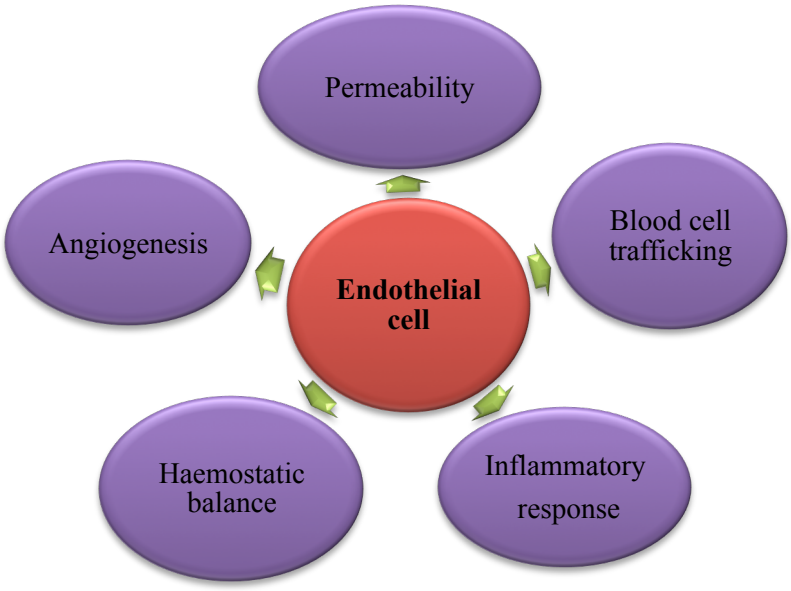

Figure 1.3 Image representing endothelial cell functions.

1.7.1 Endothelial cell activation during inflammation

A set of defensive responses to localised harmful stimuli such pathogens is called inflammation which is characterised by heat, redness, swelling, loss of function and leukocyte migration to the site of injury. The heat and redness are due to vasodilation, which is induced by many vasodilator mediators such as thrombin and cytokines. These mediators stimulate the endothelial cells to secrete the vasodilator nitric oxide (NO) (Hansson, 2005; Levick, 2003). Endothelial cells play an important part during inflammation. In response to immune surveillance as well as infection or tissue injury, ECs are activated by inflammatory stimuli and participate in inflammation by mediating trafficking of circulating white blood cells (including leukocytes and monocytes) and platelet into the tissue (Figure **1.4**) (Cines *et al.*, 1998; Zhang *et al.*, 2010). ECs stimulate inflammatory chemokines and cytokines such as tumour necrosis factor-α (TNF-α) (which is a central mediator of endothelial cell activation), interleukin-6 (IL-6) and inteleukin-8 (IL-8), which are mediators of inflammation and facilitate leukocyte movement towards the ECs (Ballermann, 1998; Cook-Mills and Deem, 2005; Zhang *et al.*, 2010). Endothelial cell then expresses adhesion molecules such as platelet-endothelial cell adhesion molecule-1 (PECAM-1), intercellular adhesion molecule-1 (ICAM-1) and vascular cell adhesion molecule-1 (VCAM-1), which provide scaffolding to the endothelium surface, which in turn regulates leukocyte adhesion and migration into the tissue at the site of inflammation (Ballermann, 1998; Cook-Mills and Deem, 2005; Zhang *et al.*, 2010). The uncontrolled platelet and leukocyte adhesion to the site of injury by ECs contributes to the thrombotic and inflammatory diseases (atherosclerosis) (Cines *et al.*, 1998). Endothelium from large and small blood vessels has functional and morphological heterogeneity as it expresses different markers (Lang *et al.*, 2003).

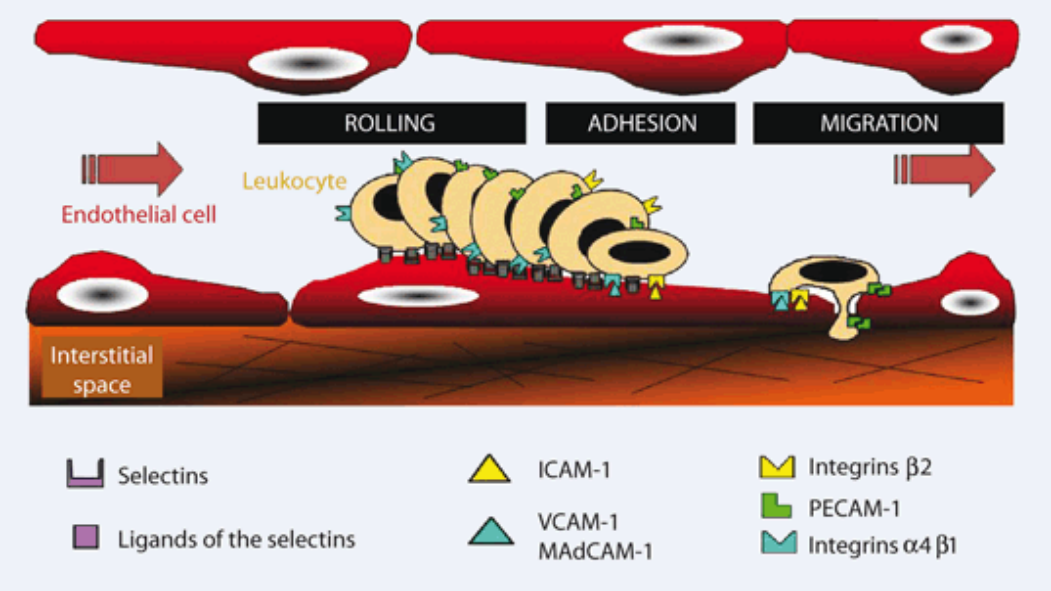

Figure 1.4 Diagram of recruitment of circulating leukocytes. The activated EC induces leukocyte movement towards the ECs by stimulating inflammatory chemokines and cytokines such as TNF-α, IL-6 and 8. The adhesion of leukocytes to the site of inflammation is facilities by adhesion molecules such as ICAM-1, VCAM-1and PECAM-1 that are expressed by ECs (Image from Arenas *et al.*, 2012).

During EC activation, its morphology and gene expression changes to generate chemokines, cytokines, adhesion molecules and pro-coagulant factors, following stimulation by infection, drugs or free radicals (radiation). However, the term "EC activation" is different from "EC injury" as morphological rearrangement is reversible and so they can return to the quiescent state without any cell loss. But if the alterations become uncontrolled resulting in EC dysfunction, it may lead to apoptosis, fibrosis, cells loss, increased permeability and haemorrhage. Therefore, uncontrolled and persistent activation of ECs could produce irreversible injury, which in turn results in the induction of pro-inflammatory and coagulant molecules, chemokines and cytokines as well as cell loss. Activation of endothelial cells has an important role in atherosclerosis, the immune response and thrombosis (Cockwell *et al.*, 1997; Zhang *et al.*, 2010).

1.7.1.1 Endothelial cells and Atherosclerosis

Atherosclerosis is a complex multifactorial syndrome affecting arterial blood vessels, which is characterised by lipid accumulation, occurring as a result of chronic inflammatory processes (Hansson, 2005; Sima *et al.*, 2009). Nowadays, atherosclerosis is one of the dominant health problems in western society. Murray *et al* predicted that atherosclerosis could become the biggest cause of death worldwide by 2020 (Andreassi, 2008; Murray and Lopez, 1997). According to epidemiological studies hyperlipidaemia, hypertension, aging, diabetes and smoking have been identified as the main risk factors in this disease (Sima *et al.*, 2009). Atherosclerotic lesions can cause stenosis or narrowing of the lumen of the vessels, which leads to reduction in oxygen and nutrition supply in the surrounding tissue. As lesions become more extensive, they can rupture and this can lead to activation of the coagulation cascade and thrombus formation. Ruptured plaques and thrombi can lead to sudden occlusion in arteries. For example, occlusion of the coronary artery in the heart can cause myocardial infarction (MI) and heart failure (Glass and Witztum, 2001).

Atherosclerosis develops from lipid accumulation especially cholesterol, which is essential for synthesis of steroid hormones, vitamins and membrane fluidity. Cholesterol is transported by

low-density lipoprotein (LDL) and taken up by high-density lipoprotein (HDL) and transported to the liver for excretion from the body (Ginsberg, 1998). There are a number of factors that can elevate levels of LDL. The deficiency in LDL receptor or low level of HDL in Tangier disease and other genetic disorders, can lead to the accumulation of LDL in peripheral tissue (Brooks-Wilson *et al.*, 1999; Glass and Witztum, 2001). Endothelial cells are involved in all stages of atherosclerosis and changes in their properties are a key early event in the developing disease (Hansson, 2005). The accumulated LDL in the vascular wall undergoes modifications such as oxidation which stimulates EC activation and endothelial dysfunction (Lusis, 2000). Once ECs become activated because of the accumulation of modified LDL they secrete various cytokines and chemokines such as interleukins, TNF-α and MCP-1. Activated endothelial cells also express adhesion molecules such as VCAM-1, ICAM-1 and E and P selectins (Rader and Dugi, 2000; Sima *et al.*, 2009). The activated endothelial cells and oxidized LDL cause the recruitment of monocytes/leukocytes and subsequently the adhesion of these inflammatory cells at vascular endothelium by endothelial VCAM-1, ICAM-1 and integrin. LDL diffuses through endothelial cell junctions into the sub-endothelial space of the vascular wall (intima). Then, migration of monocytes into the intima occurs which is mediated by modified LDL and MCP-1. Monocytes can differentiate into macrophages (stimulated by macrophage colony-stimulating factor) and produce inflammatory mediators (Linton and Fazio, 2003). LDL is taken up and degraded by macrophages, which express special receptors; mostly low-density lipoprotein receptor (LDLr) and scavenger receptor class A (SR-A). The storage of LDL leads to transformation of macrophages into foam cells. The accumulation of foam cells in the vascular wall leads to a characteristic fatty streak. The fatty streak is an initial lesion in atherosclerosis which subsequently develop into more advanced lesions known as plaques (Glass and Witztum, 2001; Stizinger, 2007).

During lesion progression, T lymphocytes join macrophages in the intima and result in cytokine and growth factor secretion that can promote the migration of smooth muscle cells (SMC) from the media. SMCs migrate into intima, proliferate and produce extracellular

matrix, take up LDL and subsequently turn to foam cells by cholesterol accumulation. Programmed cell death leads to formation of a necrotic core within the intima which consists of macrophage and SMCs and is covered by a fibrous cap (Cullen *et al.*, 2005). Ultimately, macrophages can inhibit matrix synthesis by releasing matrix metalloproteinase and induce smooth muscle cell apoptosis within the intima lesion. Therefore the reduction of matrix (collagen) and altered extracellular matrix metabolism can affect the thickness of the fibrous cap and render the plaque weak and susceptible to rupture (Libby, 2009). Following the rapture of the plaque, the contents of the lipid core are exposed to blood which leads to the initiation of coagulation, recruitment of platelets and thrombus formation. As mentioned above, the formation of thrombus or clot in blood results in ischemia due to the narrowing of the vessel lumen, and finally it can cause MI and stroke (Glass and Witztum, 2001). Figure **1.5** represents the morphology of a normal artery compared to a narrowed artery by atherosclerosis.

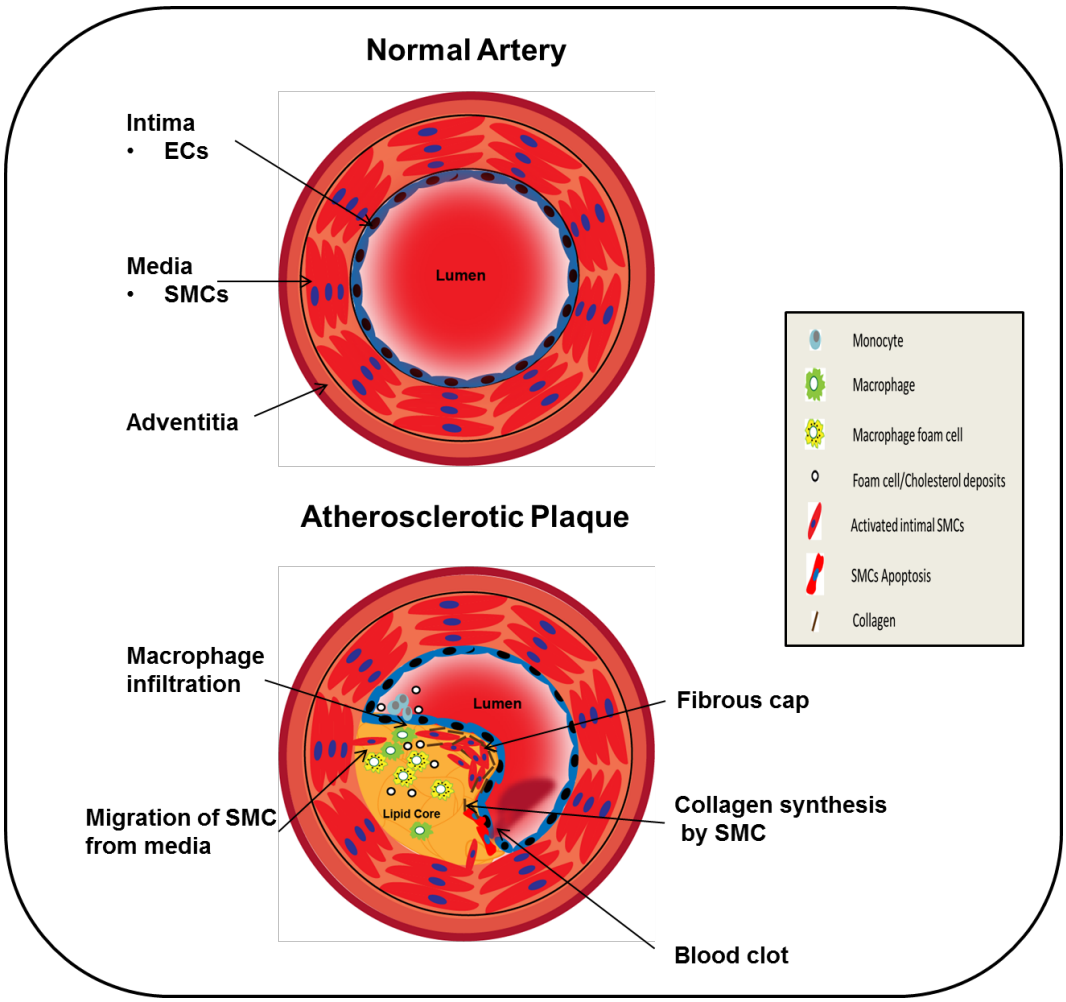

Figure 1.5 Morphology of a normal artery and an atherosclerotic artery. The first image represents a normal artery, which contains three layers: Intima, media and adventitia. The second image shows a narrowed artery by atherosclerosis. The initial steps of atherosclerosis include adhesion of monocytes, their transmigration into intima (subendothelial space) and transformation into macrophages which uptake lipids and form fatty streaks within the intima. The progression of lesion happens when SMCs migrate from media to the intima, then proliferate and produce collagen. In the advanced lesion, programmed cell death (in macrophages and SMCs) leads to formation of a necrotic core and is covered by a fibrous cap.

1.8 Mechanisms of radiation damage to the heart

1.8.1 Mechanism of endothelial radiation damage at molecular/cellular level

The first driving events leading to both micro- and macrovascular injuries are alteration of endothelial cells and pro-inflammatory responses (Schultz-Hector and Trott, 2007). EC damage and excessive cell death caused by high doses of radiation are thought to contribute to CVD. Moreover, it has been reported from both human and animal studies that radiation increased the risk of ischemic heart disease and myocardial infarction at moderate doses (≥ 2 – 5 Gy) by inducing persistent changes in capillaries and ECs. Radiation-induce CVD results from damage to both heart microvasculature and microvasculature (Schultz-Hector and Trott, 2007; Stewart et al, 2013).

Endothelial injury is one of the earliest features of atherosclerosis that promotes inflammatory cell migration. Inflammation has been proven to participate in the development of cardiovascular disease especially atherosclerosis (reviewed by Little *et al.*, 2008). An elevated level of systemic inflammation has been reported in many studies showing radiation-induced damage to the heart (Stewart *et al.*, 2006; Hoving *et al.*, 2008). There are experimental (animal and *in vitro* studies) evidence of inflammatory changes in ECs after radiation exposure at doses of ≥ 1 Gy (reviewed by Little *et al.*, 2008).

According to Hallahan *et al*, the expression of cell adhesion molecules such as E-selectin (at 1 Gy) and ICAM-l (at 5 Gy) increased following radiation (X-ray) in a dose- and time-dependent manner in human umbilical vein endothelial cells (HUVECs) (Hallahan *et al.*, 1995; Hallahan *et al.*, 1996). The levels of other cytokine-inducible adhesion molecules (P-selectin or VCAM-1) were unaffected. Activated NFκB was shown to regulate the expression of E-selectin following radiation. E-selectin expression at low doses of 0.5 Gy was regulated through binding of NFκB to promoter regions of the E-selectin gene (Hallahan *et al.*, 1995; Hallahan *et al.*, 1996; Little *et al.*, 2008).

The up-regulation of ICAM-1 and VCAM-1 was shown to occur in human dermal microvascular endothelial cells (HDMECs) at doses of 2.5 Gy and 5 Gy respectively (Quarmby *et al.*, 2000). Irradiation of transformed human bone marrow endothelial cells at doses of 2. 5 -10 Gy (^{60}Co γ rays) caused EC damage and increased production of cytokines such as IL-8, IL-6, IL-11, MIP-1 alpha and G-CSF, GM-CSF as well as ICAM-1 and vWF. However the levels of some other cytokines such as TNF-alpha and LIF did not change (Gaugler *et al.*, 1998).

In the Hallahan and Virudachalam study, C3H mice were treated with thoracic radiation at 2 Gy (X-rays). The results showed an increased ICAM-1, E-selectin and P-selectin expression in the pulmonary endothelium. E-selectin expression was induced more in the endothelium of large vessels whereas ICAM-l was expressed more in the pulmonary capillary endothelium (Hallahan and Virudachalam, 1997). Another *in vivo* animal study (using mice) also observed an increase in inflammatory cytokines and adhesion molecules as well as increased permeability in mice vessels (Tribble *et al.*, 1999).

Anti-inflammatory effects of low to medium radiation doses, ranging between 0.1-1 Gy have been demonstrated in some *in vitro* and *in vivo* experimental studies and clinical studies (reviewed by Arenas *et al.*, 2012). Radiation at lower doses induced an anti-inflammatory response with inhibition of leukocyte recruitment (maximal at 0.3-0.7 Gy), decreased production of adhesion molecules (P-, L-, E-selectins, ICAM, VCAM), increased expression of anti-inflammatory cytokines such as IL-10, TGF-β_1, induction of ECs apoptosis and increased activation of NF-κB (reviewed by Little *et al.*, 2008). This was followed by decreased iNOS production, which resulted in a decrease in ROS and NO. This anti-inflammatory effect could be due to the dose-dependent modulation of different inflammatory pathways such as the inducible NO synthase pathway by low dose radiation (Hildebrandt *et al.*, 1998; Little *et al.*, 2008; reviewed by Arenas *et al.*, 2012). The anti-inflammatory effect of low dose radiation could have inhibitory effects on the development of atherosclerotic lesions

in large arteries since they are initiated with sustained increased in inflammatory responses (Stewart *et al.*, 2013).

The up-regulation of cell adhesion molecules, inflammatory cytokines (IL6, TNF-α) and chemokines at doses > 0.5 Gy has been observed in studies of Japanese's atomic bomb survivors. These indicate acute radiation damage. Radiation induces killing of ECs and other heart cells. However in occupational doses where people are exposed to very low doses of about 0.5 mSv or less, the radiation is unlikely to play a part in killing cells as ECs have the ability to regenerate and compensate for the small cell number reduction caused by radiation (Hayashi *et al.*, 2005; Little *et al.*, 2008).

DNA damage, general somatic mutations and chromosome aberrations have been linked to increased levels of CVD. The elevated formation of reactive oxygen species (ROS), which contribute to the DNA damage has also been observed during inflammation (Little *et al.*, 2008; Mercer *et al.*, 2007). Radiation is one of the risk factors of endothelial dysfunction in atherosclerosis, which functions through ROS and oxidant stress and production of radicals that oxidise LDL. A more complex atherosclerotic lesion is produced following persistent endothelial dysfunction and apoptosis by radiation. EC death and apoptosis, as well as p53 (which is a marker of DNA damage) expression have been observed in atherosclerotic lesions. Increased ROS formation contributes to DNA damage in cardiovascular disease (Little *et al.*, 2008; Mercer *et al.*, 2007).

Apoptosis is important to maintain homeostasis and if apoptotic cells are not cleared by phagocytes, they undergo necrosis and contribute to disease pathogenesis. Radiation induces apoptosis at doses of between 2 and 10 Gy in ECs (mostly in microvasculature) which leads to the induction of pro-inflammatory signals, chemokine synthesis as well as leukocyte adhesion following interaction of healthy ECs with apoptotic and necrotic ECs (Kirsch *et al.*, 2007; Langley *et al.*, 1997;).

1.8.2 Mechanism of radiation damage in the heart microvasculature

Damage to myocardium primarily results from injury to microvessels that lead to pro-inflammatory and thrombotic changes, capillary loss and subsequently ischemia, focal fibrosis and myocardial degeneration (Stewart *et al*., 2013). Based on many experimental studies the congestive heart, arrhythmias and rheumatic heart disease are delay effects of radiation on heart due to microvascular injury that contributes to myocardial cell death and pathogenesis of radiation-induced heart disease (Fajardo, 1989; Fajardo, 1999; Schultz-Hector and Trott, 2007; Stewart *et al*., 2013). This result has also been supported by clinical studies showing patches of diffuse fibrosis and myocardial degeneration in myocardium of left and right ventricles of heart after radiation exposure (Marks *et al*, 2005; Stewart *et al*, 2010).

For many years, radiation damage to heart microcirculation has been reported. Fajardo and Stewart's study on New Zealand white rabbits showed that damage, especially in small vessels within the myocardium, developed in 94% of the animals after about 70 days following radiation exposure (1970). The severity of damage was shown to be dose-dependent. They reported that there was a silent phase during which ECs went through some changes and this eventually led to myocardial damage (Fajardo and Stewart, 1970). Another study of Fajardo and colleagues suggested that fibrosis of the myocardium (in New Zealand white rabbits) occurred due to EC damage of the myocardial capillaries (Fajardo and Stewart, 1972). As the heart cardiomyocyte is dependent on the function of EC and capillary blood vessels, it can be assumed that injury to EC function by irradiation could result in myocardial degeneration and fibrosis. Therefore, ECs of microvessels, which are actively proliferating radiosensitive cells, were demonstrated to be main radiation targets and early morphological changes in EC could trigger many other mechanisms which eventually can result in congestive heart failure (Fajardo and Stewart, 1970; Schultz-Hector and Balz, 1994; Stewart *et al.*, 1995).

Changes in ECs due to radiation exposure have been reported to be associated with important physiological alterations. EC injury is followed by increased permeability, EC swelling and enlargement, detachment of EC from basement membrane, exposure of subendothelium and

platelet aggregation. Furthermore, damage to ECs also induced pro-inflammatory and pro-coagulant responses following increased expression of adhesion molecules (ICAM, VCAM), cytokines (IL-6), TF, vWF and plasminogen activator inhibitor-1 (PAI-1) (Fajard, 1989; reveiwed by Schultz-Hector and Trott, 2007; Stewart *et al.*, 1995). When damage and loss of ECs following apoptosis and necrosis exceed a critical level by radiation, damage to ECs preceded myocardial damage (Fajardo and Stewart, 1970; Schultz-Hector, 1993).

Moreover, endothelial alkaline phosphatase (ALP) is found in the plasma membrane of ECs and has a functional activity such as regulation of EC proliferation and control of blood flow. A study by Lauk showed that there was a loss of the ALP enzyme in myocardial capillaries of irradiated hearts of Wistar and Sprague-Dawley rats (10-25 Gy). Focal loss of ALP activity was evident after 40 weeks exposure (Lauk, 1987). The same result was observed, in the Schultz-Hector and Balz study (Schultz-Hector and Balz, 1994). They showed that cardiomyocyte injury in both strains of rats occurred as a result of a decrease in ALP activity following 20 Gy radiation exposure. According to their study, the ALP loss was not related to EC death and was caused by radiation-induced ultrastructure alteration in EC. They suggested that ALP loss could be associated with signs of EC activation, swelling, enlargement and lymphocyte adherence Additionally an enzyme-negative area in myocardium was observed and it was shown that myocardial degeneration developed in this area (Schultz-Hector, 1993; Schultz-Hector and Balz, 1994).

The mechanism of damage to myocardium therefore is as follow: early EC alteration results in pro-inflammatory responses which, leads to adhesion and transmigration of monocyte and its transformation to activated macrophages in capillary ECs. This is then followed by thrombus formation, obstruction of microvessels and causes reduction in capillary density (Stewart *et al*., 2010; Stewart *et al*., 2013). Additionally loss of ALP happens which has been observed at doses of $\geq$ 2 Gy in the mouse heart (Seemann *et al.*, 2012). Following injury to capillary EC by radiation, proliferation may occur in remaining capillary ECs to compensate in response to the damage; however this is not sufficient enough to maintain proper microvascular function

(Fajardo and Berthrong, 1988; Fajardo, 1989; Stewart *et al.*, 1995; Steawrt *et al*., 2010). All of these EC changes in turn result in narrowing, thrombosis and vascular occlusion, which are subsequently followed by damage and loss of myocardial microvessels. The progressive decrease in capillary density causes ischemia because of the lack of oxygen and nutrient supply and this eventually leads to myocardial cell death and fibrosis (Fajardo, 1989; Lauk, 1987; Stewart *et al.*, 1995). A summary of radiation effects in heart microvasculature is shown in Figure **1.6**.

Experimental studies have shown damage to microvessels by radiation is the main contributor to myocardial fibrosis and heart failure. There is a silent phase during which ECs go through some changes and this eventually led to myocardial damage (Stewart *et al.*, 2013). Myocardial degeneration coincides with the first sign of reduced heart function have been observed 10-20 weeks after radiation in rats (Schultz-Hector, 1993). In spite of increasing focal myocardial degeneration and fibrosis, further decreased in cardiac function appear shortly before the onset of congestive heart failure, which is fatal (Stewart *et al.*, 2010; Stewart *et al.*, 2013).

The severity of radiation damage to heart microvasculature has been shown to be dose-dependent. In the case of lower doses the onset of radiation damage in the heart is delayed. Different studies showed that radiation increases inflammatory resonance at doses ≥ 1 Gy and also based on the recent study radiation causes microcirculation changes at doses of ≥ 2 Gy in the mouse heart (Schultz-Hector and Trott, 2007; Seemann *et a l.*, 2012). This suggests that exposure to low dose radiation cause functional damage in heart microcirculation, which can cause late radiation-induced heart disease (Fajardo and Stewart, 1970; Lauk, 1987).

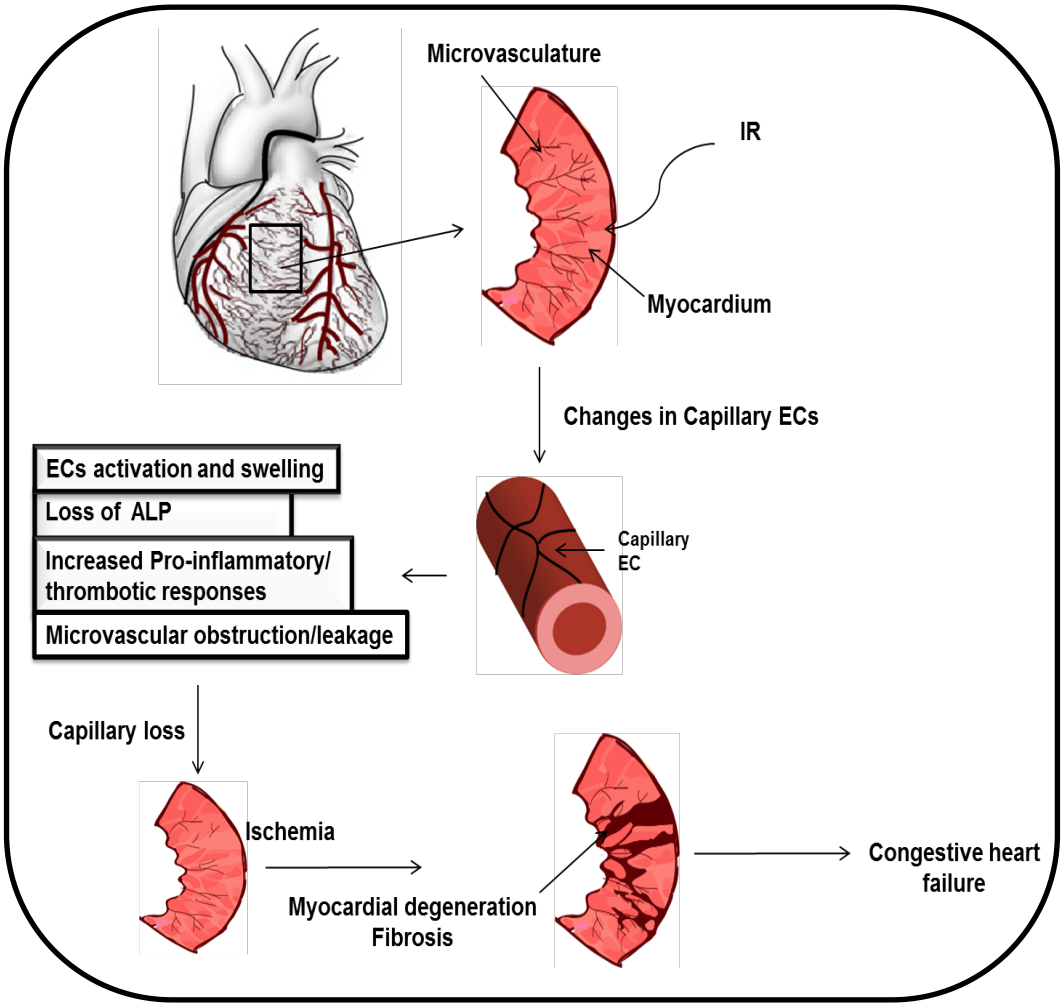

Figure 1.6 A summary of radiation effects in heart microvasculature. Radiation causes moderate and persistent reduction in capillary density, which may result in tissue damage at later times. Initially radiation induces alteration in capillary EC functions that subsequently results in EC loss, EC swelling, pro-inflammatory changes and loss of ALP. These changes are followed by vessel occlusion, reduced capillary density and tissue ischemia, which eventually lead to focal fibrosis and congestive heart failure.

1.8.3 Mechanisms of radiation damage to large blood vessels

Injury to large vessels is different from small vessels and is less common. As ECs of large arteries have strong vascular walls (three layers) and a large lumen, they are less affected by radiation compared to microvascular ECs (one layer) (Fajardo, 1999). However, the rupture of large arteries, narrowing of the lumen and thrombosis have been reported to be results of radiation damage. The accumulation of foam cells, collagen and fibrin deposition in exposed large arteries leads to the formation of plaque, followed by narrowing of the lumen and ischemia. It has been suggested that radiation, like other factors such as smoking, hyperlipidaemia and hypertension can predispose large arteries to the development of atherosclerosis (Patel *et al.*, 2006; Zidar *et al.*, 1997). There are two major CVD resulting from damage to large vessels: carotid artery disease (cause stroke) and coronary artery atherosclerosis, which is associated with myocardial infarct (Stewart *et al.*, 2013).

A study by Stewart and colleagues on $APOE^{-/-}$ mice that received 14 Gy dose showed that radiation could accelerate the risk of atherosclerotic plaque formation (Stewart *et al.*, 2006). $APOE^{-/-}$ mice are suitable animal models since they lack low-density lipoprotein receptor and, have elevated levels of plasma cholesterol. Therefore this animal could develop atherosclerosis with age unlike the wild-type (Zhang *et al*., 1992). In Stewart study it was noted that quality of the plaque, which is formed after radiation exposure in those animals, is influenced by radiation (Stewart *et al.*, 2006).

Changes in EC lining the large arteries play an important role in the development of atherosclerosis. It was reported that radiation-induced early EC changes and dysfunction resulted in increased permeability and production of inflammatory adhesion molecules and cytokines (E-selectin, ICAM1 and VCAM1) at doses of ≥ 2 Gy as well as induction of vWF in irradiated ECs. Additionally radiation decreased the production of anticoagulant thrombomodulin (Hoving *et al*., 2012; Stewart *et al.*, 2006; Stewart *et al*., 2013). These early changes caused recruitment of monocyte (via MCP-1) and their attachment and transmigration into the subendothelial space. After monocytes transform into activated macrophages, they

take up lipids and LDL and form fatty streak in intima, initiating early atherosclerotic lesion (Hoving *et al.*, 2008; Hildebrandt *et al*., 2002; Stewart *et al*., 2006; Stewart *et al*., 2013).

Another study on APOE$^{-/-}$ mice by Hoving *et al* using single dose (14 Gy) and fractionated doses (20x2 Gy), confirmed the previous results that radiation exposure predisposes large vessels to develop inflammatory atherosclerotic plaque (Hoving *et al.*, 2008). Later, it was found out that radiation at doses of ≥ 8 Gy in combination with elevated cholesterol levels in hypercholesterolaemic animals enhanced the atherosclerotic lesions formation and increased their numbers and sizes (Hoving *et al*., 2012). Moreover it was shown that radiation predisposed large arteries to the development macrophage-rich, unstable lesions with thrombotic phenotype rather than the collagenous stable atherosclerotic lesions. These lesions are more likely to rapture and cause heart attack (Hoving *et al.*, 2008; Stewart *et al*., 2013; Yu *et al*., 2011). Furthermore, in studies by Vos J *et al* (1983) and Cottin et al (2001), similar results were observed in irradiated rabbits (5, 10 and 15 Gy). The irradiated plaques had a macrophage rich and lipid filled phenotype compared to non-irradiated lesions (Cottin *et al.*, 2001; Vos *et al.*, 1983). Therefore it was proposed that the damage and local changes (e.g. increased inflammatory EC cells) to endothelium by radiation could accelerate atherosclerosis, rendering the atherosclerotic plaques more vulnerable and prone to rapture (Fajardo, 1989; Stewart *et al.*, 2006).

1.8.4 Mechanism of radiation damage to heart after exposure to low dose radiation

Based on the published studies, radiation is more likely to cause acceleration of atherosclerosis and myocardial infarct following exposure to higher doses of radiation (≥ 8 Gy) (Hoving *et al.*, 2008; Hoving *et al.,* 2012; Yu *et al*., 2011). There is an increase in inflammatory responses following radiation exposure at medium and high doses (> 1 Gy) (reviewed in Schultz-Hector and Trott, 2007; Stewart *et al.*, 2013). The inflammatory responses decrease at doses < 1 Gy and this resulted in inhibition of leukocyte adhesion to ECs *in vitro* and *in vivo* models (Arenas *et al*., 2006; Hildbrandt *et al.*, 2002). A study by Michel *et al* reported that the whole body irradiation of APOE$^{-/-}$ mice at doses of < 0.5 Gy is associated with reduction in size and

number of atherosclerotic plaque (2011). No evidence of radiation-induced coronary atherosclerosis has been reported at doses < 2 Gy yet. The increased inflammatory and cholesterol levels could only be associated with the increased risk of heart disease (Stewart *et al.*, 2013).

Microvascular changes at lower dose (≥ 2 Gy) were reposted to cause capillary loss, myocardial ischemia and fibrosis, which eventually contributed to myocardial degeneration and heart failure. Based on the analysis of risk of heart disease at lower doses, the incidence of some CVD such as congestive heart failure and rheumatic heart disease, which are caused from damage to microvessels, is found to be increased (Stewart *et al*., 2013). Radiation-induced microvascular injury at doses < 0.5 Gy needs to be studied since this could potentially participate in pathogenesis of radiation-induced CVD at lower doses which manifests years later.

Although low doses of radiation may not lead to significant levels of apoptosis and cell loss, mutation and genetic changes might result in mutated viable cells that could possibly lead to long-term damage. An increase in somatic mutation at very low radiation doses could explain the association of radiation with CVD developing a long time after exposure (Mahmoudi *et al.*, 2006; Mercer *et al.*, 2007). Indeed there is evidence of persistent genetic instability by radiation at doses of ≤ 1 Gy. This effect could be involved in mechanism of radiation damage at low doses and the formation of atherosclerotic plaques and may persist for many years after exposure (Andreassi and Botto, 2003). Therefore, DNA damage and somatic mutation caused by radiation play a role in the aetiology of heart disease at low doses (≤ 0.5 Gy) (Schultz-Hector and Trott, 2007).

Radiation-induced CVD is a multifactorial process (Schultz-Hector and Trott, 2007). The mechanism of radiation damage depends on dose and dose rate (unlike other CVD existing risk factors). Doses of > 1 Gy could induce more inflammatory, initial cell killing, apoptosis and tissue effects. Whereas at low doses ≤ 0.5 Gy the mechanism of radiation actions is different

(anti-inflammatory effects), and it could be that somatic mutation damage induces genetic lesions. More studies need to be performed on low radiation doses to elucidate the effect of radiation on environmental and occupational exposures, which proceed to CVD (Little *et al.*, 2008). One obstacle in designing study to investigate the mechanism of low doses is that development of heart diseases occurs many years after exposure and this can not be followed in *in vitro* and animal studies.

1.9 Angiogenesis and the role of endothelial cells during angiogenesis

The lymphatic and blood vascular system penetrates every tissue and organ in order to supply cells with oxygen and nutrients, providing for fluids circulation and various signaling molecules. The emergence of the blood vascular system is one of the earliest events during embryogenesis and is called vasculogenesis. This involves vascular cells differentiating from undifferentiated precursors and forming the initial vascular network. The term angiogenesis is referred to the formation of new blood vessels from pre-existing ones. Angiogenesis is required for many pathological and physiological conditions, including embryonic development, tissue growth, tissue repair, wound healing, tumour growth and tissue regeneration (Goodwin, 2007; reviewed by Karamysheva, 2008).

A variety of events are involved during angiogenesis including activation of endothelial cells, degradation of both the endothelial basement membrane and surrounding ECM, endothelial proliferation and migration, followed by the assembly of endothelial cells into tubular structures with lumens. Finally, construction of the mural cell layer of the vessel wall, which consists of smooth muscle cells and pericytes occurs (Figure **1.7**). A balance between pro- and anti-angiogenic agents regulate the whole process of angiogenesis including many pro-angiogenic growth factors such as vascular endothelial growth factor (VEGF), acidic and basic fibroblast growth factor (aFGF, bFGF), angiopoietin, platelet-derived growth factor (PDGF) and epidermal growth factor (EGF) (Goodwin, 2007; Lamalice *et al.*, 2007; reviwed by Karamysheva, 2008).

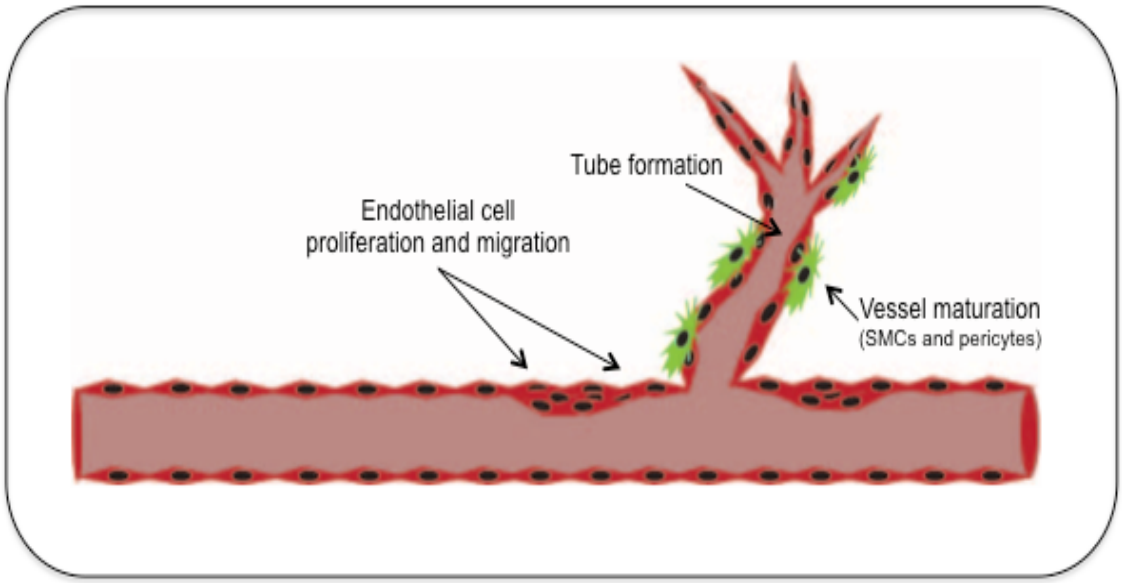

Figure 1.7 Schematic images of angiogenesis process. Angiogenesis is the formation of new blood vessels from pre-existing ones. Angiogenesis is a multistep process. Activated ECs migrate, proliferate, and re-organise into tubular structures with lumens. The recruitment of pericytes and SMCs to the vessel wall results in vessel maturation and stabilisation.

VEGF is the most well studied and potent growth factor, which plays a crucial role in regulating endothelial cell function. VEGF regulates proliferation and migration of endothelial cells during angiogenesis. Thus endothelial cells are the primary and most important constituents of vessels and have many essential functions during angiogenesis, including matrix degradation, migration, proliferation and morphogenesis (Goodwin, 2007; Lamalice *et al.*, 2007; van Hinsbergh and Koolwijk, 2008).

There are some diseases related to angiogenesis in which the new blood vessels form and grow insufficiently or excessively. The generation of blood vessels are not only required for embryonic development but is also known to be involved in the pathogenesis of some diseases such as many cancers, rheumatoid arthritis and diabetic retinopathy. In these conditions, there is excessive formation of blood vessels, which can in turn damage normal tissues (Karagiannis and Popel, 2008). Angiogenesis is triggered during tumours growth and expansion. The induction of angiogenesis in cancer cells has been shown in many humans and animals models (Folkman, 1995; Khurana *et al.*, 2005). Anti-angiogenic therapy has become an interesting and widely used approach. Avastin is an anti-angiogenic drug (antibody specific for VEGF) used in the treatment of some cancers (e.g. kidney, lung and ovarian cancers) and has been approved by the Federal Drug Administration (FDA) (Khurana *et al.*, 2005).

1.9.1 Role of angiogenesis in cardiovascular disease

The coronary artery disease can be used as an example of insufficient angiogenesis. Left ventricular remodelling, dilation, myocyte hypertrophy and contractile dysfunction are some of the characteristic of MI. Infarct size is one major factor in ventricular remodelling. Myocyte loss happens as a result of infarction, which in turn causes ventricular dysfunction and myocyte hypertrophy. After the damage or blockage of blood vessels in coronary artery disease, there is insufficient oxygen and nutrient supply to cells like myocytes and this leads to tissue cell death. The angiogenesis process can re-vascularise the damaged tissue helping the deprived heart muscles regain sufficient blood flow (Maulik, 2004; Simons and Ware, 2003; Ucuzian and Greisler, 2007).

Therefore there is a need for angiogenesis after injury to the heart and coronary artery in order to repair the tissue damage to enable cardiac regeneration (Al Sabti, 2007). Therapeutic angiogenesis has proven to be a promising method for treatment of patients with CVD who are not responding well to conventional therapies (Al Sabti, 2007). Mechanical influences such as shear stress, chemical influences including hypoxia and NO production as well as molecular influences such as inflammation and angiogenic growth factors (e.g. VEGF, FGF and angiopoietin) are major angiogenesis triggering factors. Moreover, tissue ischemia and injury are factors stimulating angiogenesis and neovascularisation (Al Sabti, 2007). A variety of angiogenic therapies involving genes, proteins and cells are being investigated in patients with coronary heart diseases and myocardial infarction to stimulate angiogenesis thereby increasing perfusion of ischemic heart areas that are unable to re-vascularise (Chachques *et al.*, 2004).

1.9.1.1 Effects of radiation in angiogenesis and wound healing

As mentioned before, radiotherapy also affects normal tissues surrounding the tumour leading to acute and long-term side effects. Moreover radiation induces EC changes and apoptosis followed by persistent decrease in capillary density. It has been observed in various studies that exposure of the vasculature to radiation results in inhibition of angiogenesis. Impaired angiogenesis and EC dysfunction could contribute to radiation-induced late tissue damage including tissue fibrosis and perturbed wound healing (Dormand *et al.*, 2005; Imaizumi *et al.*, 2010; Park *et al.*, 2012). Impaired wound healing can be frequently observed in irradiated tissues. However the underlying molecular and cellular mechanisms including cytokines and growth factor interactions still needed to be studied in more detail (Haubner *et al.*, 2012). Cardiac regeneration can occur after injury to the heart and this regeneration is dependent on angiogenesis, which plays a role in tissue repair. Therefore, angiogenesis is as an important feature of the reparative response, which can be triggered by microvascular injury to the heart and mediate cardiac regeneration. Radiation may compromise Cardiac EC (CEC) angiogenic functions since ECs play an important role during angiogenesis. Therefore, any damage to

endothelial cells may result in insufficient vascularisation, which in turn contributes to the development of cardiac diseases (Ucuzian and Greisler, 2007).

1.10 Role of fibroblasts in angiogenesis and fibrosis

Fibroblasts, which are the most common cells of connective tissue, play a critical role in angiogenesis during wound healing and tissue repair, by synthesising extracellular matrix (ECM). The ECM plays a role in tissue morphogenesis and repair by providing a structural support and attachment for cells as well as being a reservoir for signaling molecules that modulate diverse processes including angiogenesis (Badylak, 2002; Tettamanti *et al.*, 2004). Fibroblasts secrete fibronectin, various collagens and heparan sulphate proteoglycans during the wound healing process (Chang *et al.*, 2004). In addition, fibroblasts secrete many growth factors including VEGF, PDGF, bFGF, TGF-β and connective tissue growth factor (CTGF), which play a crucial role in angiogenesis. During angiogenesis, ECs invade the surrounding ECM to form capillary networks in response to paracrine factors released by neighbouring cells including fibroblasts. Different studies showed that fibroblasts contribute to EC tubulogenesis (Berthod *et al.*, 2006; Newman *et al.*, 2011; Tettamanti *et al.*, 2004). In the Newman *et al* study, fibroblast-derived factors such as collagen I, TGF-β, pro-collagen C and insulin growth factor (IGF) were identified to induce an angiogenic phenotype. They also promoted EC sprouting and lumen formation in an *in vitro* model of angiogenesis in which ECs and fibroblasts were cultured together in a 3D fibrin matrix (Newman *et al.*, 2011). Additionally, it was observed that the conditioned medium (CM) from fibroblasts induced formation of capillary tubules by ECs (Montesano *et al.*, 1993).

Following damage to tissue, fibrosis may occur, resulting in the replacement of normal tissue with connective tissue. When the repair mechanism becomes uncontrolled, it causes substantial deposition of ECM components and results in scar and tissue dysfunction (Dean *et al.*, 2005; Pohlers *et al.*, 2009; Wynn, 2008). Fibrosis is one of the late effects of radiation on normal tissue after exposure and multiple studies have indicated the role of radiation-induced fibrosis (Brush *et al.*, 2007; Haydont *et al.*, 2007; Milliat *et al.*, 2006; Stone *et al.*, 2003;

Vozenin-Brotons *et al.*, 2003). The sustained production of pro-inflammatory and pro-fibrotic cytokines by radiation may contribute to development of radiation-induced fibrosis and significant fibrosis results in remodelling and failing of the tissue (Dean *et al.*, 2005; Pohlers *et al.*, 2009).

During the normal wound healing process, fibroblasts are activated; they differentiate into myofibroblasts and become a primary producer of ECM components. However, excessive and prolonged fibroblast activation can lead to fibrosis. Fibroblasts are one of the key cellular mediators of fibrosis, which when activated after radiation exposure result in excessive deposition of collagen and ECM. It has been observed that myofibroblasts from irradiated patients' mucosa show a higher density of stress fibres and produce elevated levels of CTGF (Haydont *et al.*, 2007). Radiation-induced fibrosis can also damage microvessels, causing cardiac fibrosis in the long term (Dean *et al.*, 2005; Haydont *et al.*, 2005; Pohlers *et al.*, 2009; Vozenin-Brotons *et al.*, 2003). Fibrosis, which occurs as a result of delayed radiation-induced injury and causes persistent production of ECM by fibroblasts can be associated with impaired angiogenesis, uncontrolled wound healing and vascular remodelling (Wynn, 2008).

The interaction of fibroblasts with endothelial cell providing structural support and attachment sites is known to play a role in angiogenesis. Therefore, it is hypothesised that fibroblasts may have bystander effects on ECs and changes in vascular fibroblasts following irradiation may contribute to an imbalanced cross talk between fibroblasts and endothelial cells which indirectly results in impaired angiogenesis.

1.11 Role of TGF-β in angiogenesis, fibrosis and pathogenesis of CVD

TGF-β is a cytokine, which is involved in many biological activities and incorporates a large superfamily of receptors and ligands (33 different family members) including the bone morphogenic proteins (BMPs) and activin (Orlova *et al.*, 2011). TGF-β superfamily proteins regulate many cell functions such as cell proliferation, differentiation, and migration as well as normal and pathological wound healing process and angiogenesis. The TGF-β receptors

consist of type I and type II transmembrane serine/threonine kinase receptors, which are heterodimers. TGF-β signals via receptors and intracellular transcriptional effector proteins. The TGF-β ligand binds to the TGF-β Type II receptor (TβRII) which is then associated with type I receptor and results in the phosphorylation and activation of TβR1 receptors. Smad proteins are the intracellular effectors of TGF-β signaling, which regulate transcription in the nucleus following activation of receptors (Bakin *et al.*, 2002; Derynck and Zhang, 2003; Moustakas *et al.*, 2001). The type I receptors are divided into mainly Activin receptor-Like Kinase (ALK)-1 and 5 according to their ability to induce Smad activation. The ALK5 activation induces Smad2 and 3 phosphorylation and ALK1 activates Smads1 and 5. The activated Smads translocate to the nucleus after forming a heteromeric complex with the co-factor Smad 4, and participate in gene regulation. Smad complexes in the nucleus regulate gene expression, and after that are dissociated, dephosphorylated and turn into inactive forms, which are exported to the cytoplasm (Derynck and Zhang, 2003; Moustakas *et al.*, 2001; reviewed by Orlova *et al.*, 2011; Watabe *et al.*, 2003). TGF-β protein is secreted as a complex known as large latent complex form (LLC) comprised of latency associated protein (LAP), latent TGF-β binding protein (LTBP) and mature TGF-β (Annes *et al.*, 2003; Dancea *et al.*, 2009). Matrix metalloproteinases (MMPs 2-9), thrombospondin and β6 integrin are involved in activating TGF-β from the latent form (Ruiz-Ortega *et al.*, 2007).

TGF-β plays an important role in angiogenesis. TGF-β signaling during angiogenesis is concentration-dependent and at higher concentrations signaling is via ALK 5 which further induces Smad2/3 phosphorylation, promotes a quiescent EC phenotype and results in anti-angiogenic activity, including inhibition of EC proliferation and migration as well as and vascular permeability (Orlova *et al.*, 2011; Watabe *et al.*, 2003). However, TGF-β signaling via ALK1 is also a pro-angiogenic and promotes activation of ECs resulting in increased EC proliferation, migration and enhanced EC growth factor expression such as VEGF (reviewed by Orlova *et al.*, 2011; Shao *et al.*, 2009). Therefore TGF-β regulates both EC anti- and pro-angiogenic activities. While ALK1 and ALK5 receptors could show opposing responses, there

is also crosstalk between the two receptors. ALK5 is necessary for recruitment and maximal activation of ALK1. The crosstalk between ALK1 and ALK5 signaling offers a gentle TGF-β switch to fine-tune EC activities (Goumans *et al.*, 2009; Orlova *et al.*, 2011). Figure **1.8** shows the TGF-β signaling pathway through ALK1 and ALK5.

TGF-β is additionally one of the key mediators of fibrosis by causing over production of ECM components including collagen as well as increasing expression of fibrotic factors. It has been shown that TGF-β levels are increased following radiation and this contributes to fibrosis by continuous ECM production and persistent induction of fibrogenic phenotypes of cells (Haydont *et al.*, 2005; Haydont *et al.*, 2007; Liu and Wang, 2008; Pohlers *et al.*, 2009). Furthermore, TGF-β is the main inducer of CTGF and PAI-1, which are an important profibrotic factors. During both controlled tissue repair and uncontrolled tissue scarring, CTGF is involved in matrix remodelling via increased production of ECM including collagen (Brigstock, 1999; Dean *et al.*, 2005; Haydont *et al.*, 2005; Haydont *et al.*, 2007; Liu and Wang, 2008). PAI-1 inhibits the activation of the plasminogen, therefore is an important regulator in fibrinolysis (Kohler and Grant, 2000; Sobel *et al.*, 2003). PAI-1 is an important causative agent in CVD disease and tissue fibrosis. The overexpression of PAI-1 in transgenic-engineered animals resulted in increased development of vascular fibrosis and arterial thrombosis (Samarakoon and Higgins, 2008). TGF-β is a main inducer of PAI-1. PAI-1 expression is regulated through TGF-β-directed Smad2/3 activation (Samarakoon and Higgins, 2008).

1.11.1 Radiation-induced vascular damage by activation of TGF-β

TGF-β has an important role in development of the vasculature, maintenance of vascular homeostasis and maintenance of anti-inflammatory characteristics of ECs. It directly has effects on regulation of EC growth and migration as well as playing a role in the differentiation of mural cells into fibroblasts, smooth muscle cells and pericytes (Derynck and Zhang, 2003; Orlova *et al.*, 2011). Genetic studies in mice and human have revealed that deregulation of TGF-β signaling results in multiple vascular pathologies such as tumour angiogenesis,

Hereditary Haemorrhagic Telangiectasia (HHT), pulmonary arterial hypertension (PAH) and pre-eclampsia (Govani and Shovlin, 2009; Machado *et al.*, 2009; Venkatesha *et al.*, 2006).

Radiation has been shown to induce the TGF-β signaling pathway in many studies (Barcellos-Hoff *et al.*, 1994; Imaizumi *et al.*, 2010; Martin *et al.*, 1997; Randall and Coggle, 1995). The TGF-β ligand may trigger different signaling pathways, which is dependent on the composition of the receptor complex (Derynck and Zhang, 2003; Moustakas *et al.*, 2001). In a study by Kruse *et al,* radiation increased TGF-β signaling through ALK5, resulting in EC inhibition of proliferation and migration and contributing to anti-angiogenic functions in the mouse kidney (Kruse *et al.*, 2009). Moreover the *in vitro* and *in vivo* study by Imaizumi *et al* showed induction of Smad2 phosphorylation and additionally the inhibition of ALK5 receptors increased angiogenesis in irradiated mice (Imaizumi *et al.*, 2010; Kruse *et al.*, 2009).

Furthermore, the TGF-β family is one of the major mediators of wound healing. Radiation was shown to up-regulates the TGF-β expression in irradiated wounds in ECs and fibroblasts (Dormand *et al.*, 2005). TGF-β contributes to activation and proliferation of fibroblasts, chemotaxis of mast cells, increased collagen and ECM deposition, fibrosis and extracellular matrix degradation inhibition. Therefore, TGF-β appears to play an important role as a stimulator of radiation fibrosis (Dormand *et al.*, 2005). The late normal tissue injury and fibrosis following radiation could result from the elevated level of TFG-β production by radiation as well as circulating TGF-β expression by cancer cells (Anscher *et al.*, 1995; Dancea *et al.*, 2009). There is substantial evidence showing the involvement of TGF-β in initiation, development and persistence of late tissue fibrosis in irradiated animal tissues (Anscher *et al.*, 1995; Dancea *et al.*, 2009; Martin *et al.*, 2000). The injection of TGF-β in mice and rats or over expression of TGF-β in transgenic animals resulted in development of fibrosis in tissue such as kidney and liver following radiation (Martin *et al.*, 2000; Sanderson *et al.*, 1995; Terrell *et al.*, 1993).

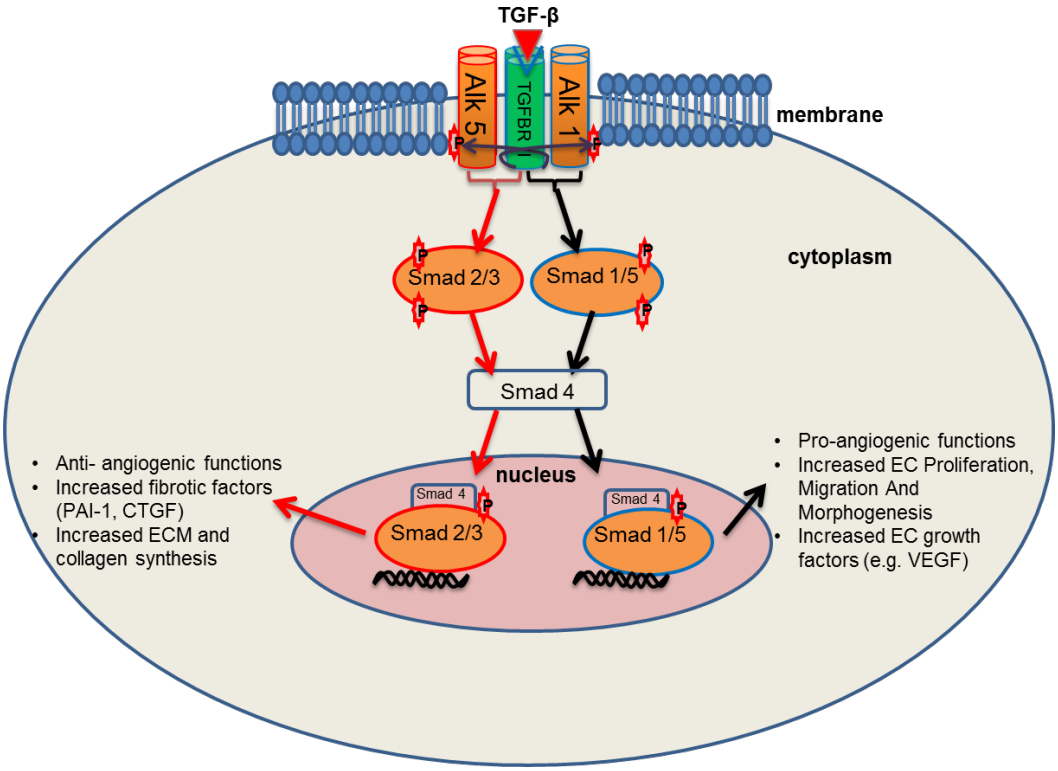

Figure 1.8 TGF-β signaling pathway. TFG-β/ALK5 signaling induces Smad2/3 phosphorylation and inhibition of angiogenesis as well as increasing production of fibrotic factors such as PAI-1. However the TFG-β/ALK1 signaling induces Smad1/5 phosphorylation, stimulating angiogenesis by increasing EC proliferation, migration and production of growth factors.

1.12 Role of Rho/Rho-kinase in angiogenesis and pathogenesis of CVD

The Rho, Ras and Ran families are GTP-binding proteins involved in intracellular signaling. There are several members of the Rho family present in mammals including: Rho (A/B/C/E/G isoforms), Rac (isoforms 1-3) and Cdc42. The Rho family proteins regulate the actin cytoskeleton, cell morphology and migration but also have many other functions including regulation of cell cycle, gene expression and cell survival, among others. Rho GTPases, when activated, associate with and activate downstream effectors (Shimokawa and Takeshita, 2005; rveiwed by Van Aelst and D'Souza-Schorey, 1997). Rho-kinase (ROCK) is a downstream target of Rho and signaling through Rho/ROCK contributes to the reorganisation of the actin cytoskeleton, cell motility and adhesion, stimulation of EC and VSMC proliferation and migration during angiogenesis and wound healing, VSMC contraction, cytokinesis and increases inflammatory cell motility. Rho/ROCK also accelerates tissue fibrosis, thrombosis and inflammatory processes through up-regulation of the fibrogenic molecules including TGF-β1, thrombogenic molecules (e.g. PAI-1 and TF) and pro-inflammatory molecules (e.g. MCP-1and IFN-γ) (Shimokawa and Takeshita, 2005; Van Aelst and D'Souza-Schorey, 1997). Different roles of Rho/Rho-kinase signaling pathways have been shown in Figure **1.9**. In many *in vitro* and *in vivo* (animal and human) studies, Rho-kinase has been shown to be involved in the pathogenesis of CVD such as arteriosclerosis, hypertension, ischemia heart disease, and heart failure (Gaugler *et al.*, 2007; Gaugler *et al*., 1998; Monceau *et al.*, 2010; Shimokawa and Takeshita, 2005).

TGF-β could activate the Rho GTPases including RhoA and enhance Rho A and B expression. The TFG-β–induced Rho activation plays a role in mediating cytoskeletal organisation, stress fibre formation as well as epithelial-to-mesenchymal transdifferentiation in human cells (Bhwmick *et al.,* 2001; Derynck and Zhang, 2003; Edlund *et al.*, 2002). The Rho/ROCK pathway also plays a critical part in CVD progression via modulation of TGF-β Smad activation as well as TGF-β association with vascular fibrosis. Additionally, Rho/ROCK pathway activation with or without TGF-β induction mediates CTGF expression following a

fibrotic stimuli and in the presence of an optimal PAI-1 expression. The Rho/ROCK pathway has been suggested to modulate Smad2/3 phosphorylation. Therefore, Rho-kinase has the potential to act as a therapeutic target in cardiovascular medicine (Bourgier *et al.*, 2005; Shimokawa and Takeshita, 2005).

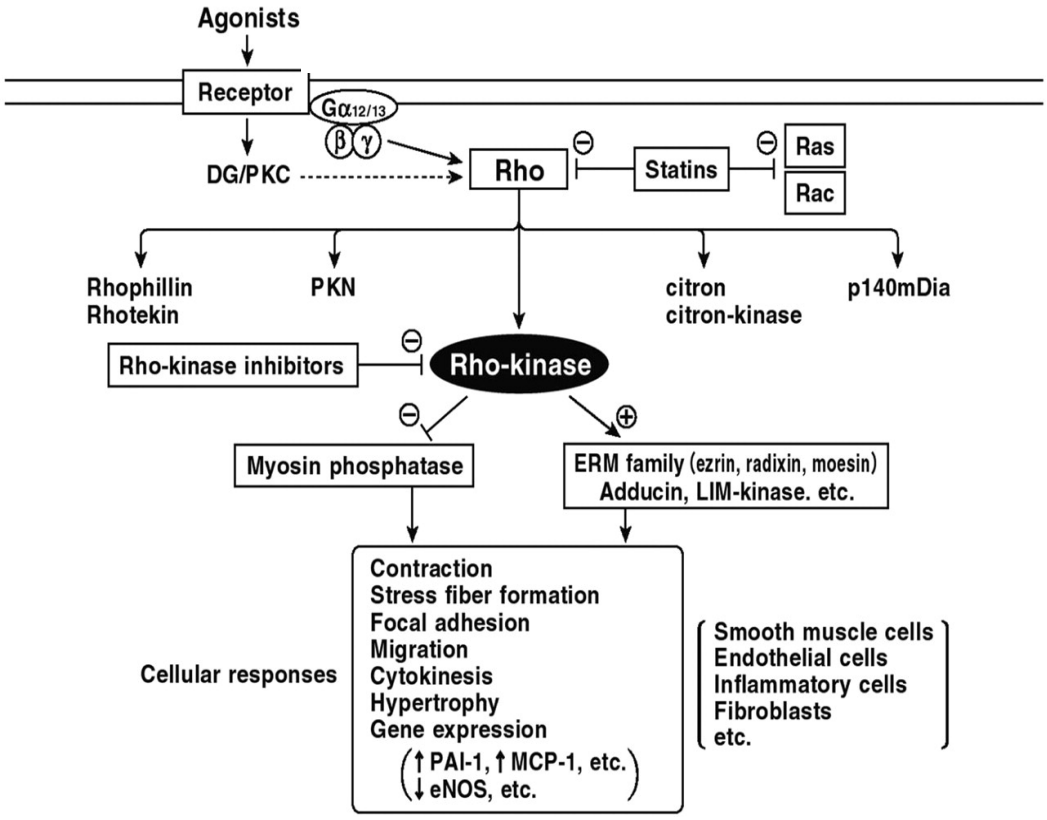

Figure 1.9 Different roles of Rho/Rho-kinase signaling pathway. Rho-kinase is involved in contraction, stress fibres formation, migration, and focal adhesion as well as expression of various genes and cytokines. Different cells including ECs, fibroblasts and smooth muscle cells express the Rho pathway (taken from Shimokawa and Takeshita, 2005).

1.13 The CARDIORISK project

The numerous experimental studies summarised above suggest that damage to blood vessels, especially microvessels, is followed by myocardial degeneration, which plays an important role in developing heart disease. Increased risk of heart disease after exposure to acute and protracted radiation doses of > 0.5 Gy manifesting years later is a growing concern for radiation protection. Therefore estimation of the potential dose threshold for the risk of radiation-induced heart diseases is required. Additionally an improved understanding of the possible mechanisms of CVD induction may offer a basis for solving the problem (Schultz-Hector and Trott, 2007).

CARDIORISK was a collaborative project funded by the European Commission in the 7th framework programme and included 12 collaborator groups. Its aim was to study the pathogenesis of early and late changes in mouse heart microcirculation after exposure to low and moderate radiation doses. *In vivo* studies were performed on locally irradiated mice hearts at low, moderate and high doses to establish late effects on coronary arteries and microvasculature as well as inflammatory and thrombotic changes following radiation. Moreover, the project aimed to study long-term alterations in irradiated endothelial cells, using endothelial cells extracted from irradiated mice in combination with *in vitro* endothelial models. The project also investigated proteomic changes following low dose irradiation in the mouse hearts (Andratschke *et al.*, 2011; Hildebrandt, 2010;).

1.13.1 Project aims and objectives

The aim of this project was to investigate the nature of the damaging effects of radiation on heart microvascular endothelial cells and the mechanisms involved. The project investigated effects of low, moderate and high doses of radiation using both *in vitro* and *in vivo* models of radiation. Angiogenesis, which mediates cardiac regeneration, is an important feature of the reparative response triggered by microvascular injury. The hypothesis here was radiation may compromise cardiac endothelial cell (CEC) angiogenic functions, which may contribute to pathogenesis of radiation-induced CVD and therefore effects of radiation on the angiogenic

functions of endothelial cells were a main focus of this study. One major aim of CARDIORISK was to develop methodology for isolating and culturing ECs from previously irradiated mouse hearts in order to further study their characteristics using *in vitro* cell culture models. In Chapter 3 methods of isolating endothelial cells from mouse hearts were developed. In addition, various endothelial cell lines were used and several assays for measuring angiogenic effects were set up in order to study the effects of radiation using cells in culture. One of the aims of CARDIORISK was to investigate late effects associated with radiation damage to the heart microvasculature. Our CARDIORISK collaborators (Professor Wolfgang Dörr and his group, Technical University of Dresden) performed *in vivo* irradiation of mice localised to the heart and using hearts excised after 20-60 weeks of irradiation a method of studying angiogenesis using ex-vivo explants was developed (Chapter **4**). A further aim of the project was to investigate the underlying mechanisms of radiation-induced ECs angiogenesis impairment. As mentioned earlier, there is cross talk between EC and fibroblasts during angiogenesis but the mechanism of interaction in the context of radiation damage is not clearly defined. Irradiation of fibroblasts may influence CEC angiogenic properties as its dysfunction has been shown to influence this process. Therefore in Chapter **5**, the effects of irradiated fibroblasts on endothelial angiogenic functions were investigated using fibroblast endothelial co-culture models. Inhibition of angiogenesis by radiation through direct effects on ECs and through bystander interactions with fibroblasts through mechanisms that may include activation of TGFβ-ALK5 and Rho/ROCK signaling pathways were investigated.

Chapter Two

Materials and Methods

2.1 Cell culture

2.1.1 Cell lines and primary cells

In order to study the biology of endothelial cells (EC) *in vitro* and establish several angiogenesis assays, different ECs and fibroblasts were used. Cultured primary cells are not like transformed cell lines with long lifespans, they become senescent in a short time. Therefore, they are mostly used from passage 2-9. Different immortalized endothelial cells with unlimited lifespan were cultured as well. All the cell culture work was conducted in a biosafety cabinet under sterile conditions. The cabinet, all equipment and bottles were cleaned using 70% ethanol before and after their use.

H5V: We kindly received H5V cell line from Dr. A. Vecchi (Instituto Clinico Humanitas, Milano, Italy). The H5V cells were derived from microvascular endothelial cells from the hearts of C57BL/6 mice (Garlanda *et al.*, 1994). They were immortalized by Polyma virus vector transfection carrying oncogene encoding the middle-sized T antigen (PmT), which is involved in ECs transformation. These PmT-transformed H5V cells could induce vascular tumour formation when injected inside the host (mice) (Garlanda *et al.*, 1994). H5V cells showed a cobblestone morphology when they were confluent. They were able to express PECAM-1 (CD31) constitutively, which is one of the main markers of ECs. Additionally, upon exposure to inflammatory stimuli (such as TNF-α) they were able to show an increase in production of adhesion molecules (VCAM-1, E-selectin, P-selectin), cytokines (as IL-6) as well as pro-coagulant activity. They were negative for the presence of Weibel-Palade bodies (Garlanda *et al.*, 1994; Sabapathy *et al.*, 1997).

bEND.3: They were purchased from ATCC (ATCC® CRL-2299™). The bEND.3 cells are immortalized endothelial cells derived from murine cerebral cortex capillaries. They are obtained by infecting of the primary culture of mouse brain endothelial cells with middle-T antigen expressing NTKmT retrovirus vector. Their endothelial nature has been validated by the expression of the von Willebrand factor (VIII) (vWF) (which is a main marker of ECs origin) (Sikorski *et al.*, 1993). The b.END.3 cell line expresses ICAM-1 constitutively, which

is consistent with its EC origin. Unlike ICAM-1, the VCAM-1 and E-selectin are expressed on stimulated b.END.3 cells by potent inducers such as TNF-α, IL-1 and LPS (Sikorski *et al.*, 1993).

HUVECs: They were purchased from PromoCell, which were supplied from pooled donors (PromoCell, Cat.no. C-12203). HUVECs are primary human endothelial cells isolated from vein of the umbilical cord. They retain endothelial cell specific properties, such as expression of surface adhesion molecules (E-selection, VCAM-1), integrin subunits (αvβ3, β1, α3), surface-bound antigens (endoglin, PECAM-1) and cytokines (IL6). They also express vWF. They are able to develop a capillary-like tube structure and exhibit a 'cobblestone' morphology. Therefore, they are the perfect candidates for studying the angiogenic properties of endothelial cells *in vitro* (Rhim *et al.*, 1998). They were maintained up to passage 10.

EA.hy 926: They were received as a kind gift from Dr Cora-Jean Edgell (University of North Carolina, USA). The Ea.hy926 cells are permanent human-humanhybrid cells (HUVECs-permanent human cell line A549) able to express factor VIII-related antigens. They were obtained from fusing human umbilical vein endothelial cells with the immortalized human thioguanine-resistant clone of A549 (human lung carcinoma). These cells displayed a number of features characteristic of vascular endothelial cells (Edgell *et al.*, 1983), for example, forming a network of tube-like structures when plated on matrigel which seem to resemble, in some respects, an *in vitro* process of angiogenesis, and therefore are a useful model for *in vitro* study of angiogenic processes. The endothelial characteristic of Ea.hy 926 cell was also confirmed by presence of cytoplasmic Weibel-Palade bodies. They could be maintained for more than 100 population doublings (Bauer *et al.*, 1992; Edgell *et al.*, 1983; Soriano *et al.*, 2003).

HDF: They were purchased from both Lonza and PromoCell (PromoCell, Cat.no. C-12302). Fibroblasts are usually found in connective tissue. Human dermal fibroblasts (HDF) are the most commonly used fibroblasts derived from the dermis of normal human skin. They have a

spindle-shaped morphology. They are able to secrete extra cellular matrix components such as collagen (type I, III and VII) and fibronectin, which are fibroblasts-specific characteristics (Chen *et al.*, 2010; Kim *et al.,* 2010). They were utilized up to passage 10. The media, solutions, antibodies, serums, consumable and equipments used have been mentioned in Appendix **I**, **II** and **III**.

2.1.2 Cell maintenance and culture procedure

In order to have healthy cells for performing bioassays, it is necessary to maintain and subculture the cells before they reach senescence. The growth media, trypsin-EDTA (ethylenediaminetetraacetic acid) and phosphate Buffered Saline/Hank's Balanced Salt Soln (PBS/HBSS) were pre-warmed to 37°C in a water bath or incubator for at least 15 min prior to harvesting the cells (to avoid any damage to cells because of temperature changes). The equipment (including tubes and pipettes) was then wiped off with a 70% ethanol solution, and cells and their growth medium were transferred into a class II biosafety cabinet. Carefully, and without disturbing cells, the old medium was pipetted off and discarded. The plate/flask was rinsed twice with 10 ml PBS before adding trypsin to remove excess serum, which inhibits trypsin activity and also removes calcium and magnesium ions, which maintain adherence of cells. After that, 5 ml sterile trypsin was added to cells in order to detach them from the plate/flask. As trypsin would kill the cells if it is left on them for a long period of time, cells were not exposed to trypsin for more than 10 min and the detachment of cells was monitored under the phase contrast microscope every 2 min. As soon as cells were separated from the plate/flask (usually between 4-6 min), the relevant cell culture media was added to stop the trypsin reaction (the volume of media was adjusted depending on the size of plate/flask). Before centrifuging the cell solution, 500 µl of solution (trypsinised cells) was added to a vial to perform a cell count. The Vi-cell XR cell viability system, which is an automated counter, was used to analyse cells and determines their concentration. The dead cells took up the dye, therefore the Vi-Cell viability analyser machine could provide data on cell numbers and the

cell viability per ml was shown on the computer screen. Cells suspensions were then centrifuged at 1000 rpm for 10 min to remove trypsin.

Cells	Full name	Growth medium	Plating densities	Passage number
HUVEC	Human umbilical vein ECs	Complete EBM-2: Endothelial cell Basal Medium-2, supplemented with growth factors (Lonza, Cat.no. CC-4147)	3 X 10^3 to 4 X 10^3 viable cells/cm^2	Up to 10
HDF	Human dermal Fibroblast, (promocell, C-12302 NHDF).	FGM-2: Fibroblast basal Medium 500ml supplemented with growth factors (Lonza, Cat.no. CC-4126) and (PromoCell, Cat.no. CC-23220)	3 X 10^3 to 4 X 10^3 viable cells/cm^2	Up to 10

Table 2.1 Primary endothelial and fibroblast cells

Cells	Full name	Growth medium	Plating densities	Passage number
H5V	Immortalised endothelial cell derived from fusion of HUVECs with human A549 cell line, Dr. A. Vecchi	10%FCS-DMEM: (Dulbecco's Modified Eagle's Medium) (Lonza, Cat.no. BE12-741F) supplemented with 10% FCS, 2mM L-glutamin, 100U/ml penicillin and 100µg/ml Streptomycin.	2 X 10^3 viable cells/cm^2	Up to 20
bEND.3	Immortalised murine endothelial cell line derived from mouse cerebral cortex tissue, (ATCC® CRL-2922™).	10%FCS-DMEM	2 X 10^3 to 3 X 10^3 viable cells/cm^2	Up to 25
EA.hy 926	Immortalised murine endothelial cell line derived from mouse heart tissue, (Dr Cora-Jean Edgell, University of North Carolina).	10%FCS-DMEM	2 X 10^3 to 3 X 10^3 viable cells/cm^2	Up to 50

Table 2.2 Endothelial cell lines

The pellet was collected in an appropriate amount of relevant growth medium, and the cell suspension was placed in the new plate/flask. The cell density was adjusted according to the cells' growth rate so that they became confluent within a week.

A list for each cell type (including primary and cell lines), growth media, seeding densities and the passage number we utilized has been summarized in tables **2.1** and **2.2**. The same culture procedure was applied to both primary and transformed cell lines. However, because most primary endothelial cells need support to adhere to substrate, we treated the plate/flask(s) with 1% gelatin for 30 min prior to placing cells in order to enhance the adhesion of primary HUVECs to their substrates.

When cell density reached confluence, the nutrient supply was diminished, waste product increased and cells proliferation activity reduced. Therefore, cells were sub-cultured when they reached 80-90% confluence in order to prevent such effects.

2.1.3 Medium renewal

The media were usually renewed 2-3 times weekly. First, the relevant supplemented medium was pre-warmed to 37°C in an incubator or water bath. Then, the spent medium was carefully pipetted off the culture plate (without disturbing the cells) and the fresh medium was added to the plate/flask.

2.1.4 Thawing out cells from the frozen stock

First, 15 ml of relevant cell culture medium was transferred into a T-75 flask and then warmed in a 37°C incubator for 30 min. A vial of cells from a liquid nitrogen tank was removed and immediately placed in a warm 37°C water bath with agitation. As soon as the cell stock was thawed, the vial was removed from the water bath, wiped with 70% ethanol and then transferred to a biosafety cabinet. The thawed cells were pipetted in the pre-warmed medium from the first step above. It was important to thaw the cells rapidly in order to have better cell viability. The medium was changed to remove DMSO when cells were completely attached to the bottom of the culture flask (24 h).

2.1.5 Freezing cells

In order to maintain enough healthy cells of early passage for further experiments, stocks of immortalized ECs (EA.hy 926, bEND.3 and H5V) were frozen in liquid nitrogen. The cells were usually frozen when they were around 80% confluent. The freezing medium was first made by adding 1 ml of Dimethyl Sulfoxide (DMSO) to every 9 ml of appropriate relevant fresh medium (10% DMSO). The solution was then mixed and filter sterilized with a 0.22 µm filter. In order to keep the medium cold during the experiment it was placed on ice. The cells from the early passage were washed, trypsinised and centrifuged to remove the medium. The pellet was resuspended in an appropriate volume of the freezing medium so that there were approximately 10^6 cells per ml. After that, cells were transferred into 1ml aliquots pre-labelled cryovials (label with cell type, date and passage number). They were immediately placed in a freezing container (Mr Frosty) and put in -80°C freezers for 24 h. Finally, vials were transferred into liquid nitrogen for storage.

2.1.6 Growth curve assay

Cell proliferation, growth rates and viability of culture curve can be measured by counting cell numbers. Moreover, this proliferation estimation could be applied to the study of angiogenic activity of vascular endothelial cells.

To determine cell growth rates, a confluent flask of the cell line of interest was trypsinised and a cell count was performed using the Vi-Cell XR viability analyser. The pre-counted cells were plated into the wells (day 0) (see Table **2.3**).

After allowing cells to grow overnight, on days 1, 2 and 3, the cell number was measured using the Vi-Cell XR viability analyser. Prior to performing a cell count of each well on each separate day, cells were first rinsed with PBS, trypsinised with 1ml of trypsin and left in an incubator for 5 min. Next, all cells were collected in15 ml tubes, centrifuged for 10 min at 1000 rpm and media were removed. To collect any drops of medium on the side of the tube or the bottom, the tubes were again centrifuged for another 5 min, and using a 200 µl Gilson

pipette, any remaining liquid from the top of the cell pellet was removed (without disrupting the pellet). At the end, 1 ml of full medium was added and the cell count performed. Irradiation induced changes in cell proliferation rate (Morris, 1996). After establishing the growth curve assay using different cell lines, in order to study the effect of radiation on EC and fibroblast proliferation, the growth curve assay was performed on irradiated and non-irradiated cells. The cells were seeded into 12 x well plates at certain densities. After they attached to the surface and were grown overnight, they were irradiated at 0.2, 2, 8 and 16 Gy the following day. For each radiation dose, cells were plated into a separate plate, and also one plate was not irradiated and kept as a control. After radiation, both irradiated and non-irradiated cells were counted (day 0) in order to establish cell numbers at the starting point of the assay. Then, cells were counted in each group at days 1, 2 and 3.

2.1.7 Inhibition of proliferation using Mitomycin C

Mitomycin C (Mit C) is a cell cycle inhibitor of S phase, stopping proliferation but not migration. Mit C was used to prevent proliferation of EC cells in migration assays. First, a condition for effectively inhibiting proliferation was established. EC cells were seeded in wells at different concentrations and allowed to grow until they became confluent. Cells were then treated with different concentrations of Mit C for 30 min to 2 h and after that Mit C was washed off and wells were rinsed with PBS 3 times. For each cell line different Mit C concentrations and treatment durations were tested as shown in Table **2.3**. Next, 2 ml of relevant full medium was added to wells and cells were incubated for another 30 min. The medium was again changed in order to completely remove Mit C, as it is toxic and would kill the cells if it remained in the culture. Finally, 2 ml of new fresh full medium was added per well and proliferation was measured over 3 days using the same method as for growth curve assay.

Cells	Cells density seeded per cm^2	Mit C concentrations and treatment duration
EA.hy 926	150,000	25µg/ml for 30 min/ 25µg/ml for 1h
bEND. 3	100,000	25µg/ml for 1 h/ 3 µg/ml for 30 min
H5V	15,000	0.5µg/ml, 2 µg/ml, 5 µg/ml and 10 µg/ml for 2 h

Table 2.3 Mitomycin C concentration and treatment duration for each cell line.

2.2 Radiation treatment

Radiation was administered to cells/heart tissue using a single-source AGO HS X-ray unit. The X-ray chamber/tube machine is designed to deliver different (low, medium and high) radiation ranges to cells/tissues. The image of the X-ray machine used in this project is shown in Figure **2.1**. In order to calculate the exact dosimetry to cells/tissues at the position they were in the X-ray tube, a member of radiological Physics department, Mr Chris Ogley from Sheffield Weston Park Hospital helped us. A Unfors Multi-O-Meter instrument which was relatively small and had a solid state detector and suitable dose range was used. Different dose rates based on the distance to the radiation chamber were measured as mentioned in Table **2.4**.

Each sample (cells/heart tissue) was placed at a distance of 40 cm from the radiation source and was treated at a dose rate of 537.6 mGy per min (200kV and 12.8 mA). Samples were treated with different radiation dose ranges between 0.2 to 16 Gy (0.2, 0.5, 1, 2, 5, 8 and 16 Gy), which were administrated as a single dose.

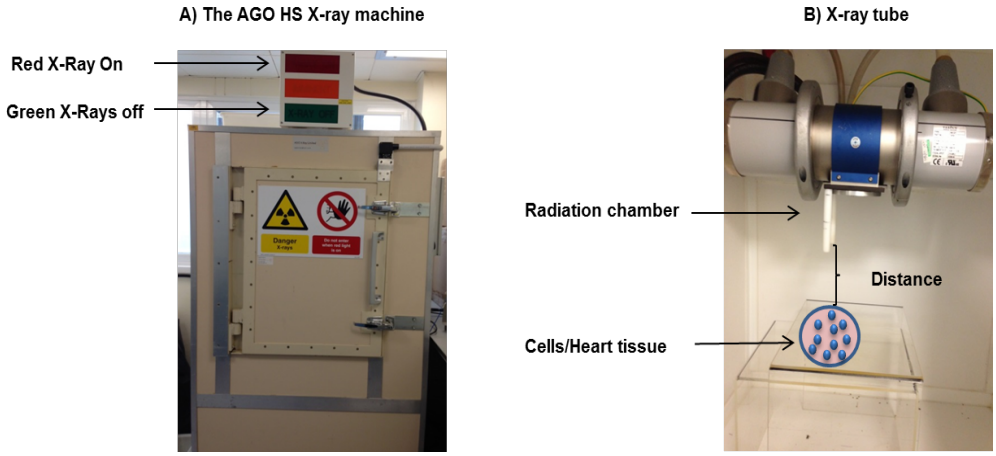

Figure 2.1 Images of the A) the AGO HS X-Ray machine, B) inside the X-ray chamber

kV	mA	Dose mGy	Time/min	Distance to IR chamber
200	12.8	537.2	1	40
200	12.8	427.4	1	46
200	12.8	177.7	1	67

Table 2.4 The average radiation dose at different distances to the chamber. The radiation dose rate per min was calculated at different distances from the radiation chamber.

2.3 Mouse cardiac endothelial cell isolation/culture

In order to study the effect of irradiation on angiogenic properties of Cardiac Endothelial Cells (CEC), isolation of mouse CEC was needed. To investigate the effects on CEC *in vitro*, different approaches were tested to optimize a method for their isolation. The basic steps involved were enzymatic digestion of heart tissue, its dissociation into single cell suspension and selection of endothelial cells from other cells (pericytes, fibroblasts, smooth muscle cells) using antibodies against specific cell surface markers and magnetic selection. Sometimes, to attain a high purity of CEC, a second sort selection was performed. The isolated CEC were characterised and then used in *in vitro* angiogenesis assays.

To isolate CEC, the hearts were first excised from the mouse. The SCID and C57BL/6 were two mouse strains, which were used here (between 6 to 22 weeks old). The mice were killed (by a person who holds the Home Office License for animal experimentation), hearts were removed and put into a 5 ml of saline solution or PBS before processing further. The tissue dissociating and CEC isolation procedures were adopted from previous publications (Marelli-Berg *et al.*, 2000; Lim and Luscinskas, 2006). The protocol for isolation of mouse heart CEC was first supplied by Dr Sheila Francis and further developed by my supervisor and Karol Jelonek, an MSc student in the Tumour Microcirculation Group.

After removing the heart, tissue was rinsed in HBSS in a petri dish, it was then cut into 3-4 pieces and washed 3 times by shaking in a tube containing HBSS to eliminate any blood and debris. Next, tissue pieces were minced into 1-2 mm^3 pieces and digested in pre-warmed enzymatic digestion solution (collagenase) in 20 ml HBSS for 45-60 min in 37°C incubator with agitation. After 30 min partial digestion the tissue was syringed through a 16 Gauge (G) needle 10-12 times for further dissociation of tissue clumps, and left in an incubator. After 15 min, it was again passed through 18 G needles and incubated for further 10-20 min until tissue clumps dissociated completely. Tissue digests were syringed one more time using 18 G needle and filtered through a sterile mesh (Miltenyi Pre-Separation Filters, Cat.no. 130-041-407) to remove any remaining tissue clumps. Then, 10%FCS-DMEM medium was added to the cell

suspension and centrifuged at 400g for 10 min at RT. At this point the cell suspension can be trypsinised or without trypsinising it performing the next step.

To trypsinise cells, they were first washed twice with PBS to remove any serum and then the pellet was resuspended in 3-5 ml of trypsin or accutase. The suspension was incubated at 37°C for 10-15 min with agitation (this step helped to dissociate cells further into a single cell suspension). Then, tubes were topped up with 10 ml of 10% FCS-DMEM and centrifuged as above to remove trypsin.

The cell suspension was washed twice with 10% FCS-DMEM to remove any red blood cells. Then, it was syringed through 18 G needle and the pellet was resuspended in 2 ml of complete 20% FCS-DMEM medium. 1-2 µl of prepared CD 31 antibody (see section **2.3.1**) bound to magnetic beads (Invitrogen, Cat.no. 110.35) was added to cell suspension and incubated for 30 min at 4°C on a rotator. After addition of antibodies, they attached to the cells expressing the antigen. The antibody-positive bound cells were then selected by using a magnet. Cell suspension was washed 6 x 3 min with 10%FCS-DMEM using a magnet (in between each magnetic separation, the cell suspension was vortexed). At the end, the selected bound cells were collected within 2 ml of complete 20%FCS-DMEM and seeded in one well of a 6 well plate which was pre-coated with 1% gelatin (Sigma). The medium was changed when cells had completely adhered to the plate (about 2-3 days). The CEC isolation procedure is shown in Figure **2.2**. Additionally, non-adherent cells including fibroblasts could be isolated and cultured. When cell suspension was washed using a magnet, the flow-through (which contains fibroblasts and any other un-selected cells including pericytes and smooth muscle cells) was collected in tubes (from the 3 first washes) and then the solution was topped up with 10%FCS-DMEM and centrifuged at 1000 rpm for 10 min. Cell suspension was washed one more time in a 10%FCS-DMEM medium. Finally, the pellet was resuspended in 10 ml of fibroblast growth medium (10% FCS-FGM) and plated in a pre-coated T-25 or T-75 flask with 1% gelatin. The medium was changed when cells adhered to the surface (usually the following day).

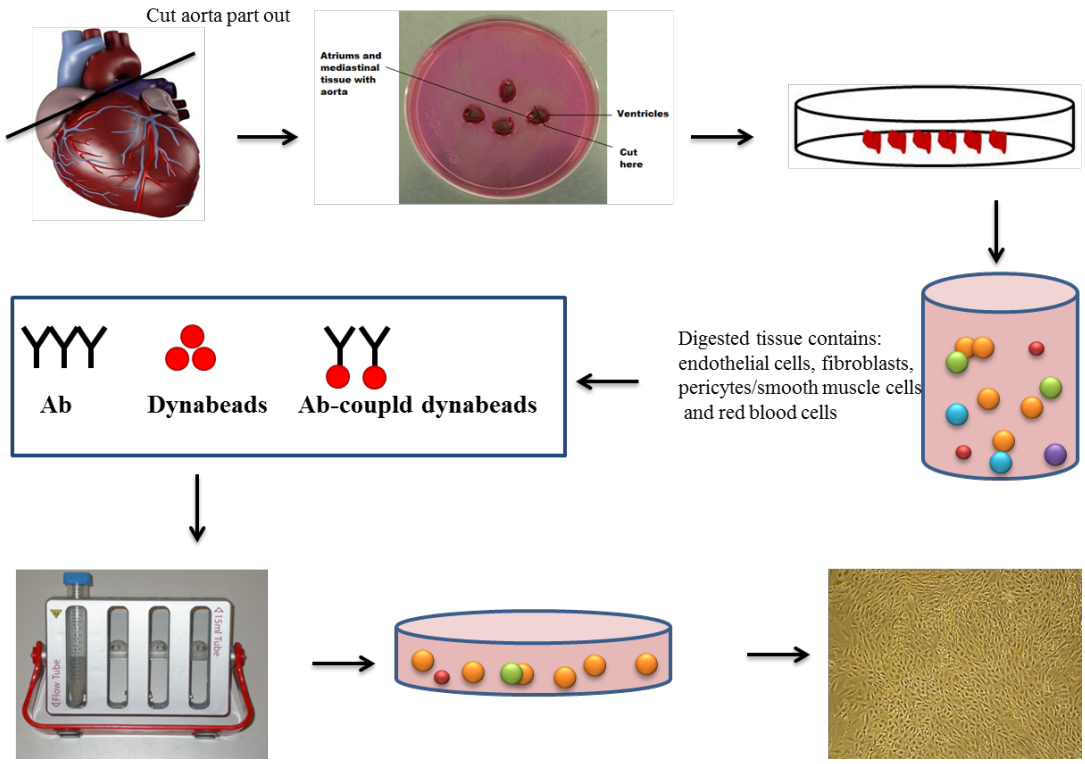

Figure 2.2 Schematic representative of mouse heart isolation procedure: First, heart aorta was cut out and the tissue was excised into small pieces. Then heart tissue was dissociated into a single cell suspension using mechanical and enzymatic dissociation. Next CEC selection was performed using antibodies to surface antigens coupled to Dynabeads. The selected CEC were isolated by magnetic means. Finally, isolated CEC were cultured in appropriate media/conditions.

2.3.1 CD31 Dynabead preparation

50 µl of Anti-Rat IgG Dynabeads (Sheep anti-rat IgG, Cat.no. 110.35) was washed twice in the magnet using 1 ml of PBS/2%FCS (washing solution). The beads were then resuspended in 50 µl of washing solution and CD31 (3 µg) was applied to the washing solution-beads. In order for the CD31 and beads to couple together, the solution was incubated overnight at 4°C on a rotator. After that, beads were washed 3 x 3 min in washing solution to remove any uncoupled CD31 antibody using the magnet. The antibody coated beads (Dynabeads) were stored at 4°C for up to 14 days.

2.3.2 Second sort selection

Occasionally, a second sort selection using CD31 was performed in order to improve the purity of isolated CEC culture and remove fibroblast contamination. When cells were near confluent they were sorted. The cell monolayer was washed with PBS, trypsinised and incubated at 37°C until all cells detached from the surface. Then, cells were collected in 10%FCS-DMEM medium, centrifuged at 1000-1500 rpm for 10 min and washed with 10%FCS-DMEM medium one more time. The cell pellet was resuspended in 2 ml of 20%FCS-DMEM medium, CD31 Dynabeads (0.5-2 µl) were added and were incubated for 30 min at 4°C with agitation. The CD31 positive cells were selected using the magnet as described before. The second sort selected CEC were then plated in one well of a 6 well plate (pre-coated with 1% gelatin).

2.3.3 Mouse cardiac endothelial cell isolation/culture using the Teflon-bag method

The Teflon cell culture bag method was another approach tested to improve the endothelial cell isolation yield. The endothelial cell surface receptors can be damaged/digested during the enzymatic treatment (collagenase A, trypsin/accutase step) and result in a reduction of EC selection by the antibody (CD31). This method was used to help CEC recover after all the enzymatic treatment and re-express their receptors, which could lead to increased CEC selection with CD31 antibody (Garland *et al.,* 1999). The cells do not adhere to the Teflon material in the bag but remain in suspension. The bag was left in the incubator.

The first steps of CEC isolation of mouse hearts were performed as described above. The heart cells were dissociated and digested. After addition of trypsin, cells were washed 3 X and then the pellet was resuspended in 15 ml of complete 20%FCS-DMEM and injected into a Teflon bag (AFC, Cat.no. 3010) as shown in Figure **2.3**. Then, the Teflon bag, which is permeable to gases, was placed in a sterile plate in the incubator at 37°C overnight. Additionally, 500µl of cell suspension was extracted in order to calculate the cell number. Next day cells were collected from the Teflon bag, centrifuged and counted again. Then, they were resuspended in 2 ml of complete 20%FCS-DMEM medium. The prepared beads (0.5-1.5 µl) bound to CD31 were added and incubated at 4°C for 30 min with agitation. After antibody addition, positive cells were selected using a magnet as described before. The selected cells were seeded in a pre-coated well of a 6 well plate with 1% gelatin. The non-selected cells were collected from flow-through during magnetic selection, topped up with 10%FCS-DMEM and centrifuged twice at 1000rpm for 10 min at RT. The pellet was resuspended in 10-15ml of complete 8%FCS-FBM and plated in a T-25 or T-75 flask (flask was pre-coated with 1% gelatin).

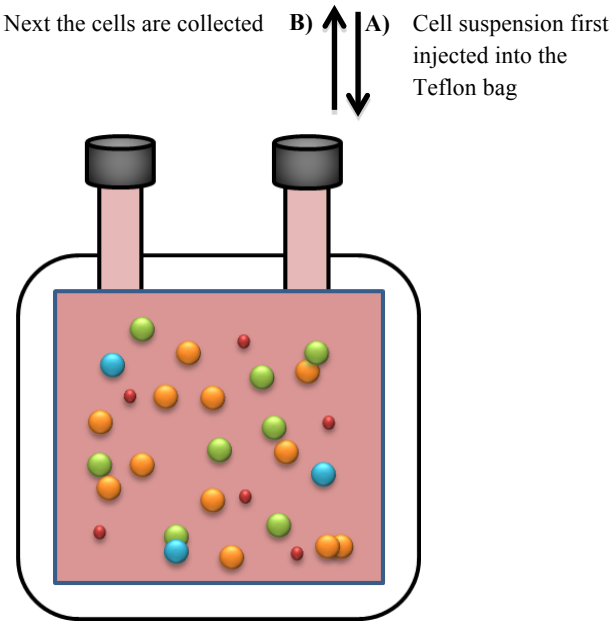

Figure 2.3 Schematic view of Teflon culture bag. A) First the mixed population of heart cells were injected into the Teflon bag. **B)** Next day cell were collected and positive cells were selected using a magnet.

2.4 *In vitro* models of Angiogenesis

Angiogenesis assays are useful tools for investigating angiogenic mechanisms of EC that modulate neovascularisation *in vivo*. *In vitro* models of angiogenesis are relatively inexpensive and rapid and can be used to study the effect of radiation on different angiogenic processes. Several angiogenesis assays, such as scratch wound assay, morphogenic matrigel assay, and "organotypic" fibroblast-endothelial co-culture assay were established using various EC types to assess effects of radiation on ECs in *in vitro* conditions.

2.4.1 Migration 'scratch wound' assay

Migration is an important step during angiogenesis. 'Scratch Wound Assay' is a straightforward method to study cell migration *in vitro* which involves creation of a scratch on a confluent cell monolayer, and is described as a two-dimensional assay. Cells migrate towards the direction of the wound (to fill the denuded area), which is eventually healed as shown in Figure **2.4**. By capturing images at zero time and at different points and then comparing these images, differences in cell migration rates can be determined (Liang *et al.*, 2007).

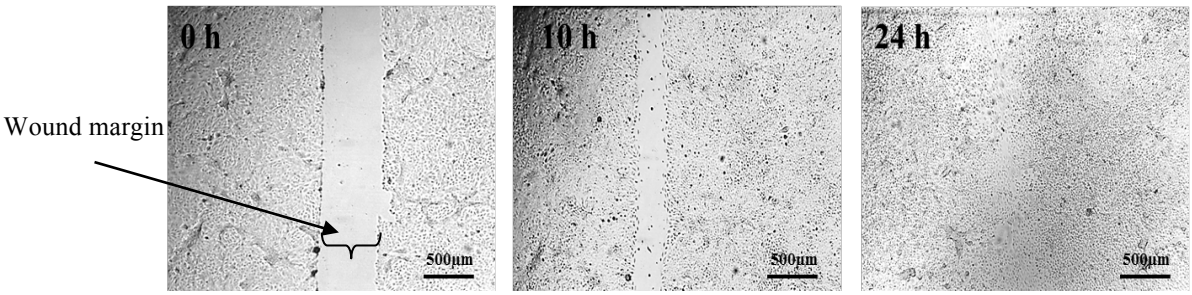

Figure 2.4 Scratch wound assay. The images of cells were captured at time '0' and at intervals up to 24 h during which time cell migration closes the wound.

The basic steps involved:

2.4.1.1 Plating and treatment of the ECs

A confluent EC lines flask was trypsinised and a cell count was performed to determine cell numbers. Next, two straight lines were marked underside of the wells using a fine marker. These lines served as reference points for imaging the "scratch wound". Then cell suspension containing certain numbers depending on the cell types was prepared and 1ml of that was plated in each well of a 12 or 24 well plate. Cells were incubated at 37°C until they became confluent (usually within 3-4 days depending on their growth rates).

To study the effect of radiation on EC migration and wound healing, one day prior to performing scratches on a confluent cell monolayer, when cells were nearly confluent they were exposed to radiation. But before performing radiation, in order to have the actual migration rate and exclude proliferation from our result, Mit C was used to stop proliferation during the wound healing process. Cells were treated with Mit C for 0.5 to 2 h. Additionally, some cells were not treated with Mit C and were used as controls. The cells after Mit C treatment were washed 3 times with fresh growth medium (10% FCS-DMEM) and incubated for 30 min. After that fresh media were added to cell cultures in order to wash off the Mit C completely. Next, irradiation of EC *in vitro* was performed at different radiation doses (between 0.2 to 16 Gy). For each radiation dose a separate plate was used and one plate was not irradiated and kept as control. The cells were incubated for 1-2 h or overnight at 37°C. The scratch wound assay was performed the following day.

2.4.1.2 Scratch wound assay

First, the confluent cell monolayer was scraped in a straight line to create a wound using a scratcher or a 200 µl pipette tip. The lines were vertical to the reference points (Figure **2.5**). Before performing the assay the culture medium was changed with fresh medium, and after creating the wound, in order to eliminate detached and damaged cells after the scratch, the old medium (from irradiated and non-irradiated cells) was returned to the culture in order to use the conditioned medium during assay. The cells were then placed under a phase-contrast

microscope and the reference points were located. The images of each well (at 4 reference points) were captured at 0, 6, 10 and 24 h to observe closure of the scratch. The plate was incubated at 37°C in between taking measurements.

2.4.1.3 Scratch wound assay using ibidi silicone inserts

In some experiments silicon ibidi inserts (Ibidi, 80206) were used which had two reservoirs with a defined gap (500 µm) between them. First they were placed inside plates. The 1% gelatin was added to each reservoir for 30 min to help cells (HUVECs) to attach to the surface. After removal of the gelatin, ECs were added to both reservoirs of the silicon inserts (70 µl each containing of 28,000 cells) and left until cells became confluent. After removing the silicon insert there should be two patches of cells which have been separated by a well-defined gap, therefore there is no need for making a scratch with 200 µl tip, which sometimes make wounds with different sizes.

2.4.1.4 Analysis of the scratch wound assay data

In order to quantify the migration rate and determine the wound diameter or area at each time point, images were analysed using Image J. The distance between one side of scratch and the other side was measured using the distance scale on the software and at least 10-20 readings of distance for each image were taken (Figure **2.5b**). The average width of the wound was measured and summarized by the image J program at each time point. Finally, the wound closure percentage (migration rate) was calculated by comparing the mean width of each wound image (in treated and non-treated cells) after 6, 10 and 24 h from the original wound (0 h).

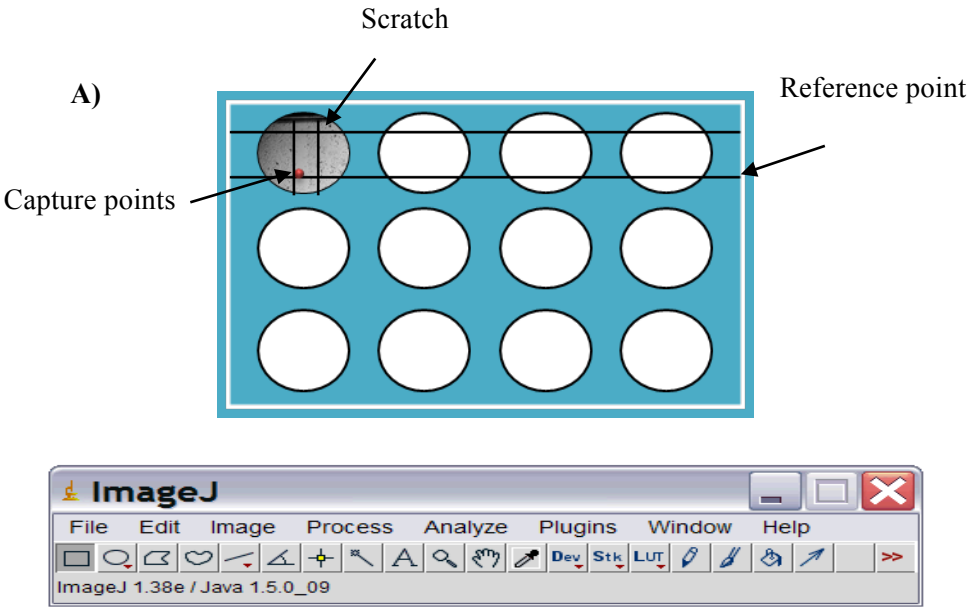

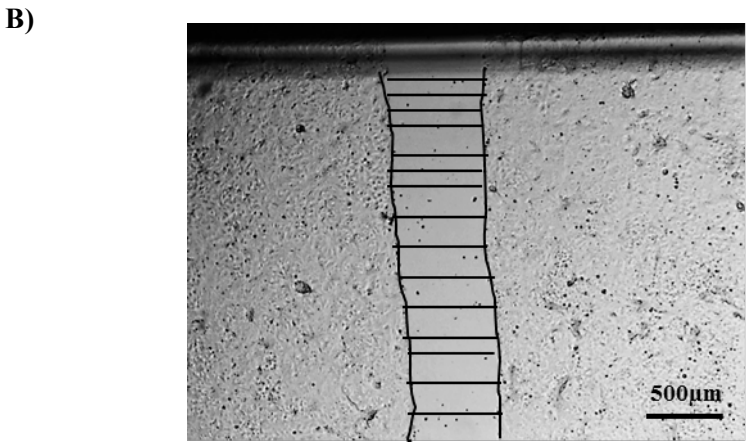

Figure 2.5 Schematic view of scratch wound assay in a 12 well plate. **A)** Cells were plated into a 12 or 24 well plate with two straight lines underside of the well **B)** the wound healing process was analysed using image J.

2.5 Clonogenic survival assay

In order to determine the ability of ECs to form a colony and to confirm the irradiation effects, the clonogenic survival assays were performed. Colony formation assay is an *in vitro* assay which determines the cell death after radiation exposure and the radiation effects on the survival of cells. This assay has been used with many different cell types for decades (Franken *et al.*, 2006). Survival of different EC lines including H5V, Ea.hy926 and bEND.3 cells and fibroblast cell line (HDF) were used here performing clonogenic assay.

First, an appropriate number of exponentially growing cells were plated into several T-25 flasks depending on the various radiation doses to be given. Once cells were approximately 80% confluent, their media were changed and they were irradiated at the required doses. Before performing radiation, culture media were pre-warmed and 10 cm dishes were prepared and labelled. Immediately following radiation, cells were trypsinised, re-suspended in medium and counted. Next, cells at appropriate plating densities were seeded into pre-labelled 10 cm plates containing pre-warmed media. Because the minimum number of cells needed to form colonies and survive differed with each cell line, different numbers of cells for each dose were plated and tested in initial experiments (Table **2.5**).

	0 Gy	0.2 Gy	0.5 Gy	1 Gy	2 Gy	5 Gy	8 Gy
H5V	100/500	100/500			500/1000		1000/2000
HDF	100/500	100/500			500/1000		1000/2000
EA.hy 926	100/200/ 500/1000		200/500	200/500		500/1000	
bEND.3	100/200/ 500/1000		200/500	200/500		500/1000	

Table 2.5 Cell seeding densities tested for different radiation doses. The table shows different numbers of cells/plates tested for each cell type and each radiation dose.

The dishes were then placed in an incubator at 37°C to allow cells to form colonies. Cells were incubated until control cells could form sufficiently large clones. The swirling of the solution and moving plates was avoided during the incubation period in order not to dislodge developing colonies. Colonies were formed between 10-14 days after plating. Once colonies formed, media were removed and colonies were fixed in 100% methanol for 10 min. Then they were stained with 0.1% methylene blue in 50% methanol and after 10 minutes dishes were washed in cold water and left to dry. Finally, the numbers of colonies in each plate were counted (by eye) to obtain the plating efficiency (PE). The plating efficiency (PE) indicated the percentages of cells plated into a dish that could grow and form a colony (Munshi *et al.*, 2005). The clonogenic assay procedure has been shown in Figure **2.6**.

A cluster of stained cells (in blue) was considered a colony when it comprised of approximately 50 cells. The number of colonies for each group was counted and averaged (3 plates for each group) and then the mean was divided by the number of cells originally seeded to give the PE. Moreover, surviving fraction as a function of dose was determined by dividing the PE of each irradiated group by the PE of the control (non-IR group). PE is a ratio of colony number to number of cells plated (multiplied by 100) and the number of colonies produced after radiation in terms of PE is called the surviving fraction (SF). The PE of different cells is different (Franken *et al.*, 2006; Munshi *et al.*, 2005; Schleicher *et al.*, 2011).

PE= Number of colonies counted/Number of cells seeded x 100.

SF= PE irradiated group / PE 0Gy control

The PE of the treated groups was normalised to the control plate, considering that to be 100%. Therefore the SF is calculated relative to the 0 Gy control group.

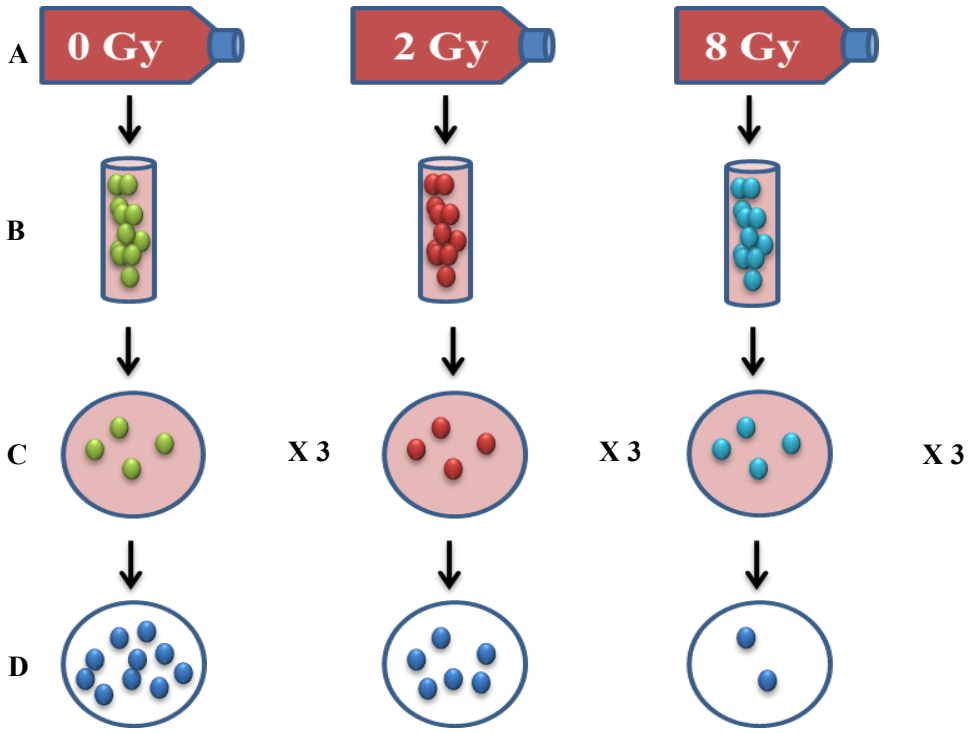

Figure 2.6 Schematic representatives of clonogenic assay procedures. The image shows **A)** Cells were first cultured in four T-25 flasks with similar density. After they became 80% confluent, there were irradiated at different radiation dose. One flask was kept as a control. **B)** Immediately after irradiation, cells were trypsinised, centrifuged, re-suspended and counted **C)**. A small number of irradiated and non-irradiated cells were seeded into 10 cm dishes (3 plates for each dose) and incubated for about 10-14 days. **D)** Once colonies formed, cells were fixed in 100% methanol for 10 min, and then stained with 0.1%methylene blue in 50 % methanol for another 10 min. A colony is defined as consisting of 50 cells.

2.6 Immunofluorescent staining of ECs for phosphorylated H2AX

Radiation causes DNA double strand breaks (DSBs) which results in phosphorylation of histone H2AX (DSBs marker) and consequently leads to recruiting DNA damage response at DSBs. In order to determine the efficacy of radiation on ECs and fibroblasts, they were first irradiated and then stained for phosphorylated histone H2AX (Marti *et al.*, 2006).

The ECs (H5V, 5000 cells/well) and fibroblasts (HDF, 10000 cells/well) were plated and cultured until they reached confluence (about 3 days). After that, HDF and H5V cells were irradiated using the X-Ray machine. Some cells were kept un-irradiated as control. After irradiation, cells were left in the incubator overnight and the next day they were fixed (both irradiated and non-irradiated cells) with 3.7% formalin (Sigma) in PBS for 20 min. After fixation, cells were permeabilised in 0.5% Triton in PBS for 5 min. Then, 3 x 2 min PBS washes were performed and blocking solution (10% horse serum, Vector labs, Cat.no. 5-2000) and 10% casein diluted in PBS were added prior to addition of the primary antibody in order to block non-specific binding of the antibody. This blocking solution was made according to the host species of secondary antibody (Table **2.6**). The solution was incubated for 30 min and removed after that. In the next step, phospho-histone H2AX rabbit antibody (Cell Signaling, Cat.no. 9718) was added to the cells as the primary antibody at dilution of 1: 50 (in 2% normal horse serum and 2% casein) for 24 h. Then, 4 x 5 min washes were applied and the secondary antibody, biotinylated anti-mouse IgG1 anti-rabbit IgG (Vector, Cat.no. BA-100) was diluted at 1:200 (in 2% normal horse serum and 2% casein) and added to plates for 1 h at RT. Then cells were incubated with fluorescent Avidin D (Vector labs, Cat.no. A-2001) at 1:250 and Texas red-X phalloidin (Molecular probes, Cat.no. H-1300) at 3 µl per filter in 10 mM HEPES, pH 7.5, 0.15M NaCl for 2 h. Finally, cells were washed 4 x 5 min in PBS, removed from the insert and mounted on a slide.

Primary Antibody	Blocking Solution	Dilution	Secondary Antibody	Dilution
Phospho-histone H2A.X rabbit Ab (Cell Signaling, Cat.no. 9718)	10% horse serum +10% casein (Vector labs, Cat.no. 5-2000)	1:50	Biotinylated anti-mouse IgG1 anti-rabbit IgG raised in horse (Vector labs, Cat.no. BA-1400)	1:200

Table 2.6 Primary and secondary antibodies were used in immunofluorescent staining of phosphorylated H2AX

2.7 Tubule formation assays

During the wound healing and angiogenesis process ECs migrate, proliferate and form a capillary-like network. There are some angiogenesis assays which can give some measurement of the ability of endothelial cells to form capillary-like structures *in vitro* such as the Matrigel assay and the fibroblast-endothelial co-culture assay.

2.7.1 Morphogenic matrigel assay

Endothelial cells are capable of forming tubules spontaneously *in vitro*. The differentiation and formation of capillary-like tubes by ECs depends on the presence of some factors such as basement membrane proteins within a three-dimensional matrix. The use of fibrin, collagen and matrigel, which are able to supply some basement membrane proteins, leads to formation of tubules by ECs in a short time by stimulating their migration and differentiation into capillary-like structures (Bishop *et al.*, 1999)

Matrigel is a basement membrane, which has been extracted from the Engelbreth-Holm-Swarm (EHS) mouse sarcoma. Matrigel, which contains some basement proteins such as collagen IV and laminin (BD Biosciences), was used as a matrix for ECs to form tubules (Ucuzian and Greisler, 2007). Matrigel converts to gel when it is at RT while it is liquid at 4°C. Different types of ECs were tested using this assay.

The required volume of matrigel was allowed to thaw out overnight on ice in the cold room, because matrigel usually sets even at low temperatures. Before starting the experiment all pipette tips and 48 well plate(s) used in this assay were cooled down to -20°C. They were kept on ice throughout the experiment. Using 48 well plates, 100 µl of matrigel was added to the wells and then allowed to set for 30 min at 37°C incubator. During this time, cells were trypsinised, counted and collected in relevant growth media. Then, cell suspensions were prepared and 300 µl added to each well containing matrigel (see Table **2.7** for specific cell numbers tested). The ECs began to form tubules within 1 h and the process was complete within 24h. After 24 h, the images of the formed channels were taken. In order to optimize this assay, different types and concentrations of ECs as well as different volumes of matrigel were tested.

Furthermore, after optimizing this assay, the effect of irradiation on formation of tubules by ECs in matrigel was tested. Cells were irradiated 1-2 hours prior to the start of the experiment, before preparing the cell suspension. After that, the matrigel experiment was performed on irradiated and non-irradiated (0 Gy) cells.

Cell type	Cell density
Eahy 926	10,000 and 15,000 cells per well
bEND.3	10,000 and 15,000 cells per well
HUVECs	20,000, 40,000 and 80,000 cells per well
CEC	50,000 and 100,000 cells per well

Table 2.7 Different endothelial cell types with different densities used in the matrigel assay.

2.7.2 Organotypic endothelial-fibroblast co-culture assay

Angiogenesis is a complex process, which involves ECs and other cell types such as fibroblasts and smooth muscle cells, as well as many different growth factors, enzymes and ECM molecules. Many *in vitro* angiogenesis assays cannot model the whole process adequately. Therefore, it was necessary to utilize an *in vitro* model which had the ability to mimic ECs behavioural activity to undergo proliferation, migration and differentiation among other cells (e.g. fibroblasts, pericytes) and form capillary structures. Fibroblasts secrete some matrix components during angiogenesis, which can act as a scaffold for the formation of EC channels (Bishop et al, 2000). The endothelial-fibroblast co-culture assay is another type of tubule formation assay, which was developed by Bishop *et al* and Donovon *et al*. They showed that ECs were able to form capillary structures in an environment where the fibroblasts were producing the ECM components including fibrillar collagen as well as growth factors such as bFGF and VEGF which promote the ECs migration and channel formation (Bishop *et al.*, 1999; Donovan *et al.*, 2001; Sorrell *et al.*, 2007). After 5-7 days in co-culture, ECs and fibroblasts started proliferating. After that ECs started segregating into cell clusters (known as ECs Island) and later sprouts emerge from those clusters. As channel formation develops the ECs sprouts elongated and thickened, forming capillary-like structures (Bishop *et al.*, 1999; Hetheridge *et al.*, 2011; Sorrell *et al.*, 2007). Moreover, the ECs formed capillary-like structures, consisting of both long and short interconnecting and more stable tubules than the matrigel assay, developing over a longer period of time (between 12-14 days) (Donovan *et al.*, 2001).

Different ECs and fibroblasts in co-culture were tested to set up and optimize this assay. The co-culture of HUVECs with HDF and isolated mouse cardiac fibroblast (CF), isolated mouse cardiac endothelial cells (CEC) with HDF and H5V cells with HDF was examined. The supplemented EGM-2, complete 20%FCS-DMEM and 10%FCS- DMEM medium were used for co-culture and cultivation of HUVEC-CF, ECE-HDF and H5V-HDFcells, respectively.

Both cell types were trypsinised, counted and mixed together at different ratios and densities. Mixtures of fibroblast and endothelial suspensions were seeded into wells of a 24-well-plate. Then, cells were cultivated for 14 days and the medium was changed every 2-3 days (Bishop *et al.*, 1999). The ECs started expanding, proliferating, migrating and forming capillary-like structures by day 12-14. At the end of co-culture assay, cells were fixed with 100% ice-cold methanol and channels were visualised by staining for CD31 and vWF. This assay has been adapted and modified from the Bishop *et al* study (1999).

2.7.2.1 Optimization of co-culture assay and irradiation treatment

First of all 24 well plates were coated with 1% gelatin 30 min prior to plating the cells, in order to help especially primary EC to adhere to the plates and grow. Then the cells were syringed several times with 18 G, 20 G and 21 G needles to separate the cells from each other and turn them into single cell suspension. Different cell ratios and densities were used as shown in Table **2.8** below. After cells were counted and mixed at shown densities and ratios the mixture of fibroblast-EC co-culture cells was seeded in a 24 well plate at a volume of 1ml in each well.

Fibroblast-endothelial Co-culture ratio	Fibroblast density per ml	Endothelial density per ml
1:1	40,000	40,000
3:1	60,000	20,000
5:1	100,000	20,000

Table 2.8. Different ratios and densities of fibroblasts and endothelial cells.

Ratio 1:1		Ratio 3:1		Ratio 5:1	
(i)	20,000 F-20,000EC	(i)	30,000 F-10,000EC	(i)	50,000 F-10,000EC
(ii)	10,000 F-10,000EC	(ii)	15,000 F-5000EC	(ii)	25,000 F-5000EC
(iii)	5000F-5000EC	(iii)	7500F-2500EC	(iii)	12500F-2500EC
(iv)	2500F-2500E C	(iv)	3750F-1250EC	(iv)	6250F-1250EC

To investigate the effect of radiation on the capacity of ECs to form capillary-like tubules in this assay, endothelial cells were irradiated at different doses prior to performing the assay. After 1 h, the irradiated and non-irradiated (0Gy, control) cells were mixed with fibroblasts and cultured for 14 days. Finally, the capillary-like structures formed by ECs were fixed and visualised to compare the quality and quantity of the capillaries made in irradiated cells to the non-irradiated group.

2.7.3 The endothelial-fibroblast self-assembling cardiac endothelial tube formation assay

The CEC self-assembly assay model was a novel assay which was established first by my supervisor Dr Chryso Kanthou in our lab in which CECs were able to form a capillary-like structure *in vitro*. In this assay mouse heart cells were digested and separated into single cell suspensions using enzymatic and mechanical digestion; but CECs were not selected during the isolation procedure.

Mouse heart from SCID and C57BL/6 animals between 14 to 40 weeks old were used. The mouse heart was first dissected and collected in a sterile petri dish. It was then minced into very small pieces. Collagenase A (2mg/ml, which was dissolved in 10 % DMEM) was added to the minced tissue for 45 min at 37°C to digest it (tissue clumps syringed with 16 G needles 6 times inbetween). Tissue again was syringed into a Miltenyi Pre-separation filter and cells were collected in a 15 ml tube. The filtered cells were topped up with pre-warmed 10% DMEM and centrifuged at 400g for 10 min. The pellet was resuspended in 10% DMEM and centrifuged 2 more times. The final pellet was resuspended in 8-10 ml of full complete 20% FCS-DMEM medium suitable for CEC growth. The mixed population of extracted cells which

contained CEC and other cells such as fibroblasts, smooth muscle cells and pericytes were then cultured. They were plated at different densities in 12 well plates to establish conditions in which the endothelial cell could form tubular structures. Therefore, one heart cell suspension was plated in 4, 5 and 6 wells coated with 1% gelatin. They were put in an incubator for 2-3 days (and not disturbed during this time) and after that every second day the media was changed (Figure **2.7**). The mixed heart cells populations were cultured for 10-12 days. Finally, cultures were fixed in 70% methanol and stained for lectin and vWF to visualize the capillary-like structures (see section **2.4.4.4-5**).

2.7.3.1 Radiation and self-assembly assay

After establishing the self-assembly assay, the effect of radiation on formation of capillary-like channels by CEC was investigated. First, the heart tissue cells were digested and dissociated into single cells suspension. Then extracted cells from one heart were plated into 12-well plates. After that the extracted heart cell population was cultured together for 10 days. When the CEC began forming tubules usually by day 5-6 (observed under phase contrast microscope) the media were changed and cultures were irradiated at different radiation doses (0, 0.2, 2, 8 and 16 Gy). The CEC capillary-like networks were fixed and characterised after 10-12 days.

2.7.4 Immuno-staining for CD31 and vWF on EC Tubules

The immuno peroxidase staining technique was used to enhance visualization of the ECs capillary-like structures. First of all cells in cultured plates were fixed in 70% methanol which had been stored at -20°C. The cell fixation was performed in order to stabilize the cells/tissue. After fixing cells for 30 min or overnight, the cells were pre-incubated in endogenous peroxidase blocking solution (3% hydrogen peroxide) which was made of 30 ml of H_2O_2 in either PBS or methanol for 30 min at 37°C. The cells/tissues were treated with hydrogen peroxide to reduce the high non-specific background from positive staining prior to incubation with conjugated antibodies.

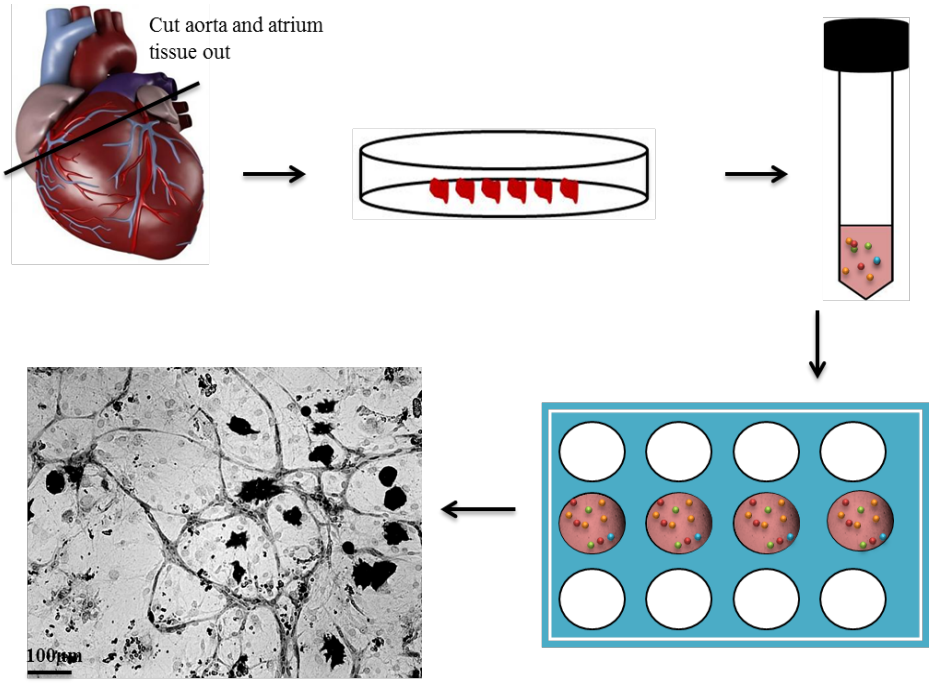

Figure 2.7 Schematic representative of self-assembling CEC tube formation assay procedures. First heart tissue was dissected into small pieces, which were then digested and dissociated into a single cell suspension using collagenase. After that, the mixed population of cells, which contained CECs along with other isolated mouse cardiac cells including fibroblasts, pericytes and smooth muscle cells were cultured together in a plate coated with 1% gelatin for 10 days. The CEC started proliferating, migrating and forming into capillary-like structures. The co-culture was fixed after 10-12 days and characterised using lectin.

After 2 x 5 min PBS washes, the blocking solution (10% normal serum and 10% casein diluted in PBS) was added prior to addition of primary antibody. This blocking solution was made according to the host species of a secondary antibody to adhere to non-specific sites. The solution was incubated for 30 min and drained off the cells without washing to prevent blocking buffer removal.

In the next step, 300 µl of primary antibody was diluted in 2% normal serum and 2% casein was applied and left for 1 h or overnight. The primary antibody is used for detecting antigens in tissue which can be either on the cell surface or in the cytoplasm. The purified rat Anti-mouse CD31 (0.5 mg, BD Pharminogen) at dilution of 1:100 and Rabbit polyclonal to vWF (abcam) at dilution of 1:500 were used as primary antibodies. The primary antibody solution was removed and cells washed 2 x 5 min with PBST (PBS+0.1 % Tween 20). Then, the secondary antibody was diluted 1:200 in 2% normal serum and 2% casein and added to plates for 1 h at RT. In the meantime, the ABC (Avidin/Biotinylated Enzyme Complex) peroxidase reagent (Vectastain ABC kit) was prepared according to the manufacturer's instruction (2 drops of reagent A and 2 drops of reagent B in 5ml PBS) and was left to stand for 30 min before adding to plates. Biotinylated secondary antibody was raised in a different species against the species in which the primary antibody was raised. Moreover, it had been biotinylated and avidin, which has affinity to biotin, was attached to several sites of biotin. Therefore, the avidin biotinylated enzyme complex was used to attach to several biotin sites of secondary antibody. Cells were incubated with ABC peroxidise reagent for about 30 min at RT and were then washed 2 x 5 min in PBST. After that, the substrate diaminobenzidine (DAB) kit (Vector) was used to convert peroxidase into dark brown insoluble end product. The DAB peroxidise substrate (2 drops of buffer solution, 4 drops of DAB, 2 drops of H_2O_2 solution in 5ml distilled water) was added for 2 to 7 min to develop the brown stain colour. Harri's haemotoxylin was used as a counter stain for nuclei staining and added for 1-2 min to each well. Then wells were rinsed in running tap water for approximately 2 min. At the end, 500µl of distilled water was added to each well and the visualised tubules were seen under a phase

contrast microscope. The images were taken by digital (Ky-F1030 JVC) camera and plate(s) were kept in the fridge.

Primary Antibody	Blocking Solution	Dilution	Secondary Antibody	Dilution
Von Willebrand	10% horse serum +10% casein	1:500	Biotinylated ani-mouse IgG1 anti-rabbit IgG raised in horse (BA-1400)	1:200
CD31	10% goat serum +10% casein	1:100	Biotinylated anti-rabbit IgG raised in goat (BA-1000)	1:200

Table 2.9. Primary and secondary antibodies used in EC channels staining

2.7.4.1 Direct staining method using biotinylated lectin

A direct staining method using biotinylated lectin was also performed for visualising ECs. In this method, there was no need for addition of a secondary antibody, as lectin had been biotinylated. The general procedure was the same as before. First cells were fixed using 70% methanol which was stored at -20°C for 30 min, then peroxidase blocking solution (3% H_2O_2 in PBS) was applied for another 30 min. After 2 x 5 min PBS washes (with agitation), serum blocking solution was made with 1% BSA in PBS and applied for 30 min to block non-specific binding of reagents. After that, biotinylated lectin (Vector, Cat.no. B-1205) was added at 20µg/ml in 1% BSA in PBS solution to cells and incubated for 1 h at RT or overnight. The Vectastain ABC reagent was made 30 min prior to their addition and applied to cells for 30 min after lectin washes. Following 2 x 5 min PBST washes (with agitation), cells were incubated with DAB for 2 to 7 min, counterstained and observed under the microscope.

2.8 Cardiac *in vitro* angiogenesis assay using heart explants

A three-dimensional (3D) cardiac angiogenesis assay, using tissue explants, was performed. This assay models multiple steps of the angiogenic process and is based on activated CECs' capacity to invade 3D substrate and form capillary-like structures. Briefly, small pieces of mouse heart tissue or aortic arch (AA) were embedded in matrigel or fibrinogen gel (as matrix substrate) and exposed to different conditions. After 3-4 days, ECs started sprouting from tissue explants and forming tubule-like structures. This assay was first developed by Kiefer *et al* (2004).

First, animals were sacrificed (a member of TMG group who held a Home Office personal license performed this step) and hearts were excised from mice. The hearts were dissected into two parts: ventricular myocardium and heart atrium. Heart from SCID (severe combined immunodeficient), C57BL/6 and $APOE^{-/-}$ mouse strains at different ages (from 14 weeks to 60 weeks old) were mostly used in this assay. Matrigel was placed on ice at 4°C overnight before starting the experiment. 120 µl of matrigel was then pipetted immediately into each of 48 well plates and matrigel was allowed to polymerize for 30 min at 37°C. After that, it was overlaid with 500 µl of serum-free media (DMEM) and placed in an incubator for another 30 min at 37°C. In the meantime, heart tissue was dissected and chopped into approximately $1mm^3$ cubes. The heart explants were placed onto the matrigel and overlaid with 120 µl of matrigel, incubated for 30 min at 37°C to allow the gel to polymerize. 500 µl of full media (EBM) were added to wells and heart explants incubated for 7 days at 37°C in the incubator. The media were replaced with fresh full media every second day. After 7 days, images of heart explants sprouts were captured by a digital camera (Leica DFC300 FX) attached to an inverted microscope (Leica DMI 4000 B).

To improve the formation of CEC sprouts from heart explants, fibrin gel was used instead of matrigel. To prepare fibrin gel, fibrinogen (Sigma) was first made at a final concentration of 3 mg/ml and diluted in serum-free DMEM (containing antibiotic and glutamine). Then, 4 µl of bovine thrombin (100U, Sigma) was added to each 4ml of fibrinogen, mixed and pipetted into

wells of a 96 well plate. As a number of growth factors can stimulate CEC migration and proliferation and induce angiogenesis *in vivo*, the heart explants were also exposed to different growth factors and media. Moreover, hypoxia (5% O_2) and normoxia (21% o_2) conditions were tested in order to mimic the *in vivo* condition more closely. Media and growth factors used were the full EBM-2 and 20% DMEM+ 5µg/ml ECGS. After 10 days explants were fixed in order to inhibit fibrin gel degradation and imaged later. Figure **2.8** shows the process of the heart explant assay.

2.8.1 Dissection of mouse aortic arch (AA) from heart tissue

After killing the animal, the mouse heart and lung with a part of the thoracic aorta were removed together and placed into a dish with PBS. After that, using the dissecting microscope, the aortic arch was located and then the lungs and fat around the heart tissue were carefully cut from the heart (all these steps were performed under the microscope). Finally, the aortic arch was cut from the heart, excised into small pieces (~ 0.5 mm) and kept (for up to 1 to 24 h) at 4°C in a tube with PBS before performing the heart explant assay.

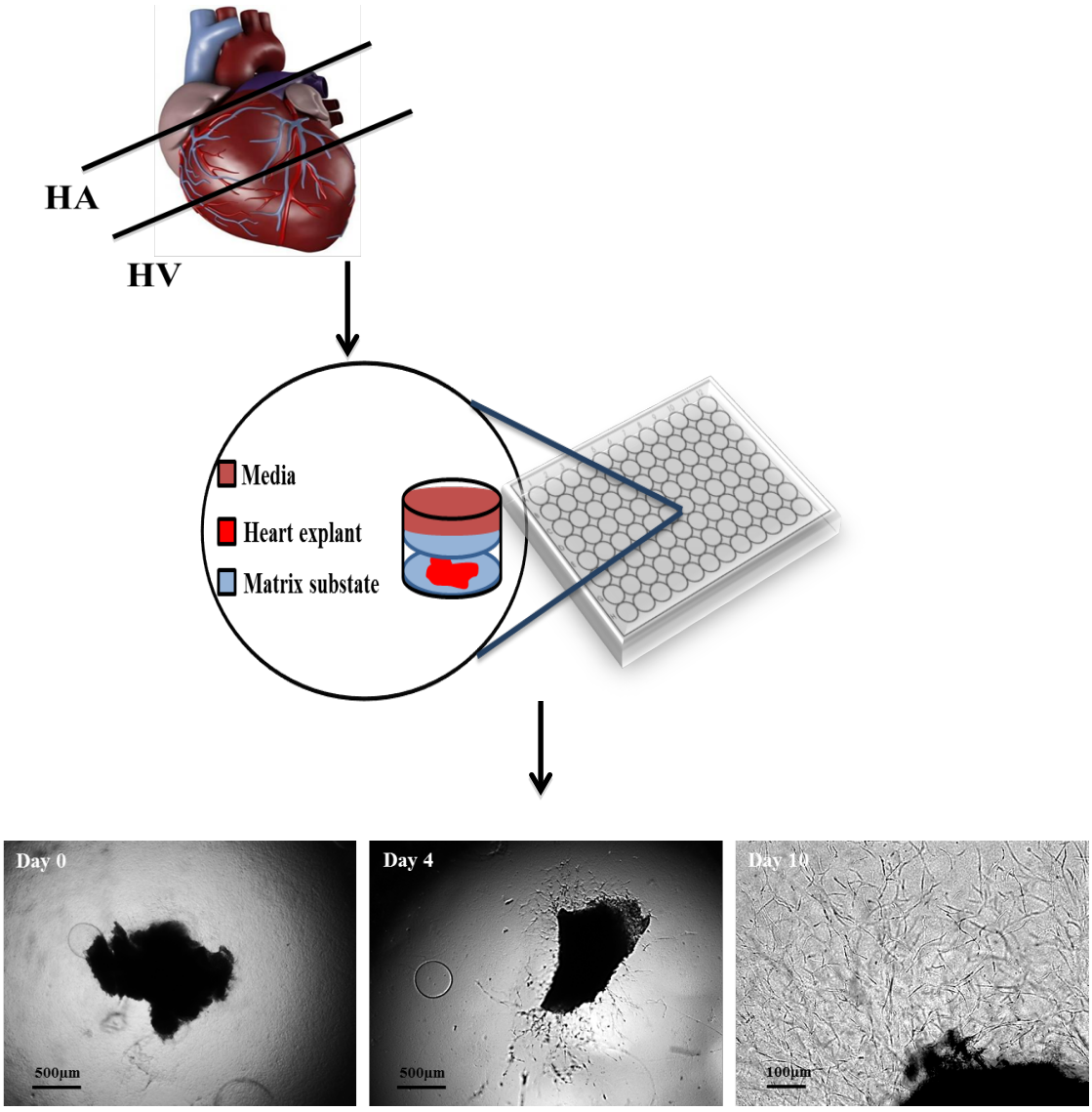

Figure 2.8 Schematic images of the heart explant assay experiments. Hearts were dissected into 2 parts: heart atrium (HA) and ventricular myocardium (HV). Each part was dissected into about 50 explants. Explants embedded in fibrin gel. Sprouts started forming between 3-5 days. After 10 days explants were fixed with 4% formalin and imaged.

2.8.2 Immunohistochemistry staining of heart explants sprouts

Immunohistochemistry (IHC) was used to visualize the angiogenic sprouts, through antigen-antibody interaction using labelled antibodies to specific tissue antigens. Different IHC methods can be used to localise antigens. Here, the fibrin gel cultures were first fixed with 4% formalin in PBS overnight after being detached from plates by a spatula. Then tissues were embedded in paraffin (for better localisation of tissue antigens) and several 5 μm sections were prepared. After sectioning, the slides were left at 37°C overnight to dry. The next day, sections were dewaxed by immersing in "dewax xylene" in 2 baths of xylene for 5 min. After that, they were hydrated for 3 min each in different concentrations of ethanol (2 x 99%, 1 x 95% and 1 x 70%) and washed in ddH_2O for 3 min. The next step was antigen retrieval. There are usually some protein cross-links, which have been formed by formalin fixation. The antigen retrieval process uncovers those antigens and improves their detection. For this step a sodium citrate buffer (2.94 g sodium citrate to 1 L ddH_2O and adjust pH to 6) was made. Then, sections were transferred in a sodium citrate solution bath and microwaved in that solution for 5 min at high power and 10 min at low power. After allowing sections to cool down for 20 min, they were washed in ddH_2O for 2 x 5min (with agitation). Next, blocking endogenous peroxidase was performed by immersing section slides in 3% H_2O_2 in either PBS (lectin staining) or methanol (CD31 and vWF antibody staining) for 30 min at 37°C. Slides were washed 2 x 5 min in PBST (with agitation), removed from the rack and placed on a slide chamber. The excess moisture was wiped off and each section on the slides was outlined using a wax pen. Prior to the addition of primary antibody, a serum blocking solution was made and sections were incubated with blocking solution for 30 min (without washing slides). Excess serum was drained and the primary antibody was then applied to sections for 1-2 h at RT or overnight in the fridge. After primary addition, slides were washed 2 x 5 min in PBST bath with agitation, and the secondary antibody was added to sections for about 1 h (in the meantime ABC reagent was made 30 min before addition). The primary and secondary antibodies were same as those antibodies listed in Table **2.9 (**with the same concentration**).**

The secondary antibody was washed off from the sections (2 x 5 min PBST bath), and sections were incubated with ABC reagent for 30 min. After another 2 x 5 min PBST bath washes, sections were stained with DAB solution for 2-7 min and washed in ddH_2O for 5 min. Cell nuclei were stained by immersing slides in Gill's Haematoxylin (Gills HTX) for 1-2 min and then rinsed in a bath of running tap water for 5 min. Tissue sections were dehydrated 3 min each through 70%, 90% and 2x 99% alcohol and then placed in mounting xylene 2 x 5 min. Finally, slides were mounted using DPX to secure the coverslips and then allowed to dry overnight at RT.

Note: For lectin immunohistochemistry antigen retrieval was not required. The secondary antibody step is eliminated and slides are incubated with ABC after adding lectin for 1h. Additionally, biotinylated lectin is applied at 20µg/ml in 1% BSA in PBS solution to cells and incubated for 1 h at RT or overnight at 4°C.

2.8.3 Haematoxylin and Eosin staining

In order to stain the cell nuclei and cytoplasm, haematoxylin and eosin (H&E) were used respectively. After fibrin gel fixation, paraffin embedding and sectioning, tissue sections were dewaxed by immersing in xylene 2 x 10 min and hydrated in 2 x 100%, 95% and 70% alcohol 5 min each. Then, they were stained in Gills HTX for 1-2 min and rinsed in a bath of running tap water for 5 min. Next, they were placed into a 70% and 95% alcohol solution for 3 min each. Following that, eosin staining was performed by immersing slides in an eosin bath for 2-5 min, and then they were transferred in a 95% alcohol bath for 5 min. At the end, tissue sections were placed in a xylene bath 2 x 5 min, mounted in DPX and coverslips were added on top.

2.8.4 Smooth muscle actin (α-SMA) staining of embedded heart explants tissue

Here the basic steps are similar to IHC staining procedure. However the primary antibody used was monoclonal anti-α smooth muscle actin (Sigma) (IgG). When a mouse primary antibody is used on mouse tissue the problem is that the secondary antibody is not able to distinguish

between the endogenous mouse IgG and the mouse primary antibody, which leads to a high non-specific background. This problem can be solved using the Vector mouse on mouse (M.O.M) immunodetection kit that reduces the unwanted binding of secondary antibody to endogenous IgG from tissue, as it contains a Mouse IgG Blocking Reagent with a specialized Biotinylated Anti-Mouse IgG. After dewaxing and hydrating the tissue sections, they were incubated with avidin D blocking solution for 15 min. Following brief washes with PBS, sections were incubated with biotin blocking solution for 15 min at RT. Blocking endogenous peroxidase was performed in pre-warmed 3% H_2O_2 in methanol at 37°C for 30 min. Sections were then washed 2 x 5 min in a PBS bath and incubated with a working solution of M.O.M mouse IgG blocking reagent (2 drops of stock solution to 2.5 ml PBS) for 1 h at RT. PBS washes were repeated and a working solution of M.O.M diluents (600 µl of protein concentration stock solution to 7.5 ml PBS) was added for 5 min at RT. Next, excess diluents was drained off and mouse monoclonal α-SMA was added (1:20,000) in M.O.M mouse diluents and applied to sections for 1 h at RT or overnight in the fridge. At this time, ABC reagent was prepared. After which, a working solution of M.O.M biotinylated anti mouse IgG (10 µl of stock solution to 2.5 ml diluents prepared as above) as secondary antibody was applied for 10 min at RT and then washed in a TBST bath. The ABC reagent was added, following which, DAB and Gills HTX staining were performed. Finally, sections were dehydrated and mounted in DPX.

2.8.5 Characterization of heart explants and outgrowing cells using Fluorescein-conjugated lectin

In this method, lectin was directly applied to heart explant cultures to characterize CEC without embedding and sectioning tissue. Explants were fixed with 4% formalin overnight. Then, they were washed with PBS 3 x 5 min. After that, they were incubated with 20 µg/ml fluorescein-conjugated lectin (GSL I-IB4) for 3-4 h. The probes were washed 3 more times with PBS and images were taken using a fluorescence microscope.

2.9 Interaction between endothelial cells and irradiated fibroblasts

In order to investigate the effect of irradiated fibroblast on ECs during angiogenesis and to study the effects of fibroblast irradiation on endothelial migration expression of pro-fibrotic proteins, several assays were performed using a new endothelial-irradiated fibroblast co-culture model.

2.9.1 Organotypic endothelial-irradiated fibroblast co-culture assay

The organotypic EC-fibroblasts co-culture assay was adopted in order to study the effect of irradiated fibroblasts on endothelial cell tubules formation. The same endothelial-fibroblast co-culture assay procedure was performed but this time fibroblasts were irradiated before they were mixed with the endothelial cells. Confluent fibroblasts in T-75 cm flasks were irradiated and 1 h after irradiation were trypsinised and mixed with trypsinised endothelial cells at a 1:3 ratio. They were cultured together as described in section 2.4.4. The media were changed every second day and after 14 days cells were fixed and ECs channels were stained using antibodies to vWF.

2.9.2 Fibroblast bed organotypic assay

This assay is basically the modified version of organotypic endothelial-fibroblast co-culture assay (Section **2.4.4**). ECs were directly plated on confluent fibroblasts. Since radiation affects the capacity of irradiated fibroblasts to adhere and grow, the fibroblast bed organotypic assay was used in place of organotypic endothelial-fibroblasts co-culture assay. In this assay fibroblasts (HDF) were plated in 24 well plates at density of 30,000 cells per well and allowed to develop over confluency, and irradiated at different radiation doses (0,0.2, 2, 8,16 Gy) prior to being co-cultured with endothelial cells. Therefore, they were able to adhere and grow properly before irradiation. Moreover, when cells reach super confluence they become quiescent and are less affected by radiation (Imaizumi *et al.*, 2010).

After irradiation of fibroblasts the HUVECs were trypsinised and plated on top of irradiated and non-irradiated fibroblast monolayers (18000 HUVECs/well). The full EBM media

containing 10% FCS and growth factors were used and cells were cultured together for 14 days. The ECs were fixed 14 days after plating on to confluent fibroblasts using 70% ethanol at −20°C for 30 min for further staining by immunohistochemistry. The channels were stained using antibodies to vWF (Figure **2.10**).

2.9.2.1 Analysis of the capillary-like structures

For obtaining data from the vessels formed by ECs, the tubule length, numbers and the number of branching points (cell junctions) were valuable parameters that could be measured. For quantifying tubules length, junctions and numbers, first their images were taken using the low-magnification (x 4) to cover the larger area of tubules. However because there were lot of capillary-like network formed in each well, 5 to 10 different images from the corner and middle of the each well were taken. Here the quantitative measurement was provided using the AngioSys software (TCS Cellworks). Each image processed was first loaded in the program to be processed. At least 2 wells (10-20 images) from each irradiated and non-irradiated group processed in each experiment and the result from multiple experiments analysed.

First tubules were separated from the surrounding tissue and background. By exploiting the differences between dark and light pixels in the AngioSys software, the tubules were extracted from background and measured. Therefore a binary image was created from the original based on the intensity level of underlying pixels by thresholding. However there were usually some dark areas at the corner of the image and sometimes the quality of images was poor which could cause spurious results. Therefore, for each image some manual interventions (changing the brightness and darkness) had to be performed to obtain a better quality image.

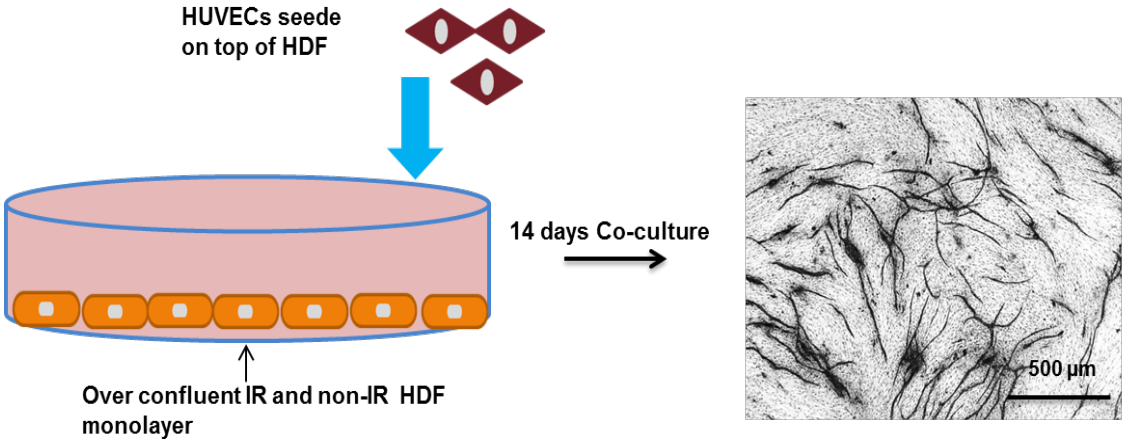

Figure 2.9 Schematic image of endothelial- and irradiated fibroblasts organotypic assay. Fibroblasts were plated to become over-confluent and were irradiated at different radiation doses. ECs were plated on top of the fibroblast bed 1 h after irradiation. Cells were cultured together for 14 days and channels stained using antibodies to vWF.

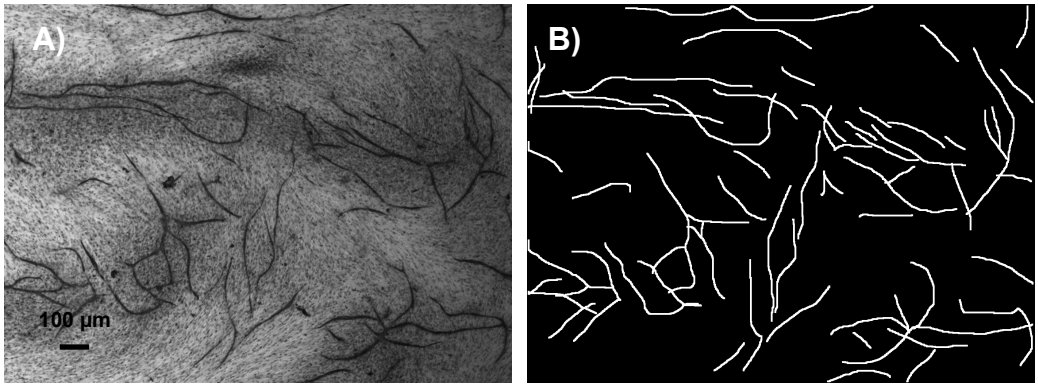

Figure 2.10 Images of capillary-like networks. A) Original image from capillary-like networks formed by HUVECs in fibroblast bed organotypic assay before AngioSys analysis **B)** the binary image of the original one from the AngioSys software (the AngioSys version).

Instead of extracting the tubules from the surrounding tissue by thresholding, they were manually traced. This was more time-consuming but more accurate with best quality of binary image. An original image and a schematic image of the binary image representing the manually traced channels are shown in Figure **2.10.** The binary images of tubules were then processed by the software; the total number of tubules, the tubules' length and junctions were measured. The results were monitored for each image to ensure they were reliable and repeatable. Because in each experiment, the numbers of capillaries formed by HUVECs in controls were different, the data for the irradiated groups was normalised and expressed as percentage of control unirradiated groups (% to control).

2.9.3 The fibroblast conditioned medium (CM)

The conditioned medium (CM) from irradiated and non-irradiated fibroblasts were added to endothelial cells to study the bystander effects of irradiated fibroblasts on EC migration and morphogenesis using the scratch wound assay and fibroblast bed assay. To condition the media, fibroblasts were plated in different T-75 flasks at equal density. After they reached confluency, the media were changed to ECs media (depending on which ECs were going to be used), and they were irradiated at different radiation doses. After 48 h CM was collected and concentrated as described in the section below.

2.9.3.1 Concentration of the fibroblast media

In order to concentrate the media (media with 2% serum or serum free media) the Vivaspin 20, 3,000 MWCO concentrator (GE Healthcare, cat.no. 28-9323-58) was used. The Vivaspin concentrators provided nondenaturing concentration of the conditioned media up to 30-fold concentration by membrane ultrafiltration. The concentrators could handle up to 20 ml of biological samples in its upper compartment (Figure **2.11**). The lower compartment is separated by a Polythersulfone membrane (PES MWCO Membranes, 3000 Daltons). The pressure applied by centrifuge forced solvent through the membrane into the lower chamber and resulted in more concentrated media in the upper compartment. The smaller size proteins

(according to the membrane molecular weight cut off) passed through the membrane and the larger proteins remained in the filter cup, which was collected.

Samples were concentrated at the speed of 4000-5000 rpm for about 4-10 times. The process took about 15-90 min, depending on the volume of media, which was between 5 to 20 ml. The more viscous the solution, the longer concentration would take. After the media were concentrated (for protein concentration the sample volume reduced to 1ml), they were collected in tubes and used for protein extraction or other experiments such as scratch wound assay. The samples were stored at -80°C.

2.11 Representative photo of Vivaspin 20 Centrifugal Concentrators.

2.9.4 The fibroblast bed organotypic assay and conditioned media from irradiated fibroblast

In the organotypic assay 20 ml HUVEC media was added to confluent HDFs before irradiation. One plate was kept un-irradiated as control. The media were left on cells for 2 days to be conditioned. On the same day (irradiation day) in parallel, HUVECs were plated on top

of the over-confluent fibroblasts. After two days, the CM from the control and irradiated HDF cells were added to the HUVECs- and HDF co-culture in organotypic assay. The media were replaced with 50% CM and 50% normal media every 2 days. The media were concentrated 4-5 times using the 20 ml concentrator (20 ml Vivaspin concentrator).

2.9.5 The Scratch wound assay conditioned media from irradiated fibroblast

In the migration assay, 20 ml of HUVEC media plus only 2% FCS and 20 ml of H5V media plus 2 % FCS (instead of 10% FCS) were utilized. The CM was then stored at 4°C to be used in the assay. While conditioning the media, ECs (HUVEC or H5V) were plated to become confluent. Near confluent ECs were incubated with irradiated and non-irradiated fibroblasts CM for 48 h. Cell migration assessed by wound scratching the monolayer and then CM were replaced by new fresh media

2.10 Analysis of molecular endothelial cells signaling pathways during angiogenesis after exposure to radiation directly or in response to irradiated fibroblasts.

2.10.1 Protein extraction from cells and conditioned media

To extract protein from EC and fibroblast monolayer cells, 1 X lithium dodecyl sulfate (LDS) reducing sample buffer was made (250 µl of 4 X NuPAGE LDS sample buffer (Invitrogen, Cat.no. NP0007), diluted at 1:4 in 650 µl distilled water and 100 µl reducing agent (Invitrogen, Cat.no. NP0009)) and heated to 70°C. Then, 50-150 µl of the buffer were added directly to the ECs or fibroblast wells. After that, the cell lysates were collected and dispersed using 27 G needles several times. The cell lysates were heated at 70°C for 10 min and then were either frozen or analysed by western blotting immediately.

In order to extract protein from media, conditioned media were added to sample buffer and reducing agent (100 µl 4 X sample buffer, 40 µl reducing agent and 260 µl conditioned media). After mixing, the sample was heated at 70°C for 10 min, then either were frozen or immediately analysed by western blotting.

2.10.2 Western blotting

Western blot is a method performed to detect a target protein from extracted protein samples. The proteins in whole cell extract or conditioned media are first separated by molecular size by gel electrophoresis, then transferred to a membrane and probed for specific antibodies to the target proteins. A list of antibodies used here and accompanying information is provided in table **2.10**. The NuPAGE electrophoresis system was used (Invitrogen, Cat.no. NP0315Box). First, precast NuPAGE® 10% Bis-Tris gels, which provide separation of small to medium-sized proteins (Da) were assembled in the electrophoresis tank. Then, 600 ml of 1X running buffer (3-(*N*-morpholino)propanesulfonic acid (MOPS) or MES (2-(*N*-morpholino)ethanesulfonic acid)) was added to the outer chamber and 200 ml of the same running buffer with addition of 500 µl antioxidant (Invitrogen, Cat.no. NP0005) was used to fill the upper buffer compartment. 20-30 µl of sample and an appropriate marker were heated for 10 min at 70°C and loaded into the gel, and then proteins were separated by gel electrophoresis (150 V, 200 mA for about 90 min). In the next step, proteins on the gel were electro-transferred onto the nitrocellulose membrane (200 V, 44mA for 1h). The gel, membrane (GE Healthcare, Cat.no. RPN3032D) and blotting paper were first soaked in 2X transfer buffer before being placed on an electrode plate. After the transfer, the membrane was first blocked in blocking solution (5% Milk in PBST or 3-5% BSA in TBST) for 2 h at RT and then it was incubated with the primary antibody at 4°C overnight. The next day, the membrane was washed 4 x 5 min in PBST/TBST and probed with secondary antibody for 2 h. After applying 4 more washes, detection of protein was performed in the dark room by enhanced chemiluminescence (ECL plus). The membrane was incubated with ECL plus (GE Healthcare, Cat.no. RPN213232) for 5 min, exposed to ECL film (GE Healthcare, Cat.no. 28906837) for 1-5 min, developed and fixed using Kodak X-ray developer and fixer reagents.

Reprobing the membrane was performed to allow use of additional antibodies. First the blot was stripped using 20-30 ml of Pierce stripping reagent (Thermo Scientific, Cat.no. 21059) for

30 min on a shaker at RT. Then, the blot was washed in PBST/TBST and after that antibody incubation and ECL detection performed as above.

2.11 Proteome Profiling

In order to investigate the changes of cytokines in the irradiated fibroblast conditioned media, antibody arrays were used. The R&D human cytokine array (Cat.no. ARY005) and a human angiogenesis array (Cat.no. ARY007) were utilised in this project. This system has different antibodies to cytokines or angiogenesis-related proteins spotted on nitrocellulose membranes supplied in the kit (Appendix **VI** and **VII**).

Fibroblast cells were plated at equal density in a number of T-75 flasks. After cells reached confluence the media was changed with 20 ml of pre-warmed EBM media in the absence of serum and growth factors. Cells were irradiated, with one flask kept unirradiated as control. Cells were incubated at 37°C for 48 h before media were collected. Next, carefully, without disturbing the cells, the media were placed in tubes and centrifuged for 10 min at 4°C to remove any cells. Media were then concentrated using Vivaspin 20 concentrators (20 ml maximum volume), which allowed the smaller size molecules less than < 3000 kDa to flow through the membrane and the larger proteins to remain in the concentrated media. Samples were concentrated in the centrifuge (4000-5000 rpm) at 4°C for approximately 10 times, which reached the volume from 20 ml to 2 ml. Samples were then collected in small Eppendorf tubes and the normal FBM media added to adjust all volumes to 2/3 ml.

The concentrated wash buffer in the kit was diluted in deionized water. One vial of biotinylated antibody cocktail was reconstituted with 100 µl of distilled water. First 2 ml of Array buffer, which served as a block buffer, was added to a 4-well multi-dish and then 4 membranes supplied were placed in wells carefully, using a tweezer, with array numbers facing upward. The membranes were incubated for 1 h with the blocking solution on a rocking platform. In the meantime, samples were prepared by adding 0.5 ml of array buffer to up to 1 ml of each sample in separate tubes.

Primary Antibody	Dilution	Wash solution	Blocking Solution	Secondary Antibody	Dilution
Phospho-histone H2A.X (Abcam, Ca.no. cb6992	1:1000	TBST	TBST+ 3% BSA	Polyclonal goat anti rabbit IgG DAKO p0448	1:2000
Anti-beta actin (Abcam, Cat.no. ab8226)	1:2000	PBST	PBST+5%M milk	Polyclonal goat anti mouse IgG DAKO p0448	1:2000
Beta III Tubulin (Abcam, Cat.no. ab52901)	1:2000	PBST	PBST+5%M milk	Polyclonal goat anti rabbit IgG DAKO p0448	1:2000
TGF-b (Abcam, Cat.no. ab66043)	1: 500	PBST	PBST+5%M milk	Polyclonal goat anti rabbit IgG DAKO p0448	1: 3000
Phospho-Smad (Cell Signaling, Cat.no. 9520)	1:1000	TBST	TBST+ 5% BSA	Polyclonal goat anti rabbit IgG DAKO p0448	1:2000
Smad 2/3 (Cell Signaling, Cat.no. 5678)	1:1000	TBST	TBST+ 5% BSA	Polyclonal goat anti rabbit IgG DAKO p0448	1:2000

Table 2.10 Primary and secondary antibodies used for Western blotting

The samples and blocking buffer were adjusted to the final volume of 1.5 ml, and array buffer 5 was added to the solution if necessary. Following which 15 µl of the reconstituted antibody was added to the sample/blocking buffer and incubated for 1 h at RT. The array buffer was aspirated from the membrane in the 4-well multi-dish and the sample/antibody mixture prepared earlier added to the membrane. The lid was placed on the dish and the mixture was incubated overnight at 4°C on a rocking platform.

The next day each membrane was placed into individual containers and washed 3 times for 10 min each, with a wash buffer on a rocking platform shaker. The lower edge of each membrane was placed onto absorbent paper to drain the excess buffer from the membrane and then returned to the 4-well multi-dish container. Then a streptavidin-HRP solution was prepared by dilution in the array buffer 5 (dilution factor 1:2000). 2 ml of diluted streptavidin-HRP was added to the membrane for 30 min at RT on a rocking platform. After washing, each membrane was exposed to 0.5 ml of chemiluminescent reagent prior to developing the blots on film. To analyse data, the transparency overlay supplied in the kit was aligned on the array image with the three pairs of positive control spots, placed in the corner of array. Therefore, following identification of the positive control spots on the array image, the remainder of the spots were identified according to their location. The array film was first scanned and the image for each irradiated and non-irradiated sample was analysed using the Quantity One 1-D analysis software (Bio-Rad). In order to compare the corresponding signals on the irradiated array to the control, the pixel density of each spot of arrays was quantified. The average pixel density of the pair of duplicate spots representing the cytokine was determined.

2.12 Statistical Analysis

Most experiments were performed in triplicates or more (exceptions have mentioned in the results chapters). All graphs presented here were plotted using GraphPad Prism software. Error bars on graph represent the standard deviation of the replicates and indicate the variability of data. Data were expressed as the Standard Error of Means (SEM) of $\geq$ 3 independent experiments.

If means of three or more independent groups were to be compared, One-way ANOVA (Analysis of variance) test performed. The Two-way ANOVA was carried out to determine the statistical differences between groups with two independent variables each (different treatments). All statistical analysis was performed using the GraphPad Prism statistical software package. The statistical differences determined through One-way and Two-way ANOVA were both followed by Tukey's honestly significant difference (HSD) post hoc test. p values of < 0.05 were considered as significant and are indicated by *.

The ANOVA Kruskal-Wallis test, which is a commonly used non-parametric technique, was performed to determine the statistical differences between several independent samples that have different sample sizes. It was performed for Heart explant data (Section **4.2.3**). The parametric equivalent of Kruskal-Wallis test is the one-way ANOVA test.

Chapter Three

In vitro models of angiogenesis to examine the effects of radiation on endothelial cell angiogenic properties

3.1 Introduction

Humans are constantly exposed to natural background radiation in low doses, with a significant body of evidence indicating that exposure, even at such low doses of radiation, causes many clinical problems (Kim *et al.*, 2007). More importantly, as discussed earlier, routine radiotherapy in the treatment of breast cancer has been reported to cause localised radiation induced damage to heart tissue (Clarke *et al.*, 2005; Preston *et al.*, 2003; Wong *et al.*, 1993), supporting a real need for the biological effects of low doses of radiation to be further studied in more detail. In terms of the biological targets of radiation, microvessels are reported to be more sensitive to radiation, and angiogenesis has been reported to be a direct target of radiation-induced damage (Ahmad *et al.*, 2007; Fajardo, 2005; Grabham and Sharma, 2013; Imaizumi *et al.*, 2010; Prionas *et al.*, 1990). However, until now, few comprehensive studies have been carried out to delineate the mechanisms involved in the anti-angiogenic effect of radiation, particularly with respect to radiation-induced heart disease. The objective of this chapter was therefore to investigate direct effects of radiation on EC angiogenesis using *in vitro* models. The first half of the chapter describes the methods that were established in order to successfully isolate CECs, whilst the second half of the chapter details various *in vitro* models of angiogenesis that were used as a means of assessing the direct effects of low, moderate and high doses of radiation on the angiogenic properties of the isolated CECs as well as established cell lines.

3.1.1 Effect of radiation on endothelial cell angiogenic properties using *in vitro* models

Several angiogenesis *in vitro* models including; assessment of endothelial clonogenic survival, proliferation, migration and tubule formation, described previously in other studies, were used in this chapter (Benndorf *et al.*, 2008; Bishop *et al.*, 1999). However, a novel self-assembly model of ECs was also developed to study the effect of radiation on mouse CEC angiogenic properties. Endothelial cells isolated and cultured from mouse hearts and/or established endothelial cell lines were used in these experiments. As the aim of this project was to investigate the effects of radiation on mouse cardiac endothelial cell angiogenic activities, the

use of H5V cell which has been derived from mouse embryo hearts and therefore resemble more closely primary CEC than the other EC lines, was preferred. However because H5V cells received later during the project, initially two EA.hy 926, bEND.3 cells were used to establish appropriate experimental working conditions (before receiving H5V cells).

Cells were irradiated at different radiation doses (0.2, 0.5, 1, 2, 5, 8 and 16 Gy), delivered at a dose rate of 0.5 to 0.58 Gy/min. The principles behind the EC isolation procedure and the angiogenesis models used are briefly described below.

3.1.1.1 Isolation of mouse cardiac endothelial cells (CEC)

Since ECs from different origins within the body could express unique and specific responses to radiation exposure, it was important to isolate cells from the mouse heart to use for modelling angiogenesis *in vitro*. The ECs are tethered to the blood vessels, in contrast to circulatory cells, making their isolation difficult (Aird, 2012). Therefore, an important consideration in this chapter was to establish an effective means of isolating intact CECs that retained their *in vivo* properties, which would allow us to study consequences of *in vivo* radiation using *in vitro* models. An isolation method based on enzymatic dissociation of heart cells to single cell suspension was used and then CEC selection was performed using antibodies to EC surface antigens (CD31 & CD105) coupled to magnetic "Dynabeads". The PECAM-1 (CD31) and endoglin (CD105) antibody against the extracellular protein as well as lectin GSL I-B4 are some of the common ECs markers used for their isolation and characterization which are not expressed on other cells such as smooth muscle cells (Lidington *et al.,* 2002; Oxhorn *et al.,* 2002). PECAM-1 is a 130-140-kDA glycoprotein, an adhesion molecule of IgG gene superfamily and a highly specific, expressed marker of ECs. It plays a role during inflammatory event by adhesion and extravasation of leukocytes toward the ECs (Oxhorn *et al.,* 2002).

The cells selected by the antibodies were then isolated by magnetic separation (Marelli-Berg *et al.*, 2000; Nistri *et al.*, 2002). The hearts of SCID mice used to optimise the isolation experiment since this strain was more available in the TMG group (between 6 to 22 weeks old). The hearts of C57BL/6 mice was also isolated as this strain was the one used in CARDIORISK project.

3.1.1.2 Evaluation of radiation effects on EC clonogenic survival and proliferation

It is well established that radiation can induce cell cycle arrest, DNA damage and ultimately cell death (Little *et al*., 2003; Nikjoo *et al*., 2001). The level of angiogenesis is related to the proliferation potential of ECs as well as their migration and morphogenesis (Maity *et al.*, 1994; Morris, 1996). Therefore, radiation effects on EC proliferation might impede angiogenesis (Juckett *et al.*, 1998; Rhee *et al.*, 1986). To examine this, assays investigating the effects of radiation on cell proliferation, clonogenic survival and DNA damage of ECs were used. The ability of cells to proliferate indefinitely and form a colony is determined using the clonogenic survival assay. The clonogenic assay or colony formation assay is an *in vitro* assay to determine cell reproductive death after radiation exposure (Franken *et al.,* 2006; Munshi *et al.*, 2005). This assay has been used to determine the radiosensitivity of ECs. In addition, growth curve experiments on ECs were performed to assess the influence of radiation on EC growth after exposure to different radiation doses. Furthermore, the level of γ-H2AX positive cells indicated those cells exhibiting DNA-damage caused by radiation (Hamer *et al.*, 2003; Lee *et al.*, 2012).

3.1.1.3 Evaluation of radiation effects on EC migration

Since migration of ECs is crucial for sprouting angiogenesis, it was important to investigate the effects of radiation on migration. Many studies have previously established the relationship between radiation and migratory effects, but importantly, not using the cell models and radiation dose regime used in this study (Imaizumi *et al.*, 2010; Rousseau *et al.*, 2011; Zheng *et al.*, 2011). Cells were exposed to different doses of radiation (0.2 to 16 Gy) in order to compare the radiation effects at low, moderate and high doses. The *in vitro* scratch wound

assay is a suitable method to study cell migration. Upon creation of a scratch (wound) on a confluent endothelial monolayer, cells on each edge of the wound migrate towards each other until they close the wound and establish cell-cell contact again (Liang *et al.*, 2007; Zheng *et al.*, 2011). This assay mimics the behaviour of cell migration in the *in vivo* context to some extent, for example during the wound healing process (Liang *et al.*, 2007).

3.1.1.4 Evaluation of radiation effects on EC capillary-like formation

ECs are capable of forming tubules spontaneously *in vitro*. Some angiogenesis assays such as the Matrigel assay and fibroblast-endothelial co-culture assay give some measurement of the ability of ECs to migrate and differentiate into capillary structures. Differentiation of ECs depends on growth factors and presence of extracellular matrix proteins.

Matrigel Assay: Matrigel is a basement membrane, which contains basement proteins such as collagen IV and laminin (BD Biosciences) and is used commonly to stimulate tubule formation in endothelial cells (Ahmad *et al.*, 2007; Bishop *et al.*, 1999). To encourage ECs to form capillary-like structures *in vitro,* a morphogenic matrigel assay was carried out, to assess the formation of capillary like tubules by ECs in a short-time period and a semi-solid media.

Organotypic fibroblast-endothelial co-culture assay: Angiogenesis is a complex process, involving interactions between ECs and other cell types such as fibroblasts, pericytes and immune cells and is dependent on the availability of growth factors, enzymes and ECM molecules (Bishop *et al.*, 1999; Goodwin, 2007; van Hinsbergh and Koolwijk, 2008). Many *in vitro* angiogenesis assays do not model the whole process adequately. However, Bishop *et al* (2000) established that co-culturing fibroblasts with ECs *in vitro*, which enabled ECs to proliferate, migrate and differentiate into capillary structures resembling the microvascular bed. Therefore this fibroblast/EC co-culture assay was used to investigate the effects of radiation on EC angiogenic properties.

3.2 Results

3.2.1 Isolation of CEC

The isolation of ECs is technically difficult, time consuming and costly. Previous studies have reported the isolation of ECs from different organs such as lung, lymph node, brain and heart. The isolation of ECs from mouse hearts was found difficult and they were capable of being passaged only 2 to 3 times before reaching senescence (Dong *et al.*, 1997; Lidington *et al.*, 2002; Marelli-Berg *et al.*, 2000), inferring the need therefore for improved and reliable methods to establish CECs, capable of being maintained in *in vitro* cell culture.

At the time of this study, Dr Sheila Francis (Cardiovascular Science Department, University of Sheffield) had initially established an 'in house' method for isolating CECs, and this had been further adapted in our laboratory by Dr Chryso Kanthou and Mr. Karol Jelonek, based on a published method by Lim and Luschinskas (2006). The method is based on dissection of heart tissue and enzymatic dissociation of heart cells to a single cell suspension using collagenase and trypsin. CEC selection is then performed using antibodies to EC surface antigens (CD31 & CD105) coupled to magnetic "Dynabeads" **(**Figure **3.1)**. The cells selected by the antibodies are then separated using a magnet, and maintained in culture in appropriate media, changed every second day with 10 ml of complete medium. In order to obtain CECs to irradiate and then test in the *in vitro* angiogenesis models, the method described above was adopted, however initial experiments yielded low numbers of CECs, unable to grow beyond 2 passages in culture, exhibiting fibroblast contamination when viewed under the light microscope (Figure **3.2**). Moreover, these issues were compounded when mouse hearts, taken from animals (both SCID and C57BL/6 mice) more than a few weeks old, were used. Figure **3.2** shows an image of primary cells growing in culture. A number of strategies were therefore adopted to try and improve these difficulties as described below:

3.2.1.1 Varying the amount of Dynabeads and centrifugation speed

In an attempt to improve the yield of isolated CECs, different amounts of antibody coupled Dynabeads were tested (between 0.5-3 µl, corresponding to approximately 4 x 10^5 – 2.4 x 10^6

beads). These experiments revealed that the higher concentration of beads was toxic to cultured cells and 8 x 10^5 beads were enough for efficient CEC selection. Moreover, by performing all steps of the procedure faster, fewer cells were lost during the isolation process. To initially improve the purity of the isolated CECs, cells were spun at varying centrifugal speeds, and centrifuging cells at 400g for 10 min was found to be optimal for separating ECs from certain cell populations such as red blood cells and any debris formed.

However, a major difficulty to overcome was contamination of isolated CEC specifically with fibroblasts **(**Figure **3.2)**. One reason for fibroblast contamination was probably due to the fact that cells could not be dissociated completely into a single cell suspension and existed always in clumps, such that upon CEC selection using antibody coupled Dynabeads, there were always some fibroblasts or other cells, possibly pericytes and smooth muscle cells, still attached to the CECs and not dissociated completely. Consequently, they were selected with the CECs during the following magnetic separation process, resulting in their growth alongside the CECs.

3.2.1.2 Use of mechanical syringing to improve tissue dissociation into single cell suspensions

By way of improving the isolation of pure CEC populations, two further approaches were adopted. First, tissue was dissected and thoroughly minced into small 1mm^3 pieces in order to reduce the size of the tissue fragments and speed up the digestion process. Partially digested tissue was then syringed, several times using different needle sizes in sequence (16G, 18G and 19G), approximately 45 min after initiating collagenase digestion, to mechanically dissociate clumps. Next, cells were passed through a sterile filter to remove undigested tissue clumps and cells were syringed a further two times to help dissociating any remaining clumps. Cell suspensions were then centrifuged to remove red blood cells and any debris formed.

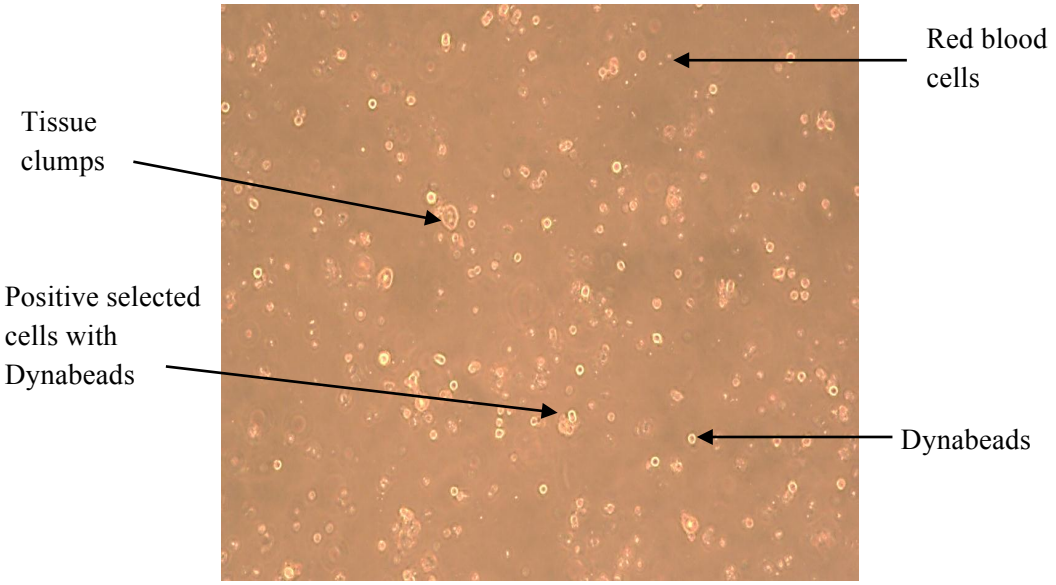

Figure 3.1 Phase-contrast microscopy of a mixed cell population from a mouse cardiac tissue digest incubated with magnetic "Dynabeads". Antibody-coupled dynabeads were used to select CECs, which were isolated by magnet separation. Positive selected cells are shown above, alongside selected cells bound to Dynabeads. In addition, non-dissociated cells were observed in the form of tissue clumps. The small-sized, round shaped bodies were red blood cells, which were present in cell suspension.

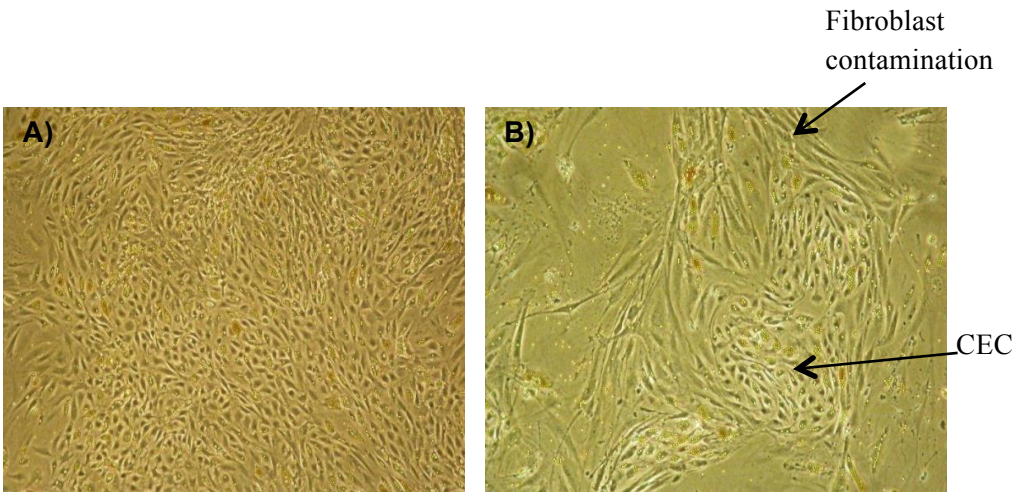

Figure 3.2 Phase-contrast images of primary CECs in culture. A) Confluent culture of mouse heart CEC one week after isolation. **B)** An example of a CEC culture contaminated with fibroblasts. All cells were viewed using the x4 objective.

By looking at the cell suspension from mouse heart tissue digest under the light microscope, it was observed that performing these steps helped to improve dissociation of tissue clumps into single cells. However since initial experiments performed to optimise the conditions, the assessment only performed visually under the microscope and no data for quantification were collected**.**

3.2.1.3 Use of enzymatic digestion to improve tissue dissociation into single cell suspension

Whilst collagenase digests and breaks down most connective tissue, previous studies have shown that trypsin can be useful for releasing cells from tissue therefore aiding separation and dissociation of tissue clumps into single cells (Marelli-Berg *et al.*, 2000). Isolation of heart cells was performed therefore with and without trypsin. However, trypsin could kill cells if left for long periods of time and more importantly, is known to damage and digest cell surface receptors such as CD31 (Marelli-Berg *et al.*, 2000). Accutase is an enzyme less toxic than trypsin, and was used instead of trypsin to overcome these problems. Accutase and trypsin were both tested in different experiments, which showed that trypsin was more successful in separating cells than accutase. However, after culturing the isolated cells, those treated with trypsin was less viable and grew slower than accutase treated cells. Data were not available for these preliminary experiments to be shown.

3.2.1.4 Dissociation of tissue with collagenase and trypsin followed by overnight growth in a Teflon-bag to improve cell yield

Another approach to optimize isolation of CEC used a Teflon bag system, a method that was established by our collaborator Dr Gabriele Multhof in Germany. After digestion and dissociation of heart tissue cells, the mixed cell suspension was incubated overnight in a Teflon bag (which is permeable to gases), which had the advantage of helping cells recover and re-express their receptors which were digested by trypsin during the isolation procedure. Importantly, the cells did not adhere to the Teflon material in the bag but remained in suspension. The following day anti-CD31 antibody-coupled Dynabeads were added to cells

and positive cells selected by magnet. Whilst these experiments improved the yield of CECs over the previous methods, comparing the number of cells before and after incubation in the Teflon bag showed that there was always some cell loss. Results from six separate experiments using the Teflon bag method showed there were 45.3% ± 5.4 calculated cell loss upon comparing the number of extracted cells from the first day through to the second day of the experiment, following Teflon bag incubation. To compare CEC isolation yield in T-bag and normal method, a parallel experiment was performed using 2 female SCID mice for each experiment, and the number of extracted cells before CEC antibody selection was calculated. Figure **3.3** shows the isolated CEC with or without using the Teflon bag after one week of culture. The result showed that although the total number of extracted cells using the Teflon-bag (before antibody selection) method was reduced compared to the enzymatic method alone (Table **3.1**), the yield of viable CEC from the T-bag method was superior with more cells proliferating and surviving in culture after 7 days. Therefore, the Teflon bag was the preferred method of CEC isolation. Whilst using Teflon bag method improved the yield of CEC antibody selection even from older mice, the isolated CEC cultures were still contaminated with fibroblasts.

Moreover, isolated CEC was required to be characterised to study whether they retained the functional properties of CEC. One of ECs specific characterisations is capillary-like tubule formation, which is not seen in other cells (e.g. smooth muscle cells) (Lidington *et al.*, 2002; Oxhorn *et a.l*, 2002). The CEC staining with specific EC markers (PECAM-1and lectin) could confirm their identity. However, due to time constraints no functional studies on isolated CEC were performed.

Number of extracted mouse heart cells using enzymatic method	Number of extracted mouse heart cells using Teflon bag (day 2)
$10x10^6$	4.5×10^6

Table 3.1 The number of isolated mouse heart cells cultured, resulting from the two methods of isolation.

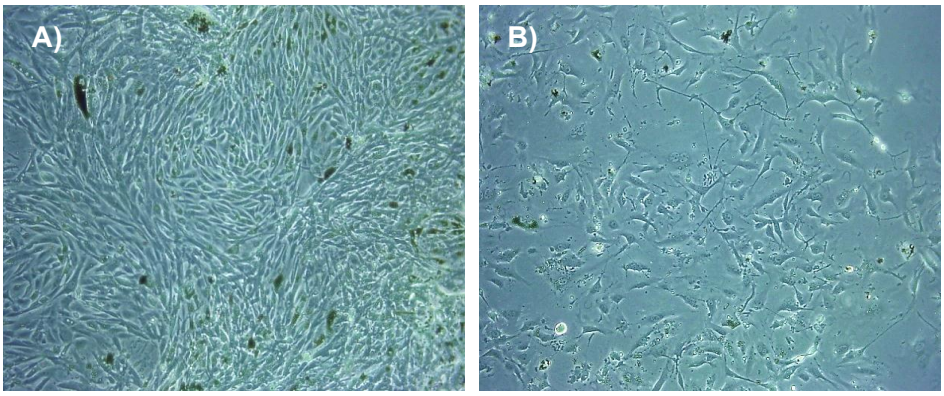

Figure 3.3 Cultured CEC isolated from 9 weeks old SCID mouse hearts with and without overnight incubation in a Teflon bag. (**A**) CEC isolated from two hearts (9 weeks SCID mouse) using the Teflon bag method and cultured for 7 days. (**B**) CEC isolated from two hearts (9 weeks SCID mouse) without using the Teflon-bag step and cultured for 7 days.

3.2.2 Radiation effects on EC survival and colony formation

Due to the problems associated with directly isolating mouse CECs (as described above), in order to examine the direct effects of radiation on EC angiogenic properties, all subsequent experiments were performed using established EC lines (Section **2.1.1**). To assess the effects of radiation on cell survival, the clonogenic assay was performed, where the ability of plated cells to form a viable colony was measured. The cell lines, H5V and HDF (fibroblasts) were grown to confluence, then irradiated at doses ranging from 0.5-8 Gy. In parallel non-irradiated cultures were used as controls. An appropriate number of cells were then sub-cultured and seeded into dishes and incubated for 10-20 days, to enable sufficient viable colonies to form for quantification. The specific seeding densities used for each radiation dose (0.5-8Gy) are presented in Table **3.2**. Cells from both irradiated and non-irradiated cultures were then fixed and stained in 0.1% methylene blue and visible colonies counted.

IR doses	H5V/HDF cells
0 Gy	500
0.5 Gy	500
2 Gy	1000
8 Gy	2000

Table 3.2 Cell seeding densities at different radiation doses. The table shows the seeding densities/dish used for each radiation dose.

The plating efficiency (PE) was calculated for both irradiated and non-irradiated cultures, as a measure of cell survival. PE was calculated, as described in previous studies (Franken *et al.*, 2006; Munshi *et al.*, 2005; Schleicher *et al.*, 2011), by dividing the number of visible colonies formed, by the number of seeded cells for each culture. The surviving fraction was then determined by dividing the PE for each irradiated culture by the PE calculated for the non-irradiated (0 Gy) control cells as described in Section **2.5**.

For H5V cells, three independent experiments were performed and in each case, cells were seeded in triplicate into three separate culture dishes, for both irradiated and non-irradiated control cells. Data from the three separate experiments were expressed as mean ± SEM and analysed using a One-way ANOVA test. However, only one experiment was performed (using triplicate dishes) for HDF cells since EC were the main focus and also due to the time constraints. The SF was then calculated for both cell lines (H5V and HDF), at the corresponding doses of radiation 0.5, 2 and 8 Gy and the data plotted graphically as shown in Figure **3.4**. This revealed that treatment with radiation resulted in a decline in cell survival in both cell lines. The effects of radiation on reduction of H5V survival were statistically significant (≥ 0.5 Gy) with the SF for H5V cells at 8 Gy being near to zero (0.004), as shown in Figure **3.4**.

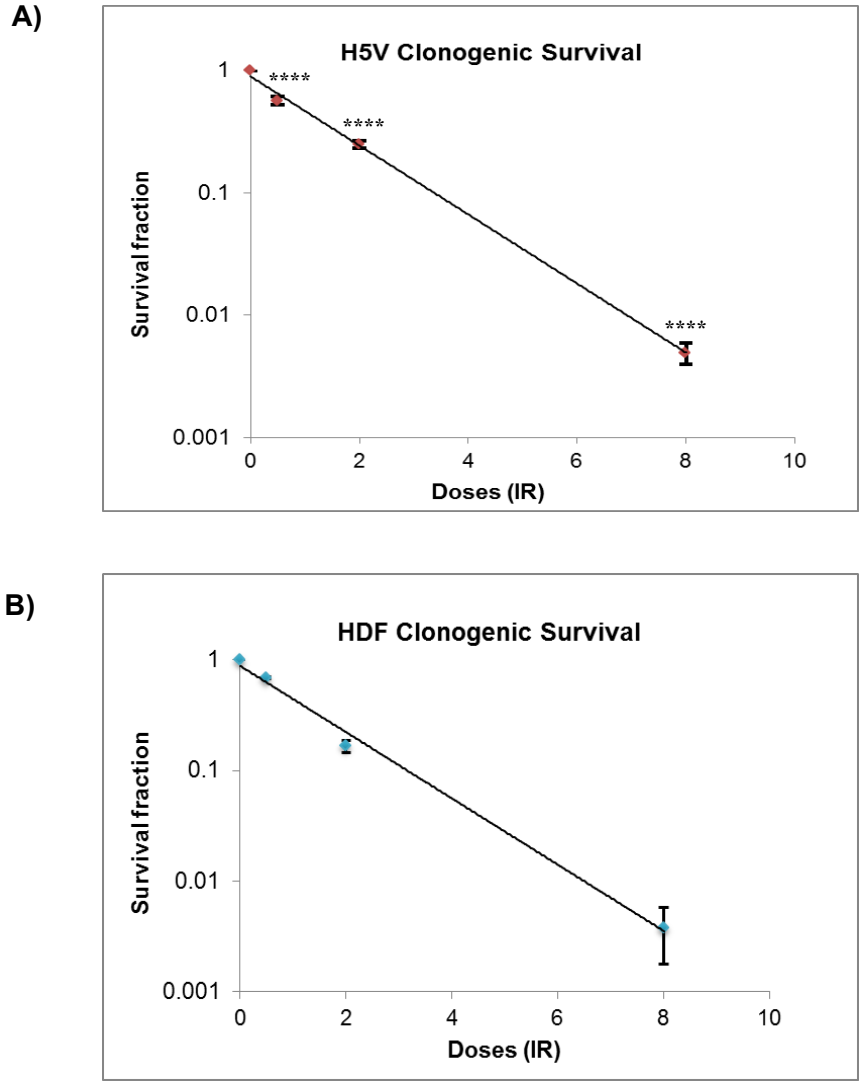

Figure 3.4 Effects of radiation on survival of H5V and HDF cells. Confluent H5V and HDF monolayers were irradiated at 0 (control), 0.5, 2 and 8 Gy and seeded immediately following irradiation. After 10 days, cells were fixed, stained and counted. Colonies consisting of more than 50 cells were counted and the SF calculated **A)** A significant reduction in H5V cell survival and colony-forming ability was observed following exposure to radiation, and this was dose-dependent. Results are expressed as mean ± SEM of 3 experiments (each performed in triplicate). Statistical analysis was performed using the One-way ANOVA test (****$p < 0.0001$) **B)** The HDF data show that exposure of HDF cells to radiation resulted in reduced cell survival and colony-forming ability, again which was dose-dependent. This result is expressed as mean ± SEM of one experiments performed in triplicate.

3.2.3 Analysis of H2AX phosphorylation to confirm radiation response

Radiation is known to cause DNA DSBs. Histone H2AX is a protein phosphorylated at serine 139 in response to DNA damage, resulting in γ-H2AX foci at DSB sites. Therefore, γ-H2AX can be used as a marker of radiation induced DNA DSB damage (Hamer *et al.*, 2003; Ismail *et al.*, 2007; Marti *et al.*, 2006). To determine the efficacy of radiation on cells, detection of γ-H2AX foci using a fluorescent γ-H2AX-specific antibody is a quantitative method to measure DSBs within irradiated and non-irradiated cells (Hamer *et al.*, 2003; Marti *et al.*, 2006).

In parallel with the clonogenic survival assays, confluent HDF and H5V cells were irradiated at 4 and 8 Gy respectively and incubated overnight. Radiation delivered at two random doses initially to test the efficiency of radiation on cells by the X-ray machine. Cell proteins were then extracted and analysed by Western blotting to detect phosphorylation of H2AX (Abcam, Cat.no. cb6992) (Figure **3.5**). Non-irradiated HDF and H5V cells were included in parallel as controls. Whilst phosphorylated γ-H2AX was detected in both cell types in the absence of radiation, the levels of phosphorylated γ-H2AX increased in irradiated HDF and H5V compared to the non-irradiated cells. This is in agreement with previous studies (Hamer *et al.*, 2003; Lee *et al.*, 2012) and importantly confirmed that the X-ray machine used in this study was working efficiently.

In addition to detecting γ-H2AX by Western blotting, fluorescence microscopy was performed using an anti-γ-H2AX antibody (Cell Signaling, Cat.no. 9718). H5V cells were plated at 5000 cells per well. Confluent H5V cells were irradiated at 8 Gy (the same dose used in western blotting) and non-irradiated cells were included as a control. After overnight incubation, both irradiated and non-irradiated H5V cells were fixed and stained with the specific γ-H2AX immunofluorescence antibody (section **2.6**), and observed under microscope. Previous studies report that DSBs, sites of radiation induced DNA damage, appear as fluorescent punctate/granular foci when using an anti γ–H2AX antibody (Marti *et al.*, 2006; Sentani *et al.*, 2008).

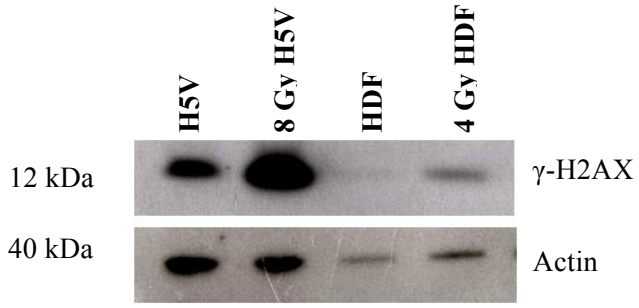

Figure 3.5 Detection of γ-H2AX by Western blotting. H5V and HDF cells were irradiated at 8 and 4 Gy respectively. Proteins were extracted 24 h after irradiation and analysed for H2AX phosphorylation (γ-H2AX) by Western blotting. The results indicate phosphorylated H2AX (12 kDa) was detectable in both cell types before and after irradiation. However, the levels of γ-H2AX increased in irradiated cells. The blot was re-probed for actin (40 kDa), a steady-state housekeeping protein, which indicates equal protein loading. This is a representative image/blot from one experiment.

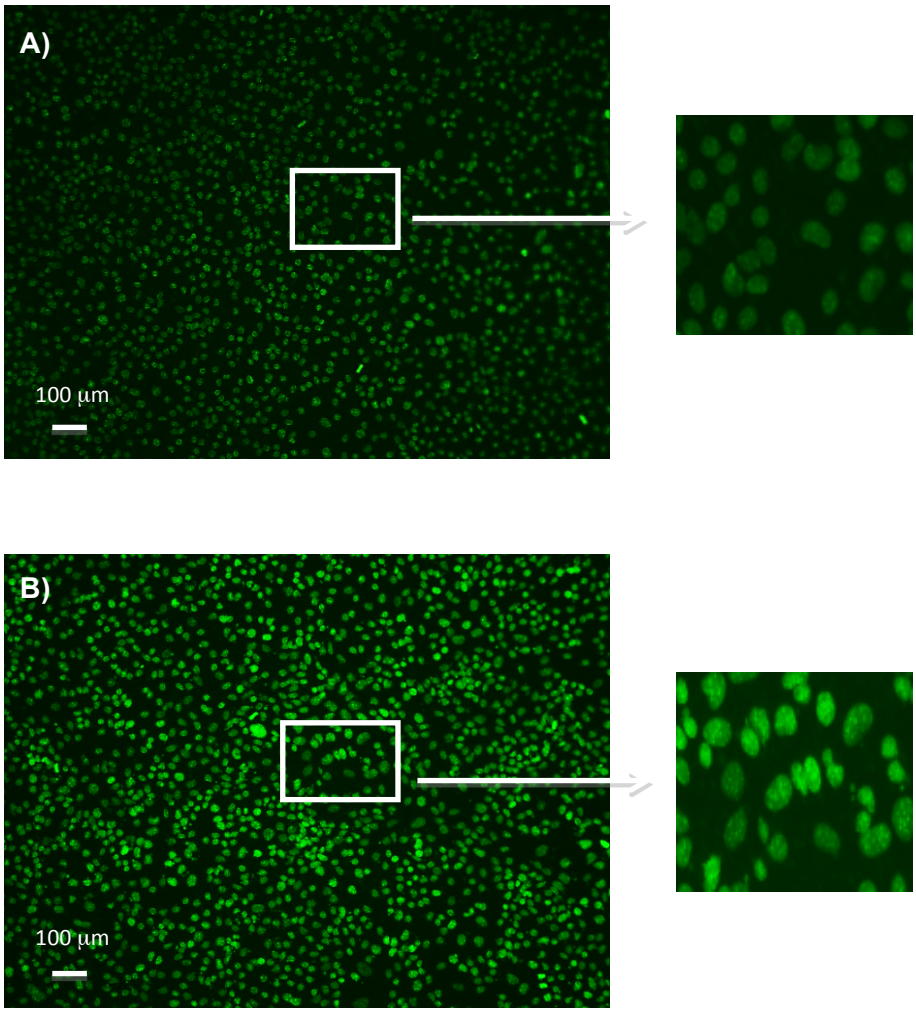

Figure 3.6 Immunofluorescent staining of H2AX. Representative images show immunofluorescent staining of γ-H2AX in (**A**) control non-irradiated H5Vcells and (**B**) cells irradiated at 8 Gy, seeded at densities of 5000 cells per well. After 24 h incubation, cells were stained using a fluorescent anti γ-H2AX antibody, and H2AX phosphorylation observed in both irradiated and non-irradiated H5V cells. However, the intensity of staining in irradiated cells was higher with bright-punctuated foci more evident following radiation exposure.

As seen in Figure **3.6**, punctate staining could be observed in both irradiated and non-irradiated H5V cells. However, the staining was much brighter in irradiated cells, suggesting an increase in DSBs. This is in agreement with the Western blot data shown above in Figure **3.5** demonstrating that low levels of DSBs are present in cells even in the absence of radiation, but there is an increase following irradiation of cells. γ-H2AX foci appear rapidly after irradiation, therefore, H2AX phosphorylation should be detected soon after radiation at different time points from 1 to 24 h (Jelonek *et al.*, 2011; Marti *et al.*, 2006). This experiment only performed once and investigating H2AX phosphorylation at different radiation doses and time points should be performed in future work. Together results confirmed the radiation response in H5V cells by inducing phosphorylation of H2AX using the X-ray machine.

3.2.4 Radiation effects on EC growth and proliferation

It is well established that radiation can causes inhibition of EC proliferation (Ahmad *et al.*, 2007). To determine the direct effect of radiation on cells, an *in vitro* growth curve was performed on irradiated (0.2-16 Gy) and non-irradiated H5V cells. First, H5V cells were plated in triplicate at a density of 30,000 cells and allowed to adhere to the plates for 24 h. Following irradiation, cells were counted to determine the initial number of cells inside the wells (day zero), H5V cells were then trypsinised after 24, 48 and 72 h and the number of cells counted. The results from three separate experiments (results presented as mean ± SEM) are shown in Figure **3.7,** and demonstrate a reduction in the number and proliferative activity of cells following irradiation compared with the non-irradiated control group. This reduction in cell proliferation was statistically significant at radiation doses between 2 and 16 Gy after 48 and 72 h compared to the non-irradiated group, which continued to grow. H5V cells exposed to a dose of 0.2 Gy did not show any reduction in cell numbers compared to the control group.

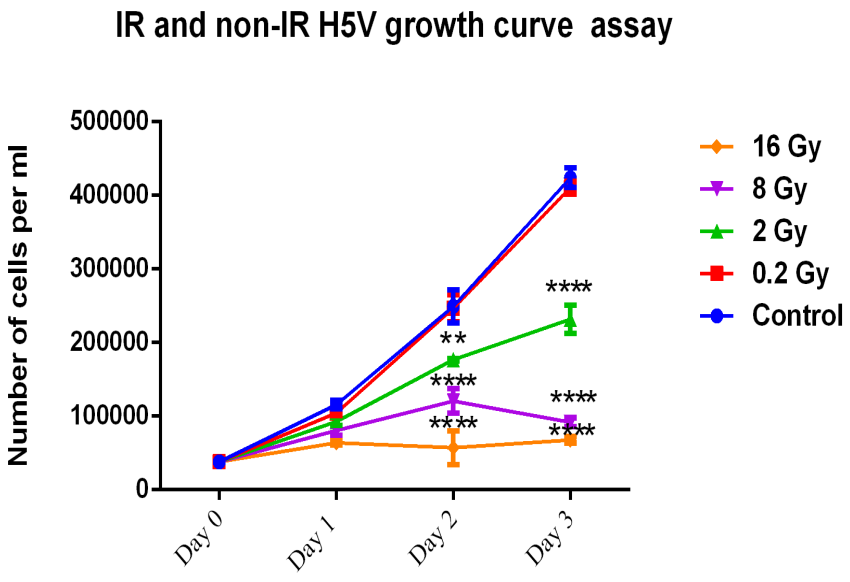

Figure 3.7 Radiation inhibition of H5V cell proliferation in growth curve assays. H5V cells were irradiated with 0 Gy (control), 0.2, 2, 8 and 16 Gy. Cells were trypsinised after 24 h and the viable cells counted after 24, 48 and 72 h. Results are expressed as mean cell counts ± SEM of 3 separate experiments (each performed in triplicate). The data show that radiation resulted in a reduction in cell proliferation, which is radiation dose-dependent. This effect is statistically significant at 2, 8 and 16 Gy as determined using the Two-way ANOVA test performed, compared to non-irradiated cells, after 48 and 72 h. (**$p < 0.01$, ****$p < 0.0001$)

3.2.5 *In vitro* models of angiogenesis

The next sets of experiments were carried out to specifically investigate the effects of radiation on EC migration and morphogenesis. Various *in vivo* angiogenesis models have been described in the literature but *in vitro* models are less expensive and more rapid (Donovan *et al.*, 2001), enabling the determination of EC migration and capillary-like structures.

3.2.5.1 Inhibition of endothelial proliferation by Mitomycin C

ECs were likely to proliferate during the migration assay, especially after 24 h. In order to exclude the proliferation effects in the migration assay and determine the wound closure accurately, cells were treated with Mitomycin C (Mit C). Mit C is a cell cycle inhibitor of S phase which stops proliferation but not migration (Seki *et al*., 2005; Mladenov *et al*., 2007).

Initially EA.hy 926, bEND.3 were used to optimise the experiment. However when H5V cell line was received, subsequent experiments were carried out using H5V, since they were the most appropriate cell line. H5V cells were grown in the presence of varying concentrations of Mit C (see section **2.1.8**), alongside untreated control cells, to establish the appropriate concentration of Mit C to effectively inhibit cell growth, without causing cell death. EC growth rate was measured over 2-3 days, and the data plotted graphically to determine the effects of Mit C on proliferative rate, as shown in Figure **3.8, 3.9** and **3.10.**

Data show that for each cell type, different concentrations of, and exposure times to Mit C were necessary to inhibit cell proliferation. The treatment of EA.hy 926 with 25µg/ml for 30 min resulted in inhibition of cell growth when compared to untreated cells (Figure **3.8**). In the case of bEND.3 cells, treatment with 30 µg/ml Mit C for 30 min was the most effective concentration in inhibiting proliferation (Figure **3.9**).

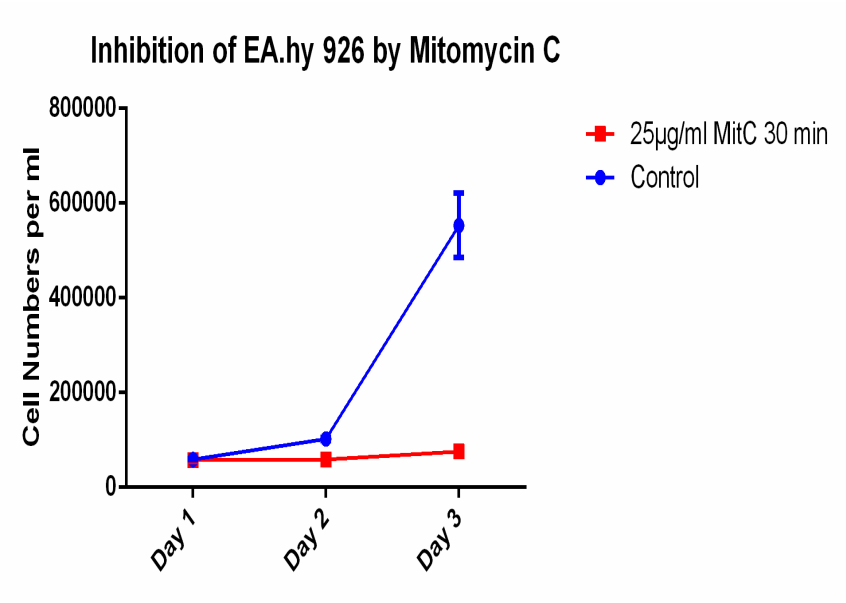

Figure 3.8 Inhibition of Ea.hy 926 cell growth by Mitomycin C. The confluent EA.hy 926 cells were treated with 25µg/ml Mit C for 30 min and its growth rate was measured over 3 days. Untreated cells were used as control. Mit C inhibited EA.hy 926 cell proliferation while the control EA.hy 926 cells continued to grow. Results are expressed as mean cell counts ± SEM of one experiment performed in triplicate.

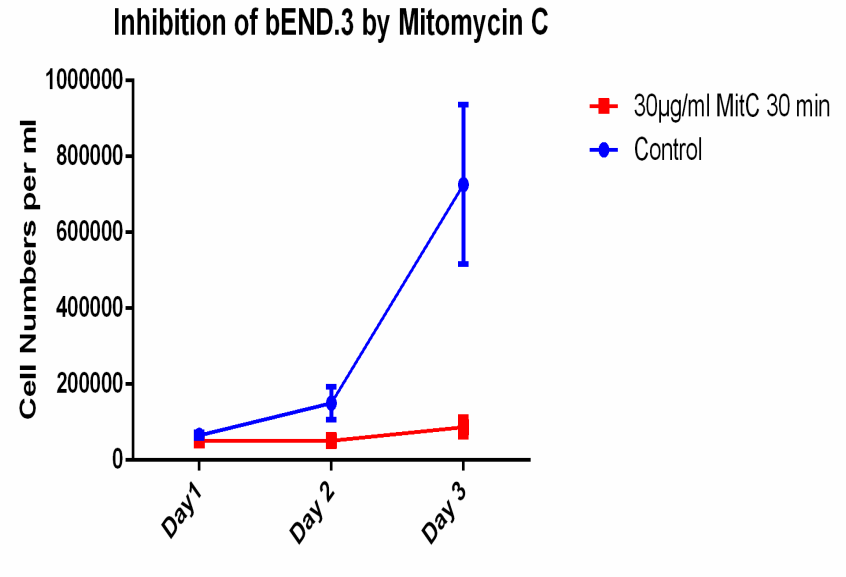

Figure 3.9 Inhibition of bEND.3 cell growth by Mitomycin C. The confluent bEND.3 cells were treated with 30µg/ml Mit C for 30 and the growth rate was measured over 3 days. Untreated cells were used as control. Mit C could stop bEND.3 cell proliferation more effectively when they were treated with 30 µg/ml for 30 min while untreated bEND.3 cells were growing significantly. Results are expressed as mean cell counts ± SEM of one experiment performed in triplicate.

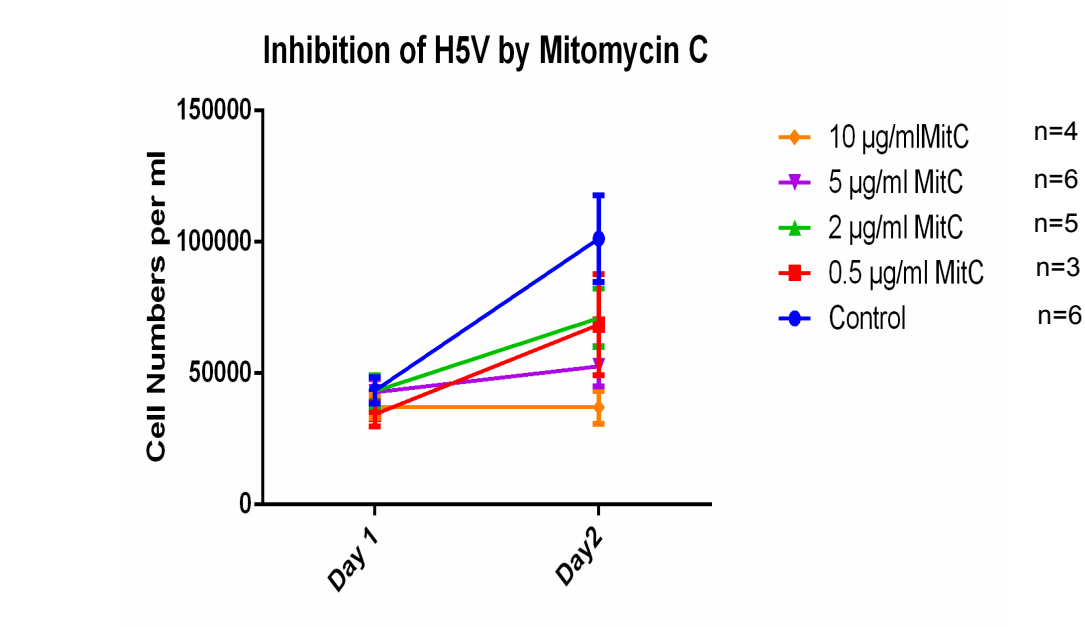

Figure 3.10 Inhibition of H5V cell growth by Mitomycin C. H5V Confluent monolayers were pre-treated with 0.5, 2, 5 and 10 µg/ml Mit C for 2 h. Untreated cell were used as control. Mit C at 5 µg/ml inhibited H5V growth effectively while 0.5 and 2 µg/ml concentrations of Mit C were efficient to stop H5V proliferation. Results are expressed as mean cell counts ± SEM of 3 to 6 separate experiments each performed in triplicate.

For H5V cells a number of different doses of Mit C were tested (0.5-10 µg/ml), to find the effective concentration of Mit C that could stop H5V growth, on the basis of conditions which were previously found to be effective in inhibiting proliferation of H5V cells (Guilini *et al.*, 2010). H5V cells were treated with 0.5 to 10 µg/ml Mit C for 2 h and then the drug was removed, before wounding the confluent monolayer. Finally, a dose of 5 µg/ml Mit C for 2 h was found to be most effective in inhibiting H5V cell proliferation (Figure **3.10**). The lower concentrations (0.5 and 2 µg/ml) did not stop the H5V growth effectively while the higher concentration of 10 µg/ml was not needed sine 5 µg/ml was enough to stop the growth (results presented as mean ± SEM).

3.2.5.1.1 Inhibition of endothelial growth by Mitomycin C during migration

Whilst the previous experiments had established the necessary doses of Mit C required to inhibit cell proliferation of ECs, it was important to confirm that the cells still retained their capacity to migrate. The scratch wound assay was therefore next performed. The method involved creating a wound on a confluent monolayer of ECs, and imaging cells at the start of the experiment and regular intervals thereafter to observe migration of cells to heal the wound. First H5V, bEND.3 and EA.hy 926 cells were treated with 5 µg/ml Mit C for 2 h, 30 µg/ml for 30 min and 25 µg/ml for 1 h, respectively as determined before. Then from the pilot study, a scratch was made on the cell monolayer and images taken between 0 and 24 h, to monitor wound closure. The average wound size (as measured by the length of the wound) at time zero for both irradiated and non-irradiated cells was calculated using Image J. The wound width determined from images taken at 24 h following wounding, was compared to time zero, to determine the rate of wound healing, as a measure of the efficiency of cell migration. Data were expressed as the percentage of wound distance observed at 24 h relative to time zero (% of original wound).

Initially experiments were performed twice using bEND.3 and once using EA.hy 926 cells. Data showed that addition of Mit C to cells retained their ability to migrate while wound

closure was slower in Mit C treated cells compared to non-treated cells, indicating proliferation was involved (data shown in **Appendix IV**). However, these cell lines were abandoned after receiving H5V cells.

Data for H5V cells from 5 experiments were expressed as mean ± SEM (Figure **3.11)**. Whilst no significant differences in migration of H5V cell were observed between treated and untreated cells at 6 and 10 h, a slight reduction in wound closure was observed at 24 h in Mit C treated group, with untreated cells migrating faster. Importantly, these results demonstrate that cells treated with Mit C do retain their capacity to migrate, albeit migrating more slowly than untreated cells upon prolonged incubation, and that wound closure in untreated cells is likely to be a combination of migration and proliferation. A similar trend was observed using bEND.3 and EA.hy 926 cells (Appendix IV) however in the case of these cells, only one experiment was performed.

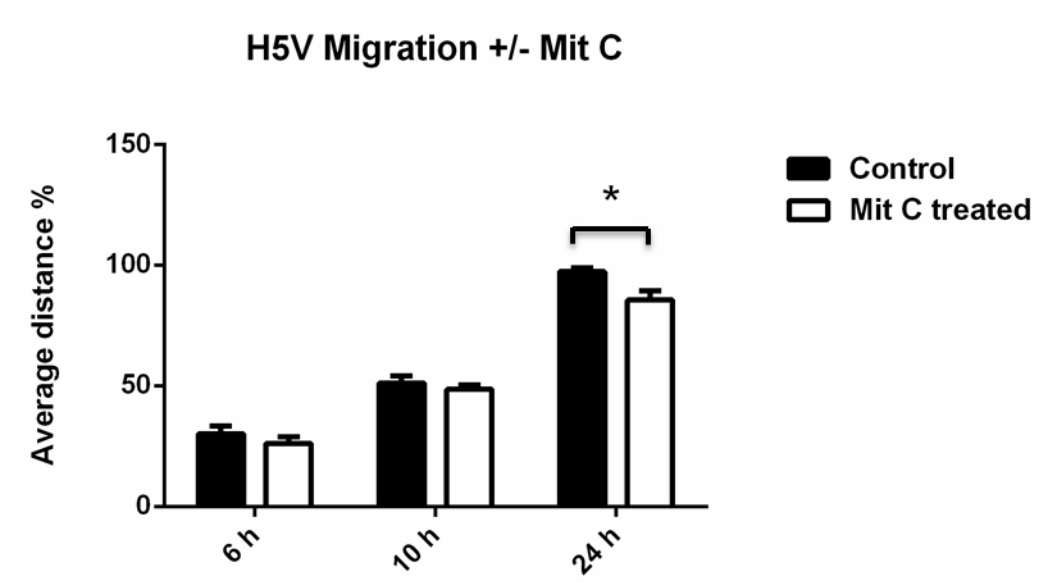

Figure 3.11 Effect of Mitomycin C on migration of H5V cells. H5V confluent monolayers were pre-treated with 5 µg/ml Mit C for 2 h and a scratch wound was created. The wound closure was monitored by a phase-contrast microscopy at 6, 10 h and 24 h. The data was expressed as the percentage of average wound distance observed at 24 h relative to the original wound. Results are expressed as mean ± SEM of 5 separate experiments (each performed in triplicate). Mit C treated group at each time point was compared to the control group of the same time point using statistical analysis t-test. Wound closures was significantly faster in control groups compared to Mic C treated H5V after 24 h. (*$p < 0.5$)

3.2.5.1.2 Effect of irradiation on migration of ECs

Having optimised the scratch wound assay in combination with treatment of ECs with Mit C, the experiment was next performed, this time to investigate the effects of exposure to radiation on EC migration. To establish appropriate experimental working conditions, initially experiments were performed using EA.hy 926, bEND.3 cells. For each cell line one experiment performed and data are shown in Appendix **V**. Subsequent experiments were performed using H5V, after receiving them and the uses of EA.hy 926, bEND.3 were abandoned. Here data are presented from experiments using H5V cells.

H5V cells were seeded in 24 well plates, and grown to confluence, and then cells were irradiated with varying doses of radiation (0.2, 0.5, 1, 2, 5, 8 and 16 Gy). The next day cells were treated with Mit C as described in the previous experiment, following which, a wound was created on the confluent monolayer of irradiated cells. Migration of cells towards the direction of wound was measured using image J at different time points (0, 6, 10 and 24h), and the data plotted graphically, as shown in Figure **3.12**. Non-irradiated cells were included as appropriate controls and a one-way ANOVA test performed to analyse data (results presented as mean ± SEM). The results show a significant inhibitory effect of radiation on H5V cell migration, which is more dramatic at shorter time intervals after irradiation (ie compared to data from 6 and 24 h). H5V cell migration was significantly reduced at all doses (0.2-16 Gy) 6 h after irradiation, whilst statistical significance was only observed at a dose of 0.5Gy and above, 10 h following irradiation. While a decreased trend was observed in the migration capacity of H5V cells after 24 h exposure to radiation, only at high doses of 8 and 16 Gy were significantly different from controls (at lower doses they retained their migratory capacity after 24 h).

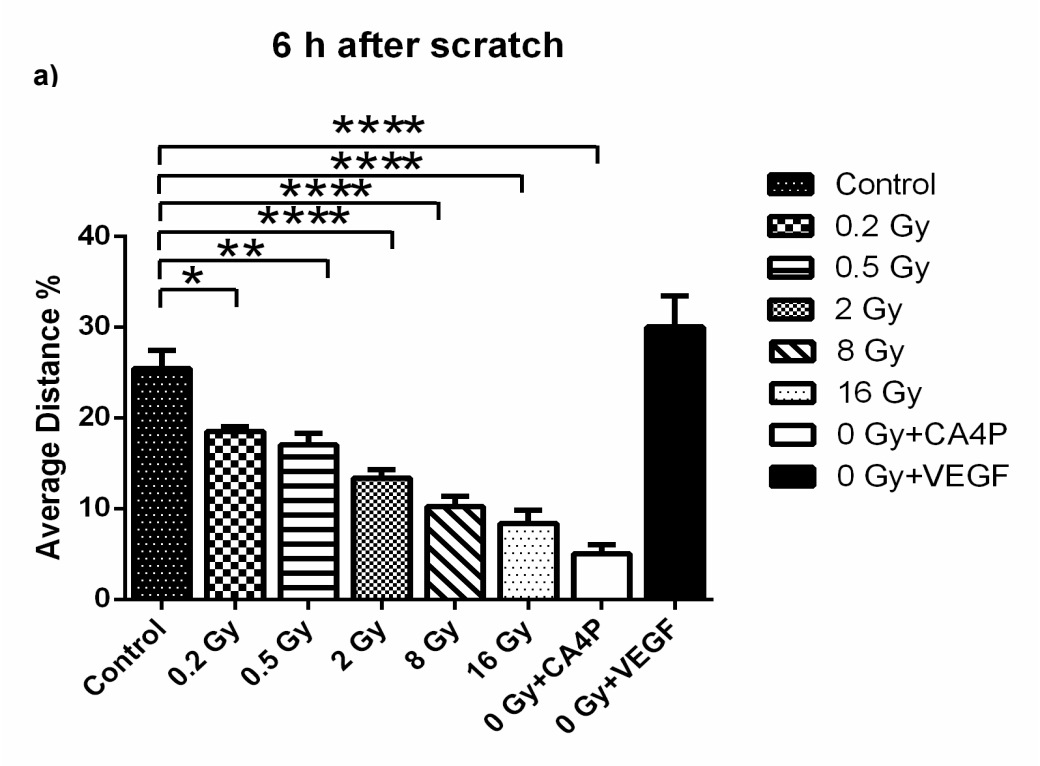
6 h after scratch
a)
Average Distance %
0
10
20
30
40
****
****
****
****
**
*
Control
0.2 Gy
0.5 Gy
2 Gy
8 Gy
16 Gy
0 Gy+CA4P
0 Gy+VEGF

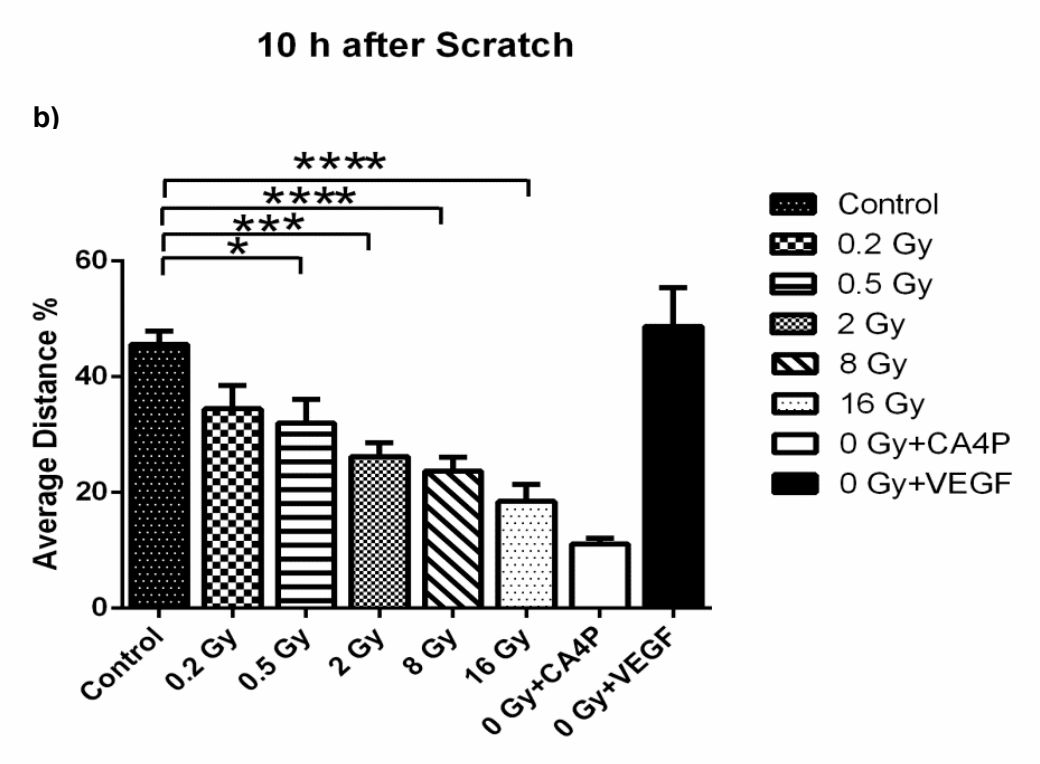
10 h after Scratch
b)
Average Distance %
0
20
40
60
****
****
***
*
Control
0.2 Gy
0.5 Gy
2 Gy
8 Gy
16 Gy
0 Gy+CA4P
0 Gy+VEGF

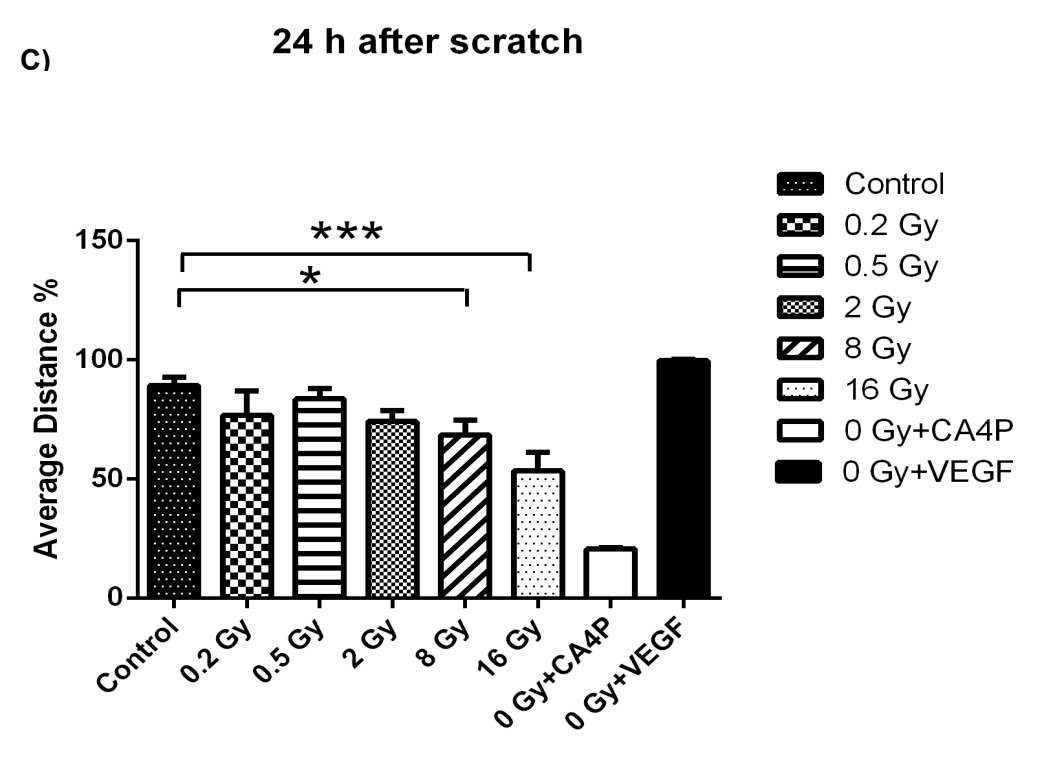

Figure 3.12 Effect of radiation on H5V migration by scratch-wound assay. Confluent H5V cells were irradiated at 0.2, 0.5, 2, 8 and 16 Gy and treated with 5 µg/ml Mit C for about 2 h. The wound closure was monitored by a phase-contrast microscopy at **a)** 6, **b)** 10 h and **c)** 24 h. The data were expressed as the percentage of wound distance observed at 24 h relative to the original wound (% of the original wound). A one-way ANOVA statistical test was performed to analyse data. A dose-dependent decrease in H5V migration in all irradiated groups after 6, 10 and 24 h was observed. Effects were significant at doses of ≥ 0.2 Gy after 6 h and ≥ 8 Gy after 24 h. The VEGF and CA4P used as positive and negative controls both showed stimulatory and inhibitory effects on migration of H5V cells respectively. Results are expressed as mean ± SEM of 3 to 7 separate experiments, each performed in triplicate. (**p < 0.01, ***p < 0.001, ****p < 0.0001)

Positive (VEGF) and negative (CA4P) control samples were also included in the experiment, and in this case 3 separate experiments were performed again using triplicate samples. As a positive control, non-irradiated cells were incubated with 50 ng/ml VEGF prior to creation of the wound. VEGF is a potent pro-angiogenic growth factor known to induce migration of endothelial cells in culture (Benndorf *et al.*, 2008; Oommen *et al.*, 2011). The VEGF treated ECs migrated at increased speed compared to the control group, as shown in the graphs plotted in Figure **3.12**. To provide a negative control, non-irradiated cells were treated with combretastatin A4 phosphate (CA4P). Since CA4P is a vascular disrupting agents that target ECs and results in inhibition of EC migration and capillary-like structure formation (Vincent *et al.*, 2005), these cells exhibited reduced cell migration in the scratch wound assay (Figure **3.12**), as evidenced by their inability to migrate and close the wound.

3.2.6 Formation of ECs tubules in morphogenic matrigel assay

In addition to EC proliferation and migration, their differentiation, sprouting and forming into tubules are other essential steps in the angiogenesis process. The morphogenic matrigel assay was developed to study the formation of capillary like tubules by ECs. The aim was to test effects of irradiation on the capacity of ECs to form capillary-like structures in matrigel. Matrigel is a basement membrane which has some extracellular components such as collagen IV and laminin (BD Biosciences) that stimulates ECs activity such as migration and their differentiation into capillary like network (Bishop *et al.*, 1999; Ahmad *et al.*, 2007). At the time of performing the matrigel assay, H5V cells were unavailable therefore, this assay was performed using bEND.3 cells and HUVECs. The use of HUVECs had been established in other studies (Benndorf *et al.*, 2008; Geng *et al.*, 2004). As described earlier (section **2.7.1**), 48 well-plates were coated with 100 µl of matrigel, and then cells were plated onto the pre-coated wells, at varying cell densities, and cell images were taken after 24 h using a phase contrast microscopy.

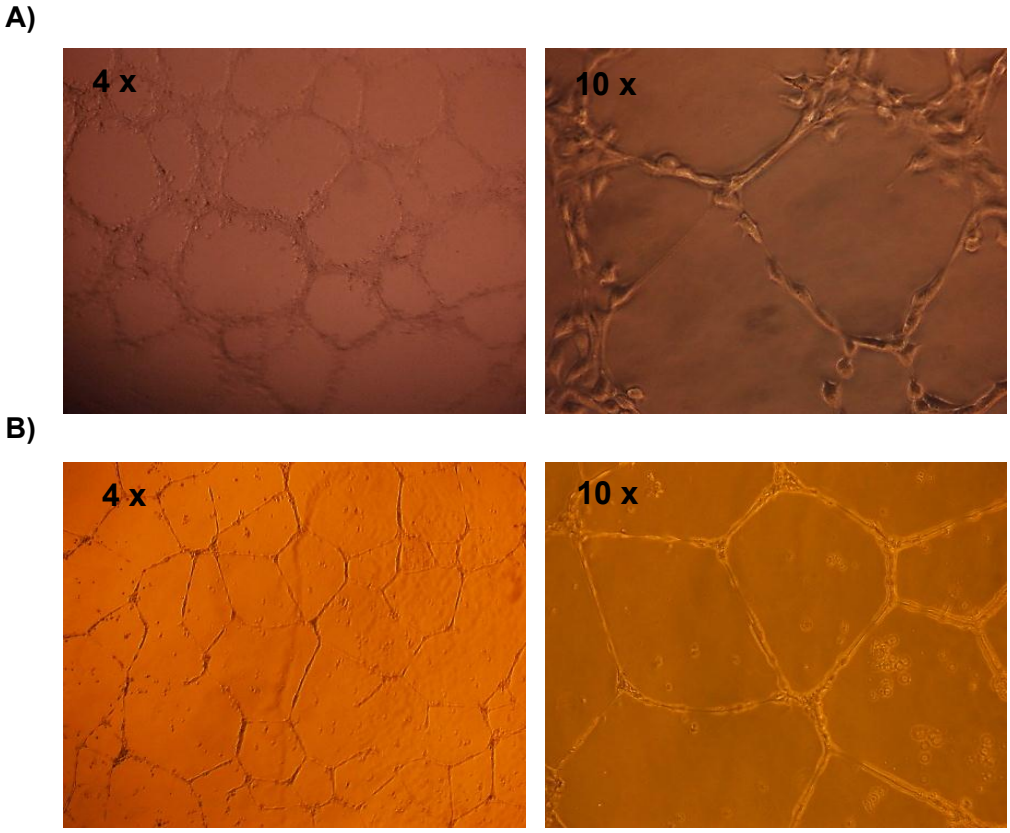

Figure 3.13 Formation of capillary-like structures by bEND.3 and HUVECs in matrigel. **A)** bEND.3 and **B)** HUVECS cells were plated at density of 10,000 and 80,000 cells respectively onto matrigel-coated 48 well-plates. Images were taken after 24 h using 4x and 10x objective, and show cells forming well-established cord-like structures.

Microscopic analysis revealed that ECs rapidly started tubules formation after 1 h and continued to form a network of tubules up to 24 h later, as shown in Figure **3.13**. Capillary-like networks formation in bEND.3 cells required seeding at a density of 10,000 cells per well (Figure **3.13A**). In contrast, cord-like structures were best observed when HUVECs were seeded at a density of 40,000 and 80,000 cells per well (Figure **3.13B**). CECs from one isolation experiment were similarly plated in matrigel, but they did not form any channels even after 24 h.

3.2.6.1 Effect of irradiation on formation of capillary-like structures in morphogenic matrigel assay

After optimisation of the matrigel assay, the effects of radiation on tubule formation of ECs were investigated using HUVECs. For this experiment HUVECs cells were irradiated at 5 Gy, 1 h prior to plating onto matrigel (40,000 cells per well). Un-irradiated cells were also included as appropriate controls. As shown in Figure **3.14**, qualitative analysis of tubule formation before (control) and after irradiation, revealed that tubule formation was reduced in HUVEC cells after exposure to 5 Gy radiation, compared to the non-irradiated cells. This experiment performed only once and organotypic co-culture model was replaced matrigel assay as it is explained in the next section **3.2.7**.

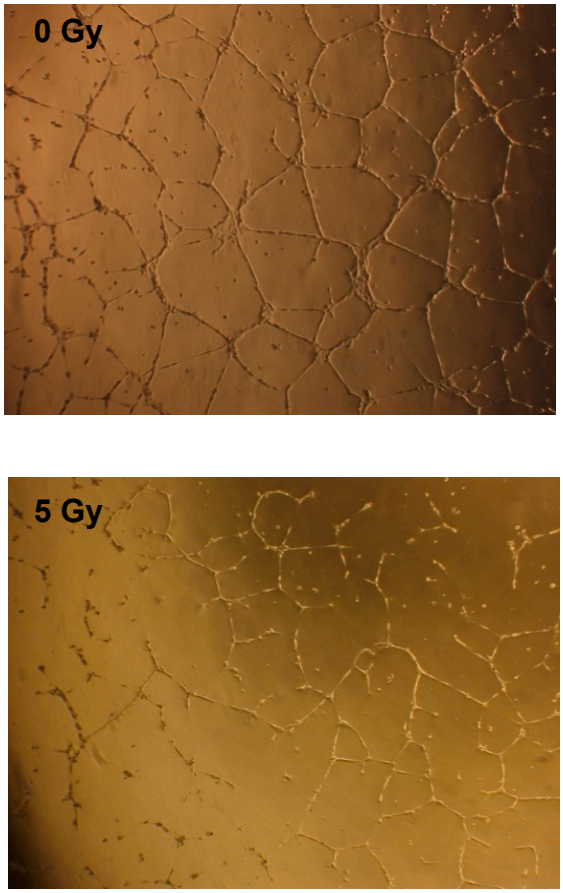

Figure 3.14 Effect of radiation on formation of channels by HUVECs. HUVECs were irradiated at 0 and 5 Gy. They were plated at density of 40,000 cells in 48 well-plates after irradiation. Tubules-like networks were formed within 24 h after culturing in matrigel. Images were taken using a 4x objective. Cord-like structures formed by irradiated cells were incomplete and disrupted compared to the non-irradiated cells.

3.2.7 Formation of capillary-like structure by ECs in organotypic co-culture assay

In the previous experiment, matrigel was required to induce tubule formation in ECs. However, it was important to next investigate EC tubule formation in a more realistic EC environment. For this reason, the organotypic co-culture assay was performed where ECs were co-cultured with fibroblasts. It is known fibroblasts secrete some extracellular matrix components as well as producing cytokines and growth factors, which stimulate EC angiogenic activity, resulting in EC capillary-like structures forming after 2-3 weeks, which are more stable. Accordingly, the co-culture assay could mimic *in vivo* microvessel bed more closely than the matrigel assay (Ahmad *et al.*, 2007; Donovan *et al.*, 2001). This assay has been adopted from Bishop *et al* work who first established this model (Bishop *et al.*, 1999).

Since HUVECs are able to develop a capillary-like structure in co-culture *in vitro* assay and express the vWF as ECs marker, they were suitable cells to establish this assay (Rhim et al., 1998). Initially the assay was set up and optimized using HUVECs and HDF cells, as described in the literature (Bishop *et al.*, 1999; Donovan *et al.*, 2001). Endothelial cells were mixed with fibroblasts and seeded into 24-well plates. The co-cultured cells were incubated at 37°C for 12-14 days and media changed every second day. After that, cells were fixed and corded structures were visualised using vWF staining. The von Willebrand factor is stored in Wiebel Palade bodies in ECs and is a classic maker of endothelium. It forms complexes with factor VIII and when it became activated, ECs produce VIII-antihemophilic factor on the membrane that have a role in the intrinsic coagulation pathway (Oxhorn et al, 2002). After optimising this assay using HUVECs other ECs (isolated CEC and H5Vcell) were tested (Section **3.2.7.2)**.

3.2.7.1 Optimisation of capillary-like networks formation using HDF and HUVEC co-cultures

During assay optimisation it was established that cells required adequate dissociation to prevent the formation of large flat clusters (endothelial islands) growing on top of the fibroblasts (see Figure **3.15A**). In some instances tubular-like structures were observed sprouting from the clusters. In contrast, when cells were syringed with different needles (19 and 21G) before mixing them, the ECs formed regular branched corded structures (Figure **3.15B**).

The ratio which cells are cultured together is really important. Optimal ratios and densities of fibroblasts to endothelial cells were established (summarised in Chapter **2**, section **2.4.4.1**), and a ratio of 3:1 and density of 30,000 HDF to 10,000 HUVEC was used in subsequent experiments. Figure **3.16** shows HDF-HUVEC in co-culture at different cell ratios (1:1, 3:1 and 5:1) and densities.

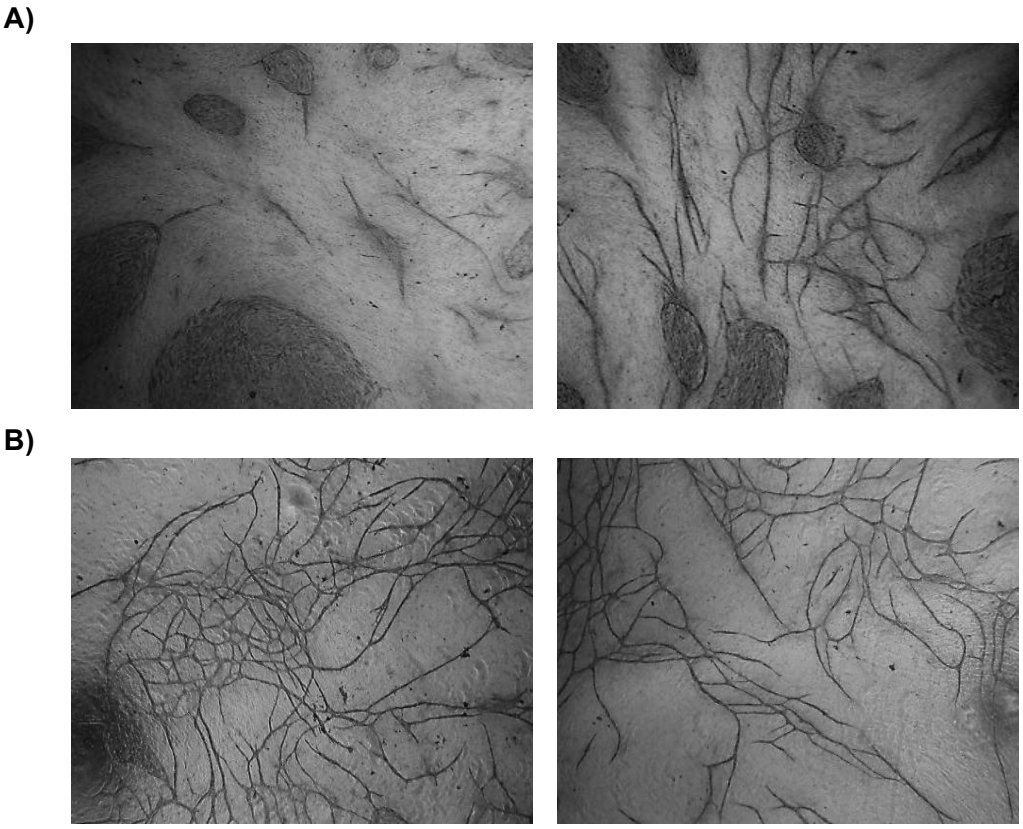

Figure 3.15 Formation of capillary-like structures by ECs in co-culture with fibroblasts. HUVECS were co-cultured with HDF cells and after 14 days the corded structures were stained with an antibody to vWF. **A)** The images show culture growth in the absence of syringing, with endothelial cells mainly growing in clusters and forming few capillary-like structures. **B)** HUVECs formed complex capillary-like structures after being well-dissociated using syringe. Images were taken using a 4x objective.

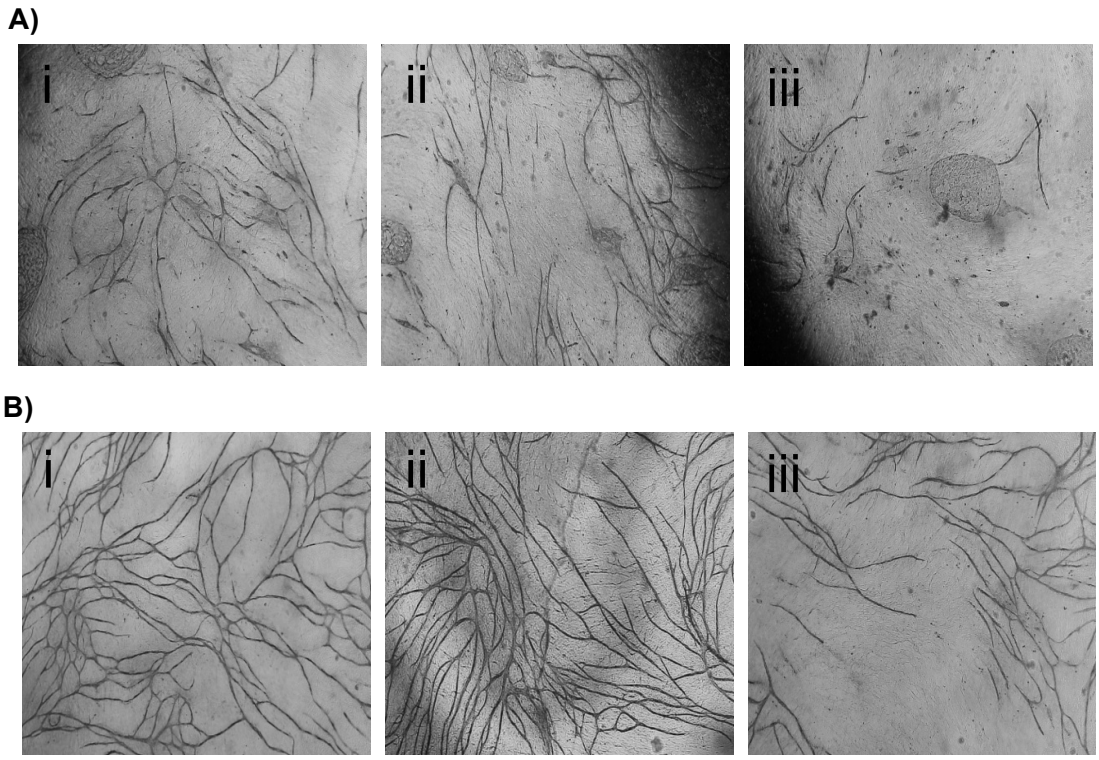

Figure 3.16 Formation of capillary-like structures by ECs in co-culture with fibroblasts at different ratios and densities. The EC thread-like structures formed by HUVECs after 14 days when co-cultured with HDF, and the corded structures were stained with an antibody to vWF. **A)** Images show the ratio of 1:1 and densities of i (40,000 HDF-40,000 HUVECs), ii (20,000 HDF-20,000 HUVECs) and iii (10,000 HDF-10,000 HUVECs). It was found out this ratios were not appropriate as ECs tended to grow in clusters and formed less capillary-like structures. However, **B)** co-culturing of HDF with HUVECs at the ratio of 3:1 resulted in an appropriate density of ECs corded structures. While ECs were able to form tubules at different densities i (60,000 HDF-20,000 ECs), ii (30,000 HDF-10,000 HUVECs) and iii (15000 HDF-5000 HUVECs), the density of (ii) 30,000 HDF to 10,000 HUVECS was used in subsequent experiments. Images were taken using a 4x objective.

3.2.7.2 Optimisation of capillary-like structures formation in the co-culture assay using different types of endothelial cells and fibroblasts

The co-culture assay was optimised using HUVECs and HDF cells as described above. However, other ECs and fibroblast cells were also tested since these were more suitable for this project.

3.2.7.2.1 Co-cultures using primary CECs and HDFs

The co-culture assay was next performed using mouse CECs with HDFs. The mouse CECs used were those isolated earlier as described in section (**2.3.1**). Again, varying ratios of HDF cells to CECs were investigated (1:1, 3:1 and 5:1), however, unfortunately no capillary-like networks were observed.

3.2.7.2.2 Co-cultures using H5V and HDF cells

HDFs and H5V cells were similarly co-cultured at varying ratios, as above, however formation of corded structures by H5V cells was inconsistent from one experiment to another (4 separate experiments performed). Moreover, thread-like networks formation generally was much less efficient than that seen when using HUVECs (Figure **3.17A**).

3.2.7.2.3 Co-cultures using HUVEC and a mixed population of cells obtained from the CEC isolation experiment

As mentioned in section **3.2.1**, after isolating CECs by magnetic separation, non-selected cells remained at the end of the experiment, which constituted smooth muscle cells, fibroblasts and pericytes. In the next experiment, the mixture of non-endothelial extracted cells from mouse heart were therefore co-cultured along with HUVECs as a source of fibroblasts that most closely resembled *in vivo* conditions. The mixture of digested heart cells including fibroblasts and HUVECs were co-cultured at ratio of 3:1 with 30,000 non-endothelial digested cells to 10,000 HUVECs density, and this resulted in the formation of cord-like structures. As shown in Figure **3.17B**, efficient formation of capillary-like structures by HUVECs was observed under these conditions.

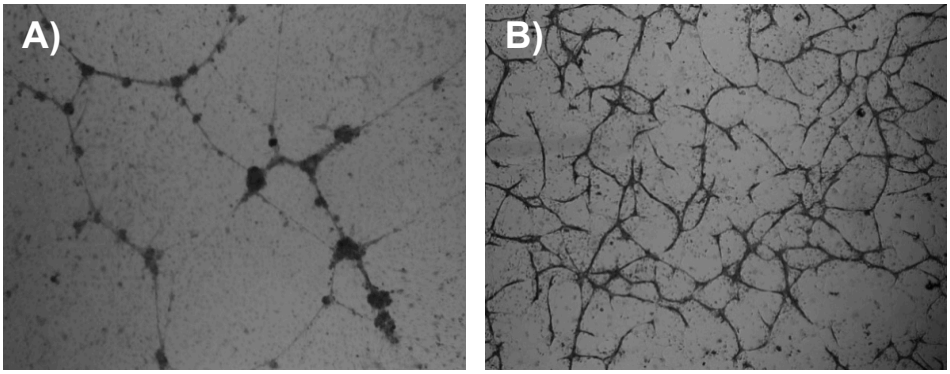

Figure 3.17 Formation of capillary-like structure by H5V-HDF and HUVECs-mixture of extracted non-EC heart cells co-cultures. A) H5V cells were co-cultured with HDF at ratio of 5:1 with density of 50,000 HDF to 10,000 H5V. They started forming thread-like networks after 14 days. The H5V corded structures were characterised with an antibody to vWF. **B)** The image represented the formation of capillary-like networks by HUVECs (density of 10,000) when co-cultured with the mixture of extracted non-EC cells including fibroblasts from mouse heart (density of 30,000) at ratio of 3:1. Images were taken using a 4x objective.

3.2.7.3 Irradiation effect on formation of ECs channels in co-culture assay

The previous experiments established that ECs do form tubules-like networks when co-cultured with fibroblasts; however this was dependent on the cells used. HUVECs were the best source of ECs, compared to others tested and they did form corded-structure in the presence of the mixture of extracted non-EC cells including fibroblasts obtained from the mouse heart isolation experiment. However, rather than use this as a model to go on and investigate the effects of radiation on EC channel formation in co-culture, HDFs were used as the source of fibroblast cells in the next experiments, since using the mixed population of cells extracted from the mouse heart isolation experiments was both time consuming and technically demanding and in addition required mouse hearts.

To investigate whether radiation modified the formation of tubule-like networks by ECs, separate experiments were performed in which HUVECs were irradiated at 0.5, 1, 2 and 5 Gy prior to co-culture with HDF cells. For each irradiation dose, a control experiment was performed in parallel, with untreated cells. After 14 days, capillary-like structures were visualised using vWF staining. Data presented in Figure **3.18** show that the number and the length of sprouts decreased after irradiation with a more profound effect at higher dose of 5 Gy compared to non-irradiated cells. A subtle effect on channel formation by HUVECs was observed at low doses of radiation (0.5 and 1 Gy). One experiment performed for each radiation dose. At the time of performing this experiment the AngioSys analysis software (TCS Cellworks) was not available, and enough images for later analysis were not taken.

The Bishop *et al* (1999) showed that the cord-like structures formed by ECs lying between fibroblast are true tubules with lumen using a transmission electron microscopy. The capillary-like networks formed by ECs in these experiments also required to be analysed by electron microscopy in order to confirm they have the true tubule structures with lumen.

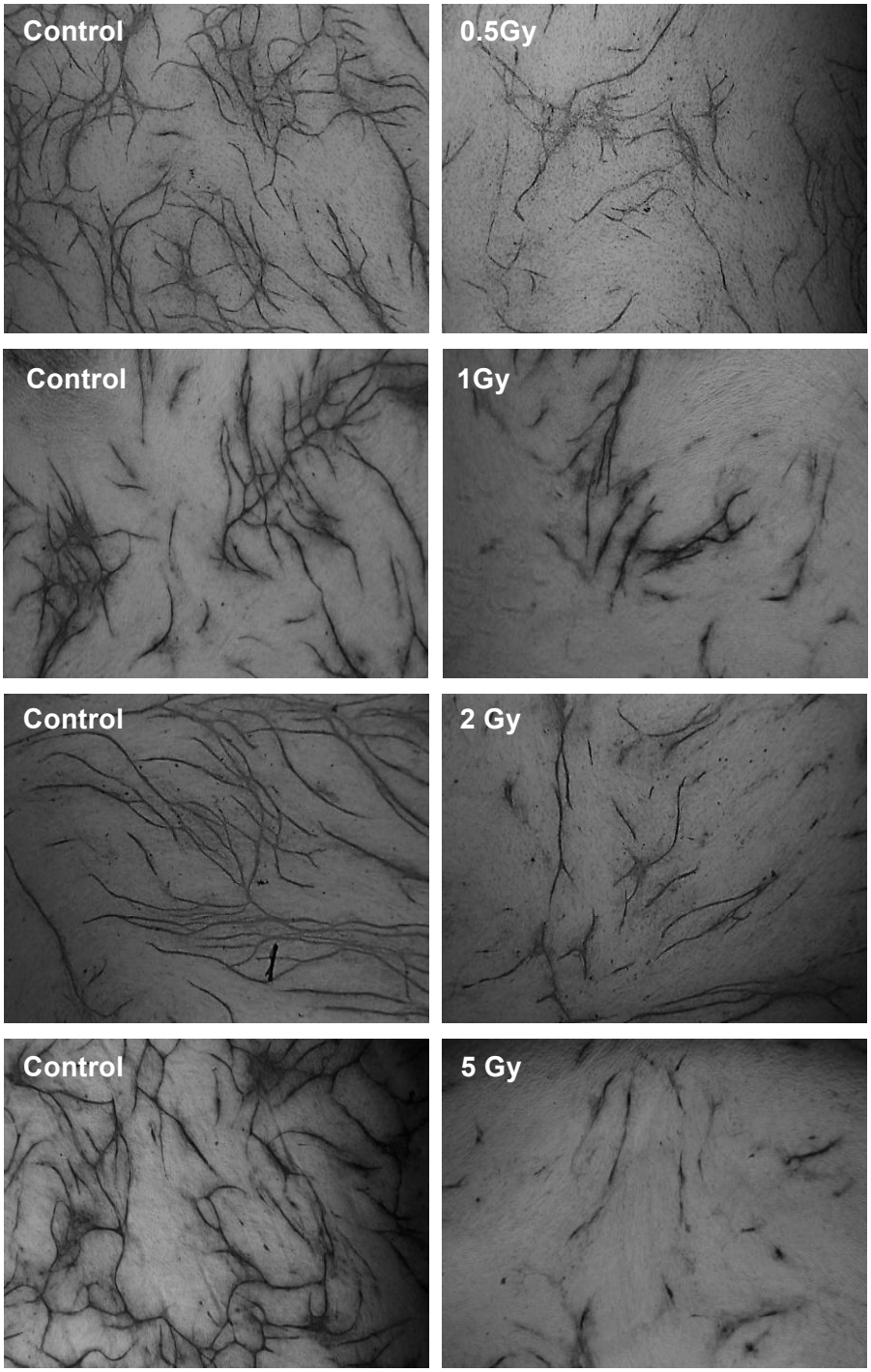

Figure 3.18 Radiation effects on the ability of HUVECs to form capillary-like structures in co-culture with fibroblasts. HUVECs were irradiated at different radiation doses and co-cultured with HDF at ratio of 3:1. After 14 days capillary-like structures were fixed and characterised with an antibody to vWF. The co-culture assay for each radiation group was performed separately and each experiment had its own control. The results show that irradiation inhibited the formation of channels by HUVECs and influenced both the length and number these structures compared to controls and effects was dose-dependent. Images were taken using a 4x objective.

Because radiation affects the ability of ECs to adhere to the surface as well as their proliferation, it was difficult to distinguish whether radiation directly damages formation of capillary-like structures by EC or whether the effects are an indirect consequence of radiation effects on EC adherence and growth. Moreover if radiation causes cell loss this could alter the ratio of plated EC cells. Therefore, this model was not performed further as it is difficult to interpret the data.

3.2.8 Formation of channels by mouse cardiac endothelial cells in the novel endothelial-fibroblast self-assembly model

A main aim of this project was to study the angiogenic properties of mouse CECs *in vitro*. However, since the previous experiments demonstrated that establishing CECs in culture was difficult and problematic, the next experiments were performed using a novel self-assembly model established more recently in our laboratory by my supervisor Dr Chryso Kanthou, subsequent to the CEC isolation experiments previously described. Using this method, CEC were able to proliferate, migrate and differentiate into capillary-like structures *in vitro* without prior separation from the rest of the cells, in a total heart cell digest. Briefly, the mouse heart was digested and cells separated using enzymatic and mechanical dissociation. After this, the mixed population of cells containing CECs along with other mouse cardiac cells including fibroblasts, pericytes and smooth cells were cultured together in a plate, which was coated with 1% gelatin (section **2.7.3**). The co-culture was fixed after 10-12 days with methanol. To establish whether corded structure were in fact ECs in nature and also visualise them, lectin stating was performed. Additionally mouse hearts from both young (2 x17 weeks old SCID) and much older mice (2 x 9 months old C57BL/6 mice) were tested. Since 20 to 60 weeks C57BL/6 mice were used in CARDIORISK project, it was important to study whether this model could be established in both young and old animals before receiving them. Moreover at the time of performing this experiment only old C56BL/6 mice were available in our lab, therefore the young SCID mice were tested instead. Result showed that capillary-like structures formed by CEC from both young and old mouse hearts as shown in Figure **3.19**.

Therefore, the advantage of this new self-assembly model was formation of tubule-like structures by mouse CEC, which is more appropriate for the purpose of this project. Additionally, it enables the long-term effects of radiation now to be examined in mice, due to working efficiently when mouse hearts from older mice are used.

3.2.8.1 Effects of radiation on formation of capillary-like structures by CEC in the self-assembly assay

After initial optimisation of the method, effects of radiation using the self-assembly assay were investigated. When the CECs started forming thread-like structures, usually by day 5-6 (as observed using phase contrast microscopy) the media was changed and cells were irradiated at different radiation doses of 0, 0.5, 2 and 8 Gy. At day 11, cells were fixed and characterised by lectin staining. As shown in Figure **3.20**, efficient capillary networks were formed by CECs irradiated at low doses of radiation (0-0.5 Gy). However radiation at higher doses of 8 Gy inhibited formation of these networks. Moreover, qualitative analysis revealed that sprout length was shorter in these cells compared to the control group. This result was consistent in further experiments performed. Whilst quantitative analysis would provide a more conclusive interpretation, the presence of many dead-cells among the tubules after staining, made any software analysis that identified only the corded structures to enable their length, area and numbers to be quantified, difficult.

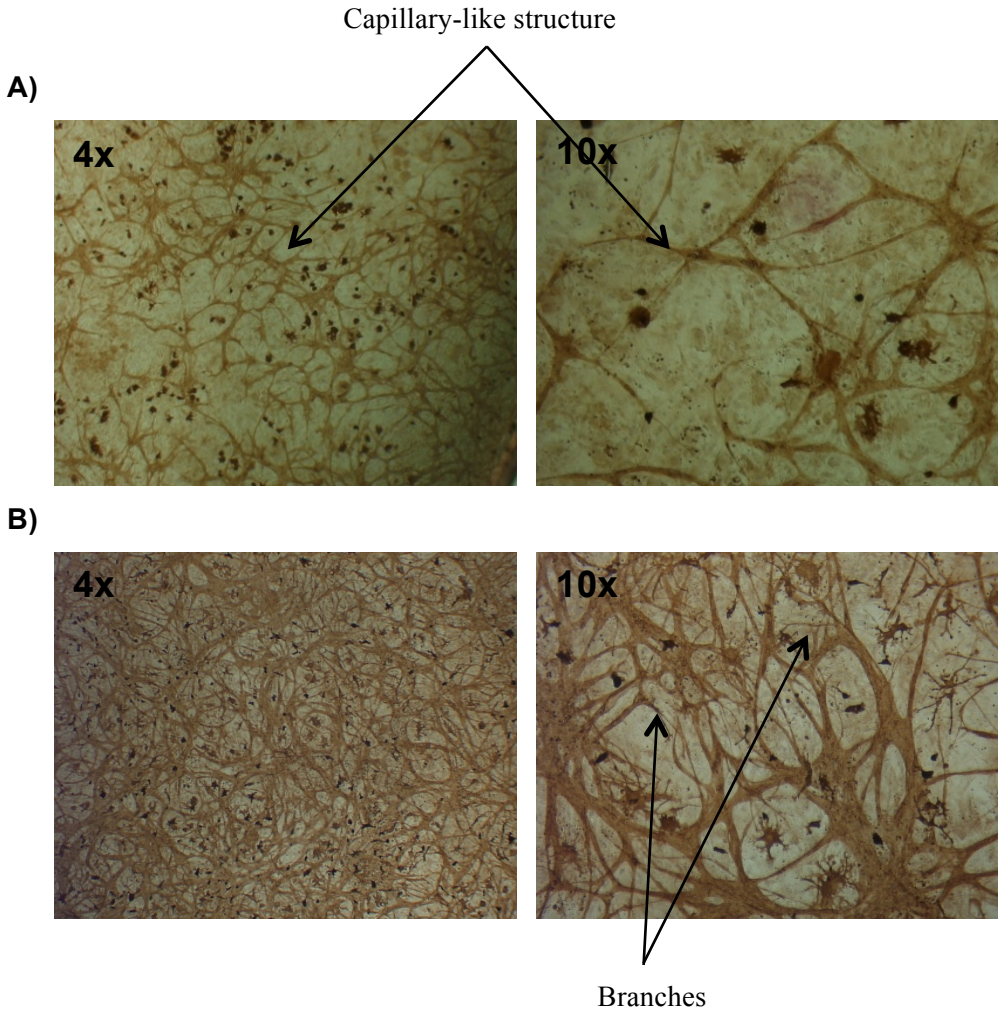

Figure 3.19 Formation of capillary-like structures by CECs in the self-assembly assay. The mouse heart cells from **A)** young mice (2 x17 weeks old SCID) and **B)** old mice (2 x 9 months old C57BL/6 mice) were cultured together after hearts were digested and cells were collected and suspended in medium. Cells were cultivated for 12 days and then corded structures were visualised by lectin staining. The formation of capillary-like networks by CEC was observed in both young and old mice. The capillary-like networks were well structured with many branches.

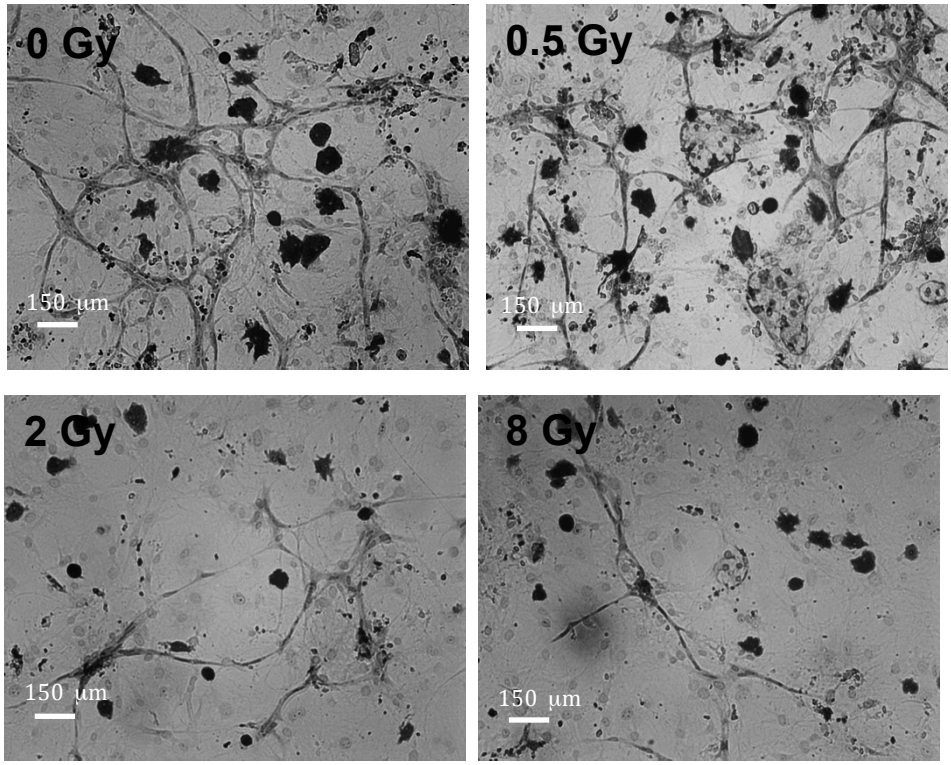

Figure 3.20 Effect of radiation on formation of capillary-like structures by mouse cardiac endothelial cell in the self-assembly model. Mouse heart cells were digested cultured together. Cultures were irradiated at 0 (control), 0.5, 2 and 8 Gy on day 6 when CEC started forming channels. After 10 days tubules were visualised by lectin. In control and 0.5 Gy well-structured capillary networks were formed whereas higher radiation doses inhibited formation of sprouts. Images were taken using a phase contrast microscope.

3.3 Discussion

Cardiac regeneration following radiation injury is dependent on neo-vascularisation. If radiation damage impairs the capacity of cardiac microvasculature to undergo repair, then investigating this aspect of endothelial function could reveal important information relating to pathogenesis of radiation-induced damage especially at lower doses. The endothelium is considered as the largest organ in body that has many roles in physiological functions as well as pathological consequences (Oxhorn *et al.*, 2002). Therefore, the study of angiogenic properties of irradiated ECs could reveal important information on the mechanisms associated with microvascular damage. The experiments performed in this chapter, were designed to investigate the effects of radiation on specific steps involved in angiogenesis, including EC migration, proliferation and capillary sprout formation. After establishing different *in vitro* angiogenesis models, the structural, morphological, and functional EC alterations were analysed *in vitro.*

3.3.1 Isolation of cardiac endothelial cell from mouse heart

The uses of isolated ECs from known origin such as H5V and HUVECs have been widely propagated. Primary and immortalised EC lines (HUVECs and H5V cells) have been used as an alternative to isolated CECs to study EC functions and properties *in vitro*, since they enable long term cultures of cells to be established, allowing many experimental repeats to be performed as well as ultimately costing less to use and being technically less demanding to work with (Lidington *et al.*, 1999; Oxhorn *et al.*, 2002). The ECs *in vitro* are heterogeneous and their functions and characteristics might be different depending on the vessel size and tissue they have been derived. They grow for month in culture therefore their properties might vary from laboratory to laboratory. Different ECs functions could be different in cell culture assays. It is better to choose a cell type for the *in vitro* angiogenesis assay more closely to the tissue of interest (Goodwin, 2007; Oxhorn *et al.*, 2002). EA.hy 926 and bEND.3 cell were used initially to optimise the migration assay before receiving the H5V. In the current project, H5V cells were predominantly chosen for the experiments described because they originate from the

mouse heart. Since the focus of this study was to investigate radiation effects on cardiac vascular injury, H5V cells provided therefore a more relevant model. However, despite these advantages, the use of primary ECs is still preferred, as cell lines might have altered cellular functions and lost some of the important EC characteristics (Marelli-Berg *et al.*, 2000; Oxhorn *et al.*, 2002).

Whilst cell lines were ultimately used in the latter part of this chapter, initial experiments describe attempts to isolate mouse CECs directly, since it was hoped that the availability of these cells would enable the direct effects of radiation on cardiac injury to be determined later in irradiated mice. However, since this was problematic (as explained below), the established cell lines enabled *in vitro* models of angiogenesis to be tested, specifically with respect to radiation.

Importantly, it was desirable to obtain CECs specifically from hearts taken from older animals to enable the long-term direct effects of radiation to be determined. However, this was found to be difficult. Many studies performed on isolation of ECs from large vessel with a defined protocol but less available for the murine ECs especially older animals (Lim and Luschinskas, 2006; Marelli-Berg *et al.*, 2000). Several different attempts were performed to achieve pure CEC cultures *in vitro.* The mechanical syringing during collagenase digestion resulted in improved tissue dissociation. Multiple washings of cells in-between incubation with the magnet helped improve the purity. The CD31 antibodies were more effective in selecting and isolating CEC than antibodies to endoglin (CD 105) as CD31 is only expressed on ECs (Lidington *et al.*, 1999). The use of trypsin enhanced dissociation and digestion of mouse heart tissue, but affected subsequent EC selection by imposing adverse effects on EC surface receptors such as CD31. Using a Teflon bag did help to optimise the isolated CEC yields, specifically from older mice. However, there was still some fibroblast contamination, which unfortunately could not be avoided. Therefore, all other experiments to examine radiation effects were performed using the cell lines described above.

Other methods of CEC isolation can be adopted in future work. Fluorescence activated cell sorting (FACS) is another method to isolate and characterise ECs. After dissociation of cells into single cell suspension, flow cytometry segregate cells expressing up to four different EC markers. Using this method, more number of cells would be expanded with initial isolation of about 5-10 x 10^6 (Oxhorn *et al.,* 2002). Another method to improve the isolation purity was to plate the isolated cells suspension in a container with a gelatin-coated surface and after 1-2 hour transfer the supernatant to a new gelatin-coated well. Therefore, the fibroblasts, which were able to attach quicker left in the first container (Hongpaisan, 2000).

More recently, the isolation of CEC from non-irradiated and irradiated C57BL/6 mice was established by Jelonek *et al*, from the same method performed here using enzymatical digestion, CD31 antibody-coupled Dynabeads and magnetic separation (only used different medium). They could achieve culture of the CEC *in vitro* up to 5 to 6 weeks (3-4 passages) in young C57BL/6 mice (6-10 weeks) and 2 to 3 weeks (2-3 passages) in older animals (6-7 months) (Jelonek *et al.*, 2011). After establishing the endothelial-fibroblast novel self-assembly assay and mouse cardiac angiogenesis *in vitro* which showed the direct effect of radiation on CEC, further attempts to isolate CEC were abandoned in order to more focus on other experiments which may assist in elucidating the mechanisms involved in radiation-induced damage.

3.3.2 Effect of radiation on endothelial cell angiogenic properties using *in vitro* models

3.3.2.1 EC clonogenic survival

Radiation induces DNA damage and apoptosis in rapidly dividing cells (Juckett *et al.*, 1998). The clonogenic assay was performed to study whether radiation affected the capacity of ECs to produce a progeny after radiation (Franken *et al.*, 2006). Previous studies have shown that treatment of HUVECS and bEND.3 cells with radiation doses of 2, 4 and 6 Gy decreased clonogenic survival in a dose-dependent manner (Abderrahmani *et al.*, 2012; Osterreicher *et al.*, 2003). Similar effects were observed also in HDF cells (Schleicher *et al.*, 2011). The

results presented here agree with these findings, since H5V and HDF cells both exhibited a decrease in clonogenic cell survival following radiation, which importantly was shown to be statistically significant in H5V cells at doses of 0.5, 2 and 8 Gy.

3.3.2.2 H2AX phosphorylation

Radiation effects were also confirmed by detecting H2AX phosphorylation. Irradiation of HDF and H5V cells at 4 and 8 Gy respectively, induced DNA breaks as demonstrated by an elevated level of γ-H2AX after 24 h in our study. This is in agreement with another study performed as part of the CARDIORISK project, where formation of γ-H2AX foci was observed in isolated mouse CECs after exposure to radiation doses of ranging between 0.2 to 16 Gy, with significant effects being observed in cells, 1 h after they received radiation doses of ≥ 2 Gy (Jelonek *et al.*, 2011). Similarly, Marti *et al* showed an increase in γ–H2AX foci in human fibroblast cells 4 h after exposure to 5 Gy radiation (Marti *et al.*, 2006).

3.3.2.3 EC proliferation

Radiation effects on cell proliferation were observed in H5V cells, where a reduction in cell proliferation was shown to be statistically significant at radiation doses ≥ 2 Gy after 48 and 72 h compared to the unirradiated group. The study by Ahmad *et al* using HUVECs similarly revealed a significant reduction in cell proliferation at radiation doses of ≥ 2 Gy compared to the sham-irradiated group (Ahmad *et al.*, 2007).

3.3.2.4 EC migration

The effects of radiation on EC migration were evaluated using the *in vitro* scratch wound assay. Radiation strongly inhibited H5V migration at very low doses of ≥ 0.2 after 6 h, such that wound healing in irradiated ECs was significantly impaired compared with control cells. These effects were only observed at higher doses of radiation after 24 h. These results are in agreement with the literature, where in a study by Zheng *et al*, irradiation of primary vascular endothelial cell at doses of 2 and 10 Gy had a significant inhibitory effect on EC migration and consequently wound healing compared to non-irradiated cells (Zheng *et al.*, 2011). Imaizumi

et al, also showed that 15 Gy irradiated HUVECS exhibited reduced wound closure compared to the sham-irradiated cells (Imaizumi *et al.*, 2010).

3.3.2.5 EC capillary-like formation in the matrigel and co-culture assay

Consistent with effects on EC migration, the experiments described here revealed defects in EC tubule formation in matrigel, following exposure of cells to radiation. Again, these data support other studies where radiation inhibited capillary-like formation by HUVECs at high doses of radiation (8 and 16 Gy) within 24 h (Benndorf *et al.*, 2008) as well as low doses (3 Gy) of radiation (Geng *et al.*, 2004). Similar results concerning radiation effects were observed here when HUVECs were grown with HDFs. However, as discussed earlier these experimental results are open to interpretation due to the nature of how the experiment is carried in terms of data being obtained over a prolonged period (14 days), it is difficult to distinguish whether the effects of radiation are direct on capillary formation or rather a consequence of direct effects on EC proliferation and adhesion. Moreover, there is an interaction between fibroblasts and ECs that make it difficult to specify the effect of radiation on EC (Bishop *et al*., 2000; Ucuzian and Greisler, 2007).

3.3.2.6 Capillary-like formation by CEC in the self-assembly assay

A relevant, novel radiobiological model to assess radiation toxicity on CEC angiogenesis properties without prior isolation of CECs was used and importantly, dose dependent radiation inhibitory effects on CEC angiogenesis *in vitro* were observed. The effects were more profound at the higher dose of 8 Gy. This self-assembly assay had more advantages over the organotypic co-culture assays. In this assay, irradiation was performed on CECs when they start forming sprouts *in vitro* among other isolated heart cells, therefore, resembling the *in vivo* conditions more closely. Additionally, the formation of channels by CEC cells was investigated in locally irradiated mouse heart mouse heart (0, 0.2, 2, 8 and 16 Gy) after 20, 40 and 60 weeks post-irradiation using the novel self-assembly model. The mouse hearts were irradiated and send by our CARDIORISK collaborators in Germany and the experiment performed by my supervisor Dr Chryso Kanthou. The results were consistent with data

obtained here from the *in vitro* irradiation of cells and revealed that there was a reduction in formation of capillary-like network by CEC in a dose-dependent manner and the effect was persistent even after 60 weeks post-radiation especially at higher dose of 8 and 16 Gy (unpublished data).

3.3.4 Summary of results

In summary, the data presented here suggest that radiation exerts anti-angiogenic effects on EC, supported by the observed inhibitory effects on EC clonogenic survival, proliferation, migration and capillary-like networks formation. Additionally some anti-angiogenic changes on ECs were observed at low doses of radiation, which could in turn result in the late radiation-induced EC angiogenic impairment and contribute to the development of CVD. Importantly, some results obtained here were shown for the first time (angiogenesis models on H5V cell line which originate from mouse CEC and self-assembly model).

Chapter Four

Determining the late effects of radiation on mouse heart angiogenesis

4.1 Introduction

The *in vitro* assays we used in the previous chapter allowed the investigation of direct effects of radiation on ECs properties, especially on processes that contribute to angiogenesis, such as migration and proliferation. *In vitro* assays are relatively inexpensive and can be performed in large-scale screenings (Goodwin, 2007; Ucuzian and Greisler, 2007). However cell culture can result in changes in ECs such as cell surface antigens and growth characteristics and their functions. EC functions and characteristics can vary depending on the vessel size and tissue of origin (Goodwin, 2007; Oxhorn *et al.*, 2002). Moreover, 2 dimensional (D) controlled *in vitro* assays are far-removed from the *in vivo* environment. EC-EC and EC-matrix interactions are important during angiogenesis. The incorporation of the 3D cell-matrix and EC-mural cell interactions into *in vitro* assays of angiogenesis is important to identify radiation-induced angiogenesis impairment more closely related to the *in vivo* condition. A different approach was needed to study the effects of radiation on the vasculature of the heart (Goodwin, 2007; Ucuzian and Greisler, 2007).

4.1.1 Using the *ex vivo* explant assays to measure angiogenesis in heart tissue

Here we focused on the 'aortic ring' and 'heart explant' angiogenesis assays which are one of the most common organ culture assays used (Goodwin, 2007; Kiefer *et al.*, 2004). These assays offer the culture of ECs together with stromal cells and matrix, which represent the *in vivo* environment more closely. The angiogenic sprouts grow from a segment of heart into a 3-dimentional arrangement with surrounding matrix (Goodwin, 2007; Ucuzian and Greisler, 2007). Additionally, it has the benefit of utilizing quiescent cells at the start of the assay, which is a characteristic of ECs *in vivo* (Ucuzian and Greisler, 2007). The neovessels that grow out from the cultured tissue resemble more closely the *in vivo* neovessels. In this assay ECs are associated with fibroblasts, pericytes and smooth muscle cells and they are recruited with ECs during their capillary-like structures formation (Goodwin, 2007; Kiefer *et al.*, 2004). Using this model we were able to study the late anti-angiogenic effects of radiation to the heart microvasculature, based on measuring EC outgrowth. Mice hearts were locally irradiated and

after 20-60 weeks of irradiation, using *ex-vivo* heart explants, the heart angiogenesis activity was studied.

4.2 Results

4.2.1 Optimization of the *in vitro* explant assay

Aortic ring and heart explant angiogenesis *in vitro* assays were used to investigate cardiovascular angiogenesis *ex vivo*. The method was based on that described by Kiefer *et al* and allow the function of endothelial cells to be studied without prior isolation from the tissue (Kiefer *et al.*, 2004). Here, pieces of mouse and rat heart/aorta were embedded in 3D fibrin gel matrix and outgrowth of endothelial sprouts quantified as a measure of efficiency of neovascularisation of the heart tissue. Sprouts comprising of endothelial cells with associated smooth muscle cells and pericytes started forming between 3 to 5 days, although the patterns of sprouts and single cells observed varied depending on experimental parameters such as the presence of different growth factors, oxygenation conditions (normoxia- 21% oxygen versus hypoxia- 3% oxygen) and the age of the donor animals.

Optimisation of the assay was achieved using hearts from non-irradiated animals. For these experiments, hearts from mice used within the Tumour Microcirculation Group (TMG) for other experiments were taken when animals were sacrificed. The age of these animals varied but they were generally between 14 and 40 weeks old and included both males and females. Experiments were conducted using both excised dissected aortic ring tissue and heart dissected into small $1mm^3$ pieces. Different conditions were tested to establish conditions for *in vitro* heart angiogenesis and to improve the formation of sprouts from mouse heart explants. First various matrices (matrigel and fibrin) were tested to find out which one is better for formation of angiogenic sprouts in *in vitro* explants assay. Different tissues (aortic ring and heart) initially were used to establish the assay, however for subsequent experiments the heart explants were utilised. Different oxygen conditions (normoxic (21% O_2) and hypoxic (5% O)) were tested to improve the assay. Additionally, mice at different ages (young and old) were tested since irradiated mice from CARDIORISK were between 20 to 60 weeks old.

4.2.1.1 Cardiac explants *in vitro* angiogenesis assay using matrigel or fibrin matrices

The angiogenesis process and formation of capillary-like structure *in vitro* occur with the support of ECM hydrogels comprised of fibrin, collagen or basement membrane that stimulate the 3-D micro vessels environment *in vivo* (Reed *et al*., 2007). The first attempt of this assay was performed using matrigel, which is a basement membrane-based gel. It converts to gel at room temperature while it is liquid at 4°C. In the first two experiments, whole hearts from SCID mice were dissected into small segments of approximately 1 mm^3. Tissue pieces were embedded on a layer of solidified matrigel and then another layer of matrigel was added on top of the explants. After 30 min, growth media were added. Two different media, the complete 20% FCS-DMEM and complete 10% FCS-EBM (both were supplemented with a maximal FCS concentrations and EC growth supplements) were tested. These two media contained some angiogenic factors as well as serum (see Appendix **I**). The heart explants were incubated for 10 days in normoxic (21% O_2) conditions and media were changed every second day. No sprouts were observed after 10 days. Further experiments were performed using the same method but this time explants were kept in normoxic (21% O_2) or hypoxic (5% O_2) conditions since previously explant sprouting was more pronounced under hypoxia (Kiefer *et al.*, 2004). However, even under hypoxic conditions, the heart explants did not demonstrate sprouting.

Since the *in vitro* assays of Kiefer *el al* (2004) and other studies used fibrin gels (Munk *et al*., 2006; Munk *et al*., 2007; Sanches de Miguel *et al*., 2008), the use of a fibrin/thrombin matrix in stimulating explant sprouting was tested in the following experiments. The fibrin matrix is generated using active thrombin to cleave soluble fibrinogen and convert it to insoluble fibrin (Senger, 1996; Wang *et al.*, 2007). In this method explants were embedded between two layers of fibrin gel, media were added and incubated at 37°C. Sprouting continued for 10 days. Figure **4.1** shows example of heart explants with sprouts after 10 days in fibrin gel. It has been previously observed that sprouting of ECs is more likely from mouse aortic explants than from heart explants (Kiefer *et al.*, 2004). Therefore, first, the aortic arch (AA) was dissected from mouse heart and tested. AA was divided into small 1mm^3 pieces, usually between 5 to 10

explants, embedded in fibrin gel and exposed to two different media under both hypoxic (5% O_2) and normoxic (21% O_2) conditions. Sprouting was observed after 2-3 days, demonstrating the viability of AA explants to sprout in different conditions including both hypoxia and normoxia when imbedded in a fibrin/thrombin matrix (Figure **4.2**).

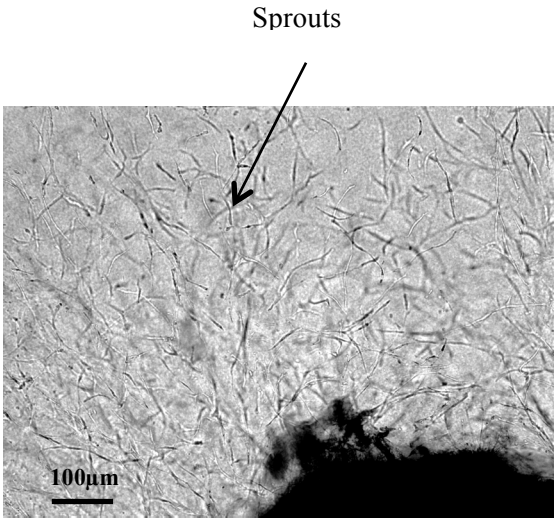

Figure 4.1 Sprouting of mouse heart explant embedded in fibrin gel. Explants were observed by phase contrast microscopy. Representative image of mouse heart tissues with outgrowing sprouts/cells is shown. The image was taken 10 days after the start of the experiment. Explants were grown in complete 20%FCS-DMEM.

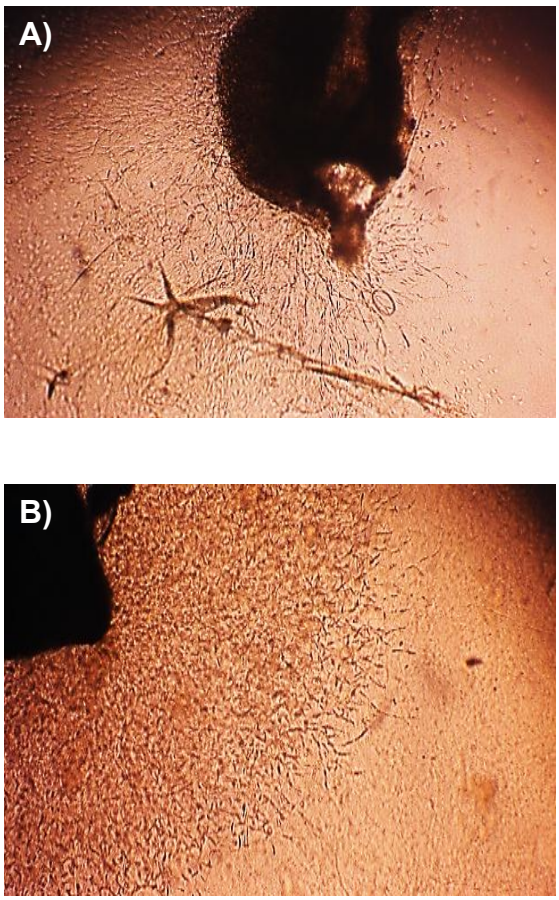

Figure 4.2 Sprouting of mouse aortic arch (AA) heart explants embedded in fibrin gel. Explants were observed by phase contrast microscopy. Representative images of mouse aortic arch (AA) heart tissue with outgrowing sprouts/cells are shown under **A)** Hypoxia (5% O_2) and **B)** Normoxia (21% O_2). Explants were grown in complete 20%FCS-DMEM. Results showed that in both conditions explants were able to sprout. Images were viewed using a 4x objective.

4.2.1.2 Optimization of the *in vitro* assay of heart angiogenesis using different media and different conditions of oxygen

Since the previous experiment demonstrated sprouting efficiency from mouse AA, even under normoxic conditions, the next experiments were designed to investigate whether regions of the heart other than the AA were able to sprout, as a way of further characterising mouse heart angiogenesis *in vitro.* Heart tissue was dissected into 2 parts: 1) heart atrium (HA) and 2) heart ventricular myocardium (HV) as shown in **Fig 4.3.** The dissection of the heart into these two parts (HA and HA) would help to better identifying the micro- and macrovascular origin of the explants for further analysis.

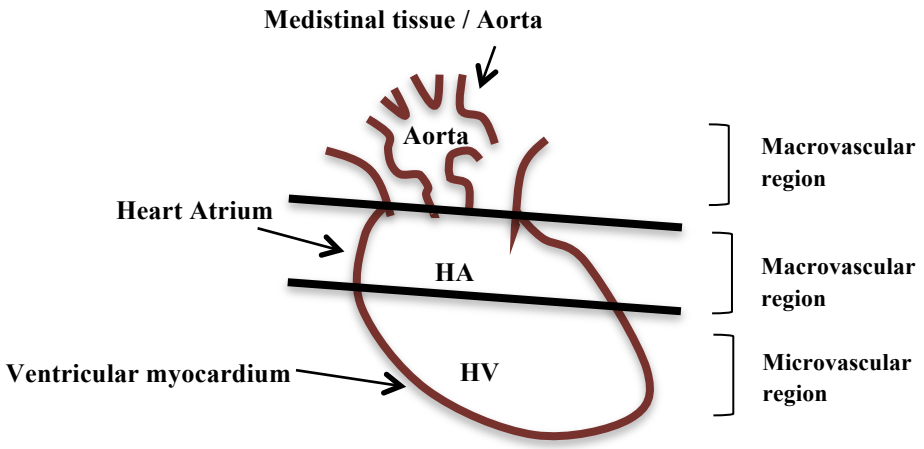

Figure 4.3 Schematic diagram of heart. The heart was dissected into two parts: heart atria (HA) and ventricular myocardium (HV).

Consistent with the study by Kiefer *et al* (2004), various parameters were tested in order to optimize the *in vitro* heart explant angiogenesis assay using HA and HV explants. Since the aim was not to assess angiogenesis response of heart explants to different angiogenic growth factors, it was possible to develop the assay using combinations of optimal FCS and angiogenic growth factors. A complete Basal EBM medium supplemented with growth factors

(hFGF-B, rEGF, hEGF,R3-1GF-1, hydrocortic and ascorbic acid) and 10 % FCS as well as a DMEM medium that was supplemented with 20 % serum plus Endothelial Cell Growth Supplement (ECGS), were tested. In previous studies, hypoxia was found to be prerequisite for *in vitro* formation of sprouts (Kiefer *et al*., 2004; Munk *et al*., 2007). Here explants were grown under both hypoxic and normoxic conditions. Heart tissue was from SCID mice, (including both males and females) 14 weeks of age (hearts were obtained from sacrificed animals used by TMG members). Explants were embedded in fibrin gel (as used previously) and angiogenic EC sprouting monitored for 10 days, after which images were taken. Results presented in this section were only based on the number of explants forming sprouts, as identified by microscopy. Data were analysed and expressed as percentage of explants demonstrating sprouts out of the total explants embedded. The extent of explants sprouting was not evaluated. Results from the two initial experiments are tabulated in Table **4.1** and **4.2**. These data show that HA and HV explants sprout in both normoxic (21% O_2) and hypoxic (5% O_2) conditions, with HA explants demonstrating the most sprouting.

Thus, all further experiments were performed using 20%FCS-DMEM under normoxia, which represents the normal *in vivo* condition. A further seven experiments using HA and HV explants from 14 to 19 weeks old SCID mice hearts were performed (using the conditions described) to further evaluate the efficiency of sprouting from HA and HV. The results were expressed as a mean ± SEM percentage of explant sprouting, with 49.3% for ventricular myocardium and 88.5% for atrial tissue (Table **4.3**). Consistent with the first set of results, HA tissue displayed a higher number of explants with sprouts compared to HV. The statistical analysis (using t-test) showed that the formation of sprouts from HA explants were significantly higher than HV explants ($^*p < 0.05$).

14 weeks SCID (Female)	Complete DMEM Normoxia	Complete DMEM Hypoxia	Complete EBM Normoxia	Complete EBM Hypoxia
Assay 1	60%	34%	23%	17%
Assay 2	20%	27%	5%	31%
Mean	40%	30.5%	14%	24%

Table 4.1 Percentages of positive HV explants with sprouts. Data are shown from 2 initial experiments under normoxia and hypoxia conditions using Complete 20%FCS-DMEM and Complete EBM media on heart HV explants taken from 14 weeks old female (F) SCID mice.

14 weeks SCID (Female)	Complete DMEM Normoxia	Complete DMEM Hypoxia	Complete EBM Normoxia	Complete EBM Hypoxia
Assay 1	100%	90%	100%	83%
Assay 2	90%	72%	75%	100%
Mean	95%	82.5%	87.5%	91.5%

Table 4.2 Percentages of positive HA explants with sprouts. Data are shown from 2 initial experiments under normoxia and hypoxia conditions using Complete 20%FCS-DMEM and Complete EBM media on heart HA explants taken from 14 weeks old female (F) SCID mice.

14-20 weeks SCID	No of explants with spouts/ Total no of explants	HV/normoxia spouts %	No of explants with spouts/ Total no of explants	HA/normoxia Sprouts%
Assay 1	**6/10**	**60%**	**10/10**	**100%**
Assay 2	**5/25**	**20%**	**9/10**	**90%**
Assay 3	**2/18**	**11%**	**16/20**	**80%**
Assay 4	**4/18**	**18%**	**12/18**	**67%**
Assay 5	**33/41**	**81%**	**21/21**	**100%**
Assay 6	**18/18**	**100%**	**15/16**	**94%**
Assay 7	**6/11**	**55%**		
Mean		**49.3** ± 12.1		**88.5%** ± 5.3

Table 4.3. Comparative percentages of positive HV and HA explants with sprouts. Data are shown from 14-19 weeks old SCID mice under normoxia condition using Complete 20%FCS-DMEM medium on hearts' atrium (HA) and ventricular myocardium (HV) explants.

4.2.1.3 Cardiac explants *in vitro* angiogenesis assay using young and old mice

After establishing the *in vitro* explant assay method using explants from SCID mouse hearts, further experiments were performed using hearts from C57BL/6 mice. This was necessary since the irradiated heart tissue forming the basis of this experimental collaborative study came from this strain of mouse. In previous studies angiogenesis was found to be restricted in aged mice (Agah *et al.*, 2004; Reed *et al.*, 2007). Furthermore, since the collaborative experiments used irradiated and non-irradiated heart tissue from both young (20 weeks) and old (up to 68 weeks) mice, with animals being approximately 8 weeks old when irradiated, it was necessary to first optimise the explant assay to accommodate potential issues associated with the effect of mouse heart age on the efficiency of explant sprouting.

Three separate assays were performed on hearts from old C57BL/6 mice (36-40 weeks). Excised heart explants were plated in fibrin gel and then monitored for 10 days. The data in Table **4.4** indicates angiogenic activity in 40 weeks old C57BL/6 mice heart explants with heart atrium (HA) and ventricular myocardium (HV) demonstrating sprouting at 76.3% and 90.3% respectively. Therefore under the established conditions heart tissues from older mice were able to form sprouts.

36-40 weeks C56BL/6	HV/normoxia	HA/normoxia
Assay 1	**61%**	**88%**
Assay 2	**68%**	**83%**
Assay 3	**100%**	**100%**
Mean	**76.3%** ± 12	**90.3%** ± 5.04

Table 4.4 Percentages of positive explants with sprouts from older animals. Data are shown from 36-40 weeks old C57BL/5 mice under normoxia condition using Complete 20%FCS-DMEM medium on hearts' atrial (HA) and ventricular myocardium (HV) explants.

As the experimental plan would also test irradiated and non-irradiated hearts from ApoE$^{-/-}$ mice, one experiment was performed using heart tissue from a 20-week-old ApoE $^{-/-}$ mouse, in which demonstrated sprout formation.

4.2.2 Semi-quantitative analysis of explants sprouting

In order to evaluate the explant sprouting response, an appropriate method of quantification was needed. This is difficult, since sprout formation was dense and developed in 3D. Some studies evaluate the angiogenic response of heart tissue according to the ratio of total explant area to sprout area (Kiefer *et al.*, 2004). However, this method fails to take into account the density of sprouts. Other studies employ a method where explant sprouting is measured according to the angiogenesis index method; this is a semi-quantitative visual rating system where sprouts are visualised by phase contrast microscopy at different levels of magnification, and scored for degree of sprouting. Explants exhibiting no sprouts are given a score of 0 and then sprouting is rated between 1-4 (Lewis *et al*., 2006) or 1-8 (Kiefer *et al.*, 2004; Sanchez de Miguel *et al.*, 2008).

In analysing data from the experiments described above, the angiogenesis index using the visual scoring method of Lewis *et al* (2006) was adopted. Explants exhibiting no sprouts were given a score of 0, whilst explants consisting of two to ten sprouts were scored 1, explants with more than 10 sprouts but fewer than 100 were scored as 2, explants with many sprouts (>100) were scored as 3 and finally explants with longer and denser sprouts were given the score of 4 (Figure **4.4**). To accommodate the fact that there were different numbers of explants in each experiment and to enable data from multiple experiments to be directly compared, the angiogenesis index for each experiment was determined by first multiplying the total number of explants (per experiment) by 4. This represents the maximum value that could be calculated assuming all explants sprouted fully and exhibited the maximum rating of 4. The experimental explant sprouting data was then calculated such that the number of explants in each score-rating category was multiplied by that score rating to create the corresponding values (e.g. if there were 13 explants with a score of 3, then this gave the number 39). All values obtained for

each score category (0, 1, 2, 3 and 4) were then added together and expressed as a ratio of the maximum (assuming all explants scored 4). Therefore, in an experiment of 50 explants (denoted as "exp" below), where 5 explants scored 0, 10 explants scored 1, 15 explants scored 2, 10 explants scored 3 and 10 explants scored 4, the angiogenic index would be calculated as follows:

$$\textbf{Angiogenesis index} = \frac{(\text{exp}\ (0)=5) + (\text{exp}\ (1)=10) + (\text{exp}(2)=15) + (\text{exp}\ (3)=10) + (\text{exp}\ (4)=10)}{\text{exp}\ (4)=50}$$

Angiogenesis index= **(0+10+30+30+40)/200 = 0.5**

In order to examine whether the semi-quantitative visual rating system is accurate and reliable to use, two independent investigators scored the heart explants angiogenesis from the 20 weeks C56/BL6 mice group. The first investigator was the person who performed the experiment and second investigator was an unbiased observer. After obtaining the angiogenesis index of each irradiated and non-irradiated group, the result from investigator one and two were compared to each other (Appendix **VI**). There were small differences between the two observers scoring which were not statistically different, indicating this semi-quantitative method was reliable and reproducible.

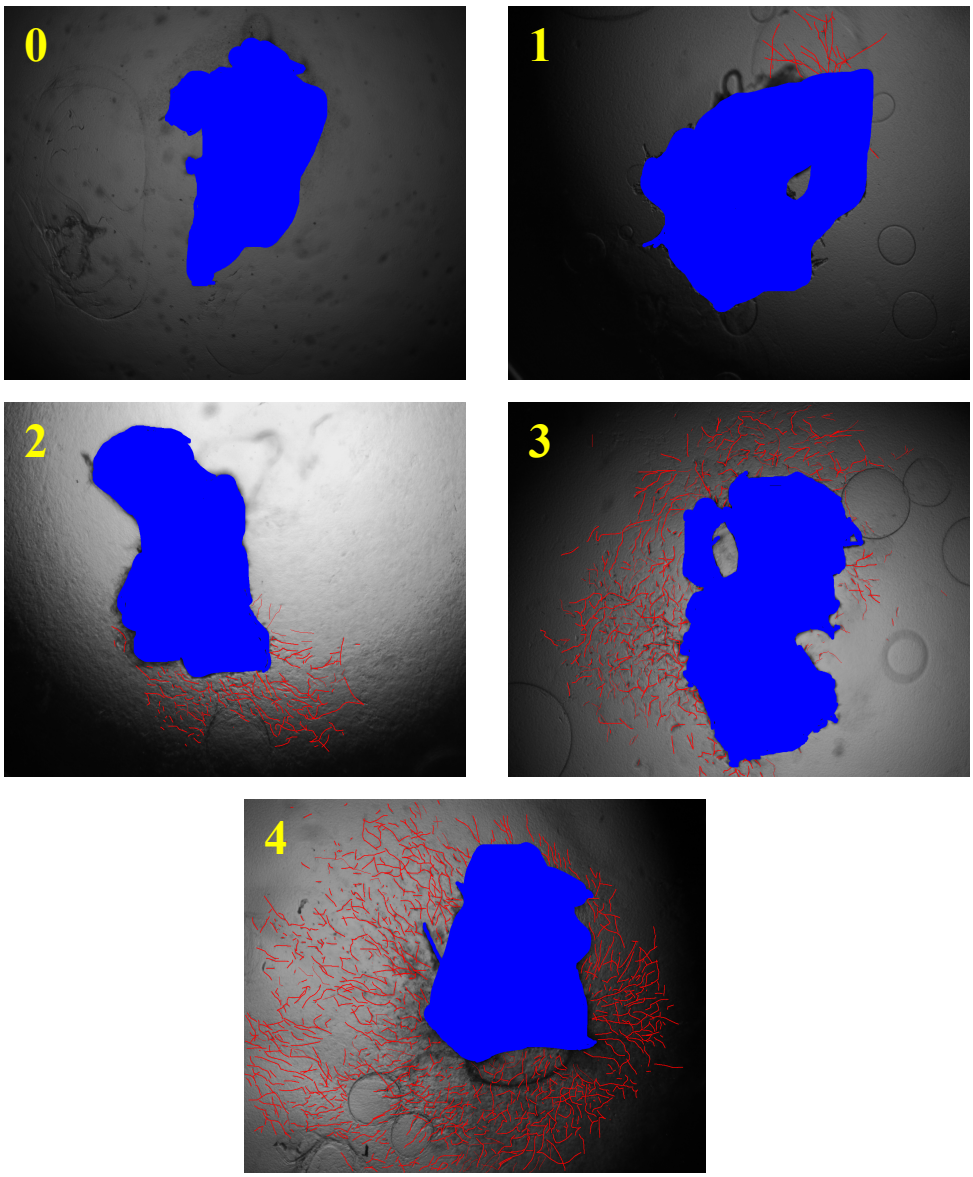

Figure 4.4 Heart explants with a different score of sprouting. A standardized scale from 0 to 4 indicates the degree of EC outgrowth/sprouting (angiogenic index). Scoring was performed as follows: No sprouts= Score 0; 2-10 sprouts=1; Sprouts<100=2; Sprouts >100=3; Very dense sprouts >100=4.

4.2.3 Effect of radiation on formation of sprouts by heart explants

Having now optimised the explant assay using heart tissue from various strains of mice including those used by our collaborators, the main objective was to investigate whether radiation affects the capacity of cardiac endothelial cells to sprout from heart explants, as a measure of their capacity to undergo repair and angiogenesis. To test the objective, hearts of the wild type C57BL/6 and ApoE$^{-/-}$ mice aged 8-12 weeks were locally irradiated by our CARDIORISK collaborators (Professor Wolfgang Dörr and his group, Technical University of Dresden) using a range of single doses of X-rays (25kV, 85mA) at low (0.2 Gy), moderate (2 Gy) and high doses (8 & 16 Gy). After 20, 40 and 60 weeks post-irradiation animals were sacrificed; their hearts then were removed and sent to the UK. Each heart was dissected into 2 parts: HA and HV and then each part was cut into about 50 explants and assessed for sprouting activity *in vitro* using the optimised assay. One issue with the way this collaborative study was set up was that the animals were sacrificed in Germany and then hearts were sent to the UK. It therefore took one to two days to start the experiment after removal of the hearts, which could have affected the viability of the tissues. However, as detailed below, the explant assays still worked and explants demonstrated sprout formation.

In the first experiment, explant assays were performed on heart tissue obtained from C57/BL6 mice (6 hearts per group), 20 weeks post irradiation (0.2, 2, 8 and 16 Gy) as well as non-irradiated heart tissue (0 Gy). Prior to performing the explant assays, hearts from each time point were weighed, to assess whether radiation had any effect on heart weight and a mean ± SEM for each time point was calculated. These data are tabulated in Table **4.5.** Heart weights were similar in control and irradiated mice from 20, 40 and 60 weeks C57/BL6 and ApoE $^{-/-}$ groups, inferring no major effects of radiation on heart weight. Explant assays were performed as described previously and sprouting assessed using the semi-quantitative angiogenesis index scoring system described above. All results represent experiments which were repeated at least 4 times (except 16 Gy) from different mouse hearts. Explant sprouting data were compared between irradiated and non-irradiated groups using a One-way ANOVA Kruskal-Wallis

statistical test for non-parametric analysis since data have not been normally distributed. As shown in Figure **4.5** the angiogenesis index varied in all C57/BL6 groups including irradiated and non-irradiated heart explants. However, despite this variation, little difference in the mean angiogenesis index score was observed between the non-irradiated HA and HV tissue compared with tissue receiving a dose of either 0.2 or 2 Gy. In contrast, a statistically significant reduction in the angiogenic index score was observed when heart tissue was exposed to doses of 8 and 16 Gy, consistent with less sprouting of explants as observed by phase contrast microscopy. The experiment was repeated again, this time using hearts from ApoE $^{-/-}$ mice (5 hearts per group). Here, the angiogenesis index scores were generally higher, compared with those obtained for C57/BL6 mouse hearts, inferring better sprouting in these explants. However, despite the qualitative and quantitative difference between mouse strains, a similar trend was observed, with a statistically significant reduction in sprouting observed for heart tissue exposed to 8 and 16 Gy irradiation compared with non-irradiated control hearts (Figure **4.6**)

In the next set of experiments, explant assays were performed on heart tissue obtained from C57/BL6 mice (5 hearts per group), 40 weeks post irradiation (2 and 16 Gy) as well as non-irradiated heart tissue (0 Gy). Only radiation doses of 2 and 16 Gy were administered in these experiments. Consistent with the data from heart tissue 20 weeks post-irradiation, evaluation of EC sprout formation in heart tissue 40 weeks post-irradiation indicated a reduction in cell outgrowth in a dose-dependent manner, which was significant at 16 Gy (Figure **4.5).** The experiment was next repeated using heart tissue from ApoE $^{-/-}$ mice (5 hearts per group, except n=4 in 16 Gy group), 40 weeks post irradiation (2 and 16 Gy) as well as non-irradiated heart tissue (0 Gy). Although a similar trend was observed, with decreased angiogenic capacity of ApoE $^{-/-}$ heart explants receiving a dose of 16 Gy, the angiogenic index in two out of four experiments was similar to the control group, which was unexpected (Figure **4.6**). One potential explanation is that the hearts were not irradiated properly.

A)

20 weeks Hearts	C57BL/6 Average Heart Weight (gr)	C57BL/6 Heart Numbers	ApoE$^{-/-}$ Average Heart Weight (gr)	ApoE$^{-/-}$ Heart Numbers
0 Gy	0.165 ± 0.0025	6	0.136 ± 0.002	5
0.2 Gy	0.153 ± 0.004	6	0.147 ± 0.007	6
2 Gy	0.174 ± 0.016	6	0.159 ± 0.006	6
8 Gy	0.151 ± 0.016	6	0.144 ± 0.003	5
16 Gy	0.143 ± 0.0025	6	0.144 ± 0.006	5

B)

40 Weeks Hearts	C57BL/6 Average Heart Weight (gr)	C57BL/6 Heart Numbers	ApoE$^{-/-}$ Average Heart Weigth (gr)	ApoE$^{-/-}$ Heart Numbers
0 Gy	0.164 ± 0.0085	5	0.159 ± 0.0092	5
2 Gy	0.167 ± 0.0086	5	0.148 ± 0.0061	5
16 Gy	0.153 ± 0.0046	5	0.162 ± 0.016	4

C)

60 Weeks Hearts	C57BL/6 Average Heart Weight (gr)	C57BL/6 Heart Numbers	ApoE$^{-/-}$ Average Heart Weight (gr)	ApoE$^{-/-}$ Heart Numbers
0 Gy	0.2 ± 0.0185	6	0.161 ± 0.0073	10
2 Gy	0.199 ± 0.0149	5	0.162 ± 0.0041	10
16 Gy	0.2	1	0.155	2

Table 4.5 The average weight and number of hearts. Data are shown from each irradiated and non-irradiated heart taken from C57/BL6 and ApoE $^{-/-}$ groups, where **A)** represents data for hearts excised 20 week post-irradiation, **B)** represents data for hearts excised 40 weeks post-irradiation and **C)** represents data for hearts excised 60 weeks post-irradiation. Data are presented as mean ± SEM of 4 to 10 separate hearts (except 16 Gy in 60 weeks group).

Therefore, following statistical analysis, it was concluded that angiogenesis formation from HA and HV explants of hearts treated with16 Gy was comparable to non-irradiated hearts.

A proportion of the mice administered with the high dose of 16 Gy to the heart had unscheduled deaths before 60 weeks. Consequently only one 16 Gy irradiated heart was received for the C57/BL6 mice and 2 for the ApoE $^{-/-}$ group. In contrast, n=10 0 Gy and 2 Gy irradiated hearts were received for the 60 weeks ApoE $^{-/-}$ group, and n=6 hearts for the C57/BL6 mice. When explant sprouting data was compared, again there was a general trend in inhibition of mouse heart angiogenic activities even after 60 weeks post irradiation. However, in contrast to the previous data (20 and 40 weeks post irradiation) more profound effects were observed at the lower irradiation doses. HA explant sprouting was significantly reduced at 2 Gy in both C57/BL6 and ApoE $^{-/-}$ mouse, and at 16 Gy in HV explants (Figure **4.5** and Figure **4.6**). Therefore, the results confirmed a general reduction of angiogenesis in irradiated mouse hearts in a dose-dependent manner compared to the control group, which was persistent after 20, 40 and 60 weeks irradiation. Additionally, profound effects on angiogenesis were observed in response to low dose irradiation (2 Gy) 60 weeks post-treatment.

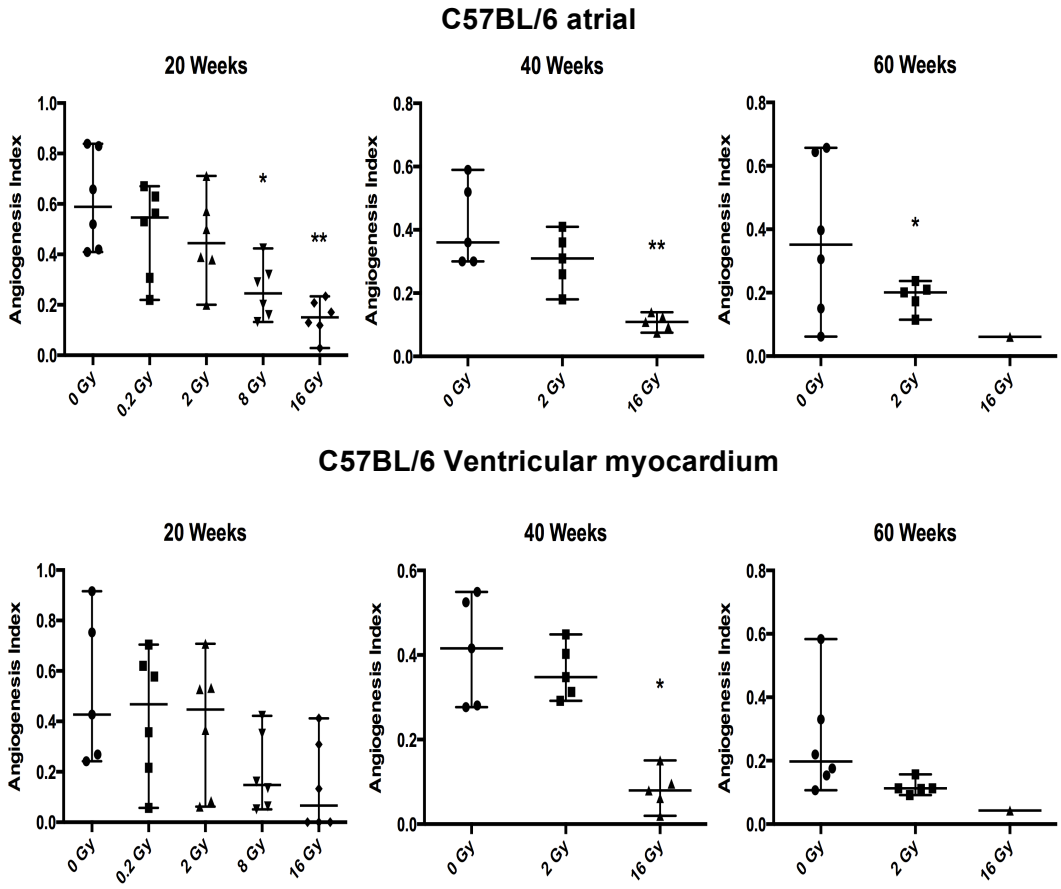

Figure 4.5 Effects of radiation on angiogenic sprouting in C57BL/6 atrial and ventricular myocardium explants after 20, 40 and 60 weeks post-irradiation. The graphs depict semi-quantitative analysis of explant sprouting at 20, 40 and 60 weeks post-irradiation in C57/BL6 hearts. Data was expressed as median of 5-6 hearts angiogenesis index (using 50 explants for each HV and HA part). Irradiated groups were compared to the control groups using non-parametric ANOVA (Kruskal-Wallis test) test. There was a reduction in angiogenic activity which increased with increasing radiation doses. Radiation inhibited the formation of angiogenic sprouts dose-dependently. Angiogenic sprouting was significantly inhibited at doses of ≥8 Gy at 20 weeks, ≥16 Gy at 40 weeks and 2 Gy at 60 weeks post-irradiation in HA explants compared to age-matched control groups. (*$p < 0.5$, **$p < 0.01$)

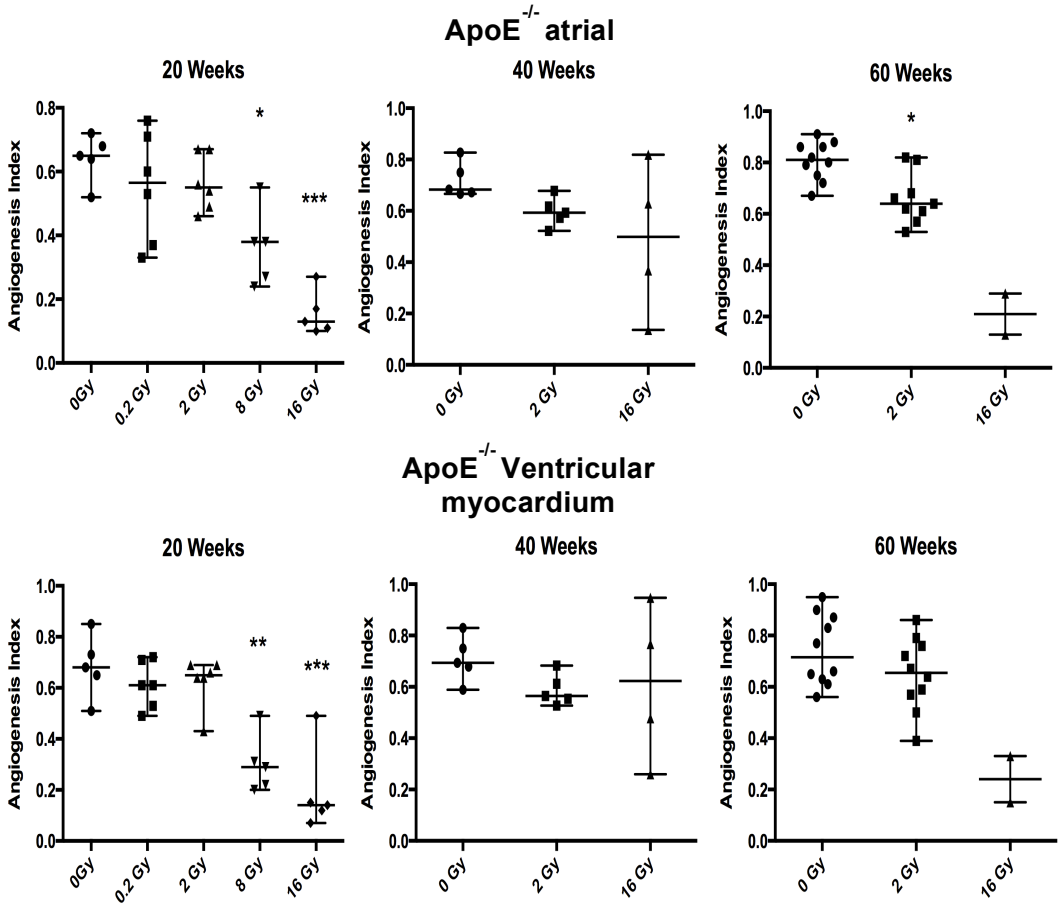

Figure 4.6 Effects of radiation on angiogenic sprouting in ApoE$^{-/-}$ atrial explants and ventricular myocardium after 20, 40 and 60 weeks post-irradiation: The graphs depict semi-quantitative analysis of explant sprouting at 20, 40 and 60 weeks post-irradiation in ApoE$^{-/-}$ hearts. Data were expressed as median of 5-6 hearts angiogenesis index (using 50 explants for each HV and HA part). Irradiated groups compared to the control groups using non-parametric ANOVA (Kruskal-Wallis test) test. There was a reduction in angiogenic index which increased with increasing radiation doses. Angiogenic sprouting was significantly regressed at doses of ≥8 Gy at 20 weeks in both HA and HV explants. Angiogenic responses were inhibited at doses 2 Gy from 60 weeks post-irradiation in HA and HV explants respectively compared to age-matched control group. (*$p < 0.5$, **$p < 0.01$, ***$p < 0.001$)

4.2.4 Characterisation of heart explant sprouts

So far the study shows that sprouting from cardiac explants was inhibited by previous irradiation of the hearts *in vivo*. It was necessary to next establish the identity of the cells in the sprouts and prove that outgrowing cells from heart explants consisted of endothelial cells. Other studies have previously shown that the angiogenic sprouts from mouse and rat heart/aorta explants are composed of a polarised layer of ECs surrounded by smooth muscle cells and pericytes (Sanchez de Miguel *et al.*, 2008).

4.2.4.1 Characterisation of CEC using immunohistochemistry method

ECs are commonly identified by immunohistochemistry using antibodies against proteins characteristically expressed in ECs. vWF is a glycoprotein stored in Weibel Palade bodies in endothelial cells and is commonly used to characterise endothelial cells and stain vessels (Lidington *et al.*, 2002; Oxhorn *et al.*, 2002). Lectin, on the other hand, can bind to the carbohydrate-rich glycocalyx on the surface of endothelial cells. The biotin-labelled form of lectin, Bandeiraea or Griffonia simplicifolia (lectin GSL I-B4) has been used to characterise vascular endothelium in different rodent species including mouse (Lang *et al.*, 1994; Mattsson *et al.*, 2002).

Immunohistochemical staining experiments using antibodies to vWF and lectin (section **2.8.2**) were performed on explant heart tissue (from the same tissue sample) as a means of confirming the explants/sprouts are ECs and representative data from these experiments are highlighted in Figure **4.7**. Haematoxylin was used as a counter stain (purple) for cell nuclei, making visualisation of cells possible **(**section **2.8.3)**. No positive (brown) vWF protein staining was identified either in the vessels of heart myocardium tissue or sprouting cells growing out into the fibrin gel (Figure **4.7a & b**).

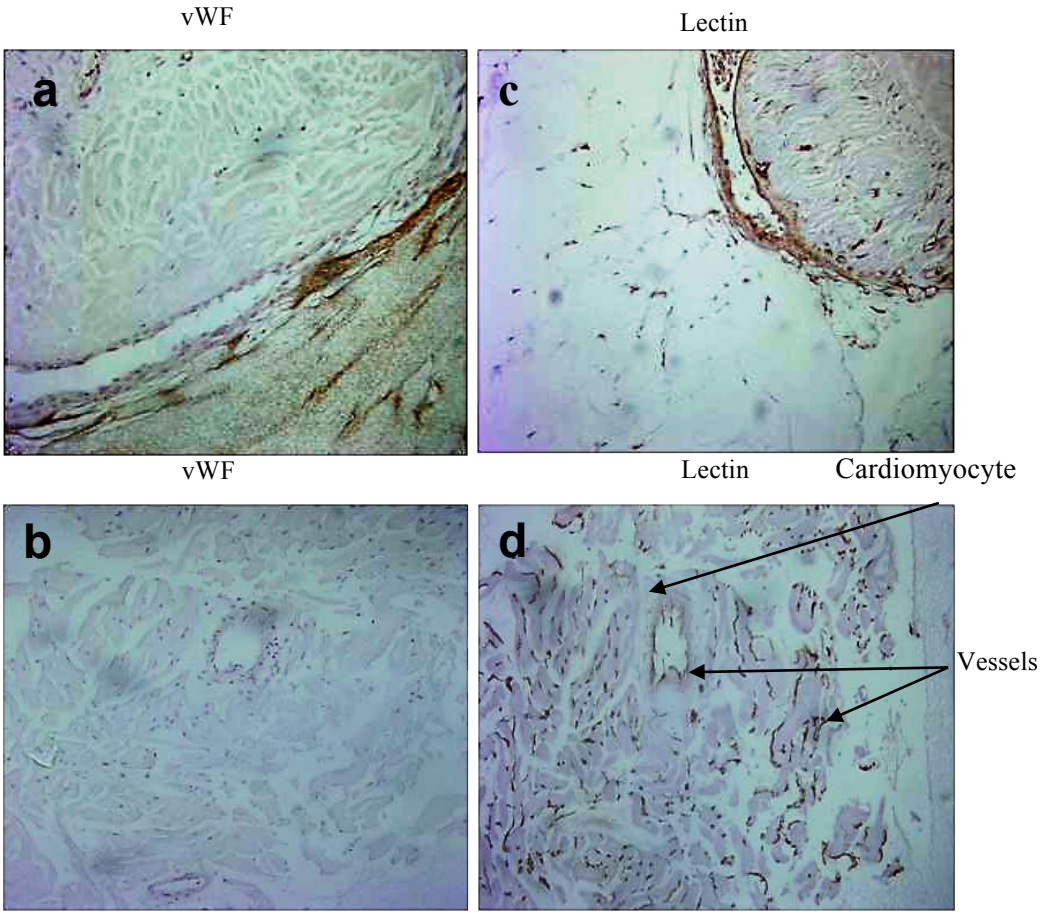

Figure 4.7 Characterisation of heart explants sprouts using vWF and lectin. Images show angiogenic sprouts from mouse heart tissues (10 x). The explants from the same heart tissue sections were fixed and stained for vWF (**a & b**) and lectin (**c & d**). No positive vWF protein staining was observed either in the microvessels of the myocardium or the sprouting cells. In contrast, microvessels in the whole mount preparation of CEC from mouse heart explants stained positively for lectin (**c & d**). Images were viewed using a 10x objective.

However, in contrast, positive (brown) lectin staining was evident not only in large and small vessels but also bound to cell sprouts within the fibrin (Figure **4.7c & d**). For this reason, all subsequent immunohistochemistry experiments were performed using lectin and no further optimisation of vWF staining was performed.

Figure **4.8** shows the identification of ECs using lectin. The microvessels of the myocardium have been characterised as well as the sprouting cells. ECs migrating from the heart explant, proliferated and formed a capillary-like network, with lumen formation (Figure **4.8**). In order to stain the cell nuclei and cytoplasm, haematoxylin and eosin (H&E) were used respectively.

During the process of vessel maturation ECs interact with mural cells, providing support and stabilisation to the newly formed vessel. Common types of mural cell are pericytes and vascular smooth muscle cells. Therefore, the sprouts can be stained with other cell markers to detect pericytes and smooth muscle cells, to establish whether other cells migrate along with the endothelial cells to form the sprouts. Additionally, such data may give additional information about the radiation effects on mural cells. Immunohistochemistry experiments were therefore next performed using an antibody to vascular α-SMA, a protein characteristically expressed in smooth muscle cells. However, whilst positive lectin staining was observed in mouse aortic arch explant, indicative of ECs, initial α-SMA staining (on the same section) was not positive (Figure **4.9)**. Based on previous studies (Kiefer *et al.*, 2004; MunK *et al.,* 2006), we expected to identify smooth muscle cells. Therefore, further experiments are needed to optimise the α-SMA staining, including a positive control tissue to confirm whether the anti-a-SMA antibody in these experiments was working. Moreover, a range of dilutions of the working a-SMA antibody will also help to optimise future experiments.

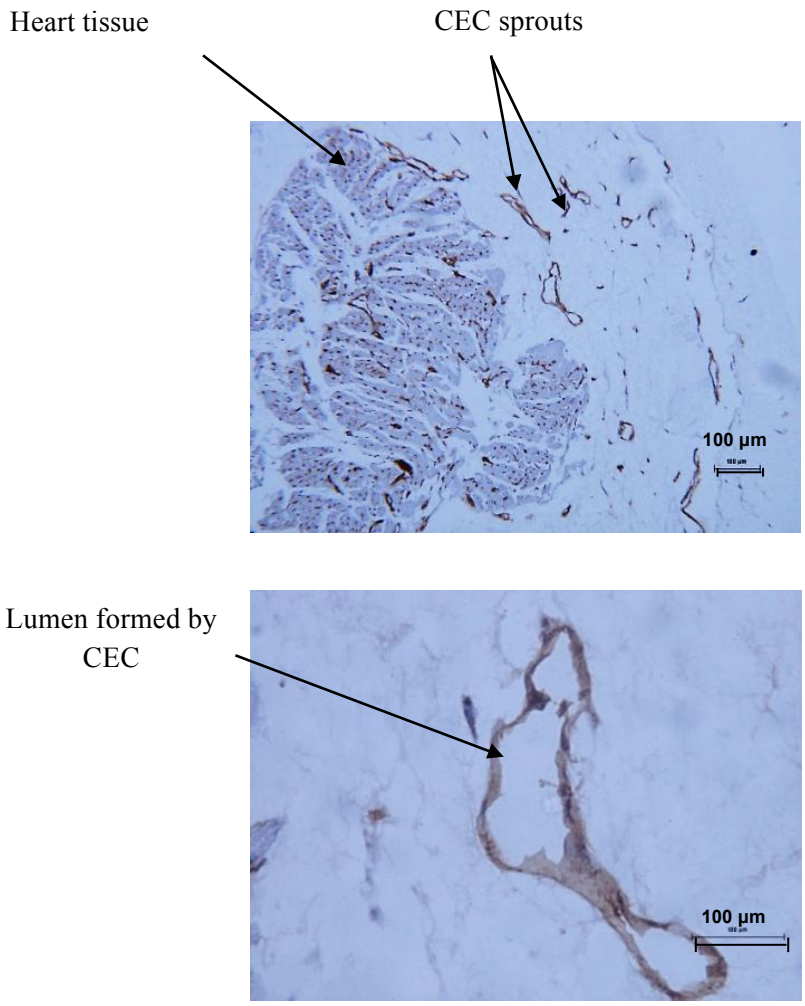

Figure 4.8 Characterisation of heart tissue explants and sprouts using EC marker lectin. Images taken from phase contrast microscopy represent the characterised CEC sprouts from the 60 weeks ApoE $^{-/-}$ mouse heart tissue, which migrated, proliferated and formed into a capillary-like structure. The microvessels in myocardium, sprouting cells and lumen (formed by EC) from embedded heart explants were stained using lectin.

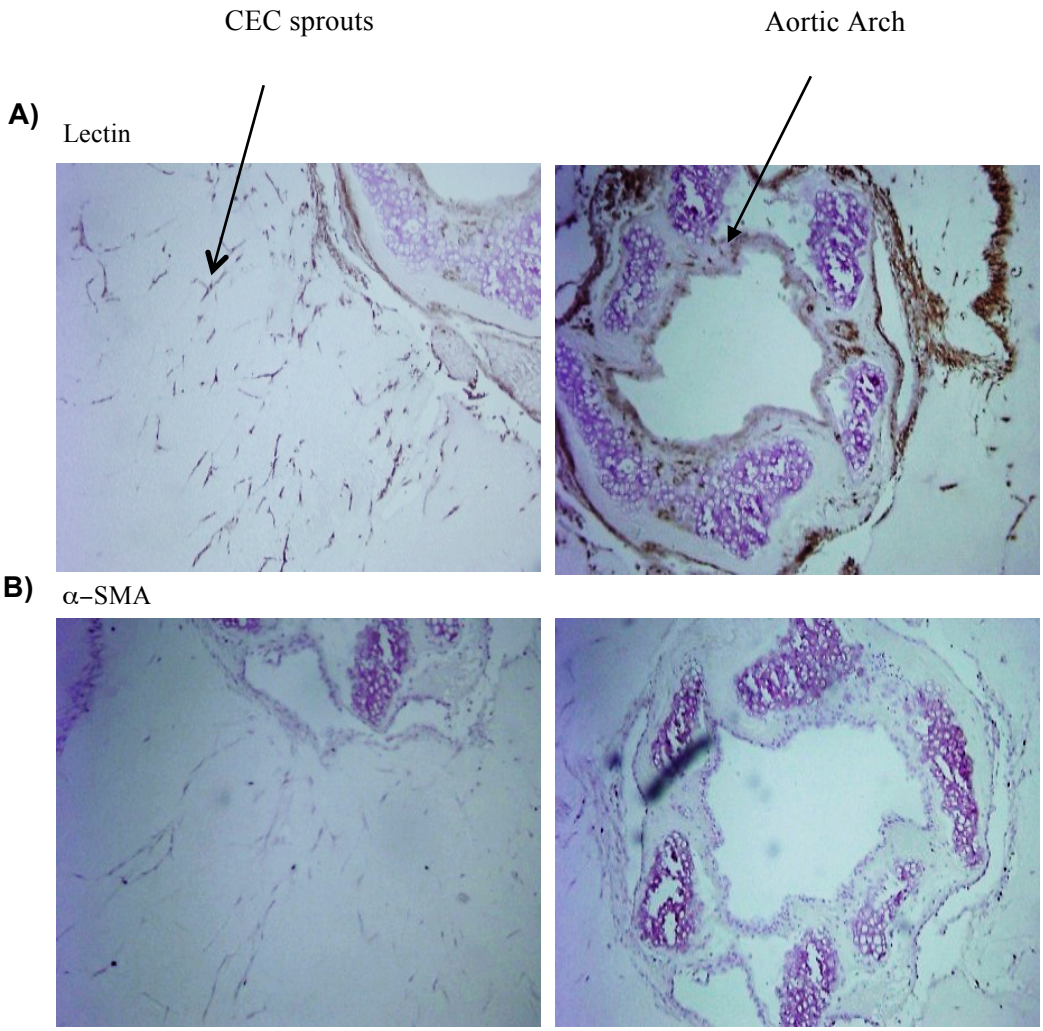

Figure 4.9 Characterisation of heart AA explants and sprouts. Images show the morphology of angiogenic sprouts from mouse aortic arch explants after 10 days. The outgrowing cells were fixed and stained for lectin (**A**), or α-smooth muscle actin (**B**), both of which stain brown with the appropriate antibodies. Haematoxylin was used as a counter stain (purple), which allowed visualisation of all cells. Lectin staining revealed the aortic arch vessel lumen (indicated by the arrow) as well as sprouting endothelial cells (positive brown staining), which was evident in explant outgrowing cells. However, the α-smooth muscle staining was negative and microvessels in myocardium did not stain for smooth muscle with the anti-α–SMA antibody (negative result). Images were viewed using 10x objective.

4.2.4.2 Characterisation of CEC using a modified method

To perform the immunohistochemistry-staining, explants were embedded in paraffin and cut into small sections. Since sprouts developed in 3D, sectioning of the explant enables only a fraction of sprouts to be assessed. Another method to characterise heart explant sprouts was using lectin conjugated to green fluorescein (GSL I-IB4) to visualise the entire outgrowing ECs. The heart tissue explants and their sprouts were first fixed with 4% formaldehyde inside the wells and then incubated with the fluorescent lectin as described in section **2.8.5**. The advantage of this method is that it removes the need to paraffin embed and section samples thus enabling the entire tissue sample to be visualised by fluorescence microscopy, where CEC glow green due to the conjugated fluorescein protein.

Since this is a much more efficient way of visualising CECs, this method was next used to stain the intact angiogenic outgrowths. Data from these experiments are shown in Figure **4.10**. Angiogenic sprouts fluoresced green showing positive lectin staining in sprouting cells as well as the channels formed by endothelial cells, indicating the presence of endothelial cells in the forming microvessels.

This experiment was only performed once, as the fibrin gel thickness interfered with antibody penetration, and therefore the results were different to interpret. It was clear that further optimisation of this method would be necessary, which was not possible within the current study due to time constraints. It is however worth noting that future studies could also use this method for co-staining pericytes, by using the EC marker (fluorescein-conjugated lectin GSL I-IB4) and smooth muscle cell marker (Cy3 labelled anti-α SMA) on the fibrin gel (Kiefer *et al.*, 2004; MunK *et al.,* 2006; Zhu and Nicosia, 2002).

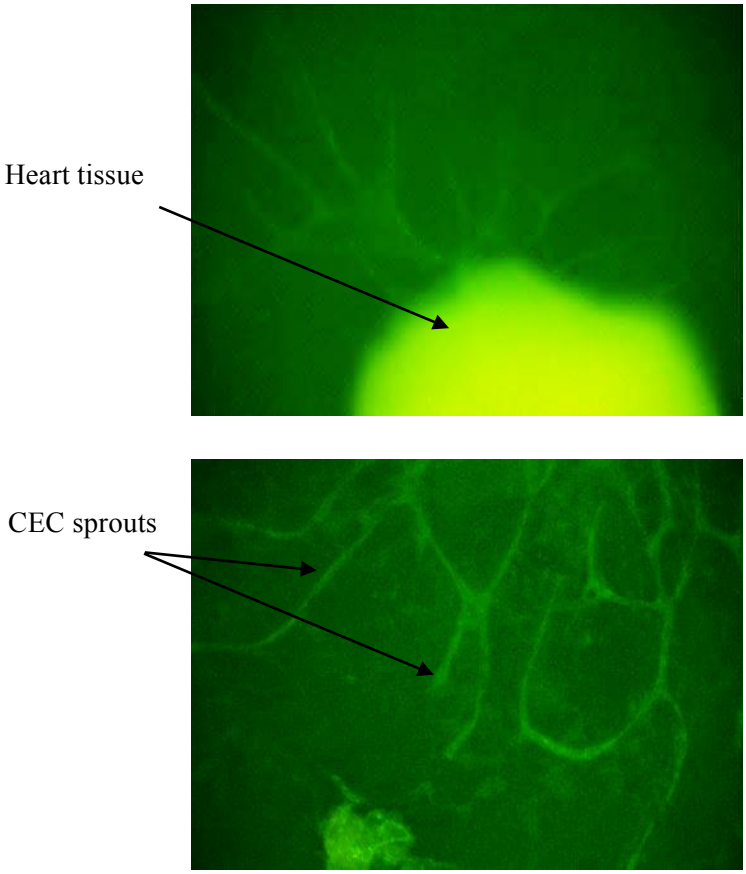

Figure 4.10 Characterisation of outgrowing cells using lectin conjugated to green fluorescein protein. Images show well-characterised channels formed by CEC stained with lectin. Wells were incubated with 25µg/ml fluorescein-conjugated GSL for 3 h. The CEC sprouts images were taken by phase contrast microscopy. Images were viewed using a 10x objective.

4.2.5 Quantitative assessment of CEC sprouts from irradiated and non-irradiated mouse heart

Since the immunohistological staining with lectin worked well (Figure **4.8** and **4.9**), the endothelial cells sprouting from 2 and 16 Gy irradiated and sham-irradiated (0 Gy) mouse heart explants were assessed further, to obtain more information about radiation influences on heart angiogenesis. Here, the aim was to identify quantitative differences between the sprouting cells from irradiated (low and high dose) and non-irradiated animals. The likelihood of sectioning areas of explants with significant numbers of visible sprouts was low, therefore only explant sections with many sprouts were selected for likely identification post-staining. Therefore, for these experiments, explants from hearts excised from 60 weeks post-irradiated $ApoE^{-/-}$ mice were selected, since previous experiments revealed these explants had increased growth.

Overall, more than 20 separate staining experiments were performed on explant tissue from each irradiated and non-irradiated group (0, 2 Gy and 16 Gy) from 60 weeks $ApoE^{-/-}$ mice. The intensity of the stain was determined visually. Representative images from these experiments, as shown in Figure **4.11**, reveal that consistent with earlier experiments, more sprouts were evident in the non-irradiated explants, staining positively for lectin (brown) indicating the presence of CEC. Moreover, these sprouts were longer with increased number of lumens compared to sprouts observed in explants excised from mice receiving either moderate (2 Gy) or high dose (16 Gy) radiation. Some explants excised from the irradiated heart failed to stain with lectin and this was most evident in explants from animals exposed to high dose (16 Gy) radiation, which exhibited only a few or no outgrowing cells.

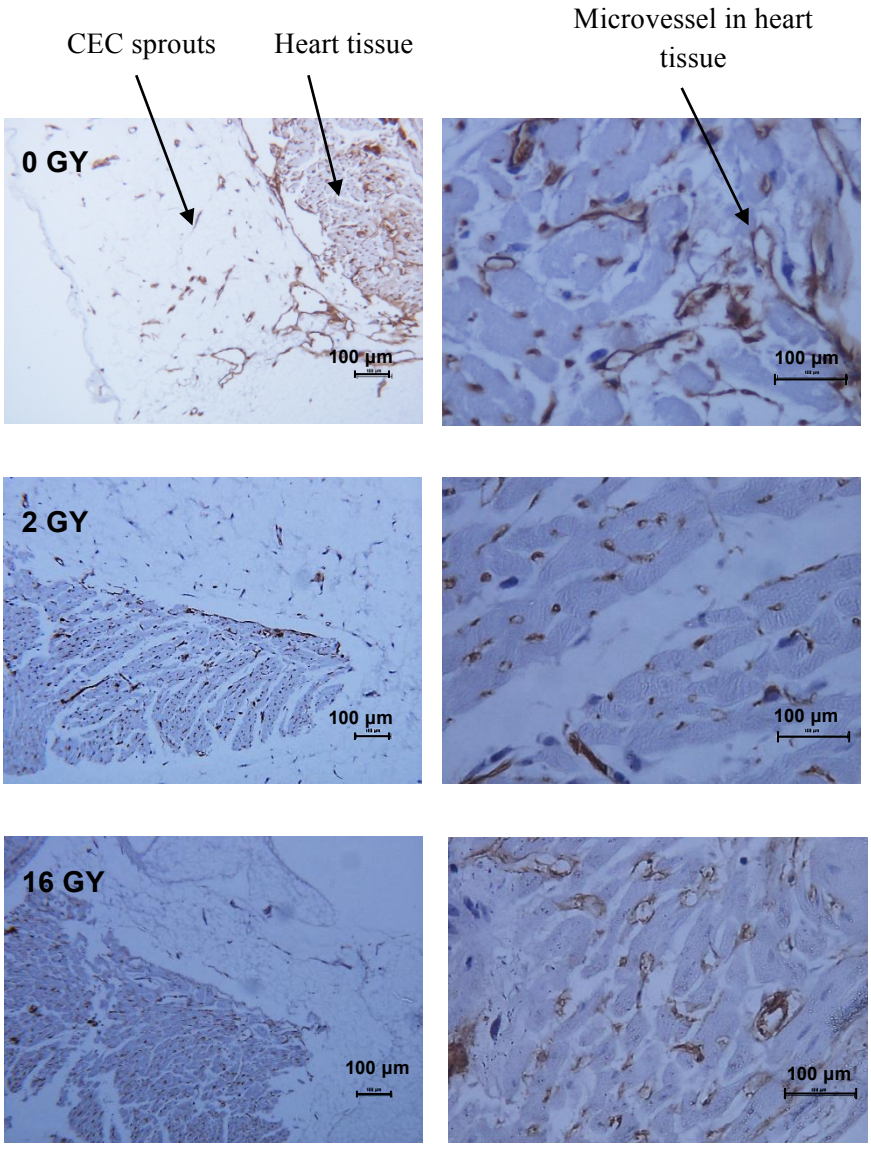

Figure 4.11 Effect of radiation on morphology and number of CEC from irradiated and non-irradiated sprouts. The images depict immunohistochemical characterisation of explant sprouting in heart tissue excised from either non-irradiated (0 Gy) or 60 weeks post-irradiated (2 Gy & 16 Gy) ApoE$^{-/-}$ mice. The explants were fixed and stained with EC marker lectin after 10 days. The number and intensity of staining of outgrowing cells stained with lectin was higher in non-irradiated explants compared to irradiated ones.

Thus, it was decided that in order to accurately evaluate the quantitative differences between the irradiated and non-irradiated sprouting cells, only 0 Gy and 2 Gy explants were compared. After identifying those explants displaying a high density of sprouts and a high intensity of staining, 10 stained sections from 0 Gy and 2 Gy 60 weeks post-irradiated hearts were scored. The number of positive stained cells and non-stained cells were counted by eye under phase contrast microscope using a cell-counter. The scoring was repeated 3 times and the average number was calculated. The result was evaluated according to the number of positively stained ECs relative to the total number of sprouting cells (including stained and non-stained cells). The data are represented in Figure **4.12** and indicates the number of lectin positively stained sprouts represented as a percentage of the total number of sprouting cells in explants from non-irradiated hearts was significantly higher than in irradiated hearts (2 Gy). These results need to be verified by an independent observer to confirm the reliability of data.

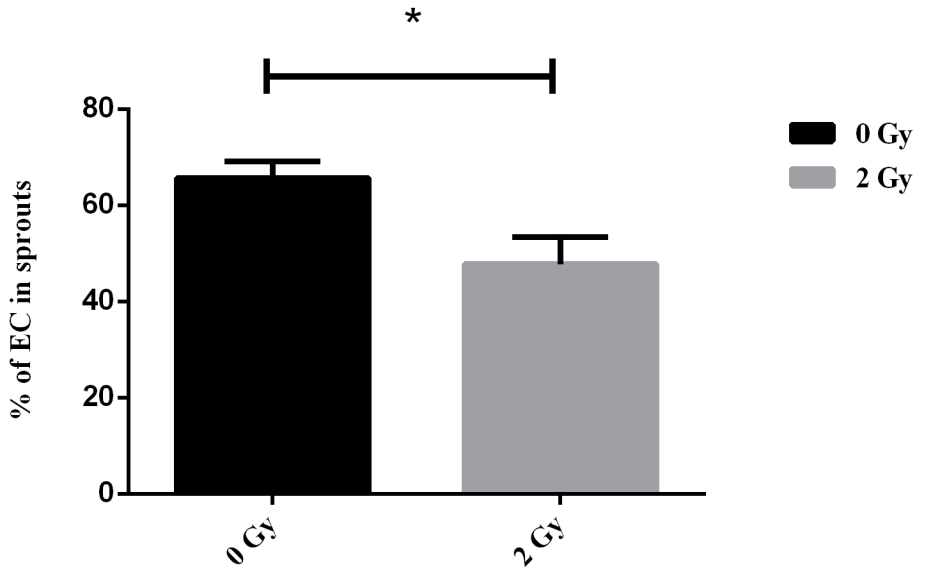

Figure 4.12 Effect of radiation on number of CEC from irradiated and non-irradiated sprouts from immunostained sections. The graphs depict quantitative analysis of explant sprouting at 60 weeks post-irradiation in $ApoE^{-/-}$ mouse hearts. The EC sprouts percentage was calculated from the number of positive outgrowing cells to the total number of sprouts. Data are expressed as mean ± SEM of 9 separate staining. 2 Gy irradiated groups were compared to the control groups using statistical analysis t-test. There was a significant reduction in the percentage of positively stained endothelial cell sprouts in 0 Gy compared to 2 Gy. (*$p \leq 0.5$)

4.3 Discussion

It is known that the long-term risk of cardio toxicity increases after radiotherapy, especially to the chest, but the underlying mechanism of radiation-induced damage such as atherosclerosis and myocardial injury is unclear (Seemann *et al.*, 2012). The main objective here was to study the late effects of radiation on mouse heart angiogenic properties using the heart explant angiogenesis *in vitro* assay.

We determined that the *in vit*ro assay of angiogenesis using heart explants was a suitable and reproducible for the purposes of investigating the effect of radiation on angiogenesis in irradiated and non-irradiated mice heart. This model recapitulates the morphogenesis at the early stage of angiogenesis (Kiefer *et al*., 2004). Non-endothelial sprouting cells were included in this assay, therefore the angiogenic responses observed were not coming from ECs responses alone but reflected an integrated interaction of ECs, mural cells and the whole myocardial tissue cells. Moreover the ECs were in quiescent state at the time of starting the experiment, which again is better representative of the natural-life situation. After ECs assembled into a new vessel, they become quiescent and remain for years (Carmeliet, 2000; Kiefer *et al.*, 2004;). Therefore our results were likely to simulate *in vivo* situations.

4.3.1 Optimization of the *in vitro* assay of heart angiogenesis

First, the assay was optimised testing different conditions, such as normoxia *vs* hypoxia and different media with growth factors, as well as different mice age. The angiogenesis process and formation of capillary-like structures *in vitro* occur with the support of ECM hydrogels comprised of fibrin, collagen or basement membrane, that stimulate the 3-D microvessels environment *in vivo* (Reed *et al*., 2007). In other studies fibrin/thrombin matrix was used to support the *in vitro* angiogenic sprouting (Kiefer *et al*., 2004; Munk *et al*., 2006; Sanchez de Miguel *et al*., 2008). Here the formation of sprouts occurred using the same fibrin-thrombin clot based gel.

4.3.1.1 Media

The 20% FCS-DMEM (supplemented with 20 % FCS and ECGS) and complete EBM (supplemented with 10% FCS and a combination of growth factors) media were tested and explants were able to from sprouts in both media. However, in other studies DMEM medium containing 5% FCS was used to prevent stimulation of angiogenesis since different growth factors on EC angiogenesis were being evaluated (Kiefer *et al*., 2004; Munk *et al*., 2006). There are several growth factors in FCS that induce angiogenesis. It has been shown that the use of 10% FCS stimulate angiogenesis (Pepper *et al.*, 1998). In the current study 20% FCS-DMEM medium were utilised for the remainder of assay, in addition to ECGS, which is a purified endothelial mitogen from bovine hypothalamus, shown to promote the growth of endothelil cells (Evans and Dipaolo, 1982).

4.3.1.2 Normoaxia vs Hypoxia

The formation of angiogenic sprouts from heart explants were observed under both hypoxia and normoxia conditions. However, this is in contrast with other studies, which observed that hypoxic conditions were required for the outgrowth cells from heart explants (Kiefer *et al.*, 2004; Munk *et al.*, 2007). Hypoxia generates angiogenic stimuli via activation of EC signaling and induction of angiogenic molecules, such as VEGF and angiopoetin II (Munk *et al.*, 2007). Kiefer *et al* (2004) found that hypoxia is a prerequisite for *in vitro* angiogenesis of mouse heart explants (Kiefer *et al.,* 2004). Under hypoxia conditions using unstimulated heart culture media (5% DMEM medium), not substantial levels of angiogenesis was observed, however, addition of growth factors such as VEGF, bFGF and PDGF improved formation of angiogenic sprouts. However it was shown under normoxia that heart explants using the same medium and growth factors did not form substantial outgrowth of cells (Kiefer *et al.*, 2004; Munk *et al.*, 2007). The only difference in the condition of experiments performed here and other previous studies is the medium was used. The DMEM medium was supplemented with optimal 20% FCS concentration and ECGS, both of which have been shown to promote the growth of endothelil cells (Evans and Dipaolo, 1982). Therefore the use of optimal FCS and ECGS could

be permissive for explants growth and helped to improve formation of angiognic sprouts under normoxic conditions.

4.3.1.3 Different tissue types (Aorta, HV and HA)

While the use of the aortic arch showed robust formation of angiogenesis in the aortic ring assay here and in other studies, but it was abandoned since the angiogenesis process is initiated from smaller vessels. The rat aorta shown to form sprouts under both normoxia and hypoxic conditions even using serum-free conditions indicates the organ-specific potential of the aorta to undergo angiogenesis *in vitro* (Humar *et al*., 2002). Moreover, removal of the adventia surrounding the aorta is difficult and time-consuming (Nicosia *et al*., 1997; Ucuzian and Greisler, 2007). In our study, the angiogenesis response observed from both mouse arterial and ventricular myocardium under hypoxia. The HA tissue showed an increased number of explants with sprouts compared to the HV tissue. The only difference in HV and HA explants is their micro- and macrovascular origin, with the HA containing more microvessels and HA contains more large vessels.

4.3.1.4 Young mice *vs* old mice

According to different studies, the capacity for reparative mechanisms and angiogenesis are decreased in aged mice (Kiefer *et al.*, 2004; Reed *et al.*, 2007). Age dependency of angiogenesis has been observed in several *in vit*ro and *in vivo* studies (Phillips and Stone, 1994; Reed *et al*., 1998; Swift *et al*., 1999). In the Kiefer *et al* study it was observed that the angiogenesis index reduced with the age of the mice. Young mice exhibited sprouts formation under serum-free conditions while older mice needed addition of stimulants (e.g. growth factors) to show angiogenesis *in vitro* (Kiefer *et al*., 2004). It has been observed that addition of growth factors (VEGF, DD-PDGF and bFGF) under hypoxia reversed the restricted sprouting in older mice hearts and induced angiogenesis (Arthur *et al*., 1998; Kiefer *et al*., 2004; Reed *et al*., 2000). Here, by utilising suitable media it was possible to obtain substantial angiogenesis from very old mice hearts up to 60 weeks old.

4.3.2 Radiation effect on mouse heart angiogenesis *in vitro*

After optimizing this angiogenesis model, it was further utilised to assess the formation of angiogenic sprouts in irradiated and non-irradiated heart explants from C57BL/6J and ApoE$^{-/-}$ treated at 8-12 weeks. The radiation-induced angiogenesis impairment in the heart of locally irradiated mice at different radiation doses (low (0.2- 2 Gy), medium (2 Gy) and high 8 and 16 Gy)) and at different time points (20, 40 and 60 weeks post-irradiation), was tested for the first time here. The angiogenesis changes in irradiated *vs* sham-irradiated (0 Gy) mice were evaluated. The statistical analysis of irradiated groups *vs* non-irradiated groups revealed that there was a decrease in angiogenic sprouts formation following radiation, which was dose-dependent. Effects were evident at high doses of radiation (8 and 16 Gy) at 20 weeks both in C57/BL6 and ApoE $^{-/-}$ mouse hearts, which persisted up to 60 weeks. Furthermore, the heart angiogenesis impairment progressed up to 60 weeks after radiation at lower doses of ≥ 2Gy in both mouse strains in HA explants. Similar results were observed in the Imazuimi *et al* study using C57/BL6 mice, irradiated with a single dose of 15 Gy, as well as fractionated doses of 3 Gy on five occasions (total of 15 Gy, performed every two days). In their study it was revealed that both single and fractionated radiation doses suppressed angiogenic responses significantly in the irradiated mouse aortic ring explants (Imaizumi *et al.*, 2010). However, their results only indicated short-term effects of radiation on heart explant angiogenesis. The novelty of the current study was to investigate the late effects of radiation damage on the angiogenic response of the heart microvasculature. Our results demonstrated for the first time a decrease in heart angiogenesis with increasing radiation doses (even at low doses), which persisted up to 60 weeks post irradiation.

Two strains of mice were used in the CARDIORISK project and hence we received irradiated hearts from both mouse strains. The C57BL/6 mice have low levels of plasma cholesterol (especially LDL), therefore are relatively resistant to developing atherosclerosis, and hence were compared with hypercholesterolemic ApoE$^{-/-}$ mice, which have elevated plasma levels of cholesterol and develop age-related atherosclerosis (Gabriels *et al.*, 2012).

Results from other CARDIORISK projects showed that the myocardium and microvasculature of murine hearts (C57BL/6J and ApoE$^{-/-}$) at 20, 40 and 60 weeks following exposure to the single doses of 2, 8 and 16 Gy radiation were affected in a dose and time-dependent manner (Gabriels *et al.*, 2012; Seemann *et al.*, 2012). The data indicated that a single radiation dose to the heart resulted in progressive alteration of the mouse heart microvasculature function and structure, which was more significant at intermediate and higher doses. It has been suggested that myocardium of mice could potentially compensate for the damage to microvasculature at the lower doses of 2 Gy due to compensatory responses of the heart, such that the damage was non-progressive (Gabriels *et al.*, 2012; Seemann *et al.*, 2012). As a result of the loss of ECs at higher doses (8 and 16 Gy) proliferation was compromised and radiation caused EC apoptosis and death. This could be one reason for a decreased in angiogenic function in the hearts of mice irradiated at higher doses in the current study, as CEC sprout formation was significantly reduced in 8 and 16 Gy irradiated groups.

4.3.3 Characterisation of heart explant sprouts

In the current study, the CEC were positively characterised with lectin as previously observed (Kiefer *et al*., 2004; Zhu and Nicosia, 2002). The staining of sprouts from the heart explants with lectin confirmed an EC phenotype.

The pericytes and smooth muscle cells are also recruited during the morphogenesis and interact with ECs (Risau, 1997; Ucuzian and Greisler, 2007). Therefore, their presence needs to be confirmed in the outgrowing cells as already been observed in other studies (Kiefer *et al.*, 2004; MunK *et al.,* 2006; Zhu and Nicosia, 2002). Characterisation of other cellular components of the outgrowths is required in order to determine any effects of radiation on associated mural cells and how the potential interaction with ECs, thus resulting in impaired angiogenesis activity. Moreover, the percentage of sprouting cells that stained positively was significantly higher at 0 Gy compared to 2 Gy. This suggests that radiation affects EC surface antigens potentially causing the failure of lectin binding and it may indicate EC damage.. Additionally, the characterisation of explants has been limited to immunohistochemistry lectin

staining. The use of fluorochrome-conjugated antibodies could help to further improve the intact sprouts characterisation.

4.3.4 Summary of results

Ischemic heart disease results from an inadequate oxygen and blood supply to the myocardium. Angiogenesis acts to repair the condition and restore the blood flow to the myocardium (Munk *et al.*, 2007). Additionally, radiation induced myocardial damage, as well as a reduction in microvessel density in mouse hearts has been identified following exposure to 2-16 Gy radiation dose-dependently reduced sprouts formation 20-60 weeks post-irradiation (Seemann *et al.*, 2012). Based on the results presented here, the impairment in angiogenesis in mice hearts following radiation (≥ 2 Gy) may contribute to an increased ischemia and a decrease in microvasculature that eventually leads to the development of CVD. Moreover, the formation of angiogenic sprouts has also been established in human cardiac tissue-based angiogenesis model (Jaquet *et al*., 2002; Lewis *et al.*, 2006). It was shown sprouts were capable of forming in serum-free and under normoxic conditions. Using this model allow the study of pathogenesis of radiation-induced CVD directly on human cardiac tissue.

Chapter Five

Investigating the mechanisms underlying radiation effects on EC angiogenesis

5.1 Introduction

Results from the previous two chapters have shown that; a) irradiation of *in vitro* ECs reduced EC proliferation, migration and capillary-like tubule formation (chapter **3**), whilst b) exposure of locally irradiated mice hearts at low (0.2-2 Gy) and 18 and 16 Gy) high doses, suppressed the formation of angiogenic sprouts, which persisted for 20 to 60 weeks post-irradiation (chapter **4**). Therefore, taken together the data confirm that radiation has the ability to modify the capacity of ECs to undergo repair and angiogenesis. In this chapter, potential mechanisms of the apparent radiation-induced inhibition of the EC angiogenesis response were investigated.

5.1.1 The influences of irradiated fibroblasts on EC angiogenesis

Fibroblasts, which are cellular mediators of fibrosis, play an important role in angiogenesis during wound healing and tissue repair. Fibroblasts act as a scaffold in angiogenesis during tissue repair by production of collagen and ECM, as well as secretion of growth factors including VEGF, PDGF, bFGF and TGF-β. This results in a defined microenvironment surrounding the ECs, which promotes their angiogenic functions (Badylak, 2002; Newman *et al.*, 2011; Tettamanti *et al.*, 2004). Additionally, fibrosis is a common consequence of therapeutic radiation, and the induction of vascular damage results in fibroblast stimulation of the production of ECM and collagen, as well as the expression of CTGF and PAI-1 (Chang *et al.*, 2004).

In the context of radiation damage, however, the cross-talk mechanisms that exist between ECs and fibroblasts have not yet been investigated. The studies presented in this chapter are therefore novel. The first aim of this chapter was to investigate whether irradiated fibroblasts influence EC angiogenic/morphogenic functions. The fibroblast bed organotypic and wound healing assays were used to investigate the effects of radiation on EC angiogenic properties. Moreover, it was hypothesised that irradiated fibroblasts influence EC migration and

morphogenesis via soluble secreted factor(s). Therefore, conditioned media, from irradiated fibroblasts were also tested on EC angiogenic function.

5.1.2 The involvement of TGF-β signaling in endothelial angiogenesis after radiation exposure

The TGF-β family control several different biological processes including: cell proliferation, differentiation, migration, ECM production, apoptosis and epithelial mesenchymal transition, as well as having an important role during embryonic development (Dancea *et al.*, 2009; Derynck and Zhang, 2003; Moustakas *et al.*, 2001). The TGF-β ligand binds to the TGF-β Type II receptor, which is then associated with the Type I receptor and this results in the phosphorylation and activation of TβR1 receptors (AlK5/ALK1). Activation of the TβR1 receptor(s) then triggers the phosphorylation of selected Smad proteins, which in turn translocate into the nucleus after binding to Smad 4, where they regulate the transcription of target genes (Bakin *et al.*, 2002; Derynck and Zhang, 2003; Moustakas *et al.*, 2001). The Smad signaling pathway, induced by TGF-β, constitutes a primary signal transduction route downstream of Type I TGF-β receptors (Edlund *et al.*, 2002).

Radiation is a known inducer of TGF-β expression/activation (Barcellos-Hoff, 1993; Imaizumi *et al.*, 2010; Martin *et al.*, 2000; Randall and Coggle, 1995). TGF-β regulates both pro- and anti-angiogenic EC functions. TGF-β signaling via ALK5 results in inhibition of EC proliferation and migration, as well as induction of PAI-1 and CTGF expression. In contrast, TGF-β signaling via ALK 1 is pro-angiogenic, promoting activation of ECs which leads to their proliferation and migration, as well as increased production of ECs growth factors, such as VEGF (Haydont *et al.*, 2005; Liu and Wang, 2008; Orlova *et al.*, 2011; Samarakoon and Higgins, 2008; Shao *et al.*, 2009). Here, the possibility that TGF-β produced by irradiated fibroblasts inhibits EC angiogenic/morphogenic responses was studied by investigating the anti-angiogenic effects of TGF-β via inhibition of the ALK 5 receptor in experimental models of angiogenesis, such as the fibroblast bed organotypic and migration assays. Experiments

were performed in the presence/absence of the TGF-β1 ALK5 receptor inhibitor SB 431542 (Tocris bioscience, Cat. no. 1614) in order to establish this.

5.1.3 The involvement of Rho/Rho A signaling in endothelial angiogenesis after radiation exposure

The Rho intracellular signaling activation is associated with the formation of the cytoskeleton, stress fibres, adhesion complex and cell movement. The Rho-kinase mediates up regulation of thrombogenic and fibrogenic molecules, such as PAI-1, TGF-β and CTGF (Shimokawa and Takeshita, 2005). Several studies using Rho-ROCK inhibitors have shown that inhibiting Rho-ROCK pathway signaling improves vascular fibrosis, as well as reducing expression of PAI-1 (Chen *et al.*, 2006; Kamaraju and Roberts, 2005; Samarakoon and Higgins, 2008). In addition to the canonical TGF-β/Smad activation following radiation, the Rho/Rock intracellular signaling cascade has also been found to be activated by radiation (Gabrys *et al.*, 2007; Haydont *et al.*, 2008; Monceau *et al.*, 2010). The radiation-induced Rho/ROCK activation is associated with changes in the actin cytoskeleton and cell permeability in the microvasculature (Gabrys *et al.*, 2007). Therefore, the EC angiogenic/morphogenic changes due to radiation could be partly dependent on the Rho/Rock pathway signaling.

Additionally, there is a cross talk between RhoA and TGF-β/Smad pathways, promoting the Smad-mediated signaling and, therefore, amplifying the TGF-β responses (Chen *et al.*, 2006; Derynck and Zhang, 2003; Edlund *et al.*, 2002; Moustakas *et al.,* 2001). Rho/ROCK activation in response to TGF-β is involved in mediating cytoskeletal organisation, stress fibre formation and epithelial-mesenchymal transdifferentiation as well as sustained phosphorylation of Smad2/3 (Bakin *et al.*, 2002; Bhowmick *et al.*, 2001; Derynck and Zhang, 2003). The inhibition of Rho A results in abrogation of TGF-β-stimulated formation of stress fibres (Edlund *et al.*, 2002). It has been reported that TGF-β induced PAI-1 and CTGF expression requires Rho/ROCK-mediated Smad2/3 activation, and the Rho/Rho kinases are involved in transforming fibroblasts into myofibrobalsts (Shimokawa and Takeshita, 2005). Rho signaling

pathways have been linked with the inhibition of EC angiogenic activities following exposure to radiation (Gabrys *et al.*, 2007; Monceau *et al.*, 2010; Zohrabian *et al.*, 2009). Thus the third aim of this chapter was to determine whether irradiated fibroblasts induce EC anti-angiogenic effects mediated through the Rho signaling pathway by investigating an anti-angiogenic efficacy of a Rho inhibitor in EC angiogenesis, using fibroblast bed organotypic and migration models. The established Rho inhibitor Y-27632, a specific inhibitor of Ser/Thr p160 Rho-associated protein kinase (ROCK) activity (downstream effectors of Rho), was used in the experimental studies (Ishizaki *et al.*, 2000).

5.2 Results

5.2.1 Effects of irradiated fibroblasts on EC angiogenesis by direct contact and via soluble secreted factors

Two approaches were taken to investigate the effects of irradiating fibroblasts on EC angiogenic/morphogenic functions. Irradiated fibroblasts were firstly co-cultured with ECs (organotypic endothelial-fibroblast co-culture assay) and the effect of irradiated fibroblasts on the formation of channels by EC was investigated. Secondly, the bystander effect(s) of irradiated fibroblasts using conditioned medium (CM) from irradiated fibroblasts was tested on EC channels formation and migration.

5.2.1.1 Effects of irradiated fibroblasts on EC capillary-like formation using the organotypic endothelial-fibroblast co-culture model

This assay was optimised as described previously in Chapter 3 section **3.2.7**. The HUVEC cells, which form channels and express ECs markers (such as VCAM-1, PECAM-1) as well as vWF, were suitable EC to study the effect of radiation on endothelial angiogenic functions (Rhim *et al.*, 1998). However the isolated CEC and H5V cells which were the best EC candidates for this project, were not able to form capillary-like structures (see section **3.2.7.2**).

Here, fibroblasts were irradiated before co-culturing with HUVECs in order to see whether exposure of fibroblasts to radiation could affect EC channel formation. The HDF cells were plated in separate T-25 flasks and upon approaching confluence, were irradiated separately at radiation doses of 0.5, 2 and 8 Gy, 1 h prior to performing the co-culture. The irradiated fibroblasts were then co-cultured with HUVECs at a ratio of 3:1 corresponding to a density of 30,000 HDF to 10,0000 HUVEC cells per 24-well plate. A control experiment with non-irradiated HDFs was performed in parallel. The co-culture medium was changed every two days and after 14 days channels were visualised by staining for vWF. The results in Figure **5.1** show that well-structured capillary networks were formed by HUVECs, when co-cultured with either non-irradiated HDFs or the HDFs exposed to low dose radiation (0.5 Gy). It was observed the number and the length of capillaries formed by the HUVECs decreased

considerably after being co-cultured with HDFs exposed to higher doses of radiation (2 and 8 Gy), with effects being most pronounced at 8 Gy. The HUVECs were not able to sprout from the EC islands and they remained in clusters, as can be seen in the cell images labelled 8 Gy. These results show that irradiated fibroblasts influenced the formation of cord-like structures by HUVECs.

Based on results from other studies, irradiation of proliferating cells results in cell death mostly through apoptosis, while the irradiation of quiescent cells can lead to cell senescence (Imaizumi *et al.*, 2010; Oh *et al.*, 2001). Therefore the results in Figure **5.1** could be explained by a reduction in the ability of the fibroblasts to adhere and grow in the co-culture system, through effects on proliferation. Additionally, the endothelial-fibroblast ratio is sensitive and changing of this ratio will affect the formation of channels by ECs. To address this, the next set of experiments was therefore performed where ECs were co-cultured on top of a bed of confluent irradiated or non-irradiated fibroblasts (fibroblast bed organotypic assay).

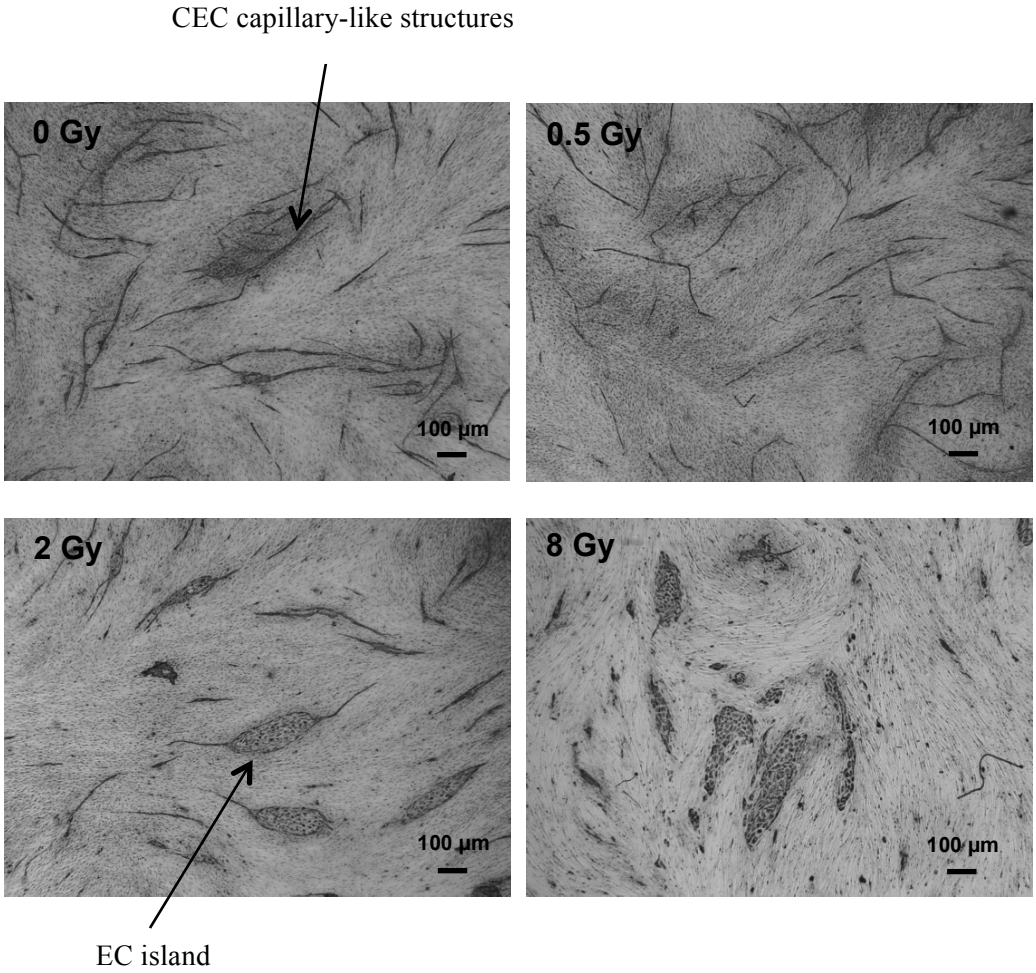

Figure 5.1 Effect of irradiated HDFs on formation of channels by HUVECs. HDF cells were irradiated at doses of 0 (control), 0.5, 2 and 8 Gy. Irradiated and non-irradiated HDFs were co-cultured with HUVECs at a ratio of 3:1, and after 14 days, channel formation was visualised using an antibody to vWF. The results show that irradiation of fibroblasts reduces HUVEC channel formation in a dose-dependent manner.

5.2.1.2 Effects of irradiated fibroblasts on EC capillary-like formation using the fibroblast bed organotypic model

These next experiments used an assay that is basically a modified version of the endothelial-fibroblasts co-culture assay described above. In this assay, ECs (HUVECs) are directly plated on fibroblasts (HDF) that have reached confluence. By allowing fibroblasts to reach confluence, they enter quiescence rather than remain in a proliferative state. Exposure of these cells to radiation does not lead therefore to cell death, meaning that the direct effects of radiation on EC sprouting can be determined more accurately and specifically.

Prior to performing the organotypic fibroblast bed assay, initial growth curve experiments were carried out using non-irradiated and irradiated HDF cells to determine that radiation did not affect the number of HDF cells during this assay. Cells were plated in separate plates at a density of 60,000 cells per well. When they became super confluent (by approximately 7 days), they were irradiated at 0.2, 2, 8 and 16 Gy. In parallel un-irradiated cells were used as controls. Before irradiation, the number of HDF cells was counted to determine the start number of cells at the beginning of the assay. Cell number was then determined at days 7 and 14 for all irradiated and non-irradiated cultures (each experiment was performed in triplicate). The results from three separate growth curve experiments are presented as mean ± SEM (Figure **5.2)** and show that the number of confluent HDF cells at the start of the assay was 271,111 ± 14,572. After 7 and 14 days, the number of cells in the non-irradiated control group was 307,777 ± 15,555 and 327,777 ± 29,123 cells respectively, implying only a very small amount of growth.

A small amount of proliferative activity was also observed in cells receiving doses of 0.2, 2 and 8 Gy. However, no change in cell number was observed when HDFs were exposed to a dose of 16 Gy. Statistical analysis of these data (Figure **5.2**) confirmed that the small differences in growth between non-irradiated and irradiated cells were not significant after 7 and 14 days, implying that radiation was not having a deleterious effect on quiescent cells.

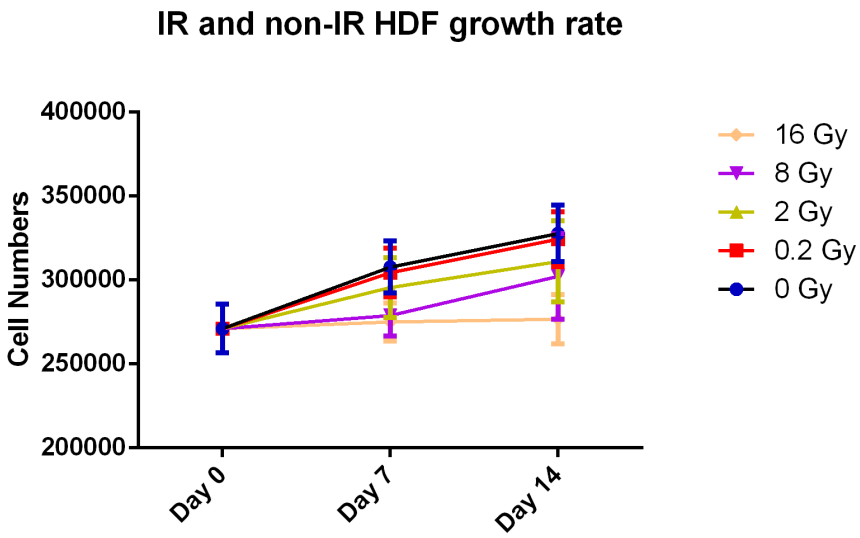

Figure 5.2 Effect of radiation on a super confluent fibroblast cell growth. HDFs were plated at a density of 60,000 cells per well and grown to confluence. Upon reaching confluence, they were irradiated at 0 (control), 0.2, 2, 8 and 16 Gy and incubated for a further 14 days. Cell numbers were determined at days 7 and 14, and the growth curve data from three separate experiments expressed as mean ± SEM. Data were statistically analysed using the Two-way ANOVA test, and this revealed that whilst non-irradiated cells and those receiving a radiation dose of 0.2, 2 and 8 Gy proliferated slightly after they reached confluence at day 7 and 14, the changes were not significant in all irradiated groups compared to the control.

Importantly, this suggested that when next performing the co-culture assay plating HUVECs on top of irradiated HDF cells, the number of fibroblasts would remain similar in each group, for up to 14 days.

Having established that radiation did not impact greatly on HDF cell number, the co-culture bed assay was performed. However, before performing the assay using irradiated HDFs and HUVECs, an initial experiment was performed plating different densities of HUVECs (10,000, 20,000 and 30,000 cells) on top of HDFs to determine that the cell density was sufficient to form enough well-organized channels in a 24 well plate. This initial experiment showed that a density of 18000 to 20,000 HUVECs cells was adequate to form enough channels after 12-14 days. HDFs were therefore plated at a density of 30,000 cells per well grown until they reached confluence (7 days). Following this, HDF cells were irradiated at doses of 0 (control), 0.2, 2, 8 and 16 Gy, and then HUVECs (18,000 cells) were directly plated on top. HUVECs medium was refreshed every two days, and cells were fixed after 12-14 days and channels visualised by staining with an antibody to vWF.

The images shown below in Figure **5.3** indicate that there was profound inhibition of capillary-like networks formation by HUVECs when they were co-cultured with irradiated HDFs, dependent on the radiation dose, with the most profound effects at higher doses. To quantify the effects of irradiated fibroblasts on EC channel formation in these experiments, 5-15 images for each irradiated and non-irradiated group from five separate experiments (results presented as mean ± SEM) were analysed for parameters such as tubule length, number of tubules and number of branching points using AngioSys software (Section **2.9.2.1**).

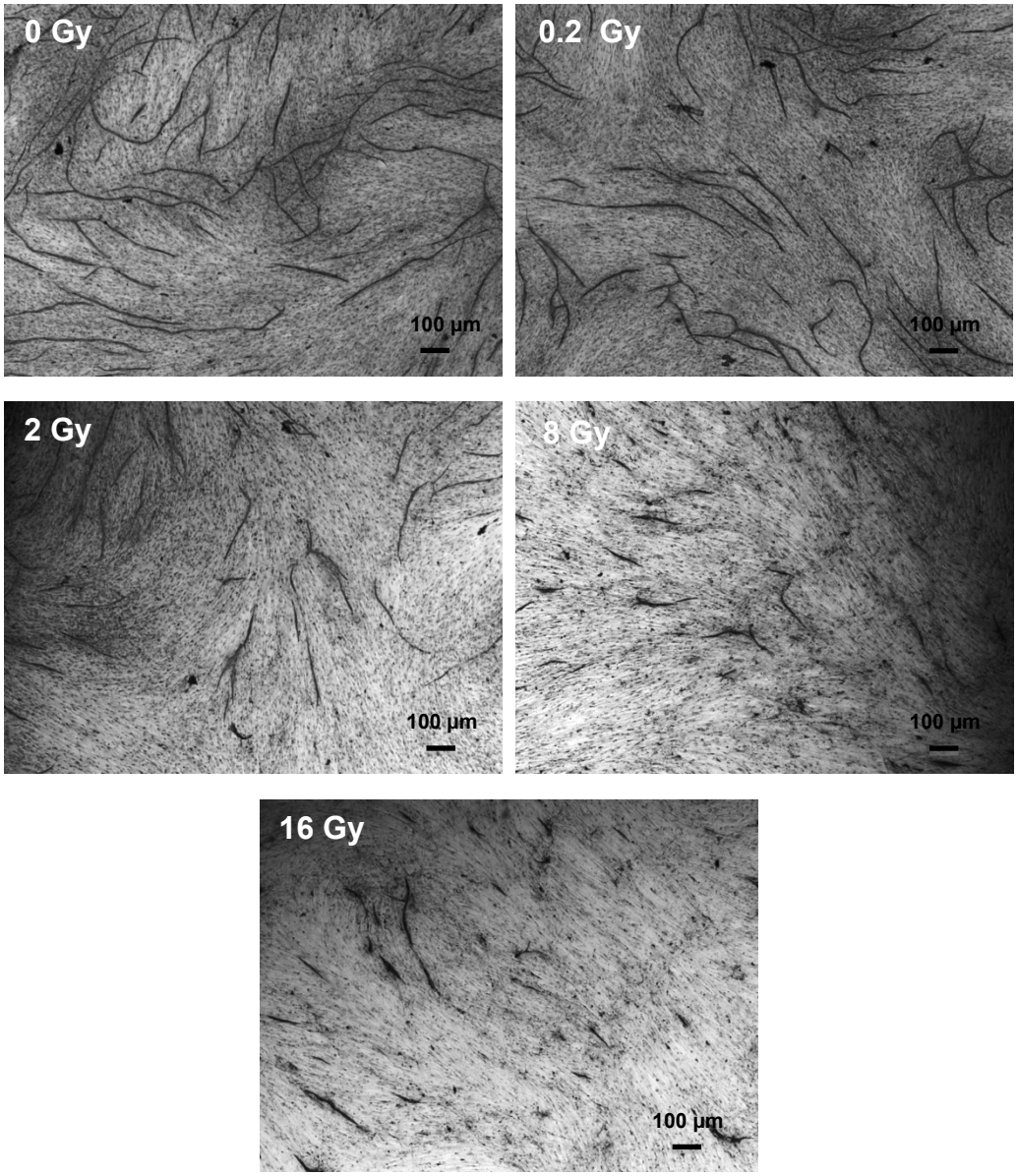

Figure 5.3 Effect of irradiated HDFs on formation of capillary-like structures by HUVECs. HDF cells were irradiated at doses of 0 (control), 0.2, 2, 8 and 16 Gy when they were super confluent. HUVECs were seeded on top of the irradiated and non-irradiated HDF. After 14 days, thread-like structures were visualised using an antibody to vWF. Images show that irradiation of fibroblasts reduced the formation of vessel like structures by the HUVECs. The number and length of sprouts formed by HUVECs when cultured with non-irradiated HDF was affected compared to when cultured with irradiated cells. The cord-like structures observed in the images denoting doses of 0 Gy and 0.2 Gy were more elongated with more branch points while in the 2, 8 and 16 Gy irradiated groups there were only a few tubules formed which were shorter with zero or few junctions.

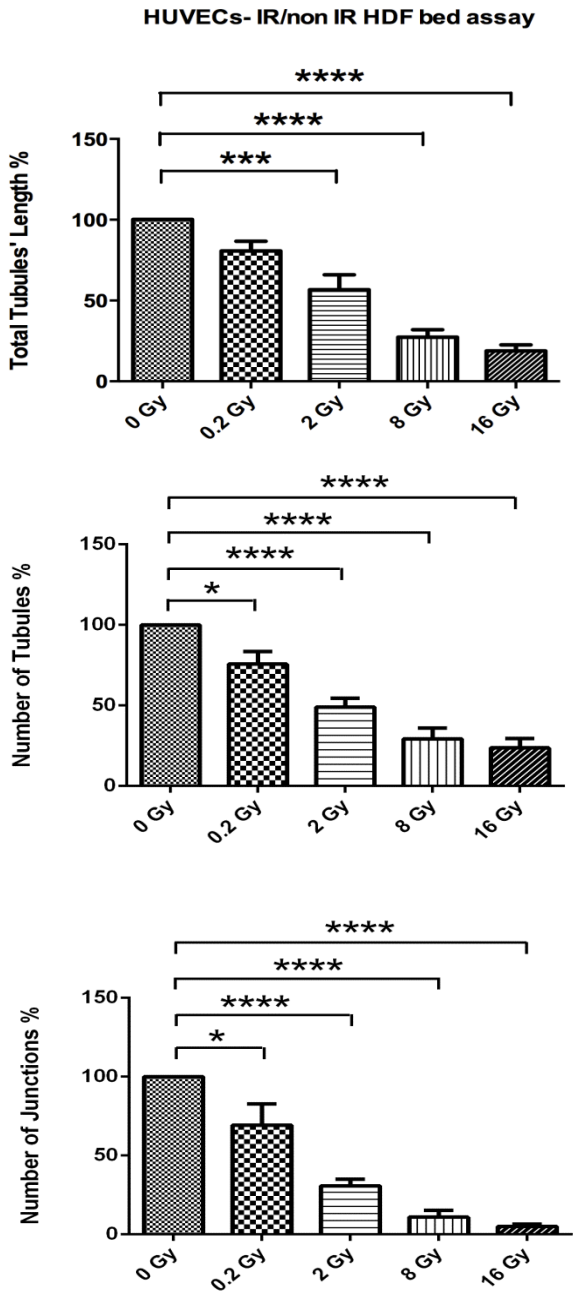

Figure 5.4 Quantification of irradiated fibroblast effects on capillary-like structure formation by HUVECs. Data from the five separate experiments were expressed as mean ± SEM and analysed using a One-way ANOVA test. The axes represent total capillary-like structure lengths, number of capillary-like structures and junctions normalised to the control (% of control). The data show that irradiation of HDFs affected the formation of channels by HUVECs. The total sprouts lengths were significantly smaller in irradiated groups (≤ 2 Gy). The number of capillaries and the numbers of their junctions formed by HUVECs when cultured with non-irradiated HDF were significantly higher compared to the irradiated 0.2, 2, 8 and 16 Gy groups. (*p < 0.5, ***p < 0.001, ****p < 0.0001)

Data were normalised to the control (100%) and a One-way ANOVA test performed to determine if effects were significant. The results show that the number of capillary-like structures formed by HUVECs after interacting with irradiated fibroblasts declined significantly at even low doses of 0.2 Gy (≤ 0.2 Gy). The total lengths of channels formed by HUVECs were considerably higher when cultured with non-irradiated HDFs compared to irradiated ones (≤ 2 Gy), and sprouts were more elongated with more junctions in the control group compared to those seen in co-cultures using irradiated HDFs. Similarly, the number of junctions was significantly decreased in the ≤ 0.2 Gy group compared to the control group (Figure **5.4**).

5.2.2 Effect of radiation on EC angiogenic functions via soluble secreted factors from irradiated fibroblasts conditioned medium (CM)

The previous experiment showed that HUVEC channel formation is significantly affected even at low doses (≤ 0.2 Gy) when HUVECs are grown on a bed of irradiated fibroblasts. The next question was whether irradiated fibroblasts inhibit endothelial morphogenesis via a soluble factor(s). To test this, the next experiments were performed using conditioned medium (CM) from irradiated fibroblasts to study whether this could reproduce the effect of irradiated fibroblasts on HUVECs morphogenesis and migration.

5.2.2.1 Effect of conditioned media from irradiated fibroblasts on HUVEC capillary-like formation

The fibroblast bed organotypic assay was again performed, this time using CM collected from non-irradiated or irradiated HDFs. Firstly, to generate conditioned media, HDFs were plated and grown to confluence. After that, the media was changed with the media used to grow HUVECs and the HDFs were then either irradiated (2 and 8 Gy) or left unirradiated (control). Following this, the media was left on cells for 48 h in order to be conditioned, and then removed for use in the co-culture assay. On the same day HDFs were irradiated, in parallel, HUVECs were plated on top of HDFs in separate wells. After two days, the collected CM (500µl) was added to the HUVEC-HDF co-culture beds, along with an equal volume of

normal media, to support HUVEC growth. Additionally, only full normal media was added to a separate plate of HUVEC-HDFs as a control. The media were changed every second day, using the conditions described above, and after 14 days, vessel-like structures were visualised, imaged and quantified as before.

Representative images from one experiment presented in Figure **5.5** show that the CM from irradiated HDFs caused a reduction in formation of cord-like networks by HUVECs, which was more evident at higher radiation doses (8 Gy). In contrast, when HUVECs grown on a fibroblast bed received either normal media or conditioned media from unirradiated HDFs, they formed a well-organized capillary networks with long channels and branching points. Quantification of the data from three experiments (results presented as a mean ± SEM) is presented in Figure **5.6** and shows that there were no significant differences in the total length of capillary-like structures and number of capillary-like structures and junctions formed by HUVECs when treated with either normal medium or CM from non-irradiated HDFs. In contrast, the length of sprouts decreased significantly to 67% ± 10 and 59% ± 9.5 in cultures treated with CM from HDFs irradiated at doses of 2 and 8 Gy. Similarly, a significant reduction in the number of sprouts and sprouts junctions formed by HUVECs was also observed using CM from HDFs irradiated at 2 and 8 Gy. Together, these data show that CM from irradiated fibroblasts inhibits EC angiogenic activity, indicating that there might be a soluble factor(s) involved that was responsible for the effects.

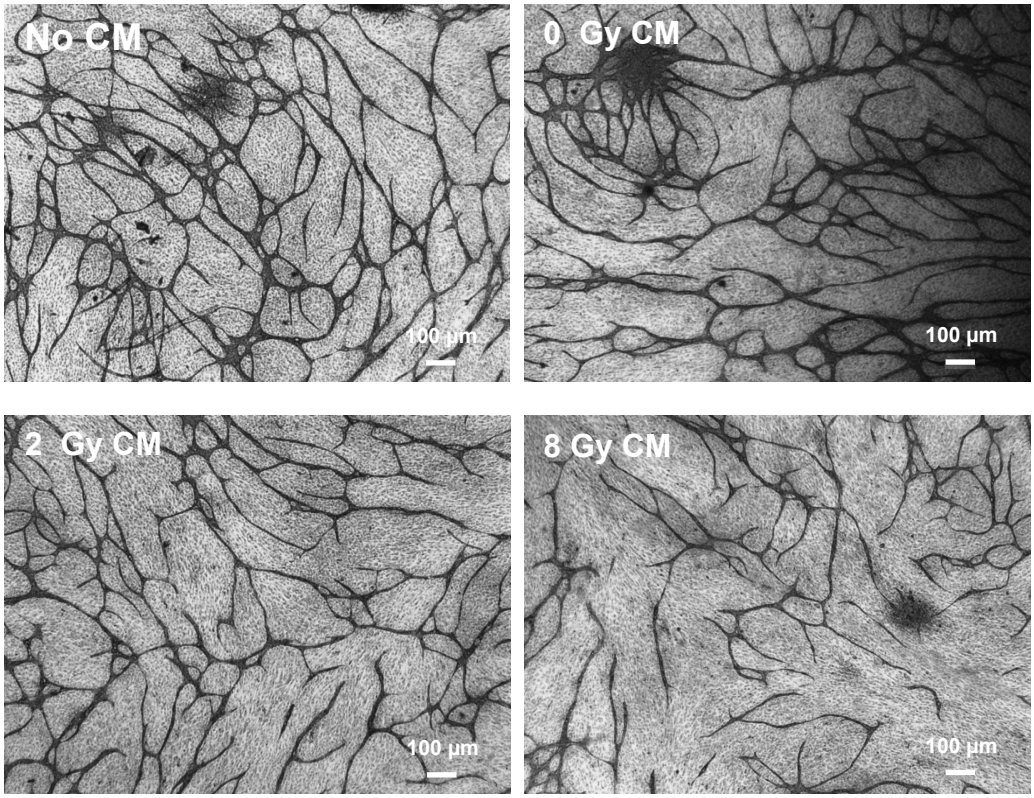

Figure 5.5 Effect of conditioned media from irradiated HDFs on formation of capillary-like structures by HUVECs. HDF cells were irradiated at radiation doses of 0 (control), 2 and 8 Gy when they were super confluent. The conditioned media from irradiated and non-irradiated HDFs were collected after 48 h and added to co-cultures of HDF-HUVECs that were already set up at a ratio of 50% CM and 50% normal media. After 14 days, cultures were stained using an antibody to vWF. The images show that CM from irradiated HDFs reduced the formation of capillary networks by HUVECs in a radiation dose-dependent manner, with fewer sprouts exhibiting shorter lengths being more evident at the higher dose (8 Gy) compared to those receiving either 100 % normal media or CM from non-irradiated HDFs.

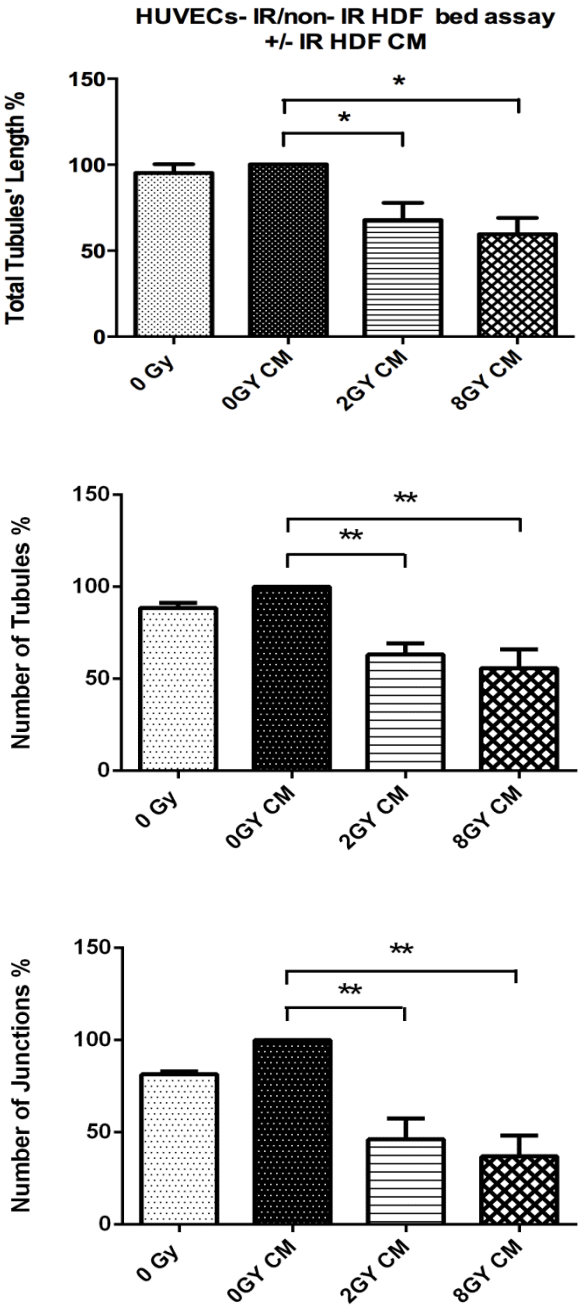

Figure 5.6 Quantification of the effects of CM from irradiated HDFs on capillary-like structures formation by HUVECs. Data from the three separate experiments were expressed as mean ± SEM and analysed using a One-way ANOVA test. The axes represent total sprout lengths, number of sprouts and junctions normalised to the control (% of control). The analysis of data show that the ability of HUVECs to form channels slightly increased when exposed to the HDF CM, however the changes were small. The addition of CM from irradiated HDFs to the HDF-HUVECs assay suppressed the number of sprouts to 62% ± 5.8 and 55% ± 10 at doses of 2 and 8 Gy respectively, compared to CM from non-irradiated HDFs. The total lengths of sprouts and number of sprouts junctions were also significantly reduced in HUVECs plated with HDFs receiving CM from HDFs irradiated at 2 and 8 Gy. (*p < 0.5, **p < 0.01)

5.2.2.2 Effect of conditioned media from irradiated fibroblasts on EC migration

The previous experiments clearly demonstrate that CM from irradiated fibroblasts exerts some changes in the formation of capillary networks by HUVECs and so further experiments were set up to investigate the effect of CM on EC migration. Moreover, it was important to determine whether the true extent of these effects might be being masked by the normal bed of HDFs on top of which the HUVECs were plated, and/or the addition of normal media alongside the CM. Therefore here, the CM from irradiated and non-irradiated HDFs was added to ECs in a scratch wound assay and the effects on migration of ECs (HUVECs and H5V cells) were assessed.

Prior to initiating the migration assay, it was necessary to firstly prepare and concentrate HDF CM. Here both H5V and HUVECs were tested, as H5V is the best EC candidate in the current project. Since the HUVECs and H5V cells are normally grown in different media, the HDFs were grown to confluence and then prior to irradiation (0.2 – 16 Gy), the media was changed to a medium appropriate for growing either HUVECs or H5V cells, and after 48 h, the media were concentrated 4-5 times. In both cases these media were supplemented with only 2% serum. In parallel, ECs were plated and when approaching near confluence, media was exchanged with CM from either irradiated or non-irradiated HDFs, and cells incubated for 48 h. Following this, a scratch was made on the EC monolayer(s) and the media changed with fresh CM. Cells were imaged after 6, 10 and 24 h, and wound closure measured. The H5V cells only were treated with 5 μg/ml Mit C for 2 h before performing the scratch wound assay for reasons described previously (see **3.2.5.1.1**).

The migration results for both HUVECs and H5V cells are presented as the percentages of the average wound distance after 6, 10 and 24 h relative to the original wound (0 h) in each group. The results showing the influence of CM from both irradiated and non-irradiated HDFs on HUVEC migration are displayed in Figure **5.7.** The analysis of data from four separate experiments expressed as mean ± SEM shows that CM from irradiated HDFs inhibited wound closure in the scratch assay. The migratory capacity of HUVECs was significantly reduced

when they were exposed to CM from HDFs irradiated at 8 Gy after 6 h. However, the significance of the effects of radiation increased at lower doses (2 Gy) upon prolonged incubation of HUVECs following addition of CM (10 and 24 h). These results are consistent with the previous effects on EC morphogenesis, confirming that there is a soluble secreted factor(s) in the CM from irradiated fibroblasts, which affects EC migration/morphogenesis.

The migratory data for H5V cells incubated with CM from irradiated (0 (control), 0.2, 2, 8 and 16 Gy) and non-irradiated HDFs are presented in Figure **5.8**. The data are presented from one experiment which is a representative of two separate experiments and show that CM from irradiated HDFs had some inhibitory effect on H5V migration, after 6 and 10 h, which was more profound at higher doses of 8 and 16 Gy. However, the migration capacity of H5V cells was rather similar (at doses of 0.2, 2 and 8 Gy) after 24 h following the addition of CM from irradiated and non-irradiated HDFs and only some inhibitory effects at dose of 16 Gy were observed. Data were obtained from only two sets of experiments, and consequently further experiments would be required to determine if any of the observed effects were significant.

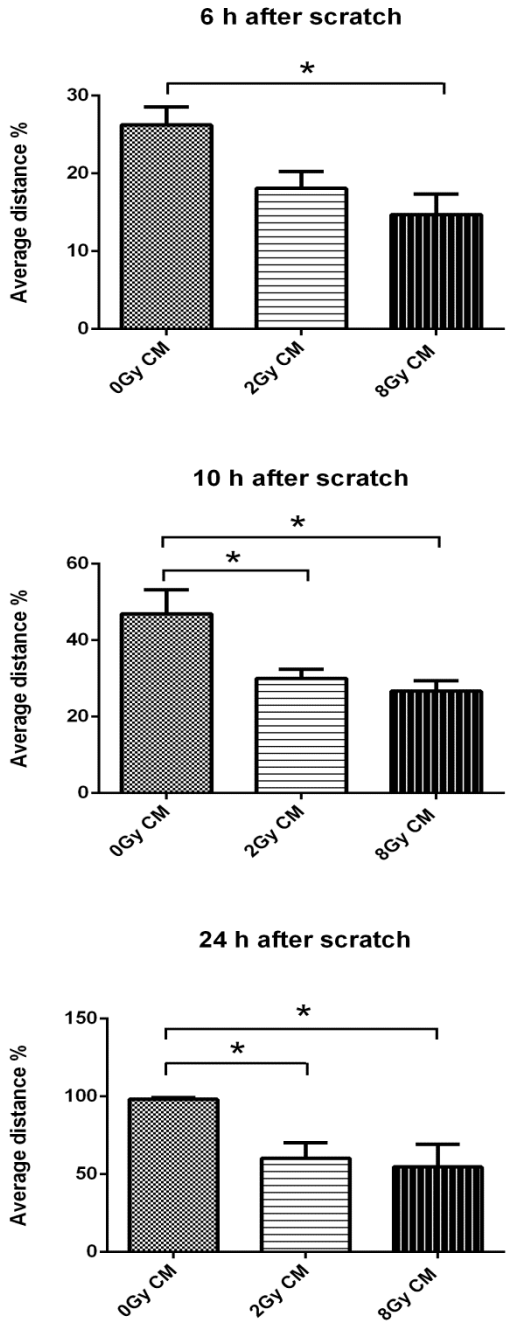

Figure 5.7 Effects of CM from irradiated HDFs on HUVEC migration. Confluent HUVEC monolayers were exposed for two days to CM obtained from HDF cells irradiated at doses of 0, 2 and 8 Gy, after which a scratch wound was performed. The wound healing process was monitored for 24 h. The results are presented as the percentages of the average wound area after 6, 10 and 24 h relative to the original wound (0 h) in each group. The graphs show data from mean of 4 separate experiments ± SEM using a One-Way ANOVA test. The CM from HDFs irradiated at 8 Gy shows a significant inhibitory effect on HUVEC migration after 6 h, which became significant at 2 and 8 Gy upon prolonged exposure for 10 and 24 h. (*$p < 0.5$)

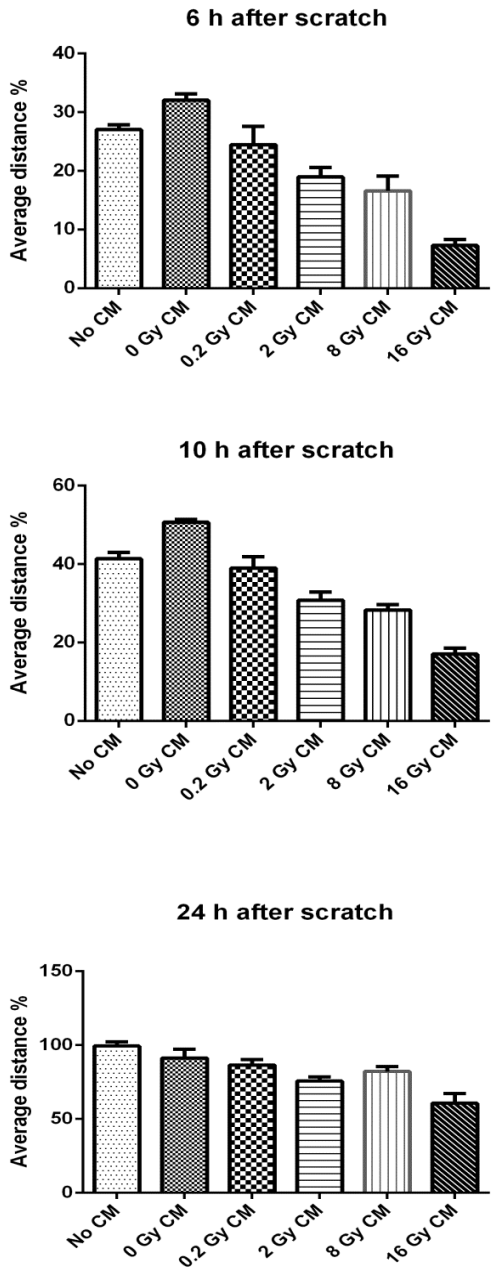

Figure 5.8 Effect of CM from irradiated HDFs on H5V migration. The effect of CM from irradiated and non-irradiated HDFs on H5V wound closure was tested using an *in vitro* scratch wound closure assay. The confluent H5V monolayers were exposed to the 0 (control), 0.2, 2, 8 and 16 HDF CM for two days. They were then treated with 5µg/ml Mit C for 2 h before starting the experiment. The scratch was made on the monolayer and the wound healing process was monitored for 24 h. The data are presented from one experiment. The CM from irradiated HDF had inhibitory effects on H5V migration after 6 and 10 h. However, the wound healing process improved after 24 h and there were some differences in H5V migratory capacity between those received CM from 16 Gy irradiated HDFs compared to non-irradiated HDFs.

5.2.3 Irradiated fibroblast/endothelial cell signaling and its impact on functional changes in endothelial cells

The results presented so far in this chapter show that irradiated fibroblasts inhibit EC formation of capillary-like structures and migration. Moreover, the data suggest that irradiated fibroblasts influence endothelial angiogenic function through bystander interactions mediated by soluble factors. To address this, the experiments outlined next investigated whether TGF-β and Rho/ROCK may be possible mediators of these bystander interactions. To study the role of Rho and TGF-β signaling on the effects of radiation on EC angiogenic responses described in the previous sections, the ALK5 inhibitor SB 431542 and Rho kinase inhibitor Y 27632 were used. The following experiments describe the use of these inhibitors in different assays (fibroblast bed organotypic and scratch wound assays) to investigate EC capillary-like formation and migration.

5.2.3.1 Investigating the influence of Rho and TGF-β signaling on irradiated fibroblast induced EC morphogenic changes

The HUVECs-HDF fibroblast bed organotypic assay was performed in the presence of SB431542 and Y27632 inhibitors. HDFs were plated and grown to confluence, and were then either non-irradiated or irradiated (0.2, 2, 8 and 16 Gy). Following this, HUVECs were directly plated on top. The SB431542 inhibitor (10 μM) and Y27632 inhibitor (10 μM) were then added to the cells every two days. After 14 days, EC capillary-like structures were visualised as described previously. The number, total length and branch points of EC capillary networks were measured relative to the different treatment groups (+/- radiation and +/- inhibitors/neutralizing antibody), and data normalised to the control (% to control). To determine the statistical significance of the data from irradiated and non-irradiated groups, with and without treatment, a Two-way ANOVA test was performed.

The treatment of cells with the TGF-β receptor (ALK5) inhibitor, SB431542 decreased the inhibitory effect of irradiated fibroblasts on EC capillary networks formation as shown in the images in Figure **5.9**. The number of capillary-like structures formed by HUVECS increased

upon addition of SB 431542, resulting in a well-structured mature network with more junctions. Quantitation of these data is presented in Figure **5.10**. Data from the three (16 Gy) and four separate experiments were expressed as mean ± SEM and analysed using a Two-way ANOVA test. EC sprouts length increased significantly (approximately 40%) upon treatment with SB 431542 in all irradiated groups (≥ 0.2 Gy) compared to non-treated control group. Even in the non-irradiated group, the addition of SB 431542 improved the number and length of cord-like structures compared to the non-treated groups, however this was not significant. A similar, significant effect on sprouts numbers was also observed, with an increase (approximately 50%) in the number of sprouts evident in the irradiated group treated with SB 431542, compared to the untreated group. Additionally, these channels had more branch points, which was statistically significant at doses of 0.2, 2 and 16 Gy (90% increases in formation of branches in 0.2 and 2 Gy treated groups and 45% in 16 Gy one). Similar to the increase in EC channels number and length observed in non-irradiated groups treated with SB 431542, inhibition of the TGF-β receptor increased the number of junctions in the non-irradiated group. However, in this case the increase was shown to be significant. The inhibition of TGF-β receptor using SB 431542 induced some morphogenesis changes in the vessels, which resulted in significant increase in formation of branch points in vessels. It is required to further investigate how this inhibitor induces its effect during angiogenesis.

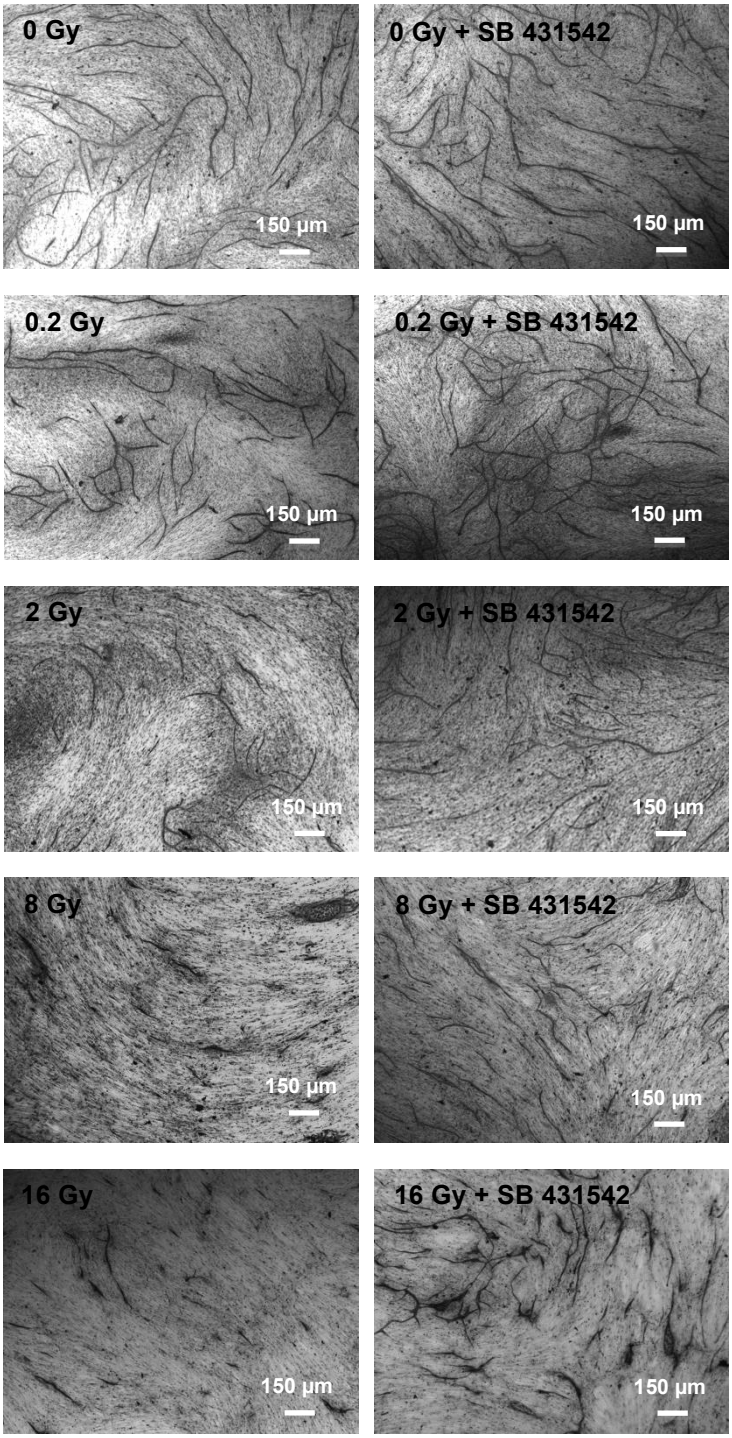

Figure 5.9 Effect of the TGF-β ALK 5 receptor inhibitor SB 431542 on the formation of capillary-like networks by HUVECs plated on a bed of irradiated fibroblasts. HDFs were irradiated at doses of 0 (control), 0.2, 2, 8 and 16 Gy upon reaching confluence. HUVECs were seeded on top of the fibroblasts and treated with 10 µM of SB431542 every two days. After 14 days, EC thread-like structures were characterised with an antibody to vWF. The results show that irradiation of fibroblasts affected the formation of sprouts by HUVECs. However, the inhibition of ALK receptor considerably increased the level of sprouts formed by HUVECs in the irradiated group with more junctions compared to the non-treated ones.

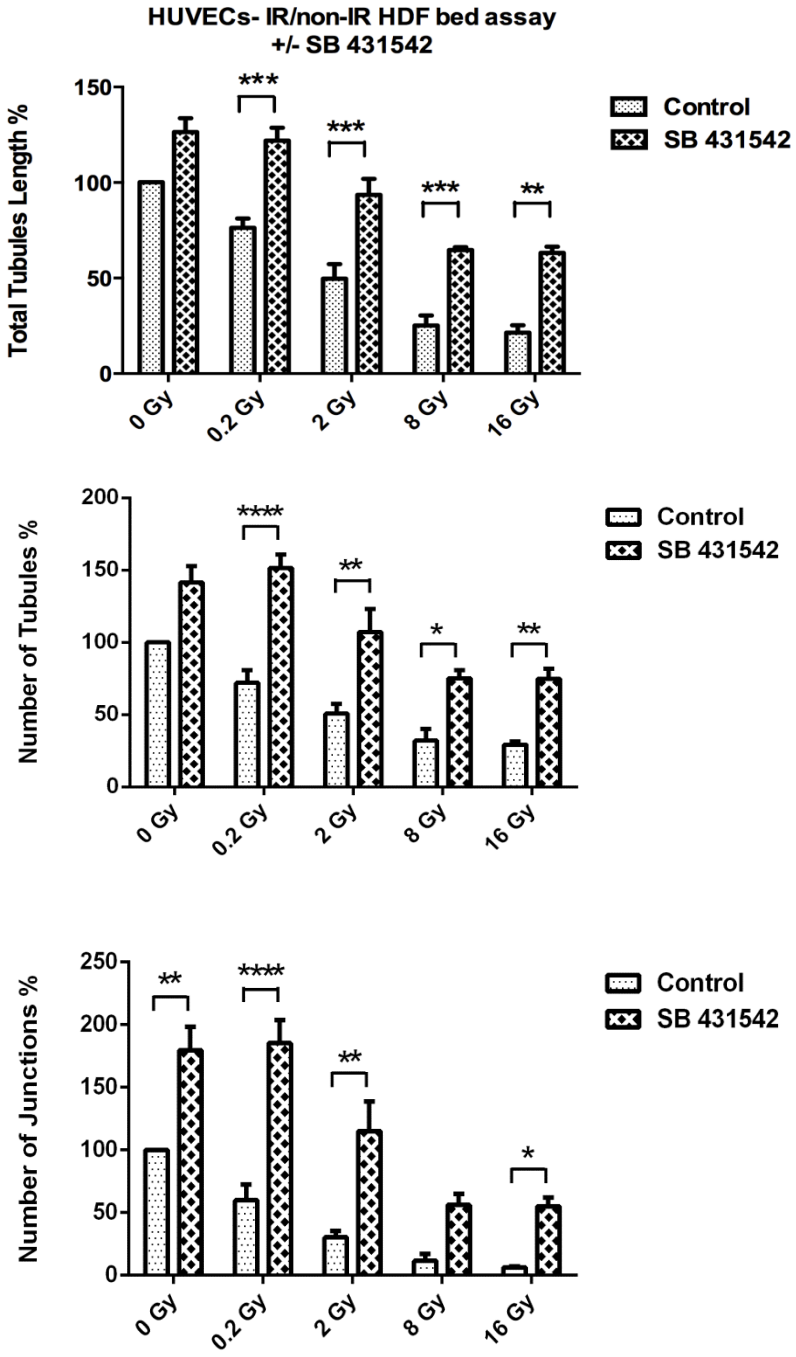

Figure 5.10 Quantification of irradiated fibroblast effects on capillary networks formation by HUVECs in the presence/absence of the TGF-β ALK 5 receptor inhibitor SB 431542. Data from the three (16 Gy) and four separate experiments were expressed as mean ± SEM and analysed using a Two-way ANOVA test. The axes represent total capillaries lengths, number of capillary-like networks and junctions normalised to the control (% of control). Inhibition of the TGF-β1 receptor, ALK5, reversed the effects of radiation and increased formation of EC channels. The number of sprouts and their total length and junctions when treated with SB431542 in irradiated groups were significantly higher compared to the non-treated irradiated groups. (*p < 0.5, **p ≤ 0.0.01, ***p < 0.0.001, ****p < 0.0001).

In the next experiments, the co-culture assay was performed in the presence/absence of the ROCK inhibitor Y27632. Images from one experiment are shown in Figure **5.11** and indicate some increase in capillary-like structures formation by HUVECs co-cultured with irradiated fibroblasts upon addition of the ROCK inhibitor, inferring that blocking the Rho pathway appears to alleviate the effects of irradiated fibroblasts on EC morphogenesis. Quantitative analysis of these data displayed in Figure **5.12**. Data were expressed as mean ± SEM of three separate experiments and analysed using a Two-way ANOVA test. Results shows that the number and total lengths of sprouts formed by HUVECs co-cultured with irradiated HDFs improved upon treatment with Y27632. This was also true when assessing EC capillary networks branching, where the number of branches increased in all irradiated groups when treated with Y 27632, which was significant in 0 and 0.2 Gy treated cells (increased 100%). However, the results from these experiments were inconsistent, as in three separate assays, one assay showed a profound increase in the formation of EC channels upon addition of the ROCK inhibitor, while only moderate changes in EC channel formation were observed in the other two assays. Therefore, further experiments are required in order to establish reliable consistent data and to determine whether any of the observed effects were significant before any definitive conclusions are made. Further, it is required to investigate how the Y 27632 inhibitor exerts their effects during EC morphogenesis/angiogenesis to find out why only the number of junctions was significant in the Y 27632 control group compared to the non-treated control.

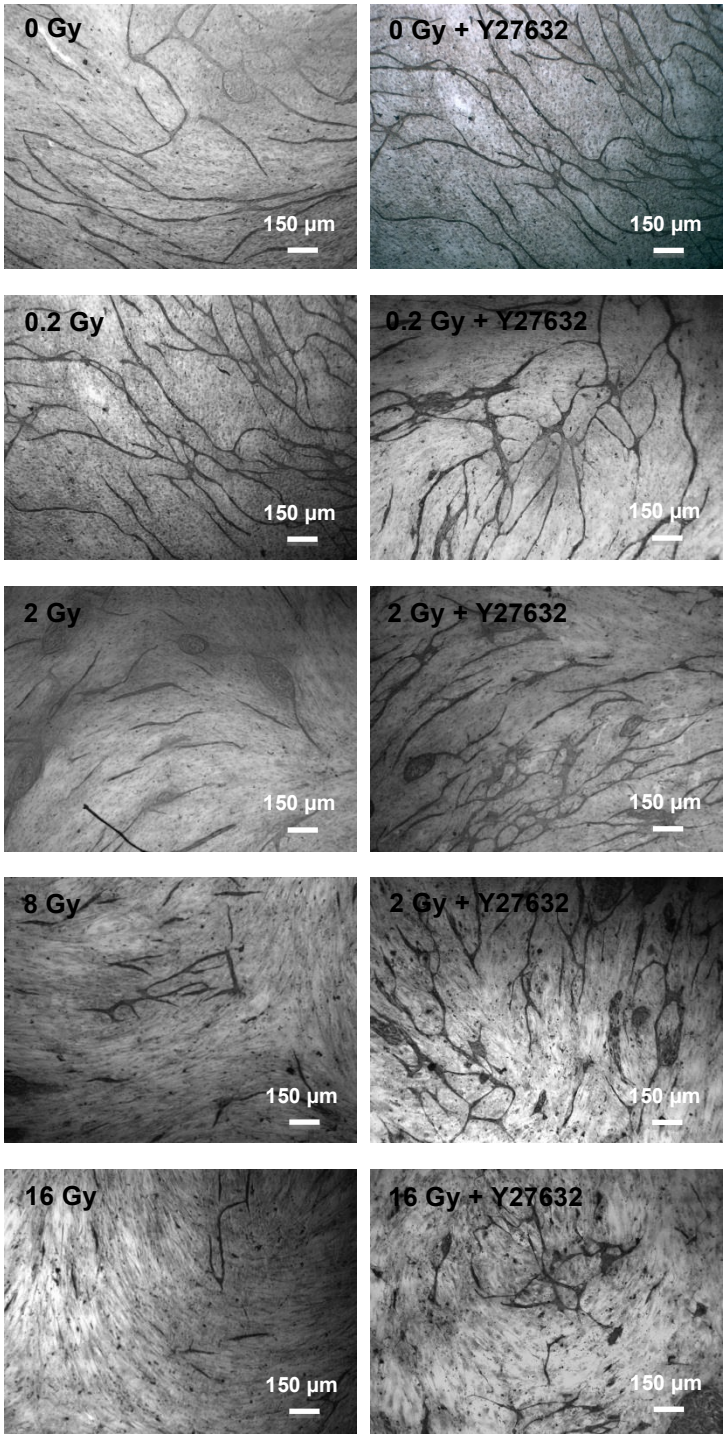

Figure 5.11 Effect of the ROCK inhibitor Y 27632 on the formation of capillary-like structures by HUVECs plated on a bed of irradiated fibroblasts. HDF cells were irradiated at radiation doses of 0 (control), 0.2, 2, 8 and 16 Gy upon reaching confluence. The HUVECs were seeded on top of the irradiated and non-irradiated HDF and treated with 10 µM of Y27632 every two days. After 14 days EC thread-like structures were visualised using an antibody to vWF. The irradiated HDFs affected the formation of vessels by HUVECs, especially at high doses of 8 and 16 Gy. However, the inhibition of ROCK reversed the radiation effects and increased the number of sprouts formed by HUVECs. The 8 and 16 Gy irradiated groups upon treatment with Y27632 showed an increase in cord-like tubes formation and they exhibited more branches points.

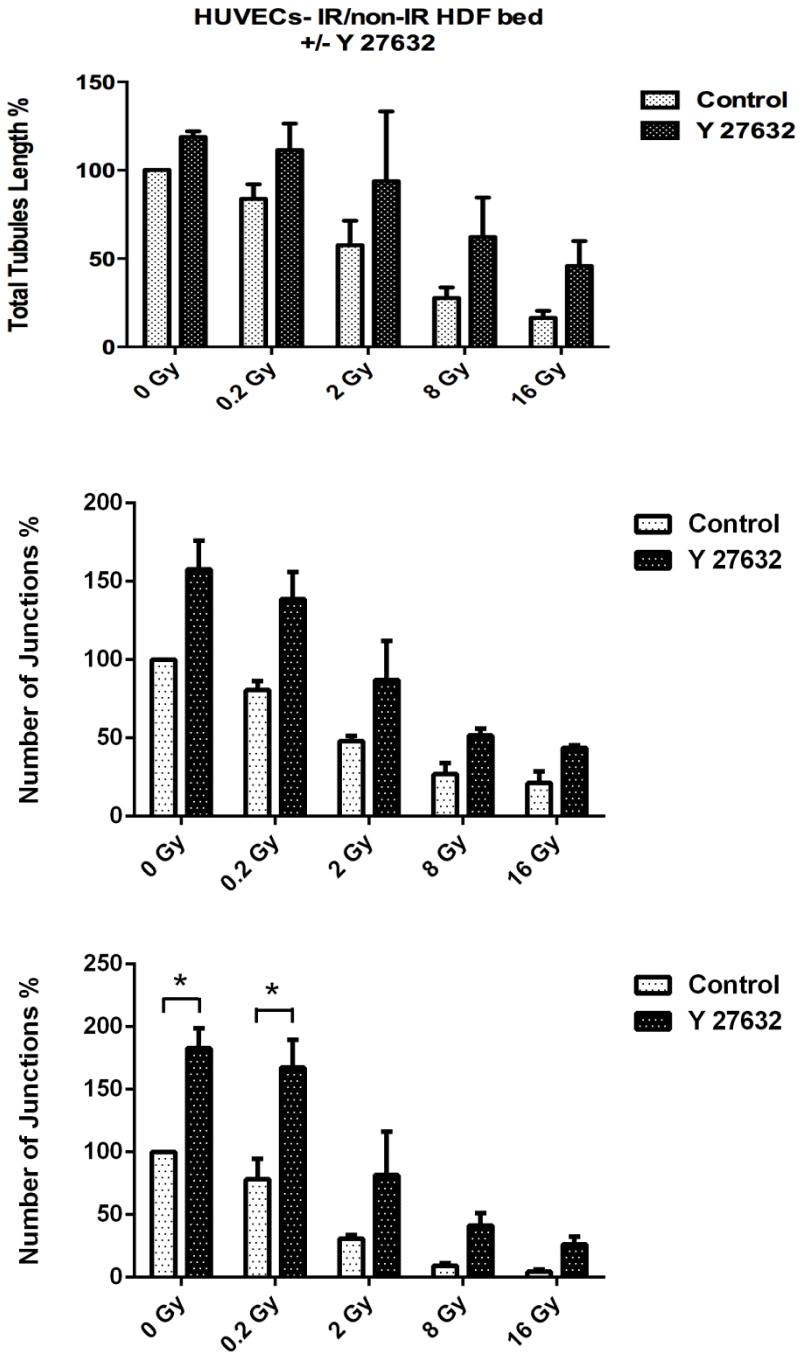

Figure 5.12 Quantification of irradiated fibroblast effects on capillary-like structures formation by HUVECs in the presence/absence of the ROCK inhibitor Y27632. Data from the three separate experiments were expressed as mean ± SEM and analysed using a Two-way ANOVA test. The axes represent total capillary-like network lengths, number of capillary-like networks and junctions normalised to the control (% of control). Data show that while HDF irradiation had a dramatic inhibitory effect on the morphogenesis capacity of HUVECs, ROCK inhibition suppressed these effects, resulting in an increase in the number and lengths of tubules as well as the forming of junctions, however, these effects were not significant.

5.2.4 Investigating the influence of Rho pathway signaling on the inhibitory effect of CM from irradiated fibroblasts on EC morphogenesis

The experiments described previously (Section **5.2.3.**1) have shown that inhibiting ROCK results in some improvement in the formation of vessel-like structures by HUVECS when cultured with irradiated fibroblasts. Therefore, the Rho pathway might play a negative role in the angiogenic activity of ECs following radiation. The fibroblasts were shown to have bystander effects on ECs angiogenic/morphogenic responses and soluble factors released by fibroblasts are likely to be involved. Here the inhibition of ROCK by Y27632 on the formation of tubules by HUVECS when cultured on a HDF bed exposed to conditioned media obtained from irradiated HDFs was investigated.

HUVECs were directly plated on a confluent bed of HDFs as described previously (section **5.2.2.1**). After two days CM collected from irradiated HDFs at 0 (control), 2 and 8 Gy were added to the co-cultures and they were also treated with +/- 10 μM Y27632. These treatments were repeated every two days for 14 days. Two independent sets of experiments were performed and the images and quantitative analysis from each separate experiment are presented in Figures **5.13** and **5.14**.

The results from both experiments clearly demonstrate the inhibitory effect of the irradiated CM on the formation of sprouts by HUVECs (Figure **5.13**), as described previously (**5.2.2.1**). The blocking of ROCK increased the formation of capillary-like networks in co-cultures receiving CM from irradiated HDFs, this effect being particularly profound at doses of 8 Gy (Figure **5.13A** and **B**). HUVECs in the control non-irradiated group exhibited similar levels of vessel-like structures in the presence or absence of Y 27632. The quantitative analysis of these data, shown in Figure **5.14** confirms that the CM from irradiated HDFs suppressed formation of capillary-like tubes in co-cultures.

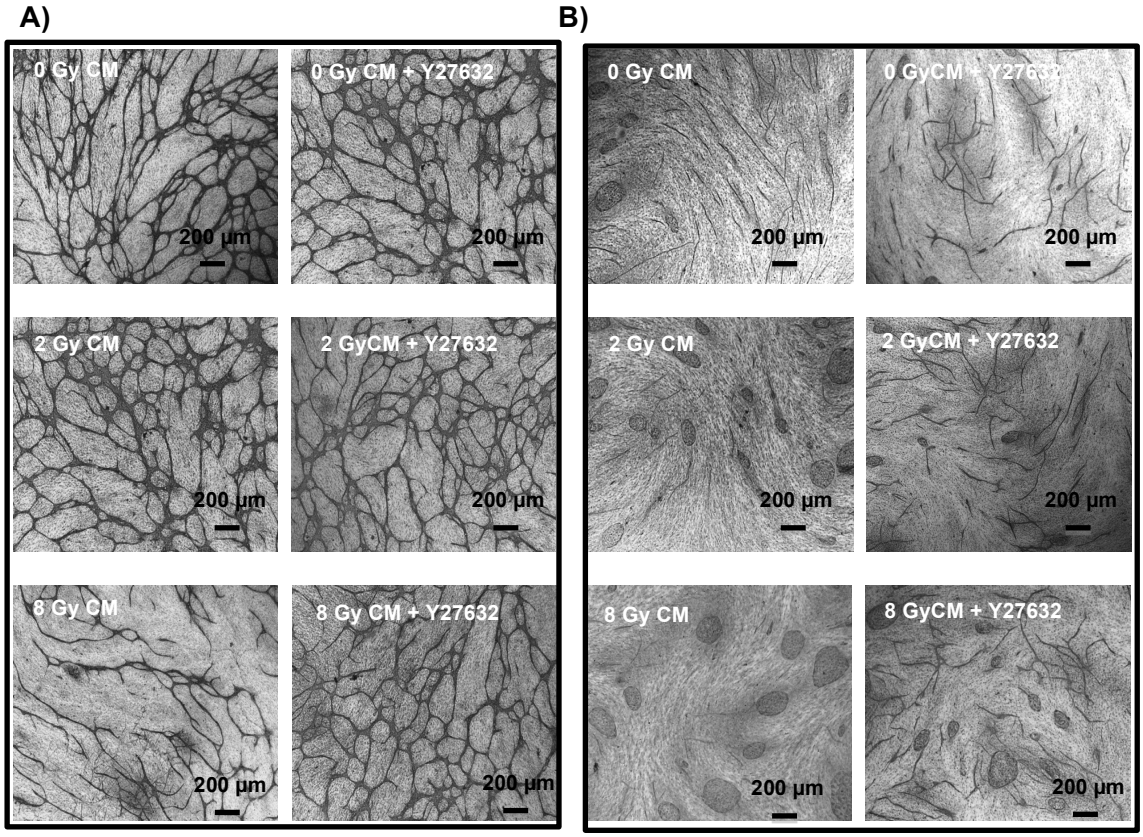

Figure 5.13 Effect of the ROCK inhibitor Y 27632 on the formation of capillary-like structures by HUVECs plated on a bed of HDFs, cultured in the presence of CM from irradiated HDFs. HDFs were irradiated at radiation doses of 0 (control), 2 and 8 Gy upon reaching confluence. CM from these experiments was then added separately to the co-culture bed along with an equal volume of normal media. The Y27632 inhibitor was then added every two days in a fresh medium and EC sprouts visualised with an antibody to vWF after 14 days. Images from experiment **A)** show that CM from irradiated HDFs affected the formation of cord-like structures by HUVECs. The number and quality (length and junctions) of capillary-like tubes formed by HUVECs increased upon addition of Y27632, which was more profound at higher doses of 8 Gy. The images from experiment **B)** show that CM from both 2 and 8 Gy irradiated HDFs affected the formation of channels in HUVECs-HDFs co-culture and HUVECs remained in clusters form at 2 and 8 Gy. However, inhibiting the ROCK improved the HUVECs sprouting and effects were most obvious in HUVECs co-cultured in the presence of CM from both 2 and 8 Gy irradiated HDFs.

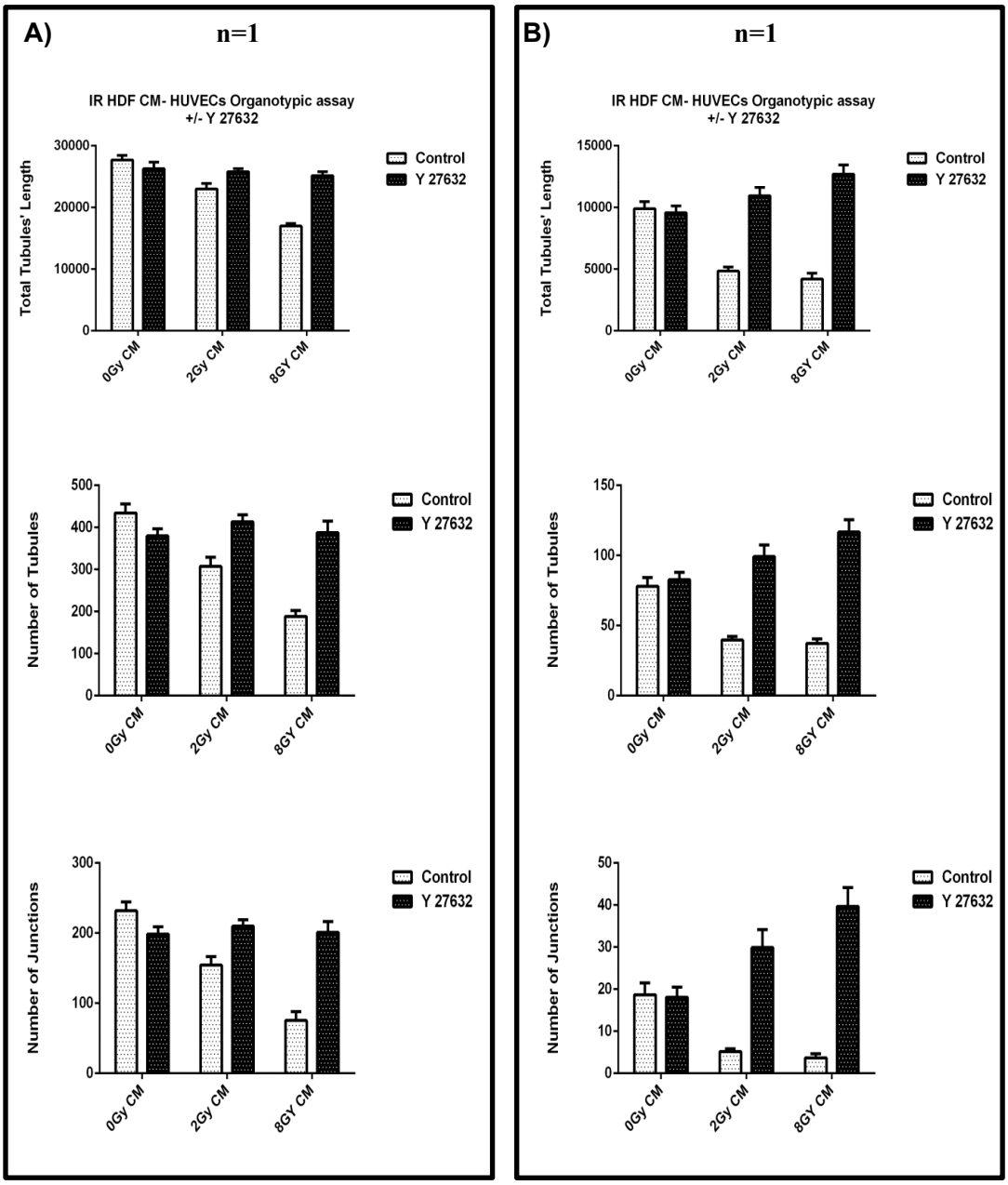

Figure 5.14 Quantification of the effect of CM from irradiated fibroblasts on formation of capillary-like structures by HUVECs in the presence/absence of the ROCK inhibitor Y27632. Quantified data, based on the number of, length of capillary-like tubes and the number of tubes branch points formed by HUVECs in the two experiments described above are presented. The results from experiment **A)** show the number, length and junctions of capillary-like tubes formed by HUVECs increased upon treatment with Y 27632 when co-cultured with CM from irradiated HDFs. This was most profound at a dose of 8 Gy. The results from experiment **B)** show there was a more profound increase in the number, length and junctions of capillary networks at doses of both 2 and 8 Gy in the presence of Y 27632 compared to non-treated groups.

Addition of Y27632 suppressed the inhibitory effect of the CM from irradiated HDFs, resulting in an increase in the number of capillary-like networks, their lengths and junctions in both experiments. However, this effect was most obvious at doses of 8 Gy in experiment **A)** (**Fig 5.14A**), whilst, a profound improvement was observed at both doses of 2 and 8 Gy in the experiment **B)** (**Fig 5.14B**). These results together imply that the Rho pathway is involved in the inhibitory effect of CM from irradiated fibroblasts on EC morphogenesis. Further experiments would be necessary in order to confirm that the observed effects are significant.

5.2.4.1 The involvement of TGF-β signaling in the inhibition of migration of HUVECs exposed to CM from irradiated fibroblasts

Previous experiments showed that inhibiting the TGF-β receptor ALK5, restored EC morphogenesis. The next set of experiments, therefore, tested the effects of CM from irradiated fibroblasts on HUVEC migration in the presence/absence of the ALK5 inhibitor (SB431542).

CM from irradiated fibroblasts (0, 2 and 8 Gy) were obtained and concentrated. HUVECs were plated in silicon ibidi inserts at a density of 28,000 cells per reservoir. Upon reaching confluence, the ibidi inserts were removed and the CM from irradiated and non-irradiated HDFs were added, with and without SB431542. Images of the wounds were taken after 6, 10 and 24 h. In initial experiments 10 μM of SB431542 was found to completely stop the migration of control HUVECs, therefore the lower concentration of 3 μM was chosen for these experiments.

The data from one experiment presented in Figure **5.15A**, shows that CM from irradiated fibroblasts reduced the migratory capacity of HUVECs, which was more apparent after 10 and 24 h. There was some improvement in HUVEC migration capacity in all groups tested, upon addition of the TGF-β/ALK5 inhibitor.

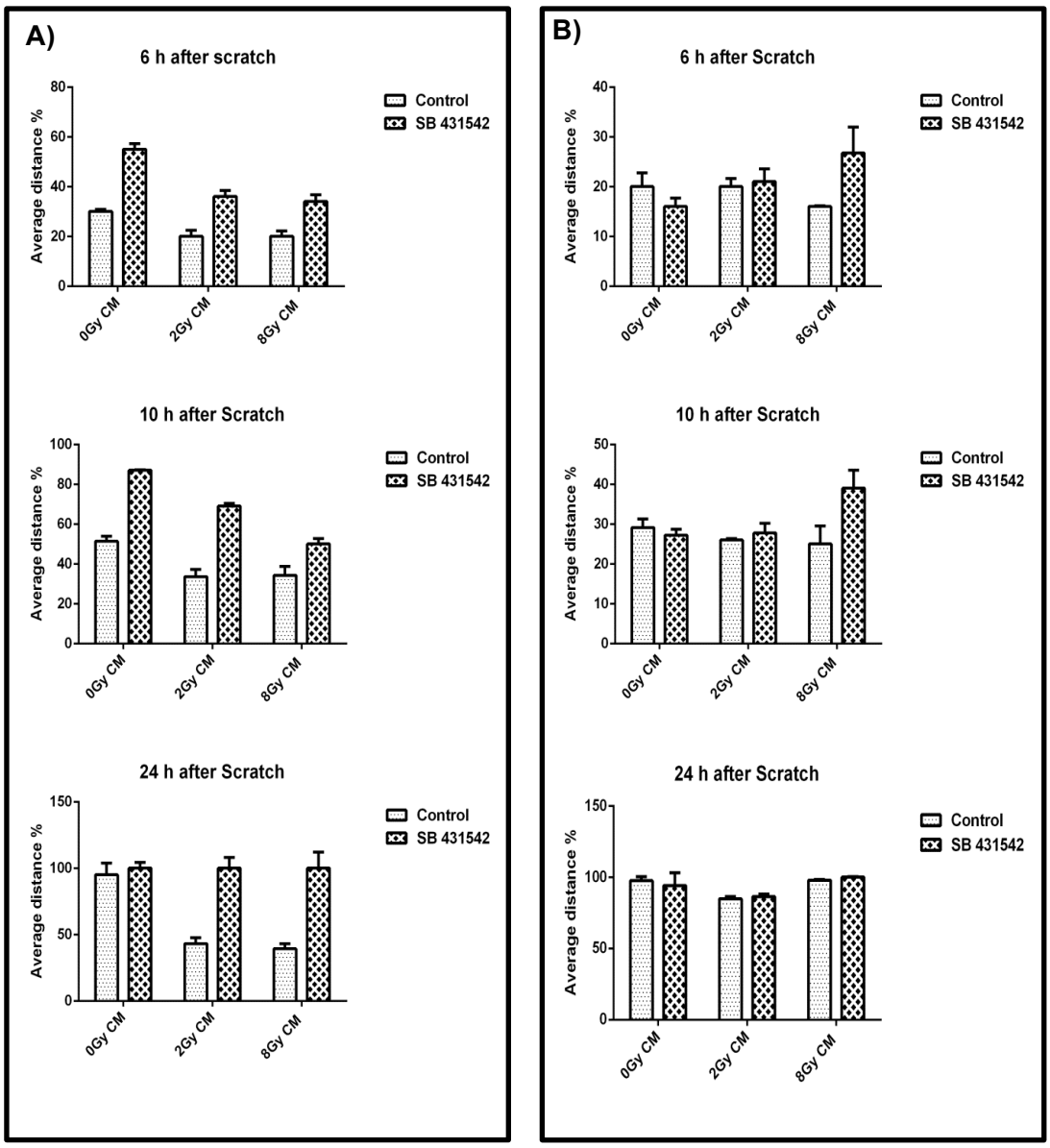

Figure 5.15 Effect of the TGF-β ALK 5 receptor inhibitor (SB 431542) on migration of HUVECs when exposed to CM from irradiated and non-irradiated HDFs. CM from irradiated and non-irradiated HDFs was added to HUVECs in a scratch wound assay, in the presence/absence of 3 μM of SB431542. Data were expressed as the percentage of the average wound distance after 6, 10 and 24 h relative to the original wound (0 h). **A)** Data show that CM from irradiated fibroblasts suppressed HUVEC migration, being most notable at 24 h. The addition of SB 431542 alleviated this effect in all groups tested (even in non-irradiated control cells), however, the effect was most obvious at 24 h in irradiated cells. **B)** Data represent that addition of CM from irradiated HDFs did not have the same inhibitory effect on HUVEC migration; only a small reduction at 8 Gy after 6 h was observed.

This appeared to be the case even in cells receiving CM from non-irradiated HDFs, as well as SB 431542 after 6 and 10 h following wound creation. However, after 24 h, HUVECs receiving CM from irradiated HDFs in the presence of the SB431542 inhibitor had the same migratory capacity as HUVECs in the control group, compared to those that did not receive the drug. Data presented in Figure **5.15B**, represents a repeat of the same experiment, however, in this experiment, the inhibitory effects of radiation on HUVEC migration were not as obvious, and therefore making it difficult to draw any informed conclusions regarding the effects of adding the ALK5 inhibitor. Further experiments are required in order to make a firm statement about the involvement of TGF-β signaling in alleviating radiation-induced inhibition of EC migration after the exposure of ECs to CM from irradiated fibroblasts.

5.2.5 Effect of radiation on expression of TGF-β in CM from fibroblasts

The inhibiting TGF-β signaling via the ALK5 receptor resulted in radiation-induced inhibitory effects on morphogenesis/migration being alleviated, inferring a role for TGF-β in mediating these effects. The next experiments were therefore designed to test whether TGF-β expression increased in CM from irradiated fibroblasts. This involved performing western blots using a commercial antibody to TGF-β (Abcam rabbit polyclonal to TGF-β, Cat no. ab66043).

HDFs were irradiated at 0 (control), 2 and 8 Gy upon reaching confluence. After two days, CM were collected and concentrated (from 4-5 ml to 100-500 µl), and the volume was adjusted in each group. Proteins were then extracted from CM and analysed for TGF-β expression. The western data from this experiment are shown in Figure **16A, B and C**. Recombinant TGF-β protein (rTGFbp) was used as positive control for the commercial antibody in the westerns (Figure **5.22A**). The TGF-β is secreted in a complex form called latent TGF- β complex (~235 kDa), which has been composed of LAP (80 kDa as dimer) and LTBP (130-160 kDa) and mature TGF-β. The active TGF- β form runs at a molecular weight of approximately 13 kDa (monomeric size), and can also be detected as a dimer of ~25 kDa (Annes *et al.*, 2003; Horimoto *et al.,* 1995; Miyazono *et al.,* 1991). A band of 25 kDa is clearly evident in the lane corresponding to rTGFbp, demonstrating that the commercial anti- TGF-β

antibody is working (Figure **5.16A**). Interestingly, a similar sized band was evident in protein extracts isolated from CM from fibroblasts irradiated at 2 and 8 Gy. However, since this same sized band was also observed in CM from non-irradiated fibroblasts, this inferred that radiation was not up-regulating TGF-β expression. A strong band was observed across the blot at ~ 60 kDa, which was evident even in normal media, but was not present in the lane corresponding to rTGFbp. This could possibly correspond to Bovine Serum Albumin (BSA) present in the media (BSA molecular size is 64 kDa). Two bands running at approximately 140 and 240 kDa are also evident in all lanes, with the exception of the lane corresponding to normal media. Since this is also evident in the rTGFbp lane, this suggests that it could correspond to unprocessed TGF-β protein (large latent TGF-β complex form). However, again, there was no observed increase in the strength of this band in CM from irradiated fibroblasts compared to non-irradiated control fibroblasts. This experiment was performed a few times (3 times), and similar results were obtained. However, depending on experiments, the monomeric form (13 kDa) of TGF-β was detected in two experiments (Figure **5.16B**). The TGF-β band was more obvious usually after longer exposure (5-10 min). Therefore, since it is difficult to detect signaling proteins in CM, in future experiment, a higher concentration of CM is required to detect TGF-β in the media.

Since the Western data from the CM showed that there were no apparent changes in the expression of TGF-β in CM from irradiated compared to non-irradiated CM, another experiment was performed as above, however, this time TGF-β expression was investigated directly in irradiated and non-irradiated HDFs. Here, (Figure **5.16C**) bands corresponding to the unprocessed form of TGF-β are evident in extracts from both irradiated and non-irradiated HDFs, but again appear with similar intensities.

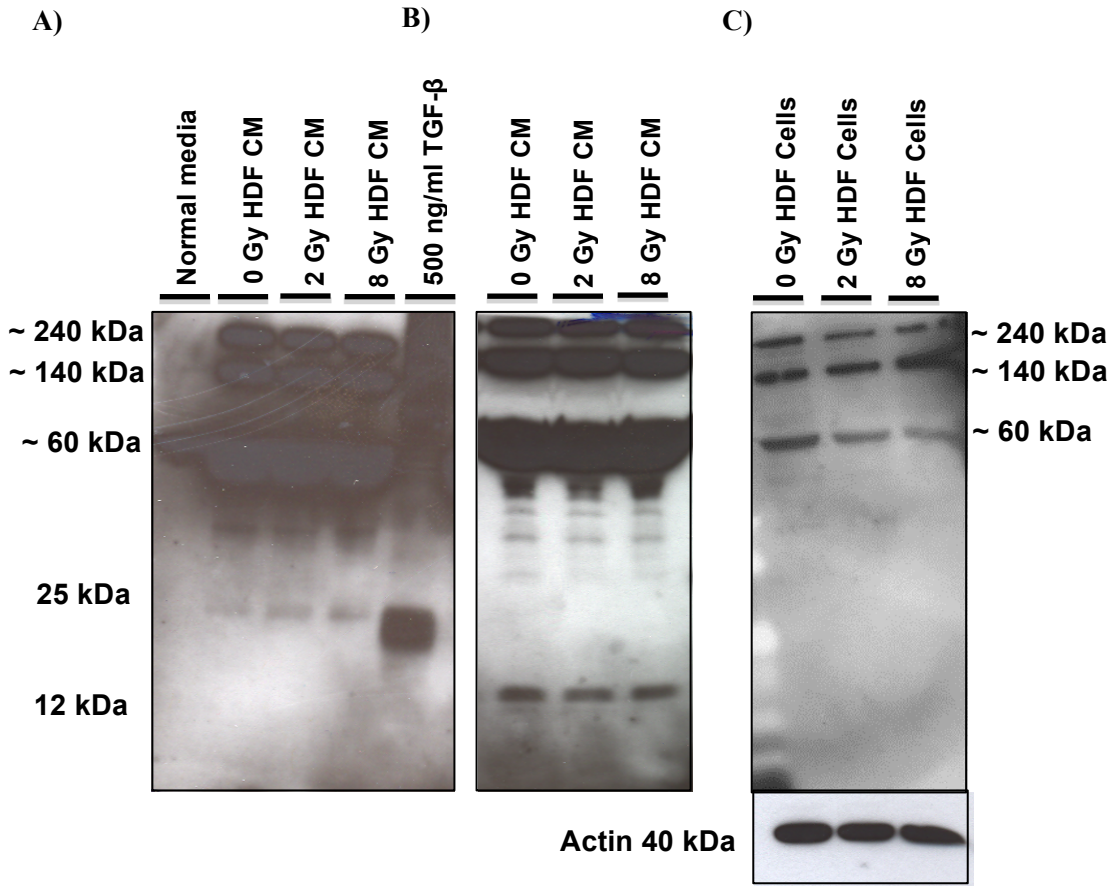

Figure 5.16 Western blot analysis of TGF-β expression. HDF cells were either irradiated or left unirradiated and protein extracts prepared from CM, as well as HDF cells themselves. Extracts were probed using an anti- TGF-β antibody. **A**) Bands corresponding to dimeric TGF-β (~ 25 kDa) are evident in all CM tested, as well as in the lane corresponding to rTGFbp. Similar levels of TGF-β expression were observed in all CM from irradiated and non-irradiated HDFs. No TGF-β protein was detected in the protein extracts from normal media. The 60 kDa band observed in all CM as well as normal media could potentially correspond to BSA. TGF-βp bands were also detected at molecular sizes of 140 and 240 kDa at same densities, which could correspond to the unprocessed, latent TGF-β protein. **B**) A representative blot from further experiments showing the same level of TGF-β protein bands observed corresponding to monomeric (12 kDa) and unprocessed latent (140-240 kDa) TGF-bp in CM from irradiated and non-irradiated HDFs. **C)** Data show the expression of TGF-β with a similar level in cell extracts derived from irradiated and non-irradiated HDFs (only TGF-β bands of 140 and 240 kDa were detected). The membrane was reprobed for actin to determine protein loading.

Reprobing of the blot for actin (40 kDa) revealed similar levels of protein loading in all lanes, again inferring that there was no obvious increase in TGF-β expression in HDFs exposed to radiation. However, since these data were only obtained from a few experiments, further experiments are required in order to make any firm conclusions about whether radiation of fibroblasts affects the overall levels of TGF-β in the CM.

5.2.6 Analysis of conditioned media from irradiated fibroblasts by angiogenesis and cytokine arrays

The irradiated fibroblast conditioned media (CM) might contain soluble factors, which could be responsible for described effects on endothelial cell functions. Therefore, the fibroblasts CM were analysed using angiogenesis and cytokine arrays (R&D human cytokine array (Cat. no. ARY005) and angiogenesis array (Cat. no. ARY007). Media were collected after 48 h, concentrated (from 20 ml to about 1-2 ml) and each was adjusted to a final volume of 3 ml. The array experiments were performed as described in the Methods (section **2.11**) and analysed by ECL. Each membrane was exposed to the to the X-ray film multiple times for 1-10 minutes. The X-ray films were then analysed by densitometry and the average pixel density of each pair of duplicate spots was determined (each set representing a different cytokine).

The data from the angiogenesis array are presented in Figure **5.17**. Of 55 angiogenesis-related proteins, 20 proteins were found to be present at detectable levels in both CM from irradiated and non-irradiated HDFs (**5.17a).** The selected angiogenesis-related proteins with higher detectable expression levels are shown in Figure **5.17b**. The analysis of data from the angiogenesis array revealed that VEGF and placenta growth factor (PIGF), which are angiogenic growth factors, had a higher relative expression compared to CM from non-irradiated HDFs. PAI-1, which is also known as Serpin E1, levels were also higher in irradiated HDF CM compared to the control CM. Additionally, there was a higher level of Thrombospodin-1 (which helps to activate the TGF-β complex) levels in CM from irradiated HDFs (**5.17b).**

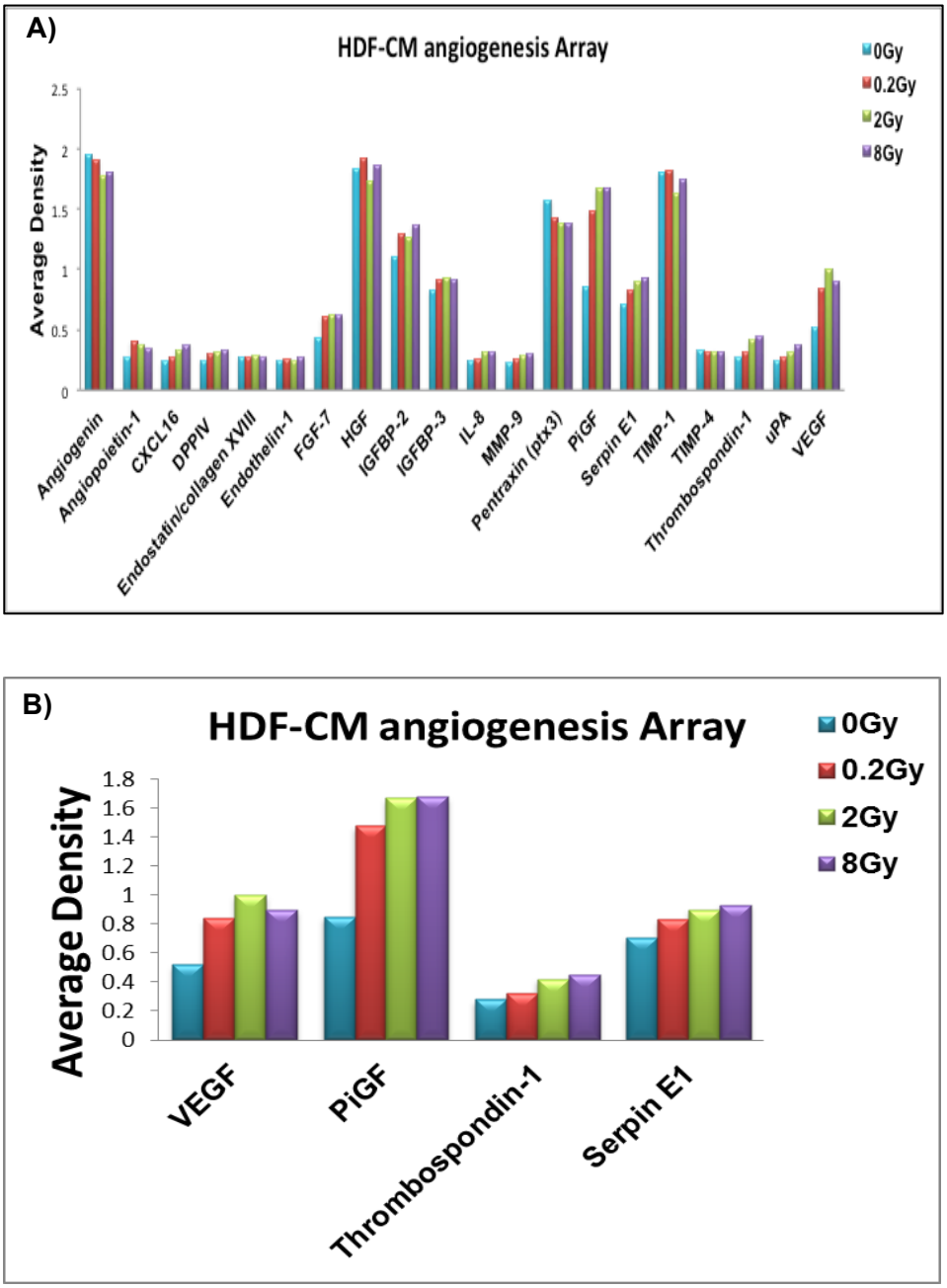

Figure 5.17 Profiling angiogenesis-related proteins in irradiated and non-irradiated fibroblast CM. A) Results show that of the 55 angiogenesis-related proteins analysed, 20 factors had detectable expression levels in CM. 13 factors showed higher relative expression in irradiated CM compared with non-irradiated CM and two proteins (pentraxin (ptx3) and angiogenin) had lower levels of expression. **B)** Data present selected angiogenesis-related proteins with higher detectable expression. The relative expression of the VEGF, PiGF, PAI-1 and thrombospodin-1 was increased in CM from irradiated HDF compared to CM from non-irradiated cells.

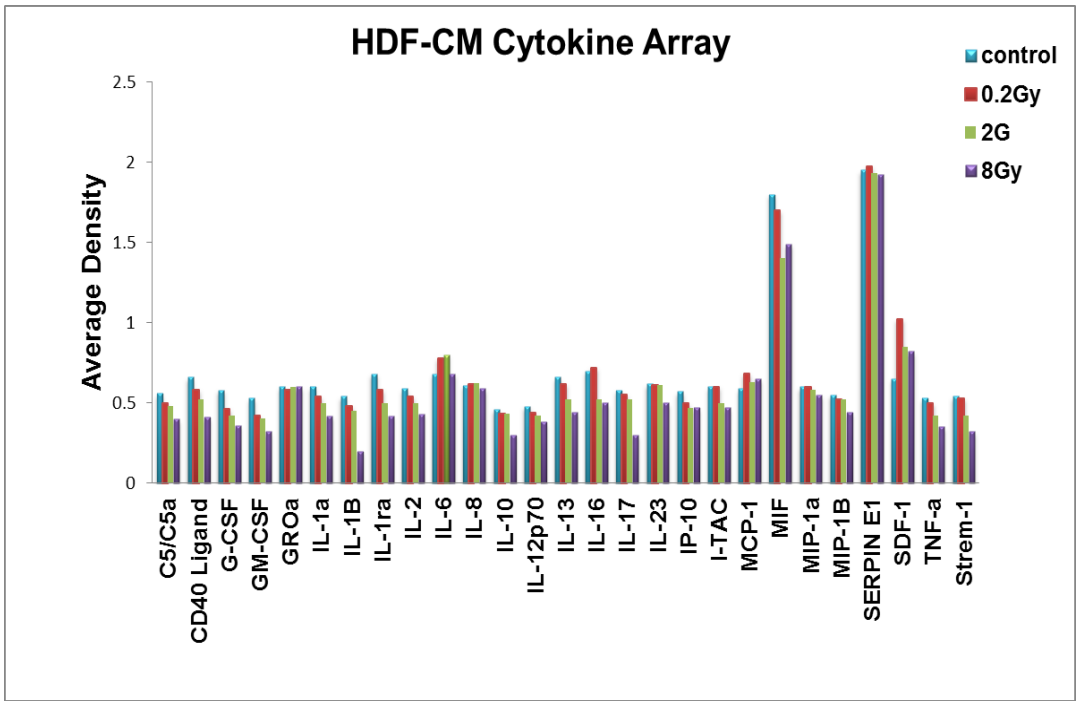

Figure 5.18 Profiling cytokines in irradiated and non-irradiated fibroblast CM. Data show that of the 36 different cytokines analysed, 20 had detectable expression levels in CM. The expression levels of 20 cytokines/chemokines, including CD40 Ligand, G-CSF, IL-1a, IL-1B, IL-1ra, IL-10/13/16/17, MIF, and TNF-α decreased in CM from irradiated HDFs compared to CM from non-irradiated cells.

Figure **5.18** shows the results of the cytokine arrays. The relative levels of 27 out of 36 different cytokines and chemokines, which were detected in the CM are shown in Figure **5.18**. Out of these 20 cytokines and chemokines showed a detectable reduction in their expression levels in CM from irradiated HDFs compared to CM from non-irradiated cells. There were lower levels of multiple interleukins, CD40 Ligand, G-CSF, MIF and TNF-α in the condition media from irradiated cells. However, since both angiogenesis and cytokine arrays experiment were only performed once, therefore, the results would need to be verified before conclusions can be made.

5.2.7 Investigating the direct involvement of Rho and TGF-β signaling in radiation effects on EC angiogenic properties

Since the previous experiments tested the effects of inhibiting Rho and TGF-β signaling in EC angiogenesis following exposure to either irradiated fibroblasts or CM from irradiated fibroblasts, the next set of experiments were designed to examine the role of these signaling pathways in the radiation induced direct effects observed previously on EC migration (chapter **3**), and heart explant angiogenic sprouting (chapter **4**).

5.2.7.1 Effects of inhibiting Rho and TGF-β signaling in radiation effects on EC migration

H5V cells were treated with Mit C, and then irradiated at 0, 0.2, 2, 8 and 16 Gy. The next day a scratch was made on the monolayer, and media changed to media containing either SB431542 (10 μM) or Y27632 (10 μM) (they were both tested in each experiment performed). The results from three separate experiments were expressed as mean ± SEM and they are presented in Figures **5.19** and **5.20.**

In the experiments using the TGF-β ALK5 inhibitor (SB 431542), the effects of radiation on migration of H5V cells were observed, whereby some reduction in H5V cell migration was measured. However, this was subtle and not consistent at all doses of radiation tested, which contrasts with the significant effects of radiation on H5V cell migration described previously

(section **3.2.5.1.2**). The analysis of data in irradiated and non-irradiated H5V revealed that decreased migration of H5V cells was only significant after 24 h at higher doses of 8 and 16 Gy. Comparison of the migratory capacity of irradiated and non-irradiated H5V cells +/- SB 431542 (10μM) shows that the treated cells exhibited a slight improvement in migration after 6 and 10 h. However, this was only obvious at higher doses of radiation (8 and 16 Gy). No notable changes were observed at 24 h. Whilst it is difficult to fully explain this discrepancy in anti-migratory effects of radiation between this experiment and previous experiments, the fact that they were carried out at different times using different cultures of cells and different vials of media could provide some explanation for experimental variation. Additionally, the Mit C used here were old and it might be possible they did not have the same effective anti-proliferative effect on H5V cells. Moreover, repeating the experiment might result in significant data. The only conclusion that can be drawn from these experiments is that there is a trend of reduced migration in response to radiation (significant at high doses after 24 h), which is marginally alleviated in the presence of the ALK5 inhibitor. However, further experiments would be required in order to confirm that TGF-β signaling was involved in radiation effects on EC migration and whether the results are significant.

The same results are observed in irradiated and non-irradiated H5V migration (without treatment) for the Y 27632 as they were also added to the cells from the same experiment performed for SB 431542. However, the results from the inhibition of the Rho kinase pathway by Y27632 showed a more profound effect. Analysis of the results presented in Figure **5.20,** reveal that ROCK inhibition increased migration in Y 27632-treated H5V irradiated cells compared to irradiated non-treated cells after 6 h, and the effect was significant at high radiation doses (16 Gy). Moreover, this effect persisted upon prolonged exposure; with effects on H5V wound healing being significant at doses of 8 and 16 Gy after 10 and 24 h. No significant effects of inhibiting the Rho/ROCK pathway were observed in non-irradiated H5V cells, with and without treatment with Y27632.

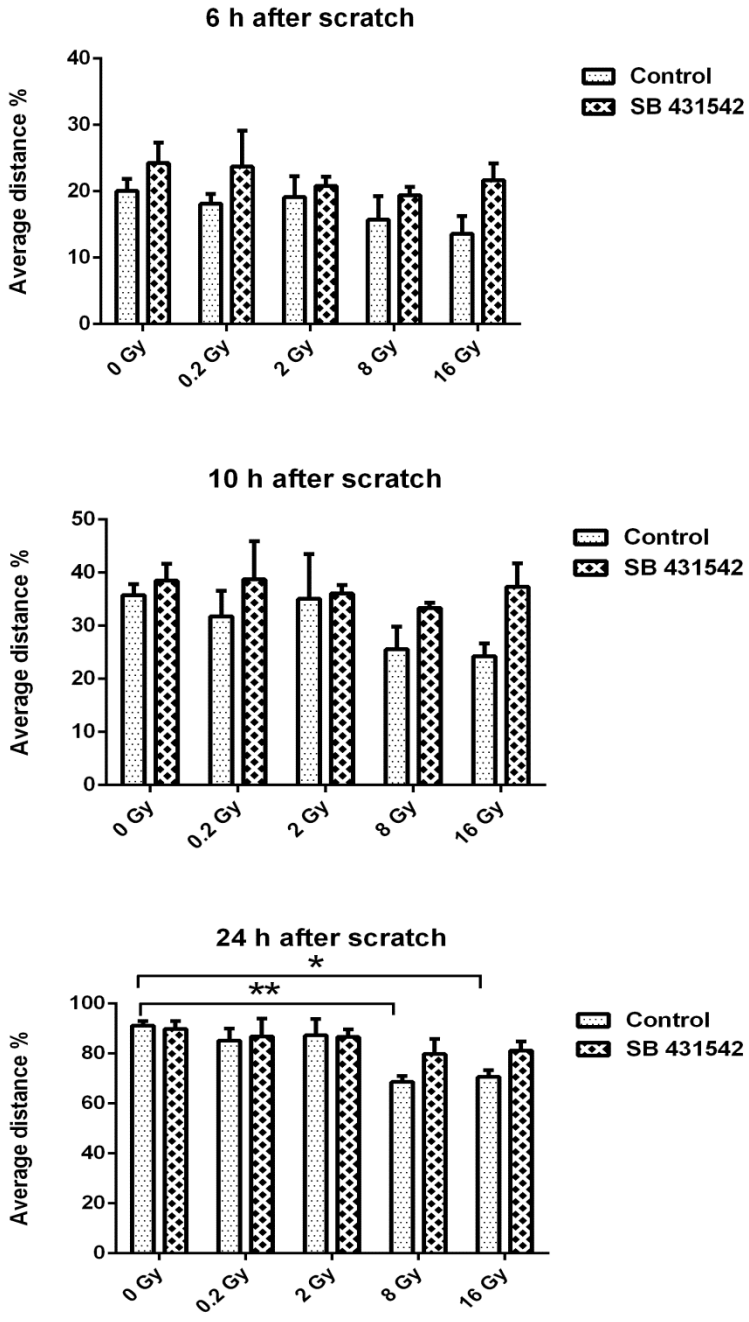

Figure 5.19 Effect of the TGF-β ALK 5 receptor inhibitor (SB 431542) on migration of irradiated and non-irradiated H5V cells. Data are expressed as the percentage of the average wound distance after 6, 10 and 24 h relative to the original wound (0 h). The effect of radiation on H5V cell wound closure was tested in the presence/absence of 10 Y 27632**.** Data from the three separate experiments were expressed as mean ± SEM and a Two-way ANOVA test was used to analyse data. Radiation only affected the H5V migration at higher doses of 8 and 16 Gy, especially after 24 h. The blocking of the TGF-β/ALK5 receptor slightly improved the H5V migration at higher doses but the effect was not significant. (*$p < 0.5$, **$p < 0.01$)

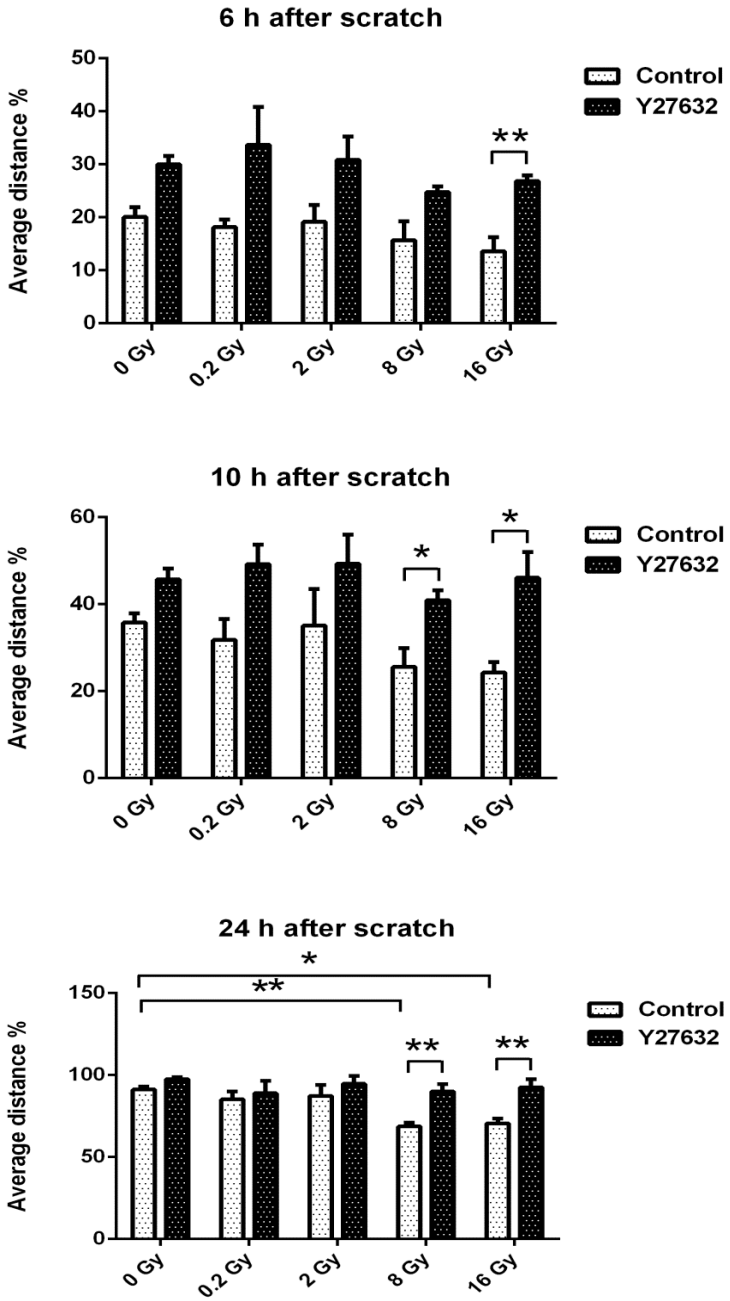

Figure 5.20 Effect of the Rho/ROCK inhibitor (Y 27632) on migration of irradiated and non-irradiated H5V cells. Data are expressed as the percentage of the average wound distance after 6, 10 and 24 h relative to the original wound (0 h). The effect of radiation on H5V cell wound closure was tested in the presence/absence of 10 μM of SB431542. Data from the three separate experiments were expressed as mean ± SEM and a Two-way ANOVA test was used to analyse data. Radiation affected H5V migration only at higher doses of 8 and 16 Gy and the effect was significant after 24 h. The inhibition of the Rho/ROCK improved migration in treated cells. The inhibitory effect of radiation on H5V migratory capacity was significantly increased at high dose of 16 Gy after 6 h and ≥ 8 and16 Gy after 10 and 24 h compared to the irradiated non-treated cells. (*$p < 0.05$, **$p < 0.01$)

The data suggest that blocking Rho/ROCK resulted in suppression of the inhibitory effect of radiation on H5V migration at high radiation doses after longer periods of time, therefore, radiation-induced effects on EC migration could be through the Rho/ROCK signaling pathway.

5.2.7.2 Effects of inhibiting Rho and TGF-β signaling in radiation effects on heart explant angiogenesis

The i*n vitro* heart angiogenesis explant experiments were also performed to study the direct involvement of ROCK and ALK5 in sprouting angiogenesis. The hearts of five SCID mice (< 20 weeks old) were used for each experiment and processed for the assay as described in the Methods (Section **4.2.1**). For these experiments only ventricular myocardial (HV) explants were used. The next day the explants were irradiated (0 (control), 0.2, 2, 8 and 16 Gy) and treated with either 3 μM SB431542 or 10 μM Y27632, for 24 h. Untreated explants were used as controls. The media was changed every second day and drugs were added fresh. After 10 days, the explants was fixed with 4% formalin and imaged. The angiogenic index was then quantified according to the extent of the explant sprouting as explained in chapters 4 and the results were analysed using a non-parametric Two-way ANOVA test. The results from three separate experiments performed are shown in **Figure 5.21**. Radiation reduced the angiogenic sprouting of the hearts dose-dependently as shown before (section **4.2.3**) and the effect was significant at high doses of 16 Gy. The inhibiting Rho/ROCK did not show any obvious effect on angiogenic sprouting in Y27632 treated irradiated explant compared to the non-treated irradiated explants. These data infer, therefore, that inhibiting ROCK has no major effect on radiation induced inhibition of heart explant sprouting.

The same heart explant technique was performed next to study the effect of the ALK5 inhibitor on radiation-induced inhibition of heart angiogenesis. While results showed there were slight increases in irradiated heart angiogenic sprouting after inhibition of ALK5, it was difficult to make any informative conclusions since the data was derived from only one experiment.

Figure 5.21 Angiogenic sprouting in irradiated SCID heart explants treated with Y27632. SCID mice hearts were dissected into ventricular myocardium (HV). Explants were embedded in fibrin gel, they were irradiated (unirradiated explants were used as control) at doses of 0.2, 2, 8 and 16 Gy, and then treated with either -/+ 10μM Y27632 after 24 h. After 10 days, the explants were fixed and the angiogenesis index measured. The results were expressed as mean ± SEM of three separate experiments. Results show that radiation inhibited formation of angiogenic sprouting dose dependently which was unaffected by inhibiting ROCK. (*$p \leq 0.05$)

5.3 Discussion

It has been observed in chapter 3 that radiation affected ECs directly and suppressed the angiogenic properties of ECs. However, the results presented in previous chapters did not exclude the possibility that radiation has effects on cells other than ECs that present in the tissue and vascular wall, including fibroblasts, could have contributed to the observed effects on ECs. These cells could be involved in EC angiogenic responses following radiation through bystander/paracrine effects. A bystander effect following radiation could possibly be secondary to EC damage, which influences the angiogenesis process. The putative mechanisms of anti-angiogenic effects of radiation need to be better understood.

5.3.1 Bystander effect of irradiated fibroblasts on EC angiogenesis

Some studies have been performed to study the bystander effects of irradiated ECs on other cells. In one study the interaction between endothelial cells and vascular smooth muscle cells (VSMCs) was investigated and it was shown that irradiated ECs could induce a fibrogenic phenotype in VSMCs by increasing the CTGF expression in these cells, as well as collagen deposition (Milliat *et al.*, 2006). It has been found that when irradiated ECs (15 Gy) were cultured with proliferating human intestinal epithelial T84 cells they imposed bystander effects, resulting in reduced proliferation and increased apoptosis in T84 cells (Gaugler *et al.*, 2007). However, to the best of our knowledge the effects of irradiated fibroblasts on EC angiogenesis and their bystander effect(s) following radiation have not been studied yet.

This study reveals for the first time that irradiation of fibroblasts can affect EC angiogenic properties. The results from several separate experiments here shown that irradiation of HDFs inhibited the morphogenesis of HUVECs *in vitro* in HUVECs-HDF bed assays. The number and quality of capillary-like tubes (length and junctions) formed by HUVECs was significantly reduced and these effects were dose-dependent. Further experiments proved that irradiated HDFs influenced HUVECs migration and morphogenesis via soluble secreted factors. The addition of CM obtained from irradiated fibroblasts to migrating HUVECs, as well as in HUVECs-HDF bed assays resulted in persistent inhibition of HUVEC migration and thread-

like networks formation. Therefore, the CM from irradiated fibroblasts contains some soluble factor(s) secreted by fibroblasts that mediate bystander effects on EC migration/morphogenesis. When the same experiments were performed using H5V cells, CM from irradiated HDFs only affected H5V migration after 6 and 10 h. H5V cells have higher proliferative activity than primary HUVECs, thus H5V cells could still be proliferating and contributing to wound closure measured at 24 h.

5.3.2 Effect of TGF-β signaling on irradiated fibroblast-induced EC angiogenic changes

TGF-β is released following radiation damage and mediates tissue injury and fibrosis. TGF-β is produced from both damaged normal tissues, as well as released as circulating TGF-β by tumours following irradiation (Dancea *et al.*, 2009; Imaizumi *et al.*, 2010; Randall and Coggle, 1995). TGF-β/ALK5 signaling has been linked with the inhibition of EC migration and capillary-like formation. The Imaizumi *et al* study showed that there was increased expression of TGF-β by HUVECs in response to radiation. Inhibition of TGF-β signaling through the ALK5 pathway restored EC migration and formation of sprouts but did not rescue the proliferation impairment by radiation. Moreover, the inhibition of the ALK5 pathway in response to radiation resulted in restored angiogenesis *in vivo*. The data suggest a dominant role of the TGF-β/ALK5 pathway in the suppression of angiogenesis following radiation (Imaizumi *et al.*, 2010).

The data presented in this chapter showed that TGF-β/ALK5 activation could contribute to impaired EC angiogenesis. The culture of HUVECs on top of a bed of irradiated fibroblasts caused a reduction in EC capillary formation compared to the control group while treatment of co-cultures with an ALK5 receptor inhibitor reversed the effect of radiation, significantly improving the number and quality of sprouts formed by irradiated groups. Therefore, these data suggest that irradiated fibroblasts could activate the TGF-β signaling through the ALK5 pathway resulting in EC anti-angiogenic functions. The activation of the TGF-β/ALK5 pathway could occur as a consequence of increased TGF-β protein concentration secreted into the media by irradiated fibroblasts, or as a result of a yet unknown mechanism(s). However,

the initial Western blot analysis of CM from irradiated HDFs, as well as extracts from irradiated HDFs, did not show any up-regulation of TGF-β protein. Detecting signaling proteins in CM is difficult and requires concentrating the medium sufficiently to detect low abundance proteins. Future experiments could involve optimising the concentration of CM. Alternatively, there might not be any up-regulation of TGF-β protein itself, but rather there is an increased activation of the TGF-β/ALK5 pathway through unknown mechanisms.

The Imaizumi *et al* study showed that radiation (15 Gy) inhibited the migratory capacity of HUVECs after 10 h while SB 431542 treatment prevented this inhibitory effect (Imaizumi *et al.,* 2010). Here the direct involvement of TGF-β signaling in EC migration after exposure to radiation doses of between 0.2-16 Gy was studied using H5V cells. However radiation had only a small effect on H5V migration, making any effect of blocking ALK5 receptor signaling difficult to assess. Nonetheless, the addition of SB 431542 showed a trend in increased migration activity of H5V cells, which was more obvious at the higher doses of 8 and 16 Gy. More experiments would help to determine whether the results are significant. In the previous chapter (**3.2.5.1.2)**, it was shown that radiation had a significant effect on H5V migration; however, in the experiments performed in this chapter, there were only small changes in H5V migration after exposure to either radiation or CM from irradiated HDFs. This was somewhat unexpected and it is difficult to make any conclusion about these discrepancies in anti-migratory effects of radiation between these and previous experiments. However, it should be noted that different stocks of H5V cells were used between the sets of experiments and the fact that the experiment were performed at a different time could mean that subtle differences in culture conditions may have been responsible for this.

5.3.3 Effect of Rho signaling on irradiated fibroblast-induced EC angiogenic changes

It has been shown that RhoA/Rho kinase signaling is activated following radiation (Gabrys *et al.*, 2007; Zohrabian *et al.*, 2009), resulting in cytoskeleton and permeability changes in ECs after radiation exposure (Gabrys *et al.*, 2007; Zohrabian *et al.*, 2009). Radiation could activate the Rho/Rock pathway and therefore play an important part in the development of TGF-β-

induced vascular damage and fibrosis (Shimokawa and Takeshita, 2005). Moreover, The Monceau *et al* study showed for the first time that radiation induced activation of Rho/ROCK and Smad signaling in human cardiomyocytes, as well as mouse heart and lungs, persisted 15-30 weeks post irradiation and correlated with late radiation-induced pulmonary and vascular diseases (Monceau *et al.*, 2010). Therefore, Rho/ROCK activation upon radiation exposure could contribute to radiation-induced EC migration/morphogenesis effects.

The experiments performed in this chapter showed that inhibiting Rho signaling improved the quality and number of capillaries formed by HUVECs when they were plated on a bed of HDFs and then exposed to CM from irradiated HDFs. This suggests, therefore, that the Rho/RhoA pathway play a role in maintaining the anti-angiogenic activity of ECs following radiation. The irradiated fibroblasts bystander effect on HUVECs angiogenic function resulted in impaired migration while the treatment with the Rho inhibitor restored the migratory capacity of cells. However, the results were not consistent across the different experiments conducted in this study. One explanation may be that the Y 27632 compounds used in some experiments was inactive since Y 27632 from old stock was used. Therefore, more experiments with new products should be performed in order to obtain consistent and reliable results.

The direct inhibition of Rho signaling pathway improved H5V migration, suppressing the anti-angiogenic function of radiation and increasing the wound healing process *in vitro*. The effects were significant at the higher doses of 8 and 16 Gy, which was consistent even after 24 h.

5.3.4 Proteome profiling of Irradiated fibroblast conditioned media

TGF-β protein is produced as an inactive protein called latent TGF-β (Annes *et al.,* 2003; Ruiz-Ortega *et al.,* 2007). The matrix metalloproteinase (MMP2-9), Thrombospondin, plasmin and β6 integrin are capable of activating the latent TGF-β complex by proteolytic cleavage (Ruiz-Ortega *et al.*, 2007). Thrombospondin1 (TSP-1) is a multi-functional protein expressed by cells including fibroblasts and ECs, which participates in the wound healing process,

stimulating cell adhesion and migration, as well as the expression of collagen and ECM. TSP-1 has been identified as one of the latent TGF-β activator proteins (Annes *et al.*, 2003; Crawford *et al.,* 1998). It also facilitates the cell-to-cell and cell-to-matrix interaction during angiogenesis (Annes *et al.*, 2003; Sabapathy *et al.*, 1997; Sweetwyne and Murphy-Ullrich, 2012). The protein array experiment described here showed that there was an increase in production of TSP-1 in CM from irradiated fibroblasts (HDFs). Therefore, it could increase the activation of TGF-β from the latent form. Additionally, there were elevated levels of Serpin E1 (PAI-1) in the CM from irradiated HDFs (TGF-β target gene). PAI-1 plays important roles in the production of ECM and, vascular remodelling, as well as modulating EC and fibroblast migration, proliferation and apoptosis. It is used as a biomarker of CVD-associated mortality. PAI-1 is a potent causative factor in tissue fibrosis and PAI-1 is one of the most expressed subsets of TGF-β induced transcripts. Rho/ROCK signaling, as well as TGF-β, directly induces PAI-1 expression in fibroblasts and VSMCs (Samarakoon and Higgins, 2008).

5.3.5 Summary of results

From the experiments using Rho/ROCK and TGF-βALK5 receptor inhibitors performed, it appeared that the inhibition of ALK5 receptors and inhibiting Rho/ROCK signaling played a negative role in the angiogenic activity of ECs following radiation. The results of this chapter demonstrate the bystander effects of irradiated fibroblasts on EC angiogenesis and suggest that the TGF-β and Rho/ROCK signaling pathways could be involved in mediating some of these effects. A greater understanding of EC/fibroblast interactions may offer, therefore, novel therapeutic options for restoring the anti-angiogenic effects of radiation, especially at low doses.

Chapter Six

Discussion

6.1 Mechanism of radiation-induced late heart diseases in CARDIORISK project

Many cancer survivors (about 70%) have received radiotherapy during their treatment (Monceau *et al.*, 2010; Wang *et al.*, 2007). According to the different epidemiological studies, about half of (100 million) cancer survivors who received radiotherapy during their treatment showed increased treatment-related side effects, most importantly cardiovascular diseases (CVD) and secondary cancers (Russell *et al.*, 2009; Stewart *et al.*, 2006; Wang *et al.*, 2007;).

Radiation-induced heart disease was found to be the common cause of death for those patients receiving thoracic radiotherapy (Abbas *et al.*, 1990; Andratschke *et al.*, 2011; Fajardo and Stewart, 1970; Hoving *et al.*, 2011; Stewart *et al.*, 2006). Long-term follow up of radiation-exposed patients in Hodgkin's disease, breast cancer patients, as well as head and neck cancer revealed incidences of ischemic stroke, atherosclerosis, myocardial infarction and coronary artery diseases (Miltenyi *et al.*, 2004; Russell *et al.*, 2009; Stewart *et al.*, 2006). Additionally, exposure to low dose radiation increases the risk of non-cancer diseases, including heart disease, many years after exposure (>10 years) (Hildebrandt, 2010). Similar evidence comes from Japanese's atomic-bomb survivors, (who received between 0.5-5 Gy whole body doses) (Andratschke *et al.*, 2011). The heart whole organ radiation tolerance dose has been estimated as approximately 40Gy (Andratschke *et al.*, 2011). In comparison, the heart receives approximately 1-2 Gy, when breast cancer patients are treated with 40-50 Gy in 2 Gy fractions (Andratschke *et al.*, 2011; Hendry *et al.*, 2008; Schultz-Hector, 1993).

Different studies on pathogenesis of radiation-induced CVD revealed that damage to both large and small vessels are important (Fajardo and Berthrong, 1988; Stewart *et al.*, 1995). Animal studies have shown that radiation induces macrovascular injury by accelerated development of age-related atherosclerosis in large vessels (Hoving *et al.*, 2008; Stewart *et al.*, 2006). For microvascular injury, radiation-induced damage to endothelial cells is a major factor (Stewart *et al.*, 1995; Wang *et al.*, 2007). EC damage leads to a decrease in capillary density, which is followed by progressive ischemia. The lack of oxygen and nutrient supply

eventually results in myocardial degeneration, which plays an important role in developing cardiac death and heart disease (Fajardo, 1989; Lauk, 1987; Stewart *et al.*, 1995). Increased awareness of radiation-induced heart disease followed from an international Congress of Therapeutic Radiology and Oncology meeting held in 2005 in Germany in 2005 (Andratschke *et al.*, 2011). However, to date, no accurate dose threshold for heart disease has been defined by the International Commission on Radiological Protection (ICRP) (Hendry *et al.*, 2008, ICRP, 2007).

The aim of the current CARDIORISK project (European framework 7 project consisting of 11 European participants) was to investigate the mechanism of radiation damage to the heart at low, medium and high doses, using C57BL/6 and ApoE$^{-/-}$ mice, at the cellular and molecular levels. Hearts were irradiated *in vitro* at X-ray dose ranging from 0.2 to 16 Gy. The project emphasis was on functional and pathological damage by local irradiation in the mouse heart, identifying early and late changes in mouse microcirculation, inflammatory, thrombotic and fibrotic factors. Additionally, the aim was to study any changes in EC properties including; permeability, cytoskeleton, migration, angiogenesis, pro-inflammatory and pro-thrombotic functions (Andratschke *et al.*, 2011; Hildebrandt, 2010). As the radiation-induced CVD showed late manifestation, the effects of radiation on mice hearts were followed up to 60 weeks (at 20, 40 and 60 weeks). It was important to investigate whether the early effects of radiation on cardiac (cell/tissue) functions were restored by compensatory mechanisms or whether effects persisted and led to manifestation of heart diseases later (Andratschke *et al.*, 2011; Hildebrandt, 2010). Different CARDIORISK *in vitro* and *in vivo* experimental studies were performed which have been summarised below.

In Gabriel *et al* (2010) an increased number of atherosclerotic lesions, as well as necrotic cores of coronary plaques (indicative of more advanced phenotype), were found in hypercholesterolemia ApoE$^{-/-}$ mice at 20 and 40 weeks radiation (8-16 Gy), which was in agreement with previous studies (Hoving *et al.*, 2008; Hu *et al.*, 2005; Stewart *et al.*, 2006). In the Seemann *et al* study (2012), the radiation damage to the microvasculature of C57BL/6

mice was evaluated at 20, 40 and 60 weeks. Data revealed that microvascular density reduced in a dose-dependent manner in irradiated hearts. The effect was found to be more significant at intermediate and higher doses, which occurred at early time points and progressed with time. Additionally, cardiac blood volume decreased in irradiated animals after 60 weeks (2-16 Gy). Gabriel *et al* observed a similar effect on the microvessels of ApoE$^{-/-}$ mice and showed that there was a persistent reduction in capillaries up to 60 weeks (Gabriels *et al.*, 2012). Despite these effects (especially at higher doses), cardiac function was maintained, only showing modest and non-progressive changes, indicating the likelihood of compensatory changes (Seemann *et al.*, 2012).

Data from studies on inflammatory changes showed a presence of iron-containing macrophages (a sign of vascular damage and indicative of haemorrhage) and CD45-positive inflammatory cells within the myocardium of irradiated animals (8 and 16 Gy) after 20 and 40 weeks (Gabriels *et al.*, 2012; Seemann *et al.*, 2012). In the Gabriels *et al* (2012) study there was a persistent increase in the amount of interstitial collagen, especially at higher doses (8-16 Gy) at different time points. This could contribute to the reduced myocardial contractility after radiation and lead to the later fibrotic injury (Seemann *et al.*, 2012). Analysis of pro-inflammatory responses in ECs showed an increase in VCAM-1 expression in irradiated hearts (Gabriels *et al.*, 2012; Seemann *et al.*, 2012). The Hoving *et al* (2012) study on irradiated large vessels suggested that large vessel response to irradiating is different from that in the small vessels (Hoving *et al.,* 2012). The level of thrombomodulin and tissue factor increased in 14 Gy irradiated ApoE$^{-/-}$ mice after 4 weeks, while it was decreased in C57BL/6 mice hearts. There was a decreased level of ICAM-1 expression in both mice hearts at 1 week after exposure to a radiation dose of 14 Gy. The results from the Hoving *et al* study revealed that there was a reduction in expression of inflammatory responses (ICAM-1) in carotid arteries (Hoving *et al.*, 2012). An increase in vWF deposition is indicative of thrombotic EC injury, which could result in vascular permeability and contribute to the lipid accumulation, eventually leading to atherosclerosis (Gabriels *et al.*, 2012). An elevated level of vWF in both

mice strains was observed at 20-60 weeks radiation, which was significant at high radiation dose (16 Gy) (Gabriels *et al.*, 2012; Seemann *et al.*, 2012).

To determine radiation damage on microvascular function, the alkaline phosphate (ALP) marker of cardiac EC (CEC) activity was quantified and shown to be significantly reduced in irradiated animal hearts (2-16 Gy). This led to vascular leakage, which developed in a time and dose-dependent manner (Seemann *et al.*, 2012). Radiation-induced changes in the cytoplasmic proteome of EA.hy 926 cells, performed at low doses (0.2 and 0.02 Gy) revealed that there was an up-regulation of the Rho/ROCK pathways, as well as changes in energy metabolism and stress responses after 24 h (Pluder *et al.*, 2011).

The biological responses of ECs to low and high dose radiation could be different. A microarray and pathway analysis of cardiac genes showed that 16 Gy irradiation resulted in up-regulation of inflammatory responses and fibrotic responses (e.g. CTGF, fibronectin 1 and endothelin) at 40 weeks. In contrast, radiation at 2 Gy triggered survival responses by regulating the cellular growth and proliferation pathway. The MMP2 and heat shock proteins (Hsp) levels increased in 2 Gy irradiated heart at 40 weeks (Gabriels *et al.*, 2012).

6.2 The contribution of results from this study to the CARDIORISK project

After tissue injury, angiogenesis is stimulated to maintain vascularisation. Radiation suppresses angiogenesis (Grabham and Sharma, 2013) and so the current study was designed to determine the capacity of CEC to undergo repair and angiogenesis after radiation exposure (an aim within CARDIORISK).

The results from the heart angiogenesis explant assay using locally irradiated mouse heart from two strains of mice revealed that heart angiogenic sprouting in the atrial and ventricular myocardium of mice hearts from both strains was inhibited in a dose-response manner. The effect was significant at higher doses, after 20 weeks post-irradiation. The inhibitory effect was persistent at 60 weeks after irradiation and significant effects in the angiogenic index were found at doses as low as 2 Gy. A “novel” fibroblast-endothelial self-assembling angiogenesis

assay was also developed in our lab to study the morphogenesis capacity of ECs after radiation exposure at different doses and time points. The results obtained were in agreement with the heart explant study and showed that there was a dose–dependent decrease in formation of capillary-like structures by CECs at 20 weeks post-irradiation, which was more profound at high doses (8 and 16 Gy). The radiation-inhibited EC morphogenesis was persistent even at 60 weeks post-radiation. The results from the experiment still need to be quantified, which could reveal possible inhibitory effects at lower doses (0.2-2 Gy). The results from the *in vitro* irradiation of cells in the self-assembly assay at day 4-5 (when CECs started forming channels) also confirmed a reduction in CEC capillary-like networks formation after 10 days co-culture of cells. Additionally, the *in vitro* radiation of H5V cells (mouse cardiac endothelial cell line) showed that radiation inhibited EC angiogenic functions. H5V proliferation reduced significantly after 48 and 72 h at doses of ≥ 2 Gy. Moreover, radiation inhibited H5V migration, which was significant even at the low dose of 0.2 Gy. However, the migratory capacity of cells was restored after 24 h in H5V cells irradiated at lower doses.

The data from the locally irradiated mouse heart experiments revealed that radiation suppressed angiogenesis, which resulted in persistent vascular damage (up to 60 weeks, which correlates with radiation-induced late CVD) in the mouse heart in a dose-response manner. While the pervious experiments showed radiation-induced inhibition of EC angiogenesis at higher doses (Ahmad *et al.*, 2007; Grabham and Sharma, 2013; Imaizumi *et al.*, 2010; Rousseau *et al.*, 2011), the data from this project confirmed suppression of EC angiogenic functions at lower radiation doses as well (0.2-2 Gy). The Girdhani *et al* (2012) study using microarray analysis and RT-PCR confirmed that some pro-angiogenic factors, including VEGF, IL-8 and hypoxia-inducible factor-1 alpha (HIF-1α), were down-regulated significantly in ECs and fibroblasts after radiation exposure at doses of 0.5-2 Gy (Girdhani *et al.*, 2012). The data suggest that impaired angiogenesis by radiation, especially at low doses, could be one potential mechanism that contributes to the late cardiac injury.

Further studies investigated the bystander effect, i.e. on non-irradiated cells and how it possibly affects EC angiogenesis, especially at lower doses. Data revealed that irradiation of fibroblasts (0.2-16 Gy) is influenced EC angiogenic functions (morphogenesis/migration), which was significant even at low radiation doses (0.2-2 Gy). The formation of capillary-like networks by HUVECs was affected significantly when these cells were cultured with either irradiated fibroblasts (≥ 0.2 Gy) or a conditioned medium (CM) from irradiated fibroblasts (≥ 2 Gy). The data together suggested that radiation suppressed EC angiogenesis even after exposure to low doses through:

1) Direct effect on ECs angiogenic function
2) Intracellular signal transduction between the target (irradiated fibroblasts) and bystander cells (direct cell-to-cell signaling)
3) Modulation of paracrine signals from targeted cells (fibroblast)

More experiments need to be performed in order to test the long-term effects of irradiated fibroblasts on EC angiogenesis, as well as investigating the effects of irradiated ECs on their neighbouring cells.

While radiation induced the expression of p53 and p21, especially at higher doses (playing roles in apoptosis and cell cycle arrest), the absence of p53 and p21 did not influence the inhibitory effects of radiation on EC proliferation and formation of sprouts. Therefore, the apoptosis response following radiation could be excluded as an important mediator of radiation-associated angiogenesis impairment (Imaizumi *et al.*, 2010). Other signaling pathways clearly contribute to the radiation-induced EC angiogenic defect. It has been revealed by different studies that radiation induces the expression of TGF-β *in vivo* in mouse skin, mammary gland and heart as well as *in vitro* in ECs, such as HUVECs (Barcellos-Hoff, 1993; Imaizumi *et al.*, 2010; Martin *et al.*, 1997; Randall and Coggle, 1995). The Imaizumi *et al* study (2010) showed that the radiation effect on EC angiogenic functions resulted from the activation of TGF-β signaling though the ALK5 receptor, which subsequently activates the

Smad2/3. The inhibition of the TGF-β/ALK5 pathway rescued the inhibitory effects of radiation on EC migration and sprouts formation *in vitro* and *in vivo* experiments (Imaizumi *et al.,* 2010). In the current project, results from the bystander/paracrine effects of irradiated fibroblasts on HUVEC angiogenic functions showed that blocking of the TGF-β ALK5 receptor increased channel formation even at low doses (0.2 and 2 Gy) after 14 days, indicating that this pathway is involved in the paracrine effects observed here. The ALK5 receptor inhibition also improved the EC migration when directly irradiated or exposed to the conditioned media from irradiated fibroblasts.

RhoA/Rho kinase signaling was found to be activated following irradiation (Gabrys *et al.*, 2007; Rousseau *et al.*, 2011; Zohrabian *et al.*, 2009). The activation of Rho kinase has been shown to lead to cytoskeleton (formation of stress fibres) and permeability changes after radiation exposure at doses of 10 and 20 Gy in microvascular ECs (Gabrys *et al.*, 2007; Rousseau *et al.*, 2011). Although a certain level of active RhoA/ROCK is required for migration, inhibition of this pathway suppressed the inhibitory effect of radiation on EC migration suggesting that ROCK activated by radiation inhibits migration (Rousseau *et al.*, 2011). The results in the current project showed that ROCK inhibition induced wound healing improvement in directly irradiated EC, which was significant at higher doses, and therefore is in agreement with the Rousseau *et al* study (20011). This project showed that blocking ROCK also improved the inhibitory bystander/paracrine effects of irradiated fibroblasts on EC morphogenic/migration properties.

The alteration of TGF-β and Rho pathways by radiation, have been reported to induce the fibrogenic phenotype in ECs and fibroblasts (Anscher *et al.*, 1995; Bourgier *et al.*, 2005; Dancea *et al.*, 2009; Martin *et al.*, 2000). TGF-β and Rho/ROCK pathways are involved in radiation-induced fibrosis by influencing CTGF and PAI-1 production (Bourgier *et al.*, 2005). CTGF and PAI-1 are downstream mediators of TGF-β-stimulated fibrosis and key regulators of angiogenesis. These proteins are also associated with TGF-β mediated increased ECM and

collagen production, as well as late normal tissue injury and fibrosis following radiation (Dancea *et al.*, 2009; Martin *et al.*, 2000; Ruiz-Ortega *et al.*, 2007).

Together, data presented in this thesis suggest that radiation effects on fibroblasts could in turn influence endothelial functions (through bystander/paracrine effects) associated with angiogenesis through activation of TGF-β/ALK5 and Rho/ROCK pathways (Figure **6.1**). Rho/ROCK could mediate radiation-induced anti-angiogenic effects on ECs directly or through the TGF-Smad 2/3 pathway activation. It has been reported that TGF-β induced PAI-1 and CTGF expression requires Rho/ROCK-mediated Smad2/3 activation (Bhowmick *et al.*, 2001; Bakin *et al.*, 2002; Derynck and Zhang, 2003; Samarakoon and Higgins, 2008). More experiments are required to confirm the involvement of Rho/ROCK and TGF-β in radiation-induced angiogenesis impairment, especially at lower doses.

Radiation induces delayed cardiac toxicity, which could result from sustained production of cytokines/growth factors. Radiation protection aims to develop treatment regimes while reducing radiation-induced side effects. The potential therapeutic targets should be able to reverse the damaging effect of radiation in normal tissue while maintaining the anti-tumour activity of radiation (Monceau *et al.*, 2010). The data from this study supports the results of other studies (summarised below), which show that inhibition of Rho/ROCK and TGF-β could reverse some of the effects of radiation. Therefore, targeting the Rho/ROCK and TGF-β pathways could have curative anti-angiogenic/fibrotic activities. The Rho/ROCK and TGF-β inhibitors could be used alongside radiotherapy to reduce delayed tissue toxicity as radiation modifies (even at low doses).

The Monceau *et al* study (2010) showed for the first time that radiation (16-19 Gy) induced activation of Rho/ROCK and TGF-β/Smad 2/3 signaling in human cardiomyocytes, as well as mouse heart and lung. Activation of these pathways was persistent after 15 and 30 weeks post-irradiation (whole thorax radiation), which correlates with late radiation-induced pulmonary and vascular diseases. They showed that the inhibition of Rho/ROCK using statin and Y-

27632 attenuated the cardiac and pulmonary radiation injury and inhibited the expression of fibrogenic markers. Other studies showed that the use of pharmacological inhibitors of the Rho/ROCK cascade (pravastatin) could reverse the effects of radiation and reduce the radiation-induced fibrosis, inflammation and cytoskeletal changes (Bourgier *et al.*, 2005; Gaugler *et al.*, 2007; Haydont *et al.*, 2008). Rho inhibition did not interfere with anti-cancer treatment, thus the inhibition of Rho/ROCK could be a safe and efficient potential therapeutic target for treatment of late radiation damage to the main thoracic organs (Monceau *et al.,* 2010). It could be applied before or after radiotherapy or in other cases where people had experienced radiation accidents (Monceau *et al.,* 2010). Interestingly, the TFG-β receptor inhibitor Ly2109761 I enhanced radiosensitivity of tumour cells and suppressed Smad2 phosphorylation (Zhang *et al.*, 2011). However, TGF-β has pleiotropic activities, and its inhibition could impair the wound healing processes, collagen synthesis, as well as angiogenesis in mice (Ruiz-Ortega *et al.*, 2007). Therefore, more specific target genes of TGF-β, such as CTGF and PAI-1, may be more appropriate targets for modulating the anti-angiogenic effects of radiation effectiveness on normal tissue without affecting the radiation effectiveness on tumour cells.

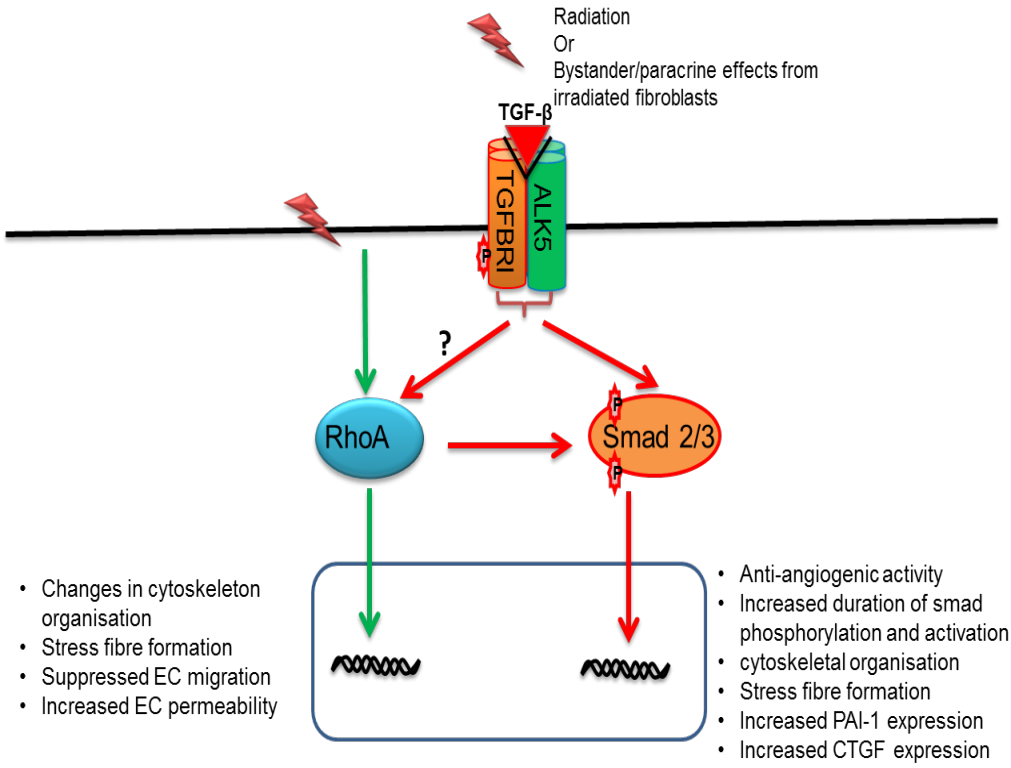

Figure 6.1 Possible mechanisms underlying radiation effects on EC angiogenesis. Radiation affects EC angiogenic properties directly or through bystander/paracrine effects by target cells (fibroblasts). Radiation could induce the anti-angiogenic effects in ECs through TGF-β/ALK5 and Rho/ROCK pathways. The activated pathways subsequently result in suppression of angiogenesis, as well as increased expression of fibrotic markers (PAI-1 and CTGF). TGF-β could induce cytoskeletal changes, increased PAI-1 and CTGF expression through Rho/ROCK-mediated Smad2/3 activation.

6.3 Conclusions, project limitations and future work

It is important to identify how different radiation doses (both low and high doses) are associated with heart disease development. It will be important to establish which part of the heart is most susceptible and sensitive to radiation (Andratschke *et al.*, 2011; Hildebrandt, 2010). The results from various *in vitro* and *in vivo* experimental studies performed in CARDRISK showed that there were early and late macrovascular and microvascular effects after exposure to high doses of radiation. The reduction in microvascular density was significant at lower doses (2 Gy). There were some changes in pro-inflammatory and pro-thrombotic activity of ECs, as well as structural changes within the microvascular networks in the heart. The results of this project correlate with these studies and show that these structural changes are also associated with changes in endothelial function. The decreased microvessel density and inhibition of angiogenesis at lower doses together could compromise the capacity of the heart to regenerate and recover from radiation damage. Together with other CARDIORISK studies the results of this project could contribute to understanding the nature of radiation-induced heart toxicity at low, moderate and high doses. Based on the results of the CARDIORSIK project, further studies could be designed in order to investigate the mechanisms and size of heart radiation risk at different doses and to develop a program for the protection of the heart from radiation risk. The findings from this project could further help to identify a drug or biological molecules that could modify the slow progression of cardiac damage in the heart after radiation exposure (Andratschke *et al.*, 2011; Hildebrandt, 2010).

There is a biological gap between experimental studies performed on animals compared to the clinical problems in humans (Andratschke *et al.*, 2011). In the experiments performed in this project, single doses of radiation were used. However, in clinical radiotherapy, fractionated low doses of between 1.5-2 Gy are delivered to patients. Therefore, to consider the clinical relevance of radiation-induced effects, fractionated low doses of radiation on EC angiogenic properties need to be studied (Brown and Koong, 2008; Imaizumi *et al.*, 2010). To fully address the radiation effect on EC angiogenic properties, further *in vivo* experiments could be

performed to investigate the possible mechanisms. Additionally, to test the radiation effect, it is best to use isolated CECs from irradiated and non-irradiated mouse hearts. The Jelonek *et al* study for the first time showed that isolation of the CECs from irradiated and non-irradiated mice up to 10 months of age was possible, although yields were very low (Jelonek *et al.*, 2011).

Based on the results obtained from this study it is concluded that the TGF-β and Rho/ROCK pathways play a role/roles in the inhibitory effects of radiation on EC angiogenesis. In the future, more experiments could be designed to fully understand the involvement of the TGF-β and Rho/ROCK pathways in these inhibitory effects and the role played by fibroblasts. The TGF-β, Smad2/3 and Rho/ROCK phosphorylation/activation in irradiated fibroblasts and normal ECs when co-cultured with either irradiated fibroblast or CM from irradiated fibroblasts should be investigated. Additionally, the involvement of Rho/ROCK in induction of TGF-β signaling following radiation exposure, could be tested by measuring the level of TGF-β (in cell lysates and CM) in the presence of a Rho/ROCK inhibitor. The nature of factors produced by irradiated fibroblasts that influence EC function need to be established. Effects of irradiation on MMP2-9, thrombospondin, integrins or Ang II may affect the activation of TGF-β from its latent form (Ruiz-Ortega *et al.*, 2007) and could contribute to the effects of irradiated fibroblasts on ECs described in this thesis. Therefore, the level of these factors would be investigated in future studies in order to establish whether they are altered in fibroblasts by radiation. To examine whether irradiated fibroblasts influence EC angiogenesis through fibrotic pathways, the expression of CTGF and PAI-1may be examined. Moreover, to study whether Rho and TGF-β activation result in the expression of these fibrotic markers, the level of their protein/gene expression could be investigated in the presence of TGF-β and Rho inhibitors.

Appendices

Appendix I: Media and Solutions

(Chapter 2)

DPBS 500ml: Dulbecco's Phosphate buffered saline (Lonza, Cat.no. BG17-512F)

HBSS 500ml: Hank's Balanced salt solution (Lonza)

Endothelial Cell Basal medium 500ml supplemented with growth factors according to the manufactures instructions (Promo Cell, Cat.no. C-22210)

DMEM: Dulbecco's Modified Eagle's Medium (Lonza, Cat.no. BE12-741F)

10% FCS-DMEM: DMEM supplemented with 10% FCS, 2mM L-glutamine, 100u/ml penicillin and 100µg/ml Streptomycin

20% FCS-DMEM: DMEM supplemented with 20% FCS, 2mM L-glutamine, 100µg/ml penicillin, 100µg/ml Streptomycin, 2mM Sodium Pyruvate, 20mM Hepes, 1% Non-Essential Amino Acid (NEAA)

Complete 20% FCS-DMEM: 25 ml 20% FCS-DMEM supplemented with 1U/ml Heparin and 0.5 µg/ml endothelial cell growth supplemet (ECGS) (Sigma, Cat.no.E2759)

EBM-2: Endothelial cell Basal Medium-2 500ml supplemented (Lonza, Cat.no. CC-4147)

Complete EBM-2: Endothelial cell Basal Medium-2 500ml supplemented with 10% FCS and growth factors (FCS, hFGF-B, rEGF, hEGF,R3-1Gf-1, hydrocortic and Ascorbic acid) according to the manufactures instructions (Lonza, Cat.no. CC-4147)

FGM: Fibroblast basal Medium 500ml supplemented with growth factors (FCS, rhFGF-B, Nsolin and GA-1000) according to manufacture's instructions (Lonza, Cat.no. CC-4126)

Enzymatic digestion solution: 20mg/ml Collagenase A dissolved in 20 ml HBSS with 10% FCS and then filter sterilised

TBS: Tris buffered saline 100mM: 12.1g Trizma and 5.84g NaCl are dissolved in 600ml H_2O and adjusted to pH 7.4 with HCl and made up to 1l with pure water

TBST: 100ml of TBS diluted in 900ml pure water plus 1ml Tween 20

PBS: 1 tablet of PBS dissolved in 200ml pure water

Appendix II: Antibodies, Serum and kits

(Chapter 2)

Phospho-histone H2A.X (Abcam, Cat.no. cb6992)

Phospho-histone rabbit H2A.X (Cell Signaling, Cat.no. 9718)

Rabbit polyclonal to Von Willebrand factor (Abcam, Cat.no. ab6994-100)

Monoclonal Anti-Actin α-smooth muscle (Sigma, Cat.no. A5228-200UL)

Anti-Beta III Tubulin (Abam, Cat.no. ab52901)

Monoclonal Anti TGF-β (Abcam, Cat.no ab66043)

Phospho-Smad (Cell Signaling, Cat.no. 9520)

Smad 2/3 (Cell Signaling, Cat.no. 5678)

SB 431542 (Tocris bioscience, Cat.no: 1614)

TGF-β antibody (R&D System, Cat.no. AB-100-NA).

α- Thrombin 100u/ml (Sigma, Cat.no. T9549)

ECGS (100 μg/ml): Endithelial Growth Supplement (BD Biosience, Cat.no. 356006)

Fibrinogen (Sigma, Cat.no. F8630)

Collagenase A (Roche, Cat.no. 70214222)

BD Matrigel Basment Membrane (BD Biosience)

Trypsin/EDTA 100ml (Lonza, Cat.no. BE17-161E)

Gelatin (Sigma, Cat.no. G1343)

Normal Rabbit Serum (Vector labs, Cat.no. 5-5000)

Normal Horse Serum (Vector labs, Cat.no. 5-2000)

Normal Goat Serum (Vector labs, Cat.no. 5-1000)

Fluorescein Avidin D (Vector labs, Cat.no. A-2001)

Vectashield with DAPI (Vector labs, Cat.no. H-1200)

Texas red-X phalloidin (Molecular probes, Cat.no. H-1300)

Dynabeads Sheep anti-rat immunoglubolin IgG magnetic beads (Invitrogen, Cat.no. 110.35)

Purified Rat Anti-mouse CD31 (PECAM-1) monoclonal Antibody (BD Pharminogem, Cat.no. 557355)

Biotinylated Anti-Rabbit IgG antibody (Vector labs, Cat.no. BA-1000)

Biotinylated Anti-Rat IgG antibody (Vector labs, Cat.no. BA-9400)

Biotinylated Anti-Mouse IgG/Anti-Rabbit IgG antibody (Vector labs, Cat.no. BA-1400)

Biotinylated GSl-isolectin B4 antibody (vactor labs, Cat.no. B-1205)

Peroxidase Substrate Kit DAB (Vector labs, Cat.no. SK-4100)

Avidin/Biotin blocking kit (Vector labs, Cat.no. Sp-2001)

M.O.M. ^{TM} Kit (Vector labs, Cat.no. BMK-2202)

Vectastain ABC kit (Vector labs, Cat.no. PK-6100)

The R&D human cytokine array kit (Cat.no. ARY005)

The R&D human angiogenesis array kit (Cat.no. ARY007)

Appendix III: Equipments and Softwares

(Chapter 2)

LE1CA DM 1000 phase contrast microscope

LE1CA DM1L phase contrast microscope

LE1CA DM4000 M LED Versatile Upright microscope

LE1CA CTR 4000 Fluorescence Microscopy

Leica DFC300 FX Digital Color Camera microscope

Digital Camera Ky-F1030 JVC

Moticam 2000 digital micrpscope camera (2.0M Pixel USB2.0)

Nikon DS-Fi1 digital microscope camera

Nikon DS-2MBWc digital microscope camera

Nikon TS100 phase contrast inverted microscope

Rotator (Luckham Rotatest Shaker Model R100)

Centrifuge (Eppendorf model 5415 R)

Centrifuge (Eppendorf model 5810 D)

MSE Harrier 18/80R refrigerated benchtop centrifuge

Water Bath (Fisherbrand, 15345802)

Vi-Cell XR cell viability analysis (Beckham Coulter, 731050)

AGO HS X-Ray machine

2.0 eppendorf tubes (Fisher Scientific UK Ltd)

Universal tubes (Scientific Laboratory Supplies Ltd)

Ibidi inserts (Ibidi, 80206)

DynaMag ^{TM} -15

Magnetic Particle Concentrator 123.01D (Invitrogen)

Surgical blade 22 (Swanm-morton)

Needel (BD Microlance)

GraphPad Prism 6

The Leica Application Suite (LAS) imaging software (DM4000 B microsystem)

Image J software

AngioSys 2.0 image analysis software (TCS Cellworks)

Quantity One 1-D Analysis software (Bio-Rad)

Appendix IV: Inhibition of bEND.3and EA.hy 926 cells by Mitomycin C during migration (Chapter 3)

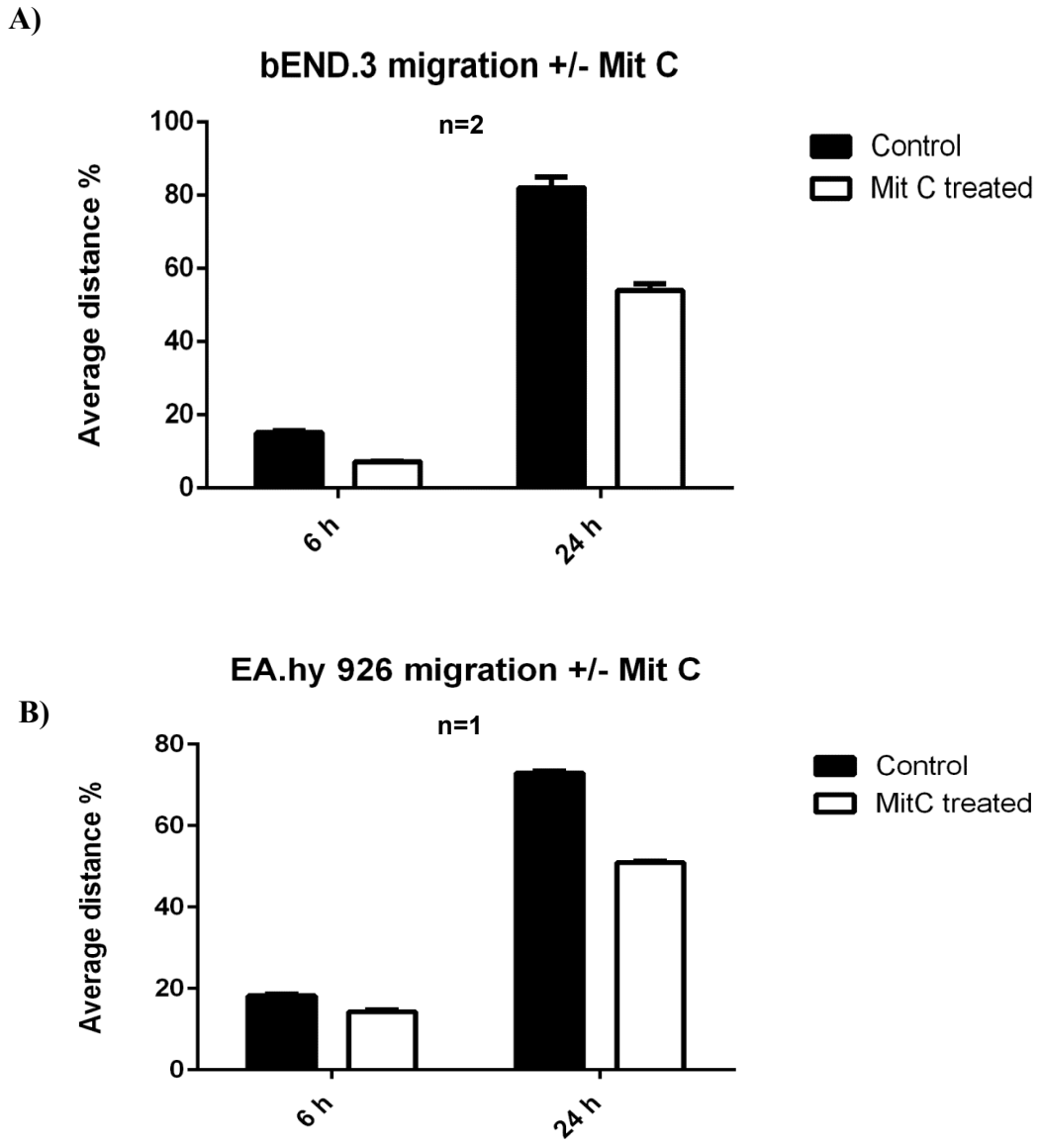

Figure I. Effect of Mitomycin C on migration of bEND.3 and EA.hy 926 cells. Confluent monolayers of **A)** bEND.3 and **B)** EA.hy 926 were pre-treated with 30 µg/ml and 25µg/ml Mit C respectively for 30 min and a scratch wound was created on each monolayer. The wound closure was monitored by a phase-contrast microscopy at 6 and 24 h. The data were expressed as the percentage of average wound distance observed at 24 h relative to the original wound (% of the original wound). In both groups the Mit C treated cells migrated slower than not-treated cells especially after 24 which has indication of cells proliferation in control groups after 24 h. Result are expressed as mean ± SEM of two separate experiments for bEND.3 and one experiment for EA.hy 926 (each performed in triplicate).

Appendix V: Effect of radiation on migration of bEND.3 and EA.hy 926 cells

(Chapter 3)

A)

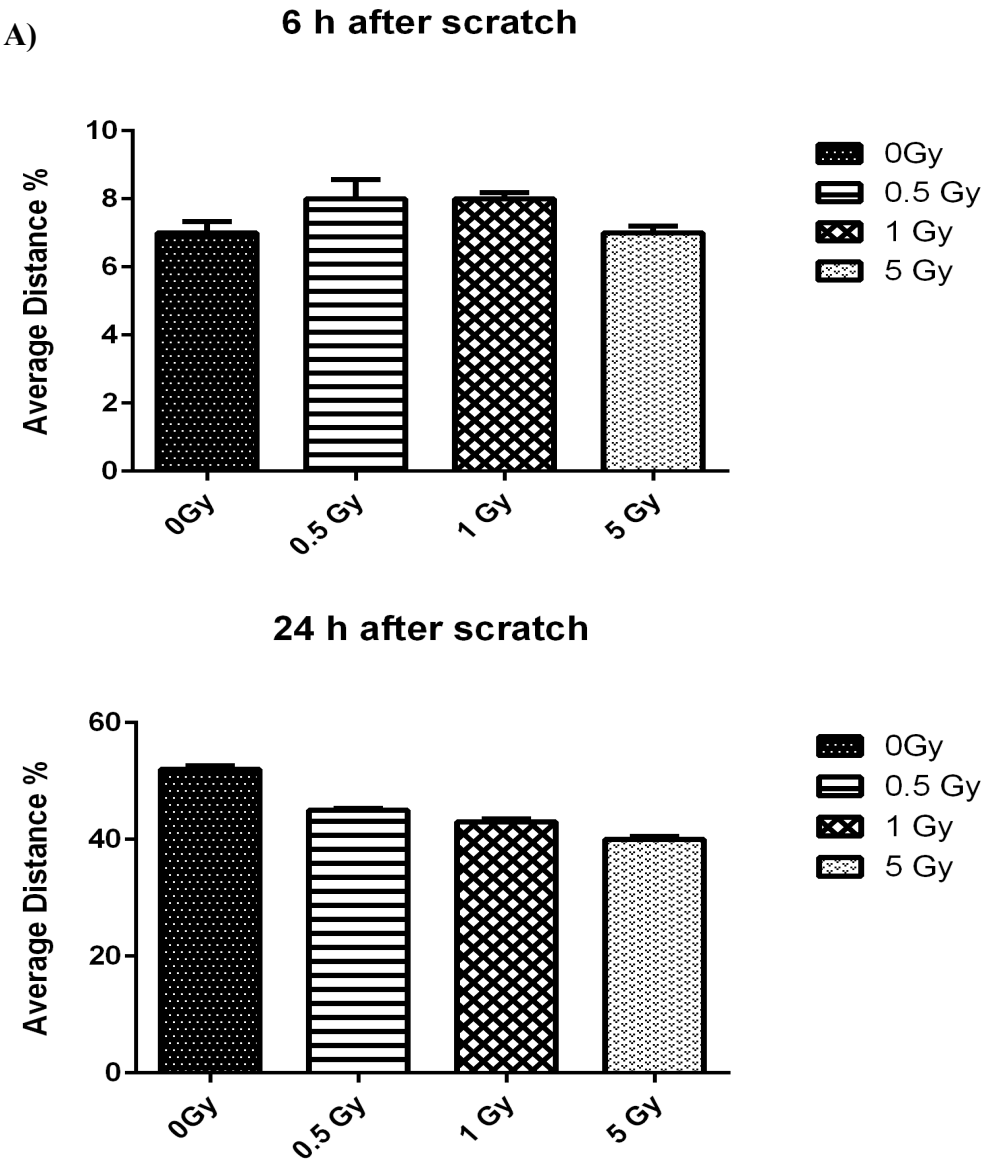

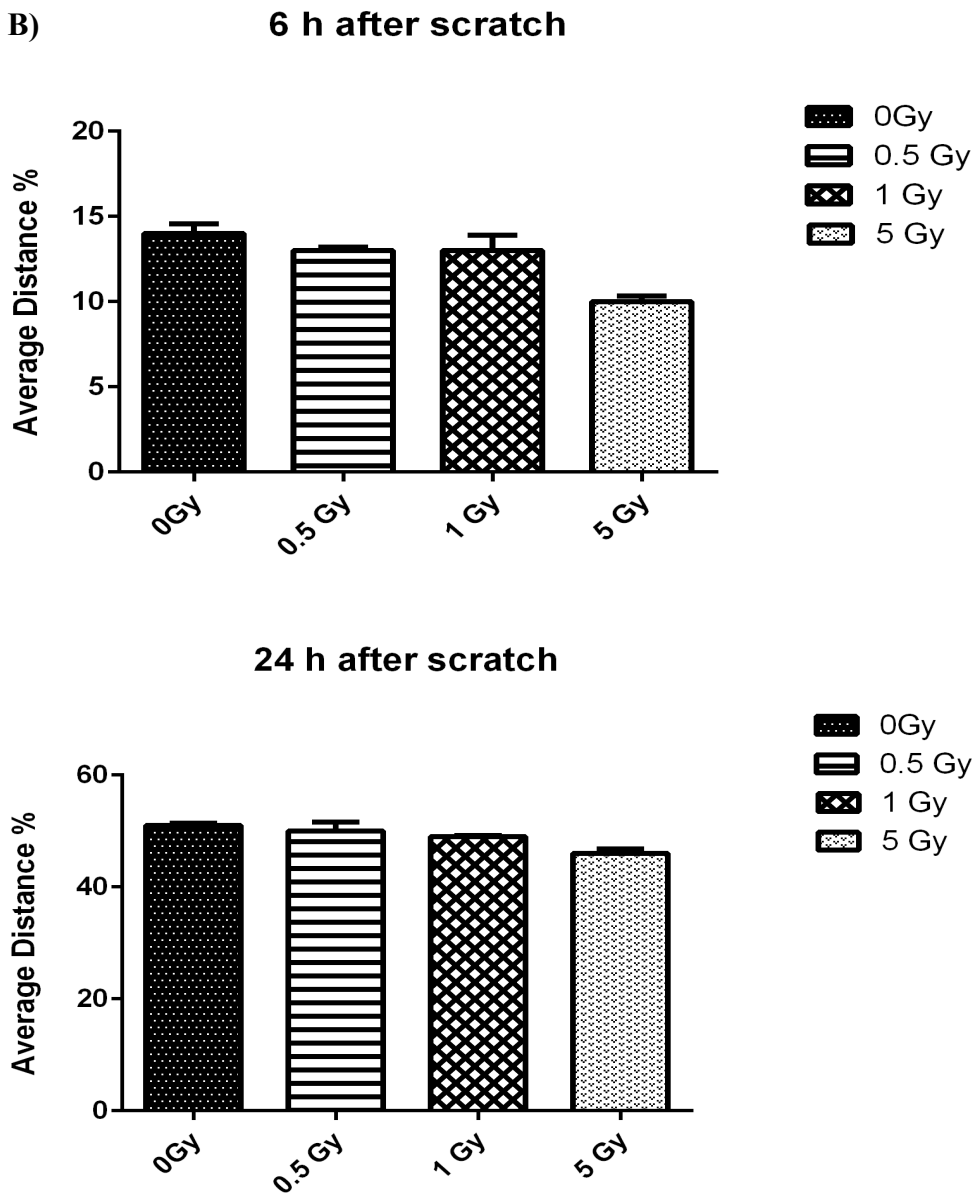

Figure II. Effects of radiation on bEND.3 and Ea.hy 926 migration by Scratch wound assay. Confluent **A)** bEND.3 and **B)** EA.hy 926 cells were irradiated at 0.5, 1 and 5 Gy and treated with 30 µg/ml and 25 µg/ml Mit C for 30 min respectively. The wound closure was monitored by a phase-contrast microscopy at 6 and 24 h. Data were expressed as the percentage of wound distance observed at 24 h relative to the original wound (% of the original wound). A dose-dependent decrease in bEND.3 cell migration observed after 24 h while EA.hy 926 cells showed only differences after 6 h and migration was same in all irradiated and non-irradiated groups after 24 h. Result expressed as mean ± SEM of one experiments performed at least in triplicate.

Appendix V: Semi-quantitative analysis of heart explants sprouting by two investigators

(Chapter 4)

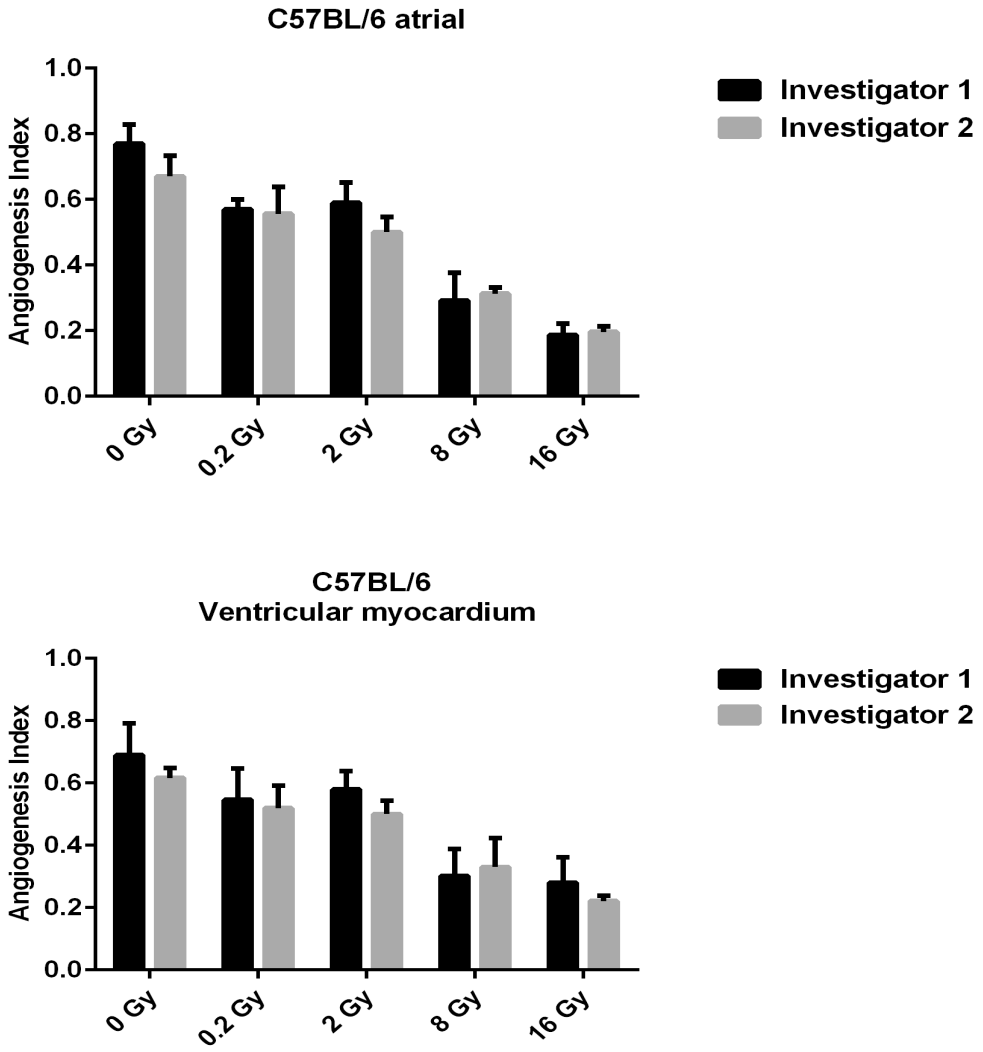

Figure III. Angiogenic index scoring in C57BL/6 atrial and ventricular myocardium explants after 20 weeks post-radiation by two investigators. The graphs depict semi-quantitative analysis of explant sprouting at 20 week post-irradiation in C57/BL6 hearts from investigator 1 and 2. Data was expressed as mean ± SEM of three independent hearts angiogenesis index (using 50 explants for each HV and HA part). The angiogenic index of each irradiated and non-irradiated group from investigator 1 were compared to the same angiogenic index obtained from investigator 2 using 2-way ANOVA test. No statistical differences were observed between results obtained from investigator 1 and 2.

Appendix VII: R&D Human Angiogenesis antibodies

(Chapter 5)

The antibodies present on the R&D Human Angiogenesis kit		
Activin A	FGF-7/KGF	PD-ECGF
ADAMTS-1	GDNF	PDGF-AA
Angiogenin	GM-CSF	PDGF-AB/PDGF-BB
Angiopoietin-1	HB-EGF	Persephin
Angiopoietin-2	HGF	CXCL4/PF4
Angiostatin/Plasminogen	IGFBP-1	P*l*GF
Amphiregulin	IGFBP-2	Prolactin
Artemin	IGFBP-3	Serpin B5/Maspin
Tissue Factor/Factor III	IL-1 beta	Serpin E1/PAI-1
CXCL16	CXCL8/IL-8	Serpin F1/PEDF
DPPIV/CD26	LAP (TGF-beta 1)	TIMP-1
EGF	Leptin	TIMP-4
EG-VEGF	CCL2/MCP-1	Thrombospondin-1
Endoglin/CD105	CCL3/MIP-1 alpha	Thrombospondin-2
Endostatin/Collagen XVIII	MMP-8	uPA
Endothelin-1	MMP-9	Vasohibin
FGF acidic	NRG1-beta 1	VEGF
FGF basic	Pentraxin 3	VEGF-C
FGF-4		

Appendix VIII: R&D Human Cytokine Array antibodies

(Chapter 5)

The antibodies present on the R&D Human Cytokine Array Kit		
C5a	**IL-4**	**IL-32 alpha**
CD40 ligand	**IL-5**	**CXCL10/IP-10**
G-CSF	**IL-6**	**CXCL11/I-TAC**
GM-CSF	**IL-8**	**CCL2/MCP-1**
CXCL1/GRO alpha	**IL-10**	**MIF**
CCL1/I-309	**IL-12 p70**	**CCL3/MIP-1 alpha**
ICAM-1	**IL-13**	**CCL4/MIP-1 beta**
IFN-gamma	**IL-16**	**CCL5/RANTES**
IL-1 alpha	**IL-17**	**CXCL12/SDF-1**
IL-1 beta	**IL-17E**	**Serpin E1/PAI-1**
IL-1ra	**IL-23**	**TNF-alpha**
IL-2	**IL-27**	**TREM-1**

References

Abbas, B., *et al*. (1990). "Radiation induced changes in the blood capillaries of rat duodenal villi: a corrosion cast, light and transmission electron microscopical study." *J Submicrosc Cytol Pathol* **22**(1): 63-70.

Abderrahmani, R., *et al*. (2012). "PAI-1-dependent endothelial cell death determines severity of radiation-induced intestinal injury." *PLoS One* **7**(4): e35740.

Adams, M. J., *et a*l. (2003). "Radiation-associated cardiovascular disease." *Crit Rev Oncol Hematol* **45**(1): 55-75.

Agah, A., *et al*. (2004). "Thrombospodin 2 levels are increased in aged mice: consequences for cutaneous wound healing and angiogenesis. " *Matnx Biol* **22**(7): 539-47.

AGIR (2010). "Circulatory Disease Risk, RCE-16". [pdf] Chilton, Oxfordshire: Public Health England. Available at: <http://www.hpa.org.uk/webc/hpawebfile/hpaweb_c/1284475204588> [Accessed at 10 August 2012]

Ahmad, M., *et al*. (2007). "Ionizing radiation decreases capillary-like structure formation by endothelial cells in vitro." *Microvasc Res* **73**(1): 14-19.

Aird, W. C. (2012). "Endothelial cell heterogeneity." Cold Spring Harb Perspect Med **2**(1): a006429.

Al Sabti, H. (2007). "Therapeutic angiogenesis in cardiovascular disease." *J Cardiothorac Surg* **2**: 49.

Aleman, B. M., *et al*. (2003). "Long-term cause-specific mortality of patients treated for Hodgkin's disease." *J Clin Oncol* **21**(18): 3431-3439.

Andratschke, N., *et al*. (2011). "Late radiation-induced heart disease after radiotherapy. Clinical importance, radiobiological mechanisms and strategies of prevention." *Radiother Oncol* **100**(2): 160-166.

Andreassi, M. G. (2008). "DNA damage, vascular senescence and atherosclerosis." *J Mol Med (Berl)* **86**(9): 1033-1043.

Andreassi, M. G. and N. Botto (2003). "DNA damage as a new emerging risk factor in atherosclerosis." *Trends Cardiovascular Med* **13**(7): 270-75.

Annes, J. P., *et al*. (2003). "Making sense of latent TGFbeta activation." *J Cell Sci* **116**(Pt 2): 217-224.

Anscher, M. S., *et al*. (1995). "Short communication: normal tissue injury after cancer therapy is a local response exacerbated by an endocrine effect of TGF beta." *Br J Radiol* **68**(807): 331-333.

Arenas, M., *et al*. (2012). "Anti-inflammatory effects of low-dose radiotherapy. Indications, dose, and radiobiological mechanisms involved." *Strahlenther Onkol* **188**(11): 975-981.

Arthur, W. T., *et al*. (1998). "Growth factors reverse the impaired sprouting of microvessels from aged mice. " *Microvasc* **55**(3): 260-70.

Auerbach, R., *et al*. (2003). "Angiogenesis assays: a critical overview. " *Clin Chem* **49**(1): 32-40.

Averbeck, D. (2009). "Does scientific evidence support a change from the LNT model for low-dose radiation risk extrapolation?" *Health Phys* **97**(5): 493-504.

Azizova, T. V., *et al*. (2010a). "Cardiovascular diseases in the cohort of workers first employed at Mayak PA in 1948–1958." *Radiat Res* **174**(2): 155–168.

Azizova, T. V., *et al*. (2010b). "Cardiovascular diseases in the cohort of workers first employed at Mayak PA in 1948–1958." *Radiat Res* **174**(2): 851–864.

Badylak, S. F. (2002). "The extracellular matrix as a scaffold for tissue reconstruction." Semin *Cell Dev Biol* **13**(5): 377-383.

Bakin, A. V., *et a*l. (2002). "p38 mitogen-activated protein kinase is required for TGFbeta-mediated fibroblastic transdifferentiation and cell migration." *J Cell Sci* **115**(Pt 15): 3193-3206.

Ballermann, B. J. (1998). "Endothelial cell activation." *Kidney Int* **53**(6): 1810-1826.

Barcellos-Hoff, M. H. (1993). "Radiation-induced transforming growth factor beta and subsequent extracellular matrix reorganization in murine mammary gland." *Cancer Res* **53**(17): 3880-3886.

Barcellos-Hoff, M. H. and A. L. Brooks (2001). "Extracellular signaling through the microenvironment: a hypothesis relating carcinogenesis, bystander effects, and genomic instability." *Radiat Res* **156**(5 Pt 2): 618-627.

Barcellos-Hoff, M. H., *et al*. (1994). "Transforming growth factor-beta activation in irradiated murine mammary gland." *J Clin Invest* **93**(2): 892-899.

Bartek, J., *et al*. (2004). "Checking on DNA damage in S phase." *Nat Rev Mol Cell Biol* **5**(10): 792-804.

Bauer, J., *et al*. (1992). "In vitro model of angiogenesis using a human endothelium-derived permanent cell line: contributions of induced gene expression, G-proteins, and integrins." J *Cell Physiol* **153**(3): 437-449.

Benndorf, R. A., *et al*. (2008). "Isoprostanes inhibit vascular endothelial growth factor-induced endothelial cell migration, tube formation, and cardiac vessel sprouting in vitro, as well as angiogenesis in vivo via activation of the thromboxane A(2) receptor: a potential link between oxidative stress and impaired angiogenesis." *Circ Res* **103**(9): 1037-1046.

Berrington, A., *et al*. (2001). "100 years of observation on British radiologists: mortality from cancer and other causes 1897-1997." *Br J Radiol* **74**(882): 507-519.

Berthod, F., *et al*. (2006). "Extracellular matrix deposition by fibroblasts is necessary to promote capillary-like tube formation in vitro." *J Cell Physiol* **207**(2): 491-498.

Bhowmick, N. A., *et al*. (2001). "Transforming growth factor-beta1 mediates epithelial to mesenchymal transdifferentiation through a RhoA-dependent mechanism." *Mol Biol Cell* **12**(1): 27-36.

Bishop, E. T., *et al*. (1999). "An in vitro model of angiogenesis: basic features." *Angiogenesis 3(4): 335-344.*

Bolotnikova, M. G., *et al*. (1994). "Mortality from cardiovascular diseases among male workers at the radiochemical plant of the 'Mayak' complex." *Sci Total Environ* **142**(1-2): 29-31.

Bourgier, C., *et al*. (2005). "Inhibition of Rho kinase modulates radiation induced fibrogenic phenotype in intestinal smooth muscle cells through alteration of the cytoskeleton and connective tissue growth factor expression." *Gut* **54**(3): 336-343.

Brigstock, D. R. (1999). "The connective tissue growth factor/cysteine-rich 61/nephroblastoma overexpressed (CCN) family." *Endocr Rev* **20**(2): 189-206.

Brooks-Wilson, A., *et al*. (1999). "Mutations in ABC1 in Tangier disease and familial high-density lipoprotein deficiency." *Nat Genet* **22**(4): 336-345.

Brooks, A. L. (2005). "Paradigm shifts in radiation biology: their impact on intervention for radiation-induced disease." *Radiat Res* **164**(4 Pt 2): 454-461.

Brown, J. M. and A. C. Koong (2008). "High-dose single-fraction radiotherapy: exploiting a new biology?" *Int J Radiat Oncol Biol Phys* **71**(2): 324-325.

Brush, J., *et al*. (2007). "Molecular mechanisms of late normal tissue injury." *Semin Radiat Oncol* **17**(2): 121-130.

Burns, P. A. (2006). "UNSCEAR 54th session and 2006 report." *J Radiol Prot* **26**(4): 442-444.

Calvo, F. A., *et al*. (2006). "Intraoperative radiation therapy first part: rationale and techniques." *Crit Rev Oncol Hematol* **59**(2): 106-115.

Cannan, R.K. (1962). "The Atomic Bomb Casualty Commission: the first fourteen years". News reports (National Academy of Science/National Reseaech Council) **12**; 1-7.

CARDIORSIK project report (2011). "The mechanism of cardiovascular risks after low radiation doses". Germany, Munich: European Commission. [pdf] Available at: <http://cordis.europa.eu/documents/documentlibrary/117238321EN6.pdf> [Accessed 25 Feb 2014].

Cardis, E., *et al*. (1995). "Effects of low doses and low dose rates of external ionizing radiation: cancer mortality among nuclear industry workers in three countries." *Radiat Res* **142**(2): 117-132.

Carmeliet, P. (2000). "Mechanisms of angiogenesis and arteriogenesis. " *Nat Med* **6**(4): 389-95.

Carr, Z. A., *et al*. (2005). "Coronary heart disease after radiotherapy for peptic ulcer disease." *Int J Radiat Oncol Biol Phys* **61**(3): 842-850.

Chachques, J. C., *et a*l. (2004). "Angiogenic growth factors and/or cellular therapy for myocardial regeneration: a comparative study." *J Thorac Cardiovasc Surg* **128**(2): 245-253.

Chang, H. Y., *et al*. (2004). "Gene expression signature of fibroblast serum response predicts human cancer progression: similarities between tumors and wounds." *PLoS Biol* **2**(2): E7.

Chargari, C., *et al*. (2011). "Cardiac toxicity in breast cancer patients: from a fractional point of view to a global assessment." *Cancer Treat Rev* **37**(4): 321-330.

Chen, S., *et al*. (2006). "RhoA modulates Smad signaling during transforming growth factor-beta-induced smooth muscle differentiation." *J Biol Chem* **281**(3): 1765-1770.

Chen, J., *et al*. (2010). "Evaluation of x-inactivation status and cytogenetic stability of human dermal fibroblasts after long-term culture." *Int J Cell Biol* **2010**: 289653.

Cines, D. B., *et al*. (1998). "Endothelial cells in physiology and in the pathophysiology of vascular disorders." *Blood* **91**(10): 3527-3561.

Clarke, M., *et al*. (2005). "Effects of radiotherapy and of differences in the extent of surgery for early breast cancer on local recurrence and 15-year survival: an overview of the randomised trials." *Lancet* **366**(9503): 2087-2106.

Cockwell, P., *et al*. (1997). "Activation of endothelial cells in thrombosis and vasculitis." *Scand J Rheumatol* **26**(3): 145-150.

Coderre, J. A., *et al*. (2006). "Late effects of radiation on the central nervous system: role of vascular endothelial damage and glial stem cell survival." *Radiat Res* **166**(3): 495-503.

Connell, P. P. and S. Hellman (2009). "Advances in radiotherapy and implications for the next century: a historical perspective." *Cancer Res* **69**(2): 383-392.

Cook-Mills, J. M. and T. L. Deem (2005). "Active participation of endothelial cells in inflammation." *J Leukoc Biol* **77**(4): 487-495.

Cottin, Y., *et a*l. (2001). "Intravascular radiation accelerates atherosclerotic lesion formation of hypercholesteremic rabbits." *Cardiovasc Radiat Med* **2**(4): 231-240.

Cox, R. (1994). "Molecular mechanisms of radiation oncogenesis." *Int J Radiat Biol* **65**(1): 57-64.

Crawford, S. E., *et al*. (1998). "Thrombospondin-1 is a major activator of TGF-beta1 in vivo." *Cell* **93**(7): 1159-1170.

Cullen, P., *et al*. (2005). "The pathogenesis of atherosclerosis." *Handb Exp Pharmacol* (170): 3-70.

Dancea, H. C., *et al*. (2009). "Role of Radiation-induced TGF-beta Signaling in Cancer Therapy." *Mol Cell Pharmacol* **1**(1): 44-56.

Darby, S. C., *et al*. (2010). "Radiation-related heart disease: current knowledge and future prospects." *Int J Radiat Oncol Biol Phys* **76**(3): 656-665.

Darby, S. C., *et al*. (2005). "Long-term mortality from heart disease and lung cancer after radiotherapy for early breast cancer: prospective cohort study of about 300,000 women in US SEER cancer registries." *Lancet Oncol* **6**(8): 557-565.

Darby, S. C., *et al*. (1995). "Radon and cancers other than lung cancer in underground miners: a collaborative analysis of 11 studies." *J Natl Cancer Inst* **87**(5): 378-384.

Dean, R. G., *et al*. (2005). "Connective tissue growth factor and cardiac fibrosis after myocardial infarction." *J Histochem Cytochem* **53**(10): 1245-1256.

Delaney, G., *et al*. (2005). "The role of radiotherapy in cancer treatment: estimating optimal utilization from a review of evidence-based clinical guidelines." *Cancer* **104**(6): 1129-1137.

Derynck, R. and Y. E. Zhang (2003). "Smad-dependent and Smad-independent pathways in TGF-beta family signaling." *Nature* **425**(6958): 577-584.

Deshpande, A., *et al*. (1996). "Alpha-particle-induced sister chromatid exchange in normal human lung fibroblasts: evidence for an extranuclear target." *Radiat Res* **145**(3): 260-267.

Doll, R. (1995). "Hazards of ionising radiation: 100 years of observations on man." *Br J Cancer* **72**(6): 1339-1349.

Dong, Q. G., *et al*. (1997). "A general strategy for isolation of endothelial cells from murine tissues. Characterization of two endothelial cell lines from the murine lung and subcutaneous sponge implants." *Arterioscler Thromb Vasc Biol* **17**(8): 1599-1604.

Donovan, D., *et al*. (2001). "Comparison of three in vitro human 'angiogenesis' assays with capillaries formed in vivo." *Angiogenesis* **4**(2): 113-121.

Dormand, E. L., *et al*. (2005). "Radiotherapy and wound healing." *Int Wound J* **2**(2): 112-127.

Dorresteijn, L. D., *et al*. (2002). "Increased risk of ischemic stroke after radiotherapy on the neck in patients younger than 60 years." *J Clin Oncol* **20**(1): 282-288.

Edgell, C. J., *et al*. (1983). "Permanent cell line expressing human factor VIII-related antigen established by hybridization." *Proc Natl Acad Sci U S A* **80**(12): 3734-3737.

Edlund, S., *et al*. (2002). "Transforming growth factor-beta-induced mobilization of actin cytoskeleton requires signaling by small GTPases Cdc42 and RhoA." *Mol Biol Cell* **13**(3): 902-914.

Evans, C. H. and J. A. DiPaolo (1982). "Equivalency of endothelial cell growth supplement to irradiated feeder cells in carcinogen-induced morphologic transformation of Syrian hamster embryo cells. " *J Natl Cancer Inst* **68**(1): 127-31.

Ewan, K. B., *et al*. (2002). "Transforming growth factor-beta1 mediates cellular response to DNA damage in situ." *Cancer Res* **62**(20): 5627-5631.

Ewing, J. (1934)."Early experiences in radiation therapy". *Am. J. Roentgenol* **31**: 153-163.

Fajardo, L. F. (1989). "The unique physiology of endothelial cells and its implications in radiobiology." *Front Radiat Ther Oncol* **23**: 96-112.

Fajardo, L. F. (1999). "Is the pathology of radiation injury different in small vs large blood vessels?" Cardiovasc Radiat Med **1**(1): 108-110.

Fajardo, L. F. (2005). "The pathology of ionizing radiation as defined by morphologic patterns." *Acta Oncol* **44**(1): 13-22.

Fajardo, L. F. and M. Berthrong (1988). "Vascular lesions following radiation." *Pathol Annu* **23 Pt 1**: 297-330.

Fajardo, L. F. and J. R. Stewart (1970). "Experimental radiation-induced heart disease. I. Light microscopic studies." *Am J Pathol* **59**(2): 299-316.

Fajardo, L. F. and J. R. Stewart (1972). "Coronary artery disease after radiation." *N Engl J Med* **286**(23): 1265-1266.

Feinendegen, L. E. (1999). "The role of adaptive responses following exposure to ionizing radiation." *Hum Exp Toxicol* **18**(7): 426-432.

Folkman, J. (1995). "Angiogenesis in cancer, vascular, rheumatoid and other disease." *Nat Med* **1**(1): 27-31.

Franken, N. A., *et al*. (2006). "Clonogenic assay of cells in vitro." *Nat Protoc* **1**(5): 2315-2319.

Gabriels, K., *et al*. (2012). "Local heart irradiation of ApoE(-/-) mice induces microvascular and endocardial damage and accelerates coronary atherosclerosis." *Radiother Oncol* **105**(3): 358-364.

Gabrys, D., *et al*. (2007). "Radiation effects on the cytoskeleton of endothelial cells and endothelial monolayer permeability." *International Journal of Radiation Oncology Biology Physics* **69**(5): 1553-1562.

Garlanda, C., *et al*. (1994). "Progressive growth in immunodeficient mice and host cell recruitment by mouse endothelial cells transformed by polyoma middle-sized T antigen: implications for the pathogenesis of opportunistic vascular tumors." *Proc Natl Acad Sci U S A* **91**(15): 7291-7295.

Garland, R. J., *et al*. (1999). "The use of Teflon cell culture bags to expand functionally active CD8+ cytotoxic T lymphocytes." *J Immunol Methods* **227**(1-2): 53-63.

Gaugler, M. H., *et al*. (2007). "Intestinal epithelial cell dysfunction is mediated by an endothelial-specific radiation-induced bystander effect." *Radiat Res* **167**(2): 185-193.

Gaugler, M. H., *et al*. (1998). "Characterization of the response of human bone marrow endothelial cells to in vitro irradiation." *Br J Haematol* **103**(4): 980-989.

Geng, L., *et al*. (2004). "A specific antagonist of the p110delta catalytic component of phosphatidylinositol 3'-kinase, IC486068, enhances radiation-induced tumor vascular destruction." *Cancer Res* **64**(14): 4893-4899.

Gerhardt, H. and C. Betsholtz (2003). "Endothelial-pericyte interactions in angiogenesis." *Cell Tissue Res* **314**(1): 15-23.

Gerhardt, H., *et al*. (2003). "VEGF guides angiogenic sprouting utilizing endothelial tip cell filopodia." *J Cell Biol* **161**(6): 1163-1177.

Ginsberg, H. N. (1998). "Lipoprotein physiology." *Endocrinol Metab Clin North Am* **27**(3): 503-519.

Girdhani, S., *et al*. (2012). "Proton irradiation suppresses angiogenic genes and impairs cell invasion and tumor growth." *Radiat Res* **178**(1): 33-45.

Glass, C. K. and J. L. Witztum (2001). "Atherosclerosis. the road ahead." *Cell* **104**(4): 503-516.

Goodhead, D. T. (1994). "Initial events in the cellular effects of ionizing radiations: clustered damage in DNA." *Int J Radiat Biol* **65**(1): 7-17.

Goodhead, D. T. (2006). "Energy deposition stochastics and track structure: what about the target?" *Radiat Prot Dosimetry* **122**(1-4): 3-15.

Goodwin, A. M. (2007). "In vitro assays of angiogenesis for assessment of angiogenic and anti-angiogenic agents." *Microvasc Res* **74**(2-3): 172-183.

Goumans, M. J., *et al*. (2009). "TGF-beta signaling in vascular biology and dysfunction." *Cell Res* **19**(1): 116-127.

Govani, F. S. and C. L. Shovlin (2009). "Hereditary haemorrhagic telangiectasia: a clinical and scientific review." *Eur J Hum Genet* **17**(7): 860-871.

Grabham, P. and P. Sharma (2013). "The effects of radiation on angiogenesis." *Vasc Cell* **5**(1): 19.

Gross, N. J. (1977). "Pulmonary effects of radiation therapy." *Ann Intern Med* **86**(1): 81-92.

Guilini, C., *et al*. (2010). "Divergent roles of prokineticin receptors in the endothelial cells: angiogenesis and fenestration." *Am J Physiol Heart Circ Physiol* **298**(3): H844-852.

Hallahan, D., *et al*. (1995). "E-selectin gene induction by ionizing radiation is independent of cytokine induction." *Biochem Biophys Res Commun* **217**(3): 784-795.

Hallahan, D., *et al*. (1996). "Cell adhesion molecules mediate radiation-induced leukocyte adhesion to the vascular endothelium." *Cancer Res* **56**(22): 5150-5155.

Hallahan, D. E. and S. Virudachalam (1997). "Ionizing radiation mediates expression of cell adhesion molecules in distinct histological patterns within the lung." *Cancer Res* **57**(11): 2096-2099.

Hamada, N., *et a*l. (2007). "Intercellular and intracellular signaling pathways mediating ionizing radiation-induced bystander effects." *J Radiat Res* **48**(2): 87-95.

Hamer, G., *et al*. (2003). "DNA double-strand breaks and gamma-H2AX signaling in the testis." *Biol Reprod* **68**(2): 628-634.

Han, W., *et al*. (2007). "Constitutive nitric oxide acting as a possible intercellular signaling molecule in the initiation of radiation-induced DNA double strand breaks in non-irradiated bystander cells." *Oncogene* **26**(16): 2330-2339.

Hancock, S. L., *et al*. (1993). "Factors affecting late mortality from heart disease after treatment of Hodgkin's disease." *JAMA* **270**(16): 1949-1955.

Hansson, G. K. (2005). "Inflammation, atherosclerosis, and coronary artery disease." *N Engl J Med* **352**(16): 1685-1695.

Haubner, F., *et al*. (2012). "Wound healing after radiation therapy: review of the literature." *Radiat Oncol* **7**: 162.

Hauptmann, M., *et al*. (2003). "Mortality from diseases of the circulatory system in radiologic technologists in the United States." *Am J Epidemiol* ***157(3): 239-248.***

Hayashi, T., *et al.* (2005). "Long-term effects of radiation dose on inflammatory markers in atomic bomb survivors." *Am J Med* **118**(1): 83-86.

Haydont, V., *et al*. (2007). "Pravastatin Inhibits the Rho/CCN2/extracellular matrix cascade in human fibrosis explants and improves radiation-induced intestinal fibrosis in rats." *Clin Cancer Res* **13**(18 Pt 1): 5331-5340.

Haydont, V., *et al*. (2007). "Rho/ROCK pathway as a molecular target for modulation of intestinal radiation-induced toxicity." *Br J Radiol* **80 Spec No 1**: S32-40.

Haydont, V. and M. C. Vozenin-Brotons (2007). "Maintenance of radiation-induced intestinal fibrosis: cellular and molecular features." *World J Gastroenterol* **13**(19): 2675-2683.

Haydont, V., *et al*. (2005). "Induction of CTGF by TGF-beta1 in normal and radiation enteritis human smooth muscle cells: Smad/Rho balance and therapeutic perspectives." *Radiother Oncol* **76**(2): 219-225.

Haydont, V., *et al*. (2008). "Specific signals involved in the long-term maintenance of radiation-induced fibrogenic differentiation: a role for CCN2 and low concentration of TGF-beta1." *Am J Physiol Cell Physiol* **294**(6): C1332-1341.

Hendry, J. H., *et al*. (2008). "Radiation-induced cardiovascular injury." *Radiat Environ Biophys* **47**(2): 189-193.

Hetheridge, C., *et al*. (2011). "Uses of the in vitro endothelial-fibroblast organotypic co-culture assay in angiogenesis research." *Biochem Soc Trans* **39**(6): 1597-1600.

Hildebrandt, G. (2010). "Non-cancer diseases and non-targeted effects." *Mutat Res* **687**(1-2): 73-77.

Hildebrandt, G., *et al*. (1998). "Mechanisms of the anti-inflammatory activity of low-dose radiation therapy." *Int J Radiat Biol* **74**(3): 367-378.

Hildebrandt, G., *et al*. (2002). "Mononuclear cell adhesion and cell adhesion molecule liberation after X-irradiation of activated endothelial cells in vitro." *Int J Radiat Biol* **78**(4): 315-25.

Hongpaisan, J. (2000). "Inhibition of proliferation of contaminating fibroblasts by D-valine in cultures of smooth muscle cells from human myometrium." *Cell Biol Int* **24**(1): 1-7.

Horimoto, M., *et al*. (1995). "Identification of a transforming growth factor beta-1 activator derived from a human gastric cancer cell line." *Br J Cancer* **72**(3): 676-682

Hoving, S., *et al*. (2011). "Anti-inflammatory and anti-thrombotic intervention strategies using atorvastatin, clopidogrel and knock-down of CD40L do not modify radiation-induced atherosclerosis in ApoE null mice." *Radiother Oncol* **101**(1): 100-108.

Hoving, S., *et al*. (2008). "Single-dose and fractionated irradiation promote initiation and progression of atherosclerosis and induce an inflammatory plaque phenotype in ApoE(-/-) mice." *Int J Radiat Oncol Biol Phys* **71**(3): 848-857.

Hoving, S., *et al*. (2012). "Irradiation induces different inflammatory and thrombotic responses in carotid arteries of wildtype C57BL/6J and atherosclerosis-prone ApoE(-/-) mice." *Radiother Oncol* **105**(3): 365-370.

Howard, A. and S. R. Pelc (1952). "Synthesis of deoxyribonucleic acid in normal and irradiated cells and its relation to chromosome breakage". *Heredity* **49(2):**261-273.

Hu, W., *et al*. (2005). "Atherosclerotic lesions in the common coronary arteries of ApoE knockout mice." *Cardiovasc Pathol* **14**(3): 120-125.

Humar, R. O. K., *et al.* (2002): "Hypoxia enhances vascular cell proliferation and angiogenesis in vitro via rapamycin (mTOR)-dependent signaling. " *FASEB J* **16**(8): 771-80.

Huo, L., *et al*. (2001). "HPRT mutants induced in bystander cells by very low fluences of alpha particles result primarily from point mutations." *Radiat Res* **156**(5 Pt 1): 521-525.

ICRP (2007a). "The 2007 Recommendations of the International Commission on Radiological Protection. ICRP publication 103." *Ann ICRP* **37**(2-4): 1-332.

ICRP (2007b). "ICRP Publication 105. Radiation protection in medicine." *Ann ICRP* **37**(6): 1-63.

Imaizumi, N., *et al*. (2010). "Radiotherapy suppresses angiogenesis in mice through TGF-betaRI/ALK5-dependent inhibition of endothelial cell sprouting." *PLoS One* **5**(6): e11084.

Ishizaki, T., *et al*. (2000). "Pharmacological properties of Y-27632, a specific inhibitor of rho-associated kinases." *Mol Pharmacol* **57**(5): 976-983.

Ismail, I. H., *et al*. (2007). "An optimized method for detecting gamma-H2AX in blood cells reveals a significant interindividual variation in the gamma-H2AX response among humans." *Nucleic Acids Res* **35**(5): e36.

Ivanov, V. K., *et al*. (2006). "The risk of radiation-induced cerebrovascular disease in Chernobyl emergency workers." *Health Phys* **90**(3): 199-207.

Iyer, R. and B. E. Lehnert (2002). "Alpha-particle-induced increases in the radioresistance of normal human bystander cells." Radiat Res **157**(1): 3-7.

Jaquet, K., *et al*. (2002). "Erythropoietin and VEGF exhibit equal angiogenic potential. " *Microvasc Res* **64**(2): 326-33.

Jelonek, K., *et al*. (2011). "Cardiac endothelial cells isolated from mouse heart - a novel model for radiobiology." *Acta Biochim Pol* **58**(3): 397-404.

Joiner, M. C., *et al*. (1996). "Hypersensitivity to very-low single radiation doses: its relationship to the adaptive response and induced radioresistance." *Mutat Res* **358**(2): 171-183.

Joiner, M. C., *et al*. (2001). "Low-dose hypersensitivity: current status and possible mechanisms." *Int J Radiat Oncol Biol Phys* **49**(2): 379-389.

Juckett, M. B., *et al*. (1998). "Desferrioxamine enhances the effects of gamma radiation on clonogenic survival and the formation of chromosomal aberrations in endothelial cells." *Radiat Res* **149**(4): 330-337.

Kamaraju, A. K. and A. B. Roberts (2005). "Role of Rho/ROCK and p38 MAP kinase pathways in transforming growth factor-beta-mediated Smad-dependent growth inhibition of human breast carcinoma cells in vivo." *J Biol Chem* **280**(2): 1024-1036.

Kamiya, K. and M. Sasatani (2012). "[Effects of radiation exposure on human body]." *Nihon Rinsho* **70**(3): 367-374.

Karagiannis, E. D. and A. S. Popel (2008). "A systematic methodology for proteome-wide identification of peptides inhibiting the proliferation and migration of endothelial cells." *Proc Natl Acad Sci U S A* **105**(37): 13775-13780.

Karamysheva, A. F. (2008). "Mechanisms of angiogenesis." *Biochemistry (Mosc)* **73**(7): 751-762.

Kassis, A. I. (2004). "In vivo validation of the bystander effect." *Hum Exp Toxicol* **23**(2): 71-73.

Kastan, M. B. and J. Bartek (2004). "Cell-cycle checkpoints and cancer." *Nature* **432**(7015): 316-323.

Khurana, R., *et al*. (2005). "Role of angiogenesis in cardiovascular disease: a critical appraisal." *Circulation* **112**(12): 1813-1824.

Kiefer, F. N., *et al*. (2004). "A versatile in vitro assay for investigating angiogenesis of the heart." *Exp Cell Res* **300**(2): 272-282.

Kim, C. S., *et al*. (2007). "Low-dose of ionizing radiation enhances cell proliferation via transient ERK1/2 and p38 activation in normal human lung fibroblasts." *J Radiat Res* **48**(5): 407-415.

Kim, H. J., *et al*. (2010). "IL-18 downregulates collagen production in human dermal fibroblasts via the ERK pathway." *J Invest Dermatol* **130**(3): 706-715.

Kirsch, T., *et al*. (2007). "Engulfment of apoptotic cells by microvascular endothelial cells induces proinflammatory responses." *Blood* **109**(7): 2854-2862.

Kodama, K., *et al*. (1996). "Profiles of non-cancer diseases in atomic bomb survivors." *World Health Stat Q* **49**(1): 7-16.

Kohler, H. P. and P. J. Grant (2000). "Plasminogen-activator inhibitor type 1 and coronary artery disease." *N Engl J Med* **342**(24): 1792-1801.

Kruse, J. J., *et al*. (2009). "Radiation-induced activation of TGF-beta signaling pathways in relation to vascular damage in mouse kidneys." *Radiat Res* **171**(2): 188-197.

Lamalice, L., *et al*. (2007). "Endothelial cell migration during angiogenesis." *Circ Res* **100**(6): 782-794.

Lang, I., *et al*. (1994). "Differential lectin binding to the fibrinoid of human full-term placenta: correlation with a fibrin antibody and the PAF-Halmi method." *Acta Anat (Basel)* **150**(3): 170-177.

Lang, I., *et al*. (2003). "Heterogeneity of microvascular endothelial cells isolated from human term placenta and macrovascular umbilical vein endothelial cells." *Eur J Cell Biol* **82**(4): 163-173.

Langley, R. E., *et al*. (1997). "Radiation-induced apoptosis in microvascular endothelial cells." *Br J Cancer* **75**(5): 666-672.

Lauk, S. (1987). "Endothelial alkaline phosphatase activity loss as an early stage in the development of radiation-induced heart disease in rats." *Radiat Res* **110**(1): 118-128.

Lawrence, T. S. (2008). "Radiotherapy for intrahepatic cancers: the promise of emerging sophisticated techniques." *J Support Oncol* **6**(1): 14-15.

Lawrence, Y. R., *et al*. (2008). "Biologically conformal treatment: biomarkers and functional imaging in radiation oncology." *Future Oncol* **4**(5): 689-704.

Lawrence, T. S., *et al*. (2008). "Principles of Radiation Oncology". Philadelphia, Lippincott Williams and Wilkins. 8th ed.

Lee, M. O., *et al*. (2012). "Effect of ionizing radiation induced damage of endothelial progenitor cells in vascular regeneration." *Arterioscler Thromb Vasc Biol* **32**(2): 343-352.

Levick, J. R. (2003). "An introduction to Cardiovascular Physiology". London, Arnold Inc. 4th ed: pp.130-149.

Lewis, J. M., *et al*. (2006). "Development of a human cardiac tissue-based angiogenesis model." *J Surg Res* **135**(1): 34-37.

Liang, C. C., *et al*. (2007). "In vitro scratch assay: a convenient and inexpensive method for analysis of cell migration in vitro." *Nat Protoc* **2**(2): 329-333.

Libby, P. (2009). "Molecular and cellular mechanisms of the thrombotic complications of atherosclerosis." *J Lipid Res* **50 Suppl**: S352-357.

Lidington, E. A., *et al*. (1999). "A comparison of primary endothelial cells and endothelial cell lines for studies of immune interactions." *Transpl Immunol* **7**(4): 239-246.

Lidington, E. A., *et al*. (2002). "Conditional immortalization of growth factor-responsive cardiac endothelial cells from H-2K(b)-tsA58 mice." *Am J Physiol Cell Physiol* **282**(1): C67-74.

Lievandot, J. and T. Asahara, (2002). "Effects of statins on angiogenesis and vasculogenesis." *Rev Esp Cardiol* **55**(38): 838-44.

Lim, Y. C. and F. W. Luscinskas (2006). "Isolation and culture of murine heart and lung endothelial cells for in vitro model systems." *Methods Mol Biol* **341**: 141-154.

Linton, M. F. and S. Fazio (2003). "Macrophages, inflammation, and atherosclerosis." *Int J Obes Relat Metab Disord* **27 Suppl 3**: S35-40.

Little, J. B., *et al*. (1973). "Repair of potentially lethal radiation damage in vitro and in vivo." *Radiology* **106**(3): 689-694.

Little, M. P., *et al*. (2009). "A model of cardiovascular disease giving a plausible mechanism for the effect of fractionated low-dose ionizing radiation exposure." *PLoS Comput Biol* **5**(10): e1000539.

Little, M. P., *et al*. (2008). "A systematic review of epidemiological associations between low and moderate doses of ionizing radiation and late cardiovascular effects, and their possible mechanisms." *Radiat Res* **169**(1): 99-109.

Little, M. P., *et al*. (2010). "Review and meta-analysis of epidemiological associations between low/moderate doses of ionizing radiation and circulatory disease risks, and their possible mechanisms." *Radiat Environ Biophys* **49**(2): 139-153.

Little, M. P., *et al*. (2012). "Systematic Review and Meta-analysis of Circulatory Disease from Exposure to Low-Level Ionizing Radiation and Estimates of Potential Population Mortality Risks." Environ Health Perspect **120**(11): 1503-11.

Liu, D. G. and T. M. Wang (2008). "Role of connective tissue growth factor in experimental radiation nephropathy in rats." *Chin Med J (Engl)* **121**(19): 1925-1931.

Lubin, J. H., *et al*. (1995). "Lung cancer in radon-exposed miners and estimation of risk from indoor exposure." *J Natl Cancer Inst* **87**(11): 817-827.

Lusis, A. J. (2000). "Atherosclerosis." *Nature* **407**(6801): 233-241.

Machado, R. D., *et al*. (2009). "Genetics and genomics of pulmonary arterial hypertension." *J Am Coll Cardiol* **54**(1 Suppl): S32-42.

Mahmoudi, M., *et al*. (2006). "DNA damage and repair in atherosclerosis." *Cardiovasc Res* **71**(2): 259-268.

Maity, A., *et al*. (1994). "The molecular basis for cell cycle delays following ionizing radiation: a review." *Radiother Oncol* **31**(1): 1-13.

Marelli-Berg, F. M., *et al*. (2000). "Isolation of endothelial cells from murine tissue." *J Immunol Methods* **244**(1-2): 205-215.

Markes, L. B., *et al*. (2005). "The incidence and functional consequences of RT-associated cardiac perfusion defects." *Int J Radiat Oncol Biol Phys* **63**(1): 214-23.

Marti, T. M., *et al*. (2006). "H2AX phosphorylation within the G1 phase after UV irradiation depends on nucleotide excision repair and not DNA double-strand breaks." *Proc Natl Acad Sci U S A* **103**(26): 9891-9896.

Martin, M., *et al*. (2000). "TGF-beta1 and radiation fibrosis: a master switch and a specific therapeutic target?" *Int J Radiat Oncol Biol Phys* **47**(2): 277-290.

Martin, M., *et al*. (1997). "Coactivation of AP-1 activity and TGF-beta1 gene expression in the stress response of normal skin cells to ionizing radiation." *Oncogene* **15**(8): 981-989.

Masse, R. (2000). "[Ionizing radiation]." *C R Acad Sci III* **323**(7): 633-640.

Matanoski, G. M., *et al*. (1975). "The current mortality rates of radiologists and other physician specialists: specific causes of death." *Am J Epidemiol* **101**(3): 199-210.

Matsumoto, H., *et al*. (2007). "Vanguards of paradigm shift in radiation biology: radiation-induced adaptive and bystander responses." *J Radiat Res* **48**(2): 97-106.

Mattsson, G., *et al*. (2002). "Histological markers for endothelial cells in endogenous and transplanted rodent pancreatic islets." *Pancreatology* **2**(2): 155-162.

Maulik, N. (2004). "Angiogenic signal during cardiac repair." *Mol Cell Biochem* **264**(1-2): 13-23.

McGale, P. and S. C. Darby (2008). "Commentary: A dose-response relationship for radiation-induced heart disease--current issues and future prospects." *Int J Epidemiol* **37**(3): 518-523.

Mercer, J., *et al*. (2007). "DNA damage, p53, apoptosis and vascular disease." *Mutat Res* **621**(1-2): 75-86.

Milliat, F., *et al*. (2006). "Influence of endothelial cells on vascular smooth muscle cells phenotype after irradiation: implication in radiation-induced vascular damages." *Am J Pathol* **169**(4): 1484-1495.

Miltenyi, Z., *et al*. (2004). "Radiation-induced coronary artery disease in Hodgkin's disease." *Cardiovasc Radiat Med* **5**(1): 38-43.

Mitchel, R. E., *et al*. (2011). "Low-dose radiation exposure and atherosclerosis in ApoE$^{-/-}$ mice." *Radiat Res* **175**(5): 665-76.

Miyazono, K., *et al*. (1991). "A role of the latent TGF-beta 1-binding protein in the assembly and secretion of TGF-beta 1." *EMBO J* **10**(5): 1091-1101.

Mladenov, E., *et al*. (2007). "Activation of the S phase DNA damage checkpoint by mitomycin C." *J Cell Physiol* **211**(2): 468-76.

Monceau, V., *et al*. (2010). "Modulation of the Rho/ROCK pathway in heart and lung after thorax irradiation reveals targets to improve normal tissue toxicity." *Curr Drug Targets* **11**(11): 1395-1404.

Montesano, R., *et al*. (1993). "Paracrine induction of angiogenesis in vitro by Swiss 3T3 fibroblasts." *J Cell Sci* **105 (Pt 4)**: 1013-1024.

Morgan, W. F. (2011). "Radiation-induced genomic instability." *Health Phys* **100**(3): 280-281.

Morgan, W. F. and M. B. Sowa (2009). "Non-targeted effects of ionizing radiation: implications for risk assessment and the radiation dose response profile." *Health Phys* **97**(5): 426-432.

Morgan, W. F. (2003). "Non-targeted and delayed effects of exposure to ionizing radiation: I. Radiation-induced genomic instability and bystander effects in vitro." *Radiat Res* **159**(5): 567-580.

Morris, G. M. (1996). "Review article: effects of radiation on the cell proliferation kinetics of epithelial tissues--therapeutic implications." Br J Radiol **69**(825): 795-803.

Mothersill, C. and C. B. Seymour (1998). "Cell-cell contact during gamma irradiation is not required to induce a bystander effect in normal human keratinocytes: evidence for release during irradiation of a signal controlling survival into the medium." *Radiat Res* **149**(3): 256-262.

Moustakas, A., *et al*. (2001). "Smad regulation in TGF-beta signal transduction." *J Cell Sci* **114**(Pt 24): 4359-4369.

Munk, V. C., *et al*. (2007). "Angiotensin II induces angiogenesis in the hypoxic adult mouse heart in vitro through an AT2-B2 receptor pathway." *Hypertension* **49**(5): 1178-1185.

Munk, V.C., *et al*. (2006). "INOS is required in vitro angiogenesis of hypoxic mouse hearts". *Seminars in Cardiology* **12**(1): 21-26.

Munshi, A., *et al*. (2005). "Clonogenic cell survival assay." *Methods Mol Med* **110**: 21-28.

Murray, C. J. and A. D. Lopez (1997). "Global mortality, disability, and the contribution of risk factors: Global Burden of Disease Study." *Lancet* **349**(9063): 1436-1442.

Nagasawa, H. and J. B. Little (1992). "Induction of sister chromatid exchanges by extremely low doses of alpha-particles." *Cancer Res* **52**(22): 6394-6396.

NCI (2010). "FactSheet, Radiation therapy for cancer". NCI FactSheet. [online] Available at: <http://www.cancer.gov/cancertopics/factsheet/Therapy/radiation> [Accessed 04 August 2012].

NCRP (2010). "Second Cancers and Cardiovascular Effects after Radiotherapy". Draft SC 1-17 Report.

Newman, A. C., *et al*. (2011). "The requirement for fibroblasts in angiogenesis: fibroblast-derived matrix proteins are essential for endothelial cell lumen formation." *Mol Biol Cell* **22**(20): 3791-3800.

Nicosia, R. F., *et al*. (1997). "Endogenous regulation of angiogenesis in the rat aorta model. Role of vascular endothelial growth factor. " *Am J Pathol* **151**(5):1379-86.

Nikjoo, H. and I. K. Khvostunov (2003). "Biophysical model of the radiation-induced bystander effect." *Int J Radiat Biol* **79**(1): 43-52.

Nikjoo, H., *et al*. (2001). "Computational approach for determining the spectrum of DNA damage induced by ionizing radiation." *Radiat Res* **156**(5 Pt 2): 577-583.

Nikjoo, H., *et al*. (1998). "Track structure in radiation biology: theory and applications." *Int J Radiat Biol* **73**(4): 355-364.

Nikjoo, H. (2003). "Radiation track and DNA damage". *Iran.J.Radiat* 1(1): 3-16.

Nistri, S., *et al*. (2002). "High-Yield Method for Isolation and Culture of Endothelial Cells from Rat Coronary Blood Vessels Suitable for Analysis of Intracellular Calcium and Nitric Oxide Biosynthetic Pathways." *Biol Proced Online* **4**: 32-37.

O'Driscoll, M. and P. A. Jeggo (2006). "The role of double-strand break repair - insights from human genetics." *Nat Rev Genet* **7**(1): 45-54.

Oh, C. W., *et al*. (2001). "Induction of a senescence-like phenotype in bovine aortic endothelial cells by ionizing radiation." *Radiat Res* **156**(3): 232-240.

Olivieri, G., *et al*. (1984). "Adaptive response of human lymphocytes to low concentrations of radioactive thymidine." *Science* **223**(4636): 594-597.

Oommen, S., *et al*. (2011). "Vascular endothelial growth factor A (VEGF-A) induces endothelial and cancer cell migration through direct binding to integrin {alpha}9{beta}1: identification of a specific {alpha}9{beta}1 binding site." *J Biol Chem* **286**(2): 1083-1092.

Orfanos, S. E., *et al*. (1994). "Radiation-induced early pulmonary endothelial ectoenzyme dysfunction in vivo: effect of indomethacin." *Toxicol Appl Pharmacol* **124**(1): 112-122.

Orlova, V. V., *et al*. (2011). "Controlling angiogenesis by two unique TGF-beta type I receptor signaling pathways." *Histol Histopathol* **26**(9): 1219-1230.

Osterreicher, J., *et al*. (2003). "Radiation-induced bystander effects. Mechanisms, biological implications, and current investigations at the Leipzig LIPSION facility." *Strahlenther Onkol* **179**(2): 69-77.

Oxhorn, B. C., *et al*. (2002). "Isolation and characterization of large numbers of endothelial cells for studies of cell signaling." *Microvasc Res* **64**(2): 302-315.

Ozasa, K., *et al*. (2012). "Studies of the mortality of atomic bomb survivors, Report 14, 1950-2003: an overview of cancer and noncancer diseases." *Radiat Res* **177**(3): 229-243.

Park, M. T., *et al*. (2012). "Radio-sensitivities and angiogenic signaling pathways of irradiated normal endothelial cells derived from diverse human organs." *J Radiat Res* **53**(4): 570-580.

Paszat, L. F., *et al*. (1998). "Mortality from myocardial infarction after adjuvant radiotherapy for breast cancer in the surveillance, epidemiology, and end-results cancer registries." *J Clin Oncol* **16**(8): 2625-2631.

Patel, D. A., *et al*. (2006). "Clinical manifestations of noncoronary atherosclerotic vascular disease after moderate dose irradiation." *Cancer* **106**(3): 718-725.

Patel, R. R. and D. W. Arthur (2006). "The emergence of advanced brachytherapy techniques for common malignancies." *Hematol Oncol Clin North Am* **20**(1): 97-118.

Peppper, M. S., *et al*. (1998). "Vascular endothelial growth factor (VEGF)-C synergizes with basic fibroblast growth factor and VEGF in the induction of angiogenesis in vitro and alters endothelial cell extracellular proteolytic activity. " *J Cell Physiol* **177**(3): 439-52.

Phillips, G. D. and A. M. Stone (1994). "PDGF-BB induced chemotaxis is impaired in aged capillary endothelial cells. " *Mech AgeingDev* **73**(3): 189-96.

Pluder, F., *et al*. (2011). "Low-dose irradiation causes rapid alterations to the proteome of the human endothelial cell line EA.hy926." *Radiat Environ Biophys* **50**(1): 155-166.

Pohlers, D., *et al*. (2009). "TGF-beta and fibrosis in different organs - molecular pathway imprints." *Biochim Biophys Acta* **1792**(8): 746-756.

Preston, D. L., *et a*l. (2003). "Studies of mortality of atomic bomb survivors. Report 13: Solid cancer and noncancer disease mortality: 1950-1997." *Radiat Res* **160**(4): 381-407.

Prionas, S. D., *et al*. (1990). "Effects of X irradiation on angiogenesis." *Radiat Res* **124**(1): 43-49.

Prise, K. M. and J. M. O'Sullivan (2009). "Radiation-induced bystander signaling in cancer therapy." *Nat Rev Cancer* **9**(5): 351-360.

Prise, K. M., *et al*. (2005). "New insights on cell death from radiation exposure." *Lancet Oncol* **6**(7): 520-528.

Quarmby, S., *et al*. (2000). "Irradiation induced expression of CD31, ICAM-1 and VCAM-1 in human microvascular endothelial cells." *Anticancer Res* **20**(5B): 3375-3381.

Rader, D. J. and K. A. Dugi (2000). "The endothelium and lipoproteins: insights from recent cell biology and animal studies." *Semin Thromb Hemost* **26**(5): 521-528.

Radiation protection No 158 (2008). "EU Scientific Seminar 2008 emerging evidences for radiation induced circulatory diseases". Luxembourg, 25 Nov 2008. Publications office of the European Union Luxembourg: European Commission.

Raicu, M., *et al*. (1993). "Radiation damage to endothelial cells in vitro, as judged by the micronucleus assay." *Mutagenesis* **8**(4): 335-339.

Randall, K. and J. E. Coggle (1995). "Expression of transforming growth factor-beta 1 in mouse skin during the acute phase of radiation damage." *Int J Radiat Biol* **68**(3): 301-309.

Rastogi, R. P., *et al*. (2010). "Molecular mechanisms of ultraviolet radiation-induced DNA damage and repair." *J Nucleic Acids* **2010**: 592980.

Reed, M. J., *et al*. (2007). "Culture of murine aortic explants in 3-dimensional extracellular matrix: a novel, miniaturized assay of angiogenesis in vitro." *Microvasc Res* **73**(3): 248-252.

Reed, M. J., *et al*. (1998). "Neovascularization in aged mice: delayed angiogenesis is coincident with decreased levels of transforming growth factor beta 1 ad type I collagen. " *Am J Pathol* **152**(1): 113-23.

Reed, M. J., *et al*. (2000). "A deficit in collagenase activity contributes to impaired migration of aged microvascular endothelial cell. " *J Cell* **77**(1): 116-126.

Rhee, J. G., *et al*. (1986). "The clonogenic response of bovine aortic endothelial cells in culture to radiation." *Radiat Res* **106**(2): 182-189.

Rhim, J. S., *et al*. (1998). "A human vascular endothelial cell model to study angiogenesis and tumorigenesis." *Carcinogenesis* **19**(4): 673-681.

Risau, W. (1997). "Mechanism of angiogenesis. " *Nature* **386**(6626): 671-4.

Rockwell, S. (1998). "Experimental radiotherapy: a brief history." *Radiat Res* **150**(5 Suppl): S157-169.

Rontgen, W. C. (1896). "On a New Kind of Rays." *Science* **3**(59): 227-231.

Roth, J., P. Schweizer, *et al* (1996). "[Basic of radiation protection]." *Schweiz Med Wochenschr* **126** (26): 1157-1171

Rousseau, M., *et al*. (2011). "RhoA GTPase regulates radiation-induced alterations in endothelial cell adhesion and migration." *Biochem Biophys Res Commun* **414**(4): 750-755.

Ruiz-Ortega, M., *et al*. (2007). "TGF-beta signaling in vascular fibrosis." *Cardiovasc Res* **74**(2): 196-206.

Russell, N. S., *et al*. (2009). "Novel insights into pathological changes in muscular arteries of radiotherapy patients." *Radiother Oncol* **92**(3): 477-483.

Rutqvist, L. E., *et al*. (1992). "Cardiovascular mortality in a randomized trial of adjuvant radiation therapy versus surgery alone in primary breast cancer." *Int J Radiat Oncol Biol Phys* **22**(5): 887-896.

Sabapathy, K. T., *et al*. (1997). "Polyoma middle T-induced vascular tumor formation: the role of the plasminogen activator/plasmin system." *J Cell Biol* **137**(4): 953-963.

Sachs, R. K., *et al*. (1992). "DNA damage caused by ionizing radiation." *Math Biosci* **112**(2): 271-303.

Samarakoon, R. and P. J. Higgins (2008). "Integration of non-SMAD and SMAD signaling in TGF-beta1-induced plasminogen activator inhibitor type-1 gene expression in vascular smooth muscle cells." *Thromb Haemost* **100**(6): 976-983.

Sanchez de Miguel, L., *et al*. (2008). "B2-kinin receptor plays a key role in B1-, angiotensin converting enzyme inhibitor-, and vascular endothelial growth factor-stimulated in vitro angiogenesis in the hypoxic mouse heart." *Cardiovasc Res* **80**(1): 106-113.

Sanderson, N., *et al*. (1995). "Hepatic expression of mature transforming growth factor beta 1 in transgenic mice results in multiple tissue lesions." *Proc Natl Acad Sci U S A* **92**(7): 2572-2576.

Schleicher, S. M., *et al*. (2011). "Autotaxin and LPA receptors represent potential molecular targets for the radiosensitization of murine glioma through effects on tumor vasculature." *PLoS One* **6**(7): e22182.

Schultz-Hector, S. (1993). "Experimental studies on the pathogenesis of damage in the heart." *Recent Results Cancer Res* **130**: 145-156.

Schultz-Hector, S. and K. Balz (1994). "Radiation-induced loss of endothelial alkaline phosphatase activity and development of myocardial degeneration. An ultrastructural study." *Lab Invest* **71**(2): 252-260.

Schultz-Hector, S., *et al*. (1995). "[Radiation sequelae in the large arteries. A review of clinical and experimental data]." *Strahlenther Onkol* **171**(8): 427-436.

Schultz-Hector, S. and K. R. Trott (2007). "Radiation-induced cardiovascular diseases: is the epidemiologic evidence compatible with the radiobiologic data?" *Int J Radiat Oncol Biol Phys* **67**(1): 10-18.

Seemann, I., *et al*. (2012). "Irradiation induced modest changes in murine cardiac function despite progressive structural damage to the myocardium and microvasculature." *Radiother Oncol* **103**(2): 143-150.

Senger, D. R. (1996). "Molecular framework for angiogenesis: a complex web of interactions between extravasated plasma proteins and endothelial cell proteins induced by angiogenic cytokines." *Am J Pathol* **149**(1): 1-7.

Seki, Y., *et al*. (2005). "In vitro effect of cyclosporin A, mitomycin C and prednisolone on cell kinetics in cultured human umbilical vein endothelial cells." *Thromb Res* **115**(3): 219-28.

Sentani, K., *et al*. (2008). "Positive immunohistochemical staining of gammaH2AX is associated with tumor progression in gastric cancers from radiation-exposed patients." *Oncol Rep* **20**(5): 1131-1136.

Shao, C., *et al*. (2002). "Nitric oxide-mediated bystander effect induced by heavy-ions in human salivary gland tumour cells." *Int J Radiat Biol* **78**(9): 837-844.

Shao, E. S., *et al*. (2009). "Expression of vascular endothelial growth factor is coordinately regulated by the activin-like kinase receptors 1 and 5 in endothelial cells." *Blood* **114**(10): 2197-2206.

Shimizu, T., *et al*. (1999). "Coordinated regulation of radioadaptive response by protein kinase C and p38 mitogen-activated protein kinase." *Exp Cell Res* **251**(2): 424-432.

Shimizu, Y., *et al*. (1990). "Studies of the mortality of A-bomb survivors. 9. Mortality, 1950-1985: Part 2. Cancer mortality based on the recently revised doses (DS86)." *Radiat Res* **121**(2): 120-141.

Shimizu, Y., *et al*. (2010). "Radiation exposure and circulatory disease risk: Hiroshima and Nagasaki atomic bomb survivor data, 1950-2003." *BMJ* **340**: b5349.

Shmizu, Y., *et al*. (1991). "Life Span study Report II, part 3. Non-cancer Mortality, 1950-1985, Based on the revised doses. RERF Technical Report series 2-91. Radiation Effects Research Foundation: Hiroshima.

Shimokawa, H. and A. Takeshita (2005). "Rho-kinase is an important therapeutic target in cardiovascular medicine." *Arterioscler Thromb Vasc Biol* **25**(9): 1767-1775.

Sikorski, E. E., *et al*. (1993). "The Peyer's patch high endothelial receptor for lymphocytes, the mucosal vascular addressin, is induced on a murine endothelial cell line by tumor necrosis factor-alpha and IL-1." *J Immunol* **151**(10): 5239-5250.

Sima, A. V., *et al*. (2009). "Vascular endothelium in atherosclerosis." *Cell Tissue Res* **335**(1): 191-203.

Simons, M. and J. A. Ware (2003). "Therapeutic angiogenesis in cardiovascular disease." *Nat Rev Drug Discov* **2**(11): 863-871.

Smith, P. G. and R. Doll (1981). "Mortality from cancer and all causes among British radiologists." *Br J Radiol* **54**(639): 187-194.

Sobel, B. E., *et al*. (2003). "Intramural plasminogen activator inhibitor type-1 and coronary atherosclerosis." *Arterioscler Thromb Vasc Biol* **23**(11): 1979-1989.

Soriano, F. X., *et al*. (2003). "Effect of beta-amyloid on endothelial cells: lack of direct toxicity, enhancement of MTT-induced cell death and intracellular accumulation." *Neurochem Int* **43**(3): 251-261.

Sorrell, J. M., *et al*. (2007). "A self-assembled fibroblast-endothelial cell co-culture system that supports in vitro vasculogenesis by both human umbilical vein endothelial cells and human dermal microvascular endothelial cells." *Cells Tissues Organs* **186**(3): 157-168.

Stewart, F. A., *et al*. (2006). "Ionizing radiation accelerates the development of atherosclerotic lesions in ApoE-/- mice and predisposes to an inflammatory plaque phenotype prone to hemorrhage." *Am J Pathol* **168**(2): 649-658.

Stewart, J. R., *et al*. (1995). "Radiation injury to the heart." *Int J Radiat Oncol Biol Phys* **31**(5): 1205-1211.

Stewart, F. A., *et al*. (2013). "Understanding radiation-induced cardiovascular damage and strategies for intervention." *Clin Oncol (R Coll Radiol)* **25**(10): 617-24.

Stewart, F. A., *et al*. (2010). "Vascular damage as an underlying mechanism of cardiac and cerebral toxicity in irradiated cancer patients." *Radiat Res* **174**(6): 865-869.

Stitzinger, M. (2007). "Lipid, inflammation and atherosclerosis". PhD. Leiden/Amsterdam Center for Drug Research, (LACDR), Leiden University. Available at:<https://openaccess.leidenuniv.nl/handle/1887/9729>.

Stone, H. B., *et al*. (2003). "Effects of radiation on normal tissue: consequences and mechanisms." *Lancet Oncol* **4**(9): 529-536.

Stucki, M. and S. P. Jackson (2006). "gammaH2AX and MDC1: anchoring the DNA-damage-response machinery to broken chromosomes." *DNA Repair (Amst)* **5**(5): 534-543.

Sweetwyne, M. T. and J. E. Murphy-Ullrich (2012). "Thrombospondin1 in tissue repair and fibrosis: TGF-beta-dependent and independent mechanisms." *Matrix Biol* **31**(3): 178-186.

Swift, M. E., *et al*. (1999). "Impaired wound repair and delayed angiogenesis in aged mice. " *Lab Invest* **79**(12): 1479-87.

Taylor, C. W., *et al*. (2007). "Cardiac exposures in breast cancer radiotherapy: 1950s-1990s." *Int J Radiat Oncol Biol Phys* **69**(5): 1484-1495.

Terrell, T. G., *et al*. (1993). "Pathology of recombinant human transforming growth factor-beta 1 in rats and rabbits." *Int Rev Exp Pathol* **34 Pt B**: 43-67.

Tettamanti, G., *et al*. (2004). "The multifunctional role of fibroblasts during wound healing in Hirudo medicinalis (Annelida, Hirudinea)." *Biol Cell* **96**(6): 443-455.

Tribble, D. L., *et al*. (1999). "Ionizing radiation accelerates aortic lesion formation in fat-fed mice via SOD-inhibitable processes." *Arterioscler Thromb Vasc Biol* **19**(6): 1387-1392.

Tubiana, M., *et al*. (1996). "One century of radiotherapy in France 1896-1996." *Int J Radiat Oncol Biol Phys* **35**(2): 227-242.

Tzoulaki, I., *et al*. (2009). "Assessment of claims of improved prediction beyond the Framingham risk score." *JAMA* **302**(21): 2345-2352.

Tzoulaki, I., *et al*. (2009). "Risk of cardiovascular disease and all cause mortality among patients with type 2 diabetes prescribed oral antidiabetes drugs: retrospective cohort study using UK general practice research database." *BMJ* **339**: b4731.

Ucuzian, A. A. and H. P. Greisler (2007). "In vitro models of angiogenesis." *World J Surg* **31**(4): 654-663.

UNSCEAR (2006). "Epidemiological evaluation of cardiovascular disease and other non-cancer diseases following radiation exposure. " United Nations: New York. Report 2006, Scientific Ann B.

UNSCEAR (1993). Source and effects of Ionizing Radiation". United Nations: New York. Report 1993, scientific Ann B.

USNRC (2011). "Natural and man-made radiation sources". USNRC Technical Training Center. [online] Available at: <http://mitnse.files.wordpress.com/2011/03/radiation_mm_06.pdf> [Accessed 20 September 2012].

Van Aelst, L. and C. D'Souza-Schorey (1997). "Rho GTPases and signaling networks." *Genes Dev* **11**(18): 2295-2322.

van Hinsbergh, V. W. and P. Koolwijk (2008). "Endothelial sprouting and angiogenesis: matrix metalloproteinases in the lead." *Cardiovasc Res* **78**(2): 203-212.

Venkatesha, S., *et al*. (2006). "Soluble endoglin contributes to the pathogenesis of preeclampsia." *Nat Med* **12**(6): 642-649.

Vincent, L., *et al*. (2005). "Combretastatin A4 phosphate induces rapid regression of tumor neovessels and growth through interference with vascular endothelial-cadherin signaling." *J Clin Invest* **115**(11): 2992-3006.

Vos, J., *et al*. (1983). "On the cellular origin and development of atheromatous plaques. A light and electron microscopic study of combined X-ray and hypercholesterolemia-induced atheromatosis in the carotid artery of the rabbit." *Virchows Arch B Cell Pathol Incl Mol Pathol* **43**(1): 1-16.

Vozenin-Brotons, M. C., *et al*. (2003). "Fibrogenic signals in patients with radiation enteritis are associated with increased connective tissue growth factor expression." I*nt J Radiat Oncol Biol Phys* **56**(2): 561-572.

Vrijheid, M., *et al*. (2007). "Mortality from diseases other than cancer following low doses of ionizing radiation: results from the 15-Country Study of nuclear industry workers." *Int J Epidemiol* **36**(5): 1126-1135.

Wang, J., *et al*. (2007). "Significance of endothelial dysfunction in the pathogenesis of early and delayed radiation enteropathy." *World J Gastroenterol* **13**(22): 3047-3055.

Wang, X. and T. Ohnishi (1997). "p53-dependent signal transduction induced by stress." *J Radiat Res* **38**(3): 179-194.

Warren, S. (1956). "Longevity and causes of death from irradiation in physicians." *J Am Med Assoc* **162**(5): 464-468.

Warters, R. L. and K. G. Hofer (1977). "Radionuclide toxicity in cultured mammalian cells. Elucidation of the primary site for radiation-induced division delay." *Radiat Res* **69**(2): 348-358.

Watabe, T., *et al*. (2003). "TGF-beta receptor kinase inhibitor enhances growth and integrity of embryonic stem cell-derived endothelial cells." *J Cell Biol* **163**(6): 1303-1311.

Wiencke, J. K., *et al*. (1986). "Evidence that the [3H]thymidine-induced adaptive response of human lymphocytes to subsequent doses of X-rays involves the induction of a chromosomal repair mechanism." *Mutagenesis* **1**(5): 375-380.

Wojta, J., *et al*. (1989a). "Functional characterization of monoclonal antibodies directed against fibrin binding domains of tissue-type plasminogen activator." *J Biol Chem* **264**(14): 7957-7961.

Wojta, J., *et al*. (1989b). "Evaluation of fibrinolytic capacity in plasma during thrombolytic therapy with single (scu-PA) or two-chain urokinase type plasminogen activator (tcu-PA) by a combined assay system for urokinase type plasminogen activator antigen and function." *Thromb Haemos*t **61**(2): 289-293.

Wojta, J., *et al*. (1989). "Vascular origin determines plasminogen activator expression in human endothelial cells. Renal endothelial cells produce large amounts of single chain urokinase type plasminogen activator." *J Biol Chem* **264**(5): 2846-2852.

Wong, F. L., *et al*. (1993). "Noncancer disease incidence in the atomic bomb survivors: 1958-1986." *Radiat Res* **135**(3): 418-430.

Wouters, B. G. and A. C. Begg (2009). "Irradiation-induced damage and the DNA damage response". Basic Clinical Radiology. Joiner, M. C. and A. J. van der Kogel. Great Britain, Hodder Arnold. 4th ed: 11-27.

Wynn, T. A. (2008). "Cellular and molecular mechanisms of fibrosis." *J Pathol* **214**(2): 199-210.

Yamada, M., *et al*. (2004). "Noncancer disease incidence in atomic bomb survivors, 1958-1998." *Radiat Res* **161**(6): 622-632.

Yu, T., *et al*. (2011). "Iron-ion radiation accelerates atherosclerosis in apolipoprotein E-deficient mice." *Radiat Res* **175**(6): 766-73.

Zhang, J., *et al*. (2010). "Biomarkers of endothelial cell activation serve as potential surrogate markers for drug-induced vascular injury." *Toxicol Pathol* **38**(6): 856-871.

Zhang, M., *et al*. (2011). "Blockade of TGF-beta signaling by the TGFbetaR-I kinase inhibitor LY2109761 enhances radiation response and prolongs survival in glioblastoma." *Cancer Res* **71**(23): 7155-7167.

Zhang, S. H., *et al*. (1992). "Spontaneous hypercholesterolemia and arterial lesions in mice lacking apolipoprotein E." *Science* **258**(5081): 468-71.

Zheng, X., *et al*. (2011). "Endothelial cell migration was impaired by irradiation-induced inhibition of SHP-2 in radiotherapy: an in vitro study." *J Radiat Res* **52**(3): 320-328.

Zhu, W. H. and R. F. Nicosia (2002). "The thin prep rat aortic ring assay: a modified method for the characterization of angiogenesis in whole mounts." *Angiogenesis* **5**(1-2): 81-86.

Zidar, N., *et al*. (1997). "Contribution to the pathogenesis of radiation-induced injury to large arteries." *J Laryngol Otol* **111**(10): 988-990.

Zielinski, J. M., *et al*. (2009). "Low dose ionizing radiation exposure and cardiovascular disease mortality: cohort study based on Canadian national dose registry of radiation workers." *Int J Occup Med Environ Health* **22**(1): 27-33.

Zohrabian, V. M., *et al*. (2009). "Rho/ROCK and MAPK signaling pathways are involved in glioblastoma cell migration and proliferation." *Anticancer Res* **29**(1): 119-123.